

MONOGRAPHS AND TEXTS IN PHYSICS AND ASTRONOMY

VOLUME XXVIII

• L. ALLEN
• J.H. EBERLY

**OPTICAL RESONANCE
AND TWO-LEVEL ATOMS**

OPTICAL RESONANCE AND TWO-LEVEL ATOMS

L. ALLEN

University of Sussex

J. H. EBERLY

University of Rochester

A WILEY-INTERSCIENCE PUBLICATION

John Wiley & Sons New York • London • Sydney • Toronto

Copyright © 1975, by John Wiley & Sons, Inc.

All rights reserved. Published simultaneously in Canada.

No part of this book may be reproduced by any means, nor transmitted, nor translated into a machine language without the written permission of the publisher.

Library of Congress Cataloging in Publication Data

Allen, Leslie.

Optical resonance and two-level atoms.

(Interscience monographs and texts in physics and astronomy, v. 28)

"A Wiley-Interscience publication."

Includes bibliographical references.

1. Optical resonance. I. Eberly, J. H., 1935–
joint author. II. Title.

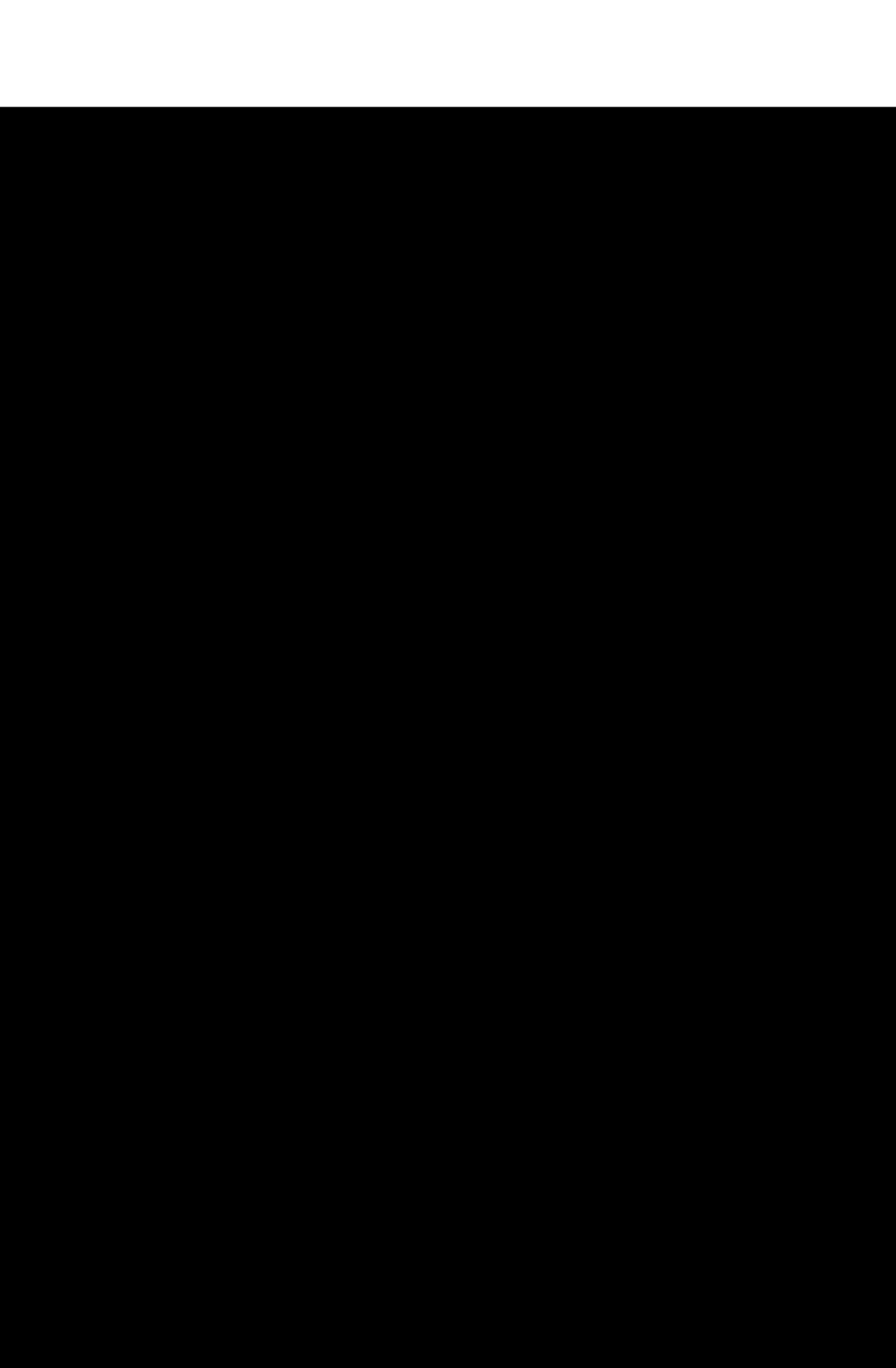
QC476.5. A44 539.2 74-18023

ISBN 0-471-02327-2

Printed in the United States of America

10 9 8 7 6 5 4 3 2 1

For Barbara and Shirley



Preface

A great deal of excitement was aroused in the world of physics by the suggestion made by Schawlow and Townes and by Prokhorov in 1958 that a maser could be operated at optical frequencies. Within a decade of the successful operation of the first optical maser, or laser, entirely new areas of physics were opened and a wave of associated technological development began. Laser physics embraced fields as disparate as photon statistics and microwelding, mensuration and two-photon absorption. The steady state theory of the laser was the subject of intensive investigations using such diverse formalisms as semiclassical rate equations and statistical quantum electrodynamics. Experimental examination of the steady state theories was carried out concurrently with the development of practical methods for producing both more intense and shorter and shorter pulses.

Presently, in the middle of the second decade of laser physics, excitement and interest continue to grow; and new results, both basic and applied, continue to flood research journals all over the world. One of the most important recent advances has been the development of the organic dye laser, offering the experimenter high power and narrow bandwidths literally anywhere in the optical spectrum. It is now possible to investigate any optical resonance at very close spectral range. Very near to resonance all dielectric absorbers can display features entirely alien to classical Lorentzian dielectrics. Some of these near-resonance optical phenomena have strong analogues in nuclear and electron spin resonance. Among these are such effects as optical nutation, photon echoes, and free induction decay. However, many other effects, particularly those involved in the propagation of intense pulses of radiation, are peculiar to the optical region of the frequency spectrum.

With all of these effects in mind we have defined the limits of this monograph. We have restricted our attention to the resonant and near-resonant interaction of coherent light with two-level atoms. To the extent that a resonant interaction calls into play only a single transition in the atom, the atom has only two energy levels, and the laser may be taken to be monochromatic. Certainly, for most lasers and most atoms this can be an excellent pair of approximations; and for an understanding of the basic

physics behind most coherent transient phenomena, completely adequate. Consequently we retain the two-level approximation for atoms throughout this book, and depart from monochromatic fields only to discuss propagating pulses, the area theorem, and self-induced transparency.

In writing the book our intention has been to concentrate on the physical essentials of resonance phenomena; therefore we have not discussed the details of the most recent experimental and theoretical work in the field. For our purposes the phenomenologically damped optical Bloch equations are adequate to express the response of near-resonant atoms to an applied field. Similarly, the classical Maxwell wave equation for the electric field is entirely sufficient to describe a wide range of absorption and amplification effects. In effect we have simply explored and interpreted, at a level requiring little sophistication, many of the consequences of coupling the Bloch and Maxwell equations.

We begin by discussing the elements of optical resonance that are contained in classical dispersion theory. This discussion allows a direct physical interpretation of the analogous quantum mechanical equations when they occur later in the book. Chapter 2 describes the semiclassical theory of radiation, and applies it to two-level atoms. In Chapter 3 the optical Bloch equations are introduced, providing the foundation for almost all of the subsequent analysis. Chapter 4 adds Maxwell's equations to the optical Bloch equations to account for propagation effects; while Chapter 5 reviews the present status of experimental studies of coherent pulse propagation. The connection between the fully coherent coupled Maxwell-Bloch equations and the most familiar semiclassical rate equations is established in Chapter 6 and used to discuss saturation phenomena. The quantization of the radiation field is introduced for the first time in Chapter 7, and used in discussions of the Jaynes-Cummings problem, and of one-atom frequency shifts and lifetimes. Many-atom spontaneous cooperative effects are treated briefly in Chapter 8, and the last chapter is devoted to a semiclassical discussion of photon echoes.

There can be no doubt that *Optical Resonance and Two-Level Atoms* will soon be guilty of omissions beyond our control as the subject develops. These omissions will be in addition to those we are already guilty of either by choice or default. Nevertheless, our hope is that the book will be useful as a primer for a reasonable length of time, and be particularly useful to someone coming into quantum optics and wanting the basic features of optical resonance explained in physical terms.

It is with such an audience in mind that we have consistently used the Heisenberg picture wherever the subject demands a quantum mechanical treatment. This is because the Heisenberg picture is almost always conceptually closer to classic physics than the Schrödinger picture. In the Heisenberg picture one deals with dynamical variables directly, rather than through probability amplitudes and state functions. The semiclassical optical Bloch equations, central to analyses of resonant phenomena, arise directly and naturally from the Heisenberg picture.

Of course atomic physics, and therefore optical resonance, is intrinsically quantum mechanical in nature. One therefore encounters equations for the behavior of dipole moments, electric field strengths, atomic inversion, field energy, and so on, which depend on Planck's constant in important ways. However, the equations themselves are rarely much different from equations often encountered in classical physics, and can often be regarded as analogues of equations familiar from, for example, Lorentzian dielectric theory, or nonlinear circuit analysis. We hope that even readers with very little exposure to quantum physics will have little trouble following discussions of coherent transients, nonlinear pulse propagation, saturation effects, and echo phenomena.

All books owe a great deal to a number of people in addition to their authors. Ours owes a particular debt to those physicists with whom we have shared countless conversations, the results of which are certainly, even if not obviously, embodied in the book: Geoff Jones, Peter Knight, Len Mandel, Carlos Stroud, and Emil Wolf. More obvious is the result achieved by our secretaries and typists. Our thanks to Jean Hafner because for six weeks she had the two of us within earshot for seven days a week, and also to Margaret Barres, Jill Biggane, Shirley Brignall, JoAnne Crane, A. Lesia Gudzowaty, and Edna Hughes, who put up with multiple retypings with commendable good humor.

We are indebted to Peter Milonni for the great majority of the computer-drawn figures and to the National Science Foundation, the U.S. Air Force Office of Scientific Research, the U.S. Army Research Office (Durham), the U.S. Atomic Energy Commission, and the Science Research Council for financial support of our own research.

We are grateful to a number of authors, and the editors of the journals they published in, for granting permission to reproduce figures from their published work. The origins of the figures are individually cited in the text of the book.

Except for a few weeks in England and a week or so in the United States, this book was a long-range collaboration. If this has meant a mode of writing that has lost the merit of a consistent individual style, we regret it. Our thanks once more to those who have helped us; we hope that they will think it all worthwhile.

L. ALLEN
J. H. EBERLY

*Sussex, England
Rochester, New York
August 1974*

Related Books and Reviews

The subject of this book can easily be seen to have its roots in a variety of established fields—for example, atomic physics, magnetic resonance, quantum electronics, and optical pumping. Readers interested in exploring the relation of optical resonance to its neighboring subjects might find the books and reviews listed below particularly helpful.

Two books which provide extensive and careful introductions to resonance physics, in the context of magnetic resonance are:

A. Abragam, *Principles of Nuclear Magnetism*, Oxford University Press, Oxford, 1961.

C. P. Slichter, *Principles of Magnetic Resonance*, Harper and Row, New York, 1963.

An excellent pedagogical review, including an introduction to the Bloch equations in the rotating coordinate frame, is provided by Pake's early articles:

G. E. Pake, "Fundamentals of Nuclear Magnetic Resonance Absorption, I and II," *Am. J. Phys.* **18**, 438; 473 (1950).

The books of Haken, Loudon, and Louisell are valuable for their thorough discussions of field quantization, quantum mechanical master equations, and quantum statistics. These subjects are central to a careful examination of the fundamental quantum theory of optical physics and have been largely bypassed in our semiclassical treatment.

H. Haken, *Laser Theory, Handbuch der Physik*, Vol. XXV/2c, Springer-Verlag, Berlin, 1970.

R. Loudon, *The Quantum Theory of Light*, Oxford University Press, Oxford, 1973.

W. H. Louisell, *Quantum Statistical Properties of Radiation*, John Wiley and Sons, New York, 1973.

Three specialized and compact discussions of recent work on the quantum theory of the interaction of radiation and matter may also be of interest:

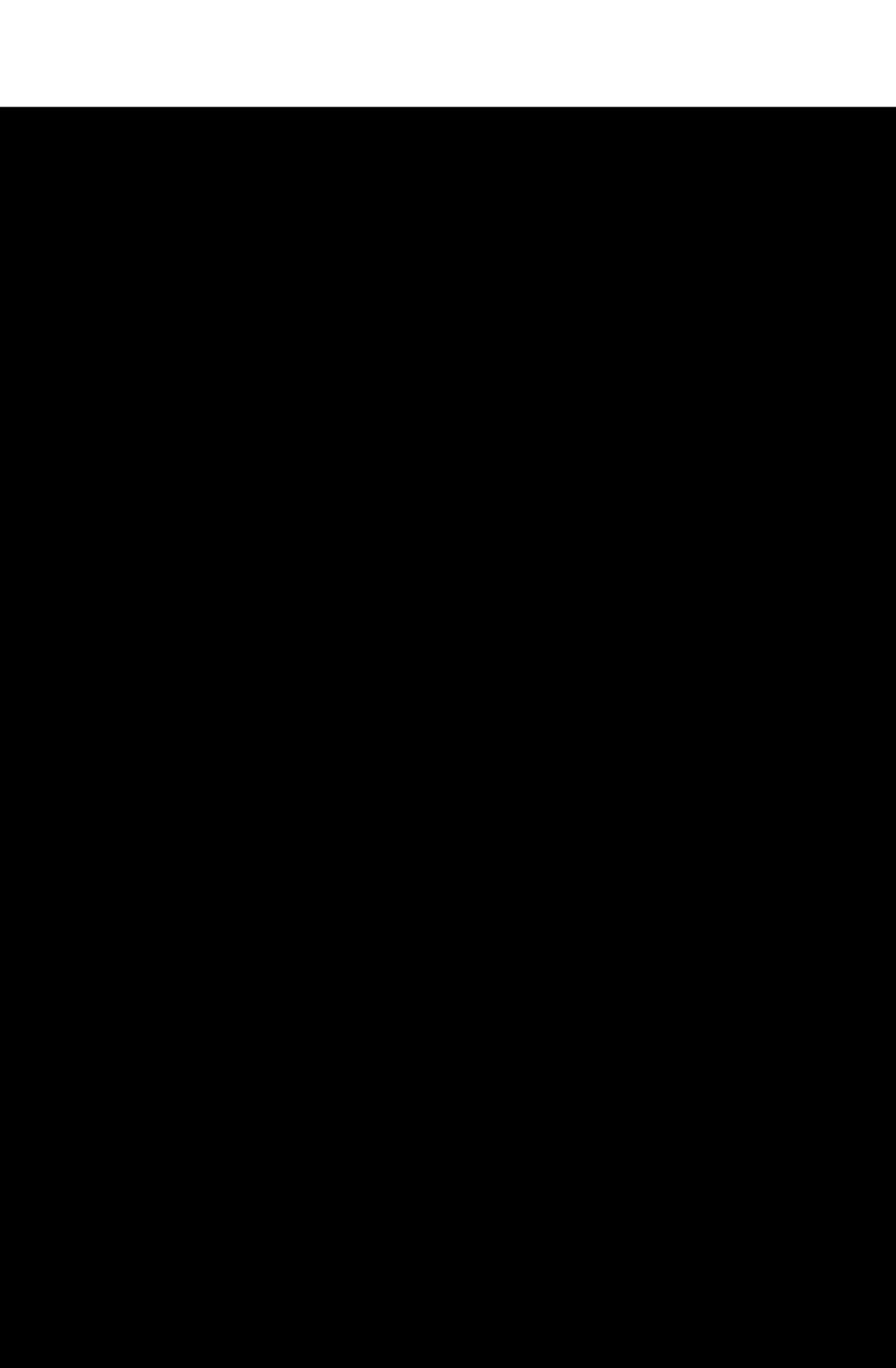
- G. S. Agarwal, "Quantum Statistical Theories of Spontaneous Emission," *Springer Tracts in Modern Physics*, Springer-Verlag, Berlin, 1974, Vol. 70.
F. Haake, "Statistical Treatment of Open Systems by Generalized Master Equations," *Springer Tracts in Modern Physics*, Springer-Verlag, Berlin, 1973, Vol. 66, p. 97.
S. Stenholm, "Quantum Theory of Electromagnetic Fields Interacting with Atoms," *Physics Reports* **6C**, 1(1973).

Finally, there are a few books already published which treat parts of the subject of optical resonance in much the way we have chosen. The semiclassical theory of radiation is used extensively, some analogies with magnetic resonance phenomena are drawn where possible, and an approach which is not exclusively theoretical is adopted. The reader of this book may find it useful to consult:

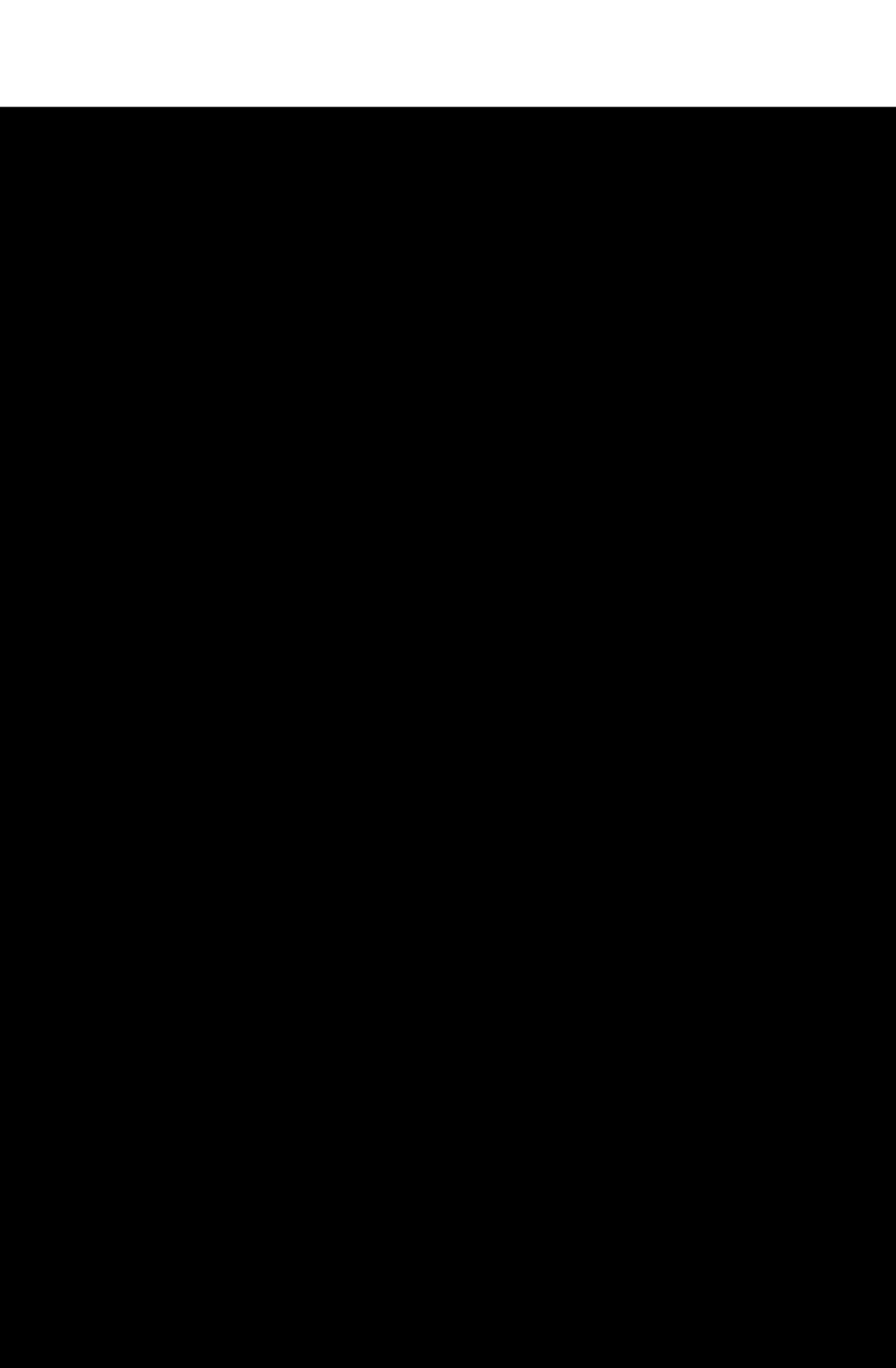
- V. M. Fain and Ya. I. Khanin, *Quantum Electronics I and II*, The M.I.T. Press, Cambridge, 1969.
H. M. Nussenzveig, *Introduction to Quantum Optics*, Gordon and Breach, London, 1973.
R. H. Pantell and H. E. Puthoff, *Fundamentals of Quantum Electronics*, John Wiley and Sons, New York, 1969.

Contents

1 Classical Theory of Resonance Optics	1
2 The Optical Bloch Equations	28
3 Two-Level Atoms in Steady Fields	52
4 Pulse Propagation	78
5 Pulse Propagation Experiments	110
6 Saturation Phenomena	130
7 Quantum Electrodynamics and Spontaneous Emission	152
8 <i>N</i>-Atom Spontaneous Emission and Superradiant Decay	174
9 Photon Echoes	195
Index	221



OPTICAL RESONANCE AND TWO-LEVEL ATOMS



CHAPTER 1

Classical Theory of Resonance Optics

1.1	Introduction	1
1.2	The Linear Dipole Oscillator	2
1.3	The Classical Rabi Problem	5
1.4	Emission Lineshape and Linewidth	7
1.5	Free Induction Decay	10
1.6	Electromagnetic Wave Propagation	12
1.7	The Classical Area Theorem	15
1.8	Anomalous Classical Absorption	21
	References	26

1.1 INTRODUCTION

The classical theory of the linear interaction of light with matter was largely the creation of H. A. Lorentz. It was Lorentz who systematically explored the idea that optical phenomena in general arise from the motion of elementary charges and dipoles that are more or less free to respond to the electric and magnetic fields associated with light waves. This view is now regarded as so obviously the correct one that it serves as the starting point of every modern study of optical properties of dielectrics.

From a practical point of view, the classical Lorentzian theory requires modifications only in the most extreme circumstances. The classical Rayleigh and Thomson optical scattering formulas do not need to be supplanted by the quantum mechanical Compton formula until the scattered light has its wavelength well into the X-ray region. Furthermore, classical Lorentzian dispersion and absorption formulas reappear in quantum mechanical treatments, and were first derived quantum mechanically by Kramers and Heisenberg simply by applying correspondence principle arguments to the classical expressions. Only for fields which are so intense as to excite intrinsic atomic nonlinearities will there be appreciable departures from the predictions of the Lorentz-Kramers-Heisenberg dispersion theory.

With the assumption that the Lorentzian oscillating-electron approach and its standard results are familiar, we devote the following sections in this chapter to a review of Lorentzian theory in unconventional notation.

This is done for two reasons. First, it will be useful to have the classical formulas at hand for comparison with the quantum mechanical expressions derived in later chapters. In this way it will be clear just how much of any given result is, in fact, quantum mechanical. Second, by introducing in an entirely classical context the notation, the near-resonance approximations, and a number of the physical phenomena to be dealt with later, we hope they will not appear puzzling or strange when encountered again. Thus, in this first chapter, the so-called Rabi problem, free induction decay, an “area” theorem, and ultrashort pulses are all discussed in addition to the standard formulas for index of refraction and attenuation coefficient.

1.2 THE LINEAR DIPOLE OSCILLATOR

According to Lorentz, the majority of optical phenomena can be accounted for by the interaction of electric charges with the electromagnetic field [1]. We begin by assuming that these charges are bound into neutral atoms, and that they oscillate about their equilibrium positions with very small amplitudes. That is, each electron-ion pair behaves as a simple harmonic oscillator, which couples to the electromagnetic field through its electric dipole moment. The motion of a collection of such dipole oscillators, comprising a gas or other dielectric system, is thus governed by the Hamiltonian:

$$\mathcal{H} = \frac{1}{2m} \sum_a (p_a^2 + \omega_a^2 m^2 r_a^2) - e \sum_a \mathbf{r}_a \cdot \mathbf{E}(t, \mathbf{r}_a), \quad (1.1)$$

where \mathbf{p}_a and \mathbf{r}_a are the canonical momentum and position of dipole a that has a natural oscillation frequency ω_a and where $\mathbf{E}(t, \mathbf{r}_a)$ is the electric field strength at the position of atom a at time t .

The specific equation of motion obeyed by a single-atom dipole oscillator is very simple. We may write it in its simplest form by recognizing that a given component of \mathbf{r}_a couples only to the same component of \mathbf{E} . Let the scalar quantities x_a and E represent a pair of coupled components. The Poisson bracket relations

$$\dot{x}_a = \{x_a, \mathcal{H}\} \text{ and } \dot{p}_a = \{p_a, \mathcal{H}\}, \quad (1.2)$$

or Hamilton's equations

$$\dot{p}_a = -\frac{\partial \mathcal{H}}{\partial q_a} \quad \text{and} \quad \dot{q}_a = \frac{\partial \mathcal{H}}{\partial p_a}, \quad (1.3)$$

lead to the familiar result

$$\ddot{x}_a + \omega_a^2 x_a = \frac{e}{m} E(t, \mathbf{r}_a), \quad (1.4)$$

which is merely the electric part of the Lorentz force law for a nonrelativistic charge. In the relativistic limit the magnetic force term $(e/c)\mathbf{v}_a \times \mathbf{B}$ is not small and must be included in equation 1.4. In the nonrelativistic limit the magnetic force may be ignored.

One of the most elementary properties of a dipole oscillator is that it radiates electromagnetic energy. Thus even if there were no other charges and currents in the universe to produce a field E at the position \mathbf{r}_a , a field due to the dipole's own radiation would still exist. The realization that this is so posed an important self-consistency problem to Lorentz: the problem of accounting for the effect of a single oscillator's own field on its own motion. One very direct way to solve this problem is to make use of energy conservation. The energy radiated into the field must be consistent with the energy lost by the oscillator. The consequences of this radiation reaction self-consistency are easily worked out.

If the oscillator has a fixed center of oscillation—because the neutral atom is very massive and slow-moving compared with the oscillating electron—then the existence of local energy conservation for the system of electromagnetic field plus oscillator is implied by the relation (Born and Wolf [2], Section 1.1.4):

$$\nabla \cdot \mathbf{S} + \frac{\partial U_{\text{em}}}{\partial t} + \frac{\partial U_{\text{mat}}}{\partial t} = 0, \quad (1.5)$$

where \mathbf{S} is the Poynting vector, U_{em} the energy density of the electromagnetic field, and U_{mat} the energy density of the matter. By integrating equation 1.5 over the volume of a small sphere centered at the oscillator we obtain a relation referring to energy, rather than to energy density:

$$\int_{\mathcal{A}} \mathbf{S} \cdot \mathbf{n} dA + \frac{\partial W_{\text{em}}}{\partial t} + \frac{\partial W_{\text{osc}}}{\partial t} = 0. \quad (1.6)$$

Here the volume integral $\int_{\mathcal{V}} \nabla \cdot \mathbf{S} dV$ has been transformed into an integral over the spherical surface area \mathcal{A} .

An assumption, to be checked later, is useful at this point: we assume the dipole's radiative energy loss to be relatively slow, at least compared with a period of atomic dipole oscillation $2\pi/\omega_a$. One consequence is that the amount of electromagnetic energy in the small volume \mathcal{V} is roughly steady in time. This means that the term $\partial W_{\text{em}}/\partial t$ makes a negligible contribution to equation 1.6. A second consequence is that the dipole oscillations are almost perfectly harmonic. Thus the energy of the a th oscillator is approximately:

$$W_a(t) = m\omega_a^2 \overline{x_a^2(t)}, \quad (1.7)$$

where the bar denotes an average over very rapid oscillations at frequency $2\omega_a$.

The rate of energy loss by electric dipole radiation through a spherical surface centered at the dipole is well-known (see Born and Wolf [2], Section 2.2.3) to be:

$$\int \mathbf{S}(t) \cdot \mathbf{n} dA = \frac{2e^2\omega_a^4}{3c^3} \overline{x_a^2(t)}, \quad (1.8)$$

which, according to relation 1.7, may be written as

$$\int \mathbf{S}(t) \cdot \mathbf{n} dA = \frac{2e^2\omega_a^2}{3mc^3} W_a(t).$$

In other words, the rate of energy flow away from the oscillating dipole is directly proportional to the energy of the dipole itself. The energy conservation relation 1.6 is thus equivalent to an exceptionally simple equation of motion for the dipole energy:

$$\frac{\partial W_a}{\partial t} = -\frac{2}{\tau_0} W_a. \quad (1.9)$$

Clearly, to the extent that these approximations are valid, the oscillation decays exponentially

$$W_a(t) = W_a(0)e^{-2t/\tau_0} \quad (1.10)$$

with an energy decay rate given by

$$\frac{2}{\tau_0} = \frac{2e^2\omega_a^2}{3mc^3}.$$

The natural lifetime τ_0 predicted in this way is of the order of 0.1 μ sec, if the dipole oscillates at optical frequencies. Thus $1/\tau_0 \ll \omega_a$ is satisfied, and the initial assumption that the oscillator energy loss is relatively slow is validated.

This slow decay of the radiating dipole's amplitude and energy, due to radiation reaction, can conveniently be incorporated directly in the dipole equation of motion. The Lorentz force equation 1.4 then becomes

$$\ddot{x}_a + \frac{2}{\tau_0} \dot{x}_a + \omega_a^2 x_a = \frac{e}{m} E, \quad (1.11)$$

where E must now be regarded as the field acting on dipole a because of all other charges and currents. It is simple to verify that, when $E=0$, equation 1.11 predicts a decay of dipole amplitude at the rate $1/\tau_0$, and thus an energy decay at the rate $2/\tau_0$.

1.3 THE CLASSICAL RABI PROBLEM

One of the simplest, but most important, special cases of the general relation 1.11 occurs when the applied field is oscillatory with a frequency ω very close to the natural frequency ω_a of one of the dipoles. Such a coincidence of driving frequency and natural frequency leads, of course, to resonance phenomena. We take a slightly unusual approach to this familiar problem, an approach designed for very-near-resonance effects.

Let the driving field be denoted by

$$E = \mathcal{E} [e^{i\omega t} + c.c.], \quad (1.12)$$

where \mathcal{E} is a constant amplitude. We then decompose x_a into a part that is approximately in-phase and a part that is approximately in-quadrature with E :

$$x_a = x_0 [u_a \cos \omega t - v_a \sin \omega t]. \quad (1.13)$$

Here x_0 may be regarded as the amplitude of oscillation at some arbitrary time, and taken to be constant. In general u_a and v_a will *not* be constant

because the natural frequency ω_a of x_a is presumed to be different from the field frequency ω . However, u_a and v_a will vary very slowly in time if the difference $\omega - \omega_a$ is small. In fact, we assume the validity of the inequalities:

$$\dot{u}_a \ll \omega u_a, \quad \ddot{u}_a \ll \omega^2 u_a, \quad \dot{v}_a \ll \omega v_a, \quad \ddot{v}_a \ll \omega^2 v_a, \quad (1.14)$$

which ensure that u_a and v_a are envelope functions, slowly varying compared with $\cos \omega t$ and $\sin \omega t$.

These assumptions allow the dipole equation 1.11 to be written as a pair of equations for u_a and v_a :

$$\dot{u}_a = -\frac{1}{2\omega}(\omega_a^2 - \omega^2)v_a - \frac{u_a}{\tau_0} - \frac{1}{\omega\tau_0}\dot{v}_a, \quad (1.15)$$

$$\dot{v}_a = \frac{1}{2\omega}(\omega_a^2 - \omega^2)u_a - \frac{v_a}{\tau_0} - \left(\frac{e}{m\omega x_0}\right)\hat{\epsilon} + \frac{1}{\omega\tau_0}\dot{u}_a \quad (1.16)$$

In these equations, since $\omega_a \approx \omega$, we may write $\omega_a^2 - \omega^2 \approx 2\omega(\omega_a - \omega)$, and for convenience denote the frequency difference by Δ_a :

$$\Delta_a \equiv \omega_a - \omega. \quad (1.17)$$

Our earlier assumption about the relative slowness of radiative decay (i.e., $\omega\tau_0 \gg 1$) justifies dropping the last term in each equation.

Furthermore, in a real physical situation radiative decay almost certainly will not be the only factor contributing to the damping of the dipole amplitude. The effective “lifetime” of the oscillator is usually shorter than its purely radiative lifetime τ_0 , because of a variety of random incoherent interactions such as collisions that were not included in the original Hamiltonian. Thus we replace τ_0 by T , where the value of T will depend on the circumstance, with the understanding that the total decay rate T^{-1} must be greater than, or at least equal to, the purely radiative rate τ_0^{-1} . With these provisions, the equations for the in-phase and in-quadrature amplitudes become:

$$\dot{u} = -\Delta v - \frac{u}{T}, \quad (1.18a)$$

where

$$\kappa \equiv \frac{e}{m\omega x_0}. \quad (1.19)$$

We have neglected to write the subscript a , since Δ serves equally well to distinguish atoms with different resonant frequencies.

Equations 1.18a and 1.18b have very simple solutions:

$$u(t; \Delta) = [u_0 \cos \Delta t - v_0 \sin \Delta t] e^{-t/T} + \kappa \mathcal{E} \int_0^t dt' \sin \Delta(t-t') e^{-(t-t')/T}, \quad (1.20a)$$

$$v(t; \Delta) = [u_0 \sin \Delta t + v_0 \cos \Delta t] e^{-t/T} - \kappa \mathcal{E} \int_0^t dt' \cos \Delta(t-t') e^{-(t-t')/T}, \quad (1.20b)$$

where $u_0 = u(0; \Delta)$ and $v_0 = v(0; \Delta)$ are the initial values of the dipole envelope functions. After a long time all initial oscillations will have died out. Then one may easily verify that the familiar result

$$x_a(t) = \frac{e}{m} \mathcal{E} \left(\frac{e^{i\omega t}}{\omega_a^2 - \omega^2 + 2i\omega/T} + \text{c.c.} \right) \quad (1.21)$$

follows from equations 1.20a and 1.20b. The driven dipole oscillates at the field frequency, but not exactly in phase with the field.

Equations 1.18 are the classical analogues of nonlinear quantum equations describing atomic dipole oscillations that will be important in later chapters. We refer to solutions 1.20 as the classical Rabi solutions because the solutions to the quantum problem in the same special limit considered here, namely $\mathcal{E} = \text{constant}$, are associated with I. I. Rabi [3] and his early work on magnetic resonance phenomena (see Chapter 3).

1.4 EMISSION LINESHAPE AND LINewidth

In a real dielectric the constituent dipoles can oscillate at many different natural frequencies. For this reason, every material exhibits a large number of emission lines. The polarization density $P(t)$ of the medium is actually due to dipole oscillations at the frequencies of all these lines. Fortunately, in most materials that have optical or near-optical emission and absorption

lines, the lines are well-separated, allowing the assumption that only the dipoles contributing to one line need be dealt with.

The spectral width of an emission line depends on many factors, and the subject of spectral lineshape is very complex. For our purposes an elementary treatment will suffice. Equations 1.20 already show that the emission line of a typical single dipole will not be infinitely sharp, but will have a width in frequency of roughly $1/T$, because of the finite lifetime T of every excited dipole moment. Because this width is the same for each dipole it is usually called the “homogeneous” width of the spectral line, and can be denoted by $\delta\omega_H$:

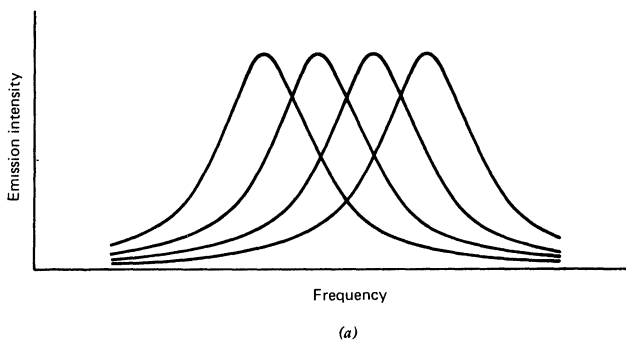
$$\delta\omega_H \sim \frac{1}{T}. \quad (1.22)$$

Since the dipole moment decay is exponential, the shape of the spectral line is Lorentzian.

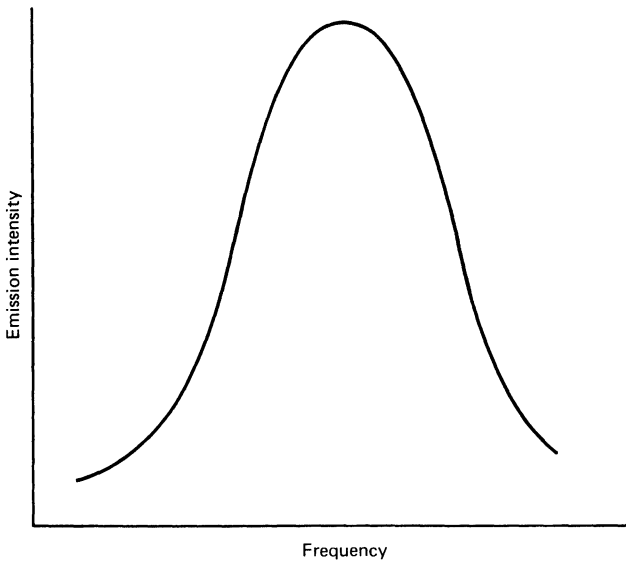
This very simple picture is unfortunately not quite adequate. Because of the Doppler effect, gas atoms with different velocities will have different effective resonance frequencies even if they are otherwise identical. In solids the same effect arises. The slightly different environments in which the resonant atoms find themselves, for such reasons as random dislocations, impurities, and strain fields, also give rise to different effective resonance frequencies for differently located but otherwise identical atoms.

Thus in many cases the actual emission line must be thought of as a superposition of a large number of Lorentzian lines, each with homogeneous width $1/T$ and each with a distinct center frequency ω_a . Figure 1.1 illustrates the unrealistically simple case in which there are only four distinct center frequencies. The overall width of the total line can be seen to be better represented by the spread between the most widely separated line centers than by the homogeneous width $1/T$. The overall line is said in this case to be “inhomogeneously” broadened to a greater extent than it is “homogeneously” broadened. The term “inhomogeneous” obviously refers to the environmental inhomogeneities that are the origin of the different effective resonance frequencies possessed by otherwise identical oscillators.

It is generally satisfactory to account for the possibility of “inhomogeneous” broadening by introducing a normalized inhomogeneous lineshape function $G(\omega_0)$. Here $G(\omega_0)d\omega_0$ is the fraction of dipoles with resonance center frequency within $d\omega_0$ of the frequency ω_0 . Obviously the



(a)



(b)

Fig. 1.1 The origin of inhomogeneous broadening. The individual Lorentzian emission lines associated with different atomic dipoles oscillating at four distinct frequencies are shown in (a). If there were a dielectric material made up of just those atoms whose individual lines are shown in (a), its emission line would be as shown in (b), the sum of the curves in (a). When the individual lines are densely scattered over a frequency range large compared with their own individual widths, the total lineshape is termed inhomogeneously broadened.

required normalization is

$$\int_0^\infty G(\omega'_0) d\omega'_0 = 1.$$

More frequently, we use an inhomogeneous lineshape *detuning* function $g(\Delta)$ obtained from $G(\omega_0)$ by a shift of ω in the frequency origin. Thus $g(\Delta)d\Delta$ is defined to be the fraction of dipoles, within the detuning interval $d\Delta$, whose resonance center frequency ω_0 is detuned from the applied field frequency by $\Delta = \omega_0 - \omega$. The normalization

$$\int_{-\infty}^\infty g(\Delta') d\Delta' = 1 \quad (1.23)$$

will be used, on the assumption that $g(\Delta')$ is so small at the true lower limit of integration $\Delta' = -\omega$, which corresponds to $\omega'_0 = 0$, that extending this limit to $-\infty$ makes no difference. Note that there need be no special significance to $g(0)$. The peak of the inhomogeneous frequency function $G(\omega_0)$ *need* not coincide with the applied field frequency ω , so that $g(\Delta)$ *need* not peak at zero detuning. However, it is near-resonance problems that are of interest. Thus it will usually be assumed that $g(0) \approx g_{\max}$ and $g(\Delta') \approx g(-\Delta')$.

1.5 FREE INDUCTION DECAY

The physical significance of inhomogeneous broadening and the role of an inhomogeneous “lifetime” are closely connected. Consider a collection of dipoles spread uniformly with density \mathcal{N} throughout a small region. The polarization density associated with these dipoles may be written as

$$P(t) = \mathcal{N} e x_0 \int \operatorname{Re} [\{u(t; \Delta') + i v(t; \Delta')\} e^{i\omega t}] g(\Delta') d\Delta', \quad (1.24)$$

by combining relation 1.13 with $g(\Delta')$ and the atomic density \mathcal{N} . The radiation emitted by such a polarization density will be qualitatively the same for any smooth detuning function. For simplicity we take $g(\Delta')$ to be Lorentzian, peaked at $\Delta' = \Delta$, which corresponds to a peak at $\omega + \Delta$ in the frequency function $G(\omega'_0)$:

$$g(\Delta') = \frac{\delta\omega_I}{\pi} \frac{1}{(\Delta' - \Delta)^2 + (\delta\omega_I)^2}, \quad (1.25)$$

where $\delta\omega_I$ is obviously the inhomogeneous halfwidth at halfmaximum. Both $u(t; \Delta')$ and $v(t; \Delta')$ may be taken from the undriven parts of the solutions given in equations 1.20, with the simplifying assumption that u_0 and v_0 are Δ' -independent. The Δ' integral in equation 1.24 is then easily done, and the resultant polarization density,

$$P(t) = \mathcal{N}ex_0 \operatorname{Re} [\{u_0 + iv_0\} e^{i(\omega+\Delta)t}] e^{-t/T} e^{-\delta\omega_I t}, \quad (1.26)$$

exhibits a number of notable features. First, $P(t)$ oscillates at the peak of the frequency distribution function $\omega + \Delta$. Second, the oscillation decays because of the homogeneous lifetime T . Neither of these features is really new. A new feature is provided by the factor $\exp[-\delta\omega_I t]$, which indicates that the total decay rate is increased due to the inhomogeneous broadening. Because no new loss mechanisms were coupled to the dipoles when we took account of inhomogeneous broadening, the appearance of a new damping factor in the solution requires an explanation.

The explanation is simple enough. The decay factor $\exp[-\delta\omega_I t]$ is due to the interference of all of the dipoles with frequencies distributed throughout the inhomogeneous line. Thus damping due to inhomogeneous broadening may be thought of as a kind of dephasing process that damps only the macroscopic polarization density $P(t)$. Each individual dipole continues to oscillate for a time T . Well before that time, however, $P(t)$ may be effectively zero because the dipoles may have drifted completely out of phase with one another.

Since the electric field radiated by a collection of dipoles depends on the density $P(t)$ and not directly on the individual dipoles themselves, a collection of dipole oscillators can cease radiating long before they cease oscillating if $\delta\omega_I \gg 1/T$. This phenomenon was observed very early in nuclear magnetic resonance studies by Hahn [4]. Its name, free induction decay, indicates that the free oscillation of the dipoles appears to decay, or rather that their radiated field terminates, in only a fraction of the natural lifetime T . We mention in Chapter 3 the recent observations by Brewer and Shoemaker [5] of quantum optical free induction decay.

Finally, the expression for $P(t)$ in equation 1.26 makes it clear that $\delta\omega_I$ does serve as an inverse lifetime. For future use we define an inhomogeneous lifetime, denoted T^* , in terms of the maximum of the detuning function:

$$T^* \equiv \pi g(\Delta')_{\max}. \quad (1.27)$$

This definition is exactly consistent with the relation $\delta\omega_I = 1/T^*$ only if the inhomogeneous lineshape is Lorentzian. Occasionally it is also convenient to speak qualitatively of a total linewidth, $\delta\omega_{\text{tot}} = \delta\omega_H + \delta\omega_I$. As equation 1.26 suggests,

$$\frac{1}{T} + \frac{1}{T^*} \equiv \frac{1}{\mathfrak{T}} \quad (1.28)$$

is suitable for a rough definition of the “total” relaxation rate \mathfrak{T}^{-1} .

1.6 ELECTROMAGNETIC WAVE PROPAGATION

An optical wavelength is so small that almost all practical optical experiments involve the propagation of radiation through an extended system of some kind. The framework of our discussion must be enlarged to allow $E(t)$ and $P(t)$ to depend on a spatial dimension as well as on time. Therefore we now turn to the question of traveling electromagnetic waves. We imagine a pulse of electromagnetic radiation traveling through a dielectric medium composed of oscillators like those already discussed. For simplicity we restrict our attention to plane wave propagation in the $+z$ direction, and study the traveling pulse of radiation far from the surface where it entered the dielectric. These restrictions present no very severe difficulties to experimental practice.

Questions immediately arise similar to the one posed in Section 1.2. We wish to know how the dipoles act to modify the field as it propagates, as well as how the field drives the dipoles. Thus self-consistency is again important. We now are concerned with a continuous dielectric, rather than with a single oscillator. In fact, we imagine the dielectric to be infinite in extent. One consequence is that the term $\partial W_{\text{em}}/\partial t$ in the basic energy-conservation relation 1.6 can not now be ignored.

However, rather than rely on a transport equation such as equation 1.6 to describe the radiation, we use the Maxwell wave equation itself as part of the self-consistent analysis. It is sufficient to write it in the one-dimensional form:

$$\left[\frac{\partial^2}{\partial z^2} - \frac{1}{c^2} \frac{\partial^2}{\partial t^2} \right] E(t, z) = \frac{4\pi}{c^2} \frac{\partial^2}{\partial t^2} P(t, z), \quad (1.29)$$

where the polarization density is given by relation 1.24 suitably generalized

to include dependence on z as well as t :

$$P(t, z) = \mathcal{N} ex_0 \int d\Delta' g(\Delta') \operatorname{Re} [\{u(t, z; \Delta') + iv(t, z; \Delta')\} e^{i(\omega t - Kz)}]. \quad (1.30)$$

The implication is that $E(t, z)$ has also been generalized from equation 1.12 to

$$E(t, z) = \mathcal{E}(t, z)[e^{i(\omega t - Kz)} + \text{c.c.}] . \quad (1.31)$$

A self-consistent analysis of these equations must determine the wave vector K , as well as the envelope functions $\mathcal{E}(t, z)$, $u(t, z; \Delta)$, and $v(t, z; \Delta)$.

The expressions 1.30 and 1.31 for P and E , together with Maxwell's wave equation 1.29, lead to so-called in-phase and in-quadrature equations for \mathcal{E} , u , and v if the coefficients of $\cos(\omega t - Kz)$ and $\sin(\omega t - Kz)$ are separately equated:

$$[K^2 - k^2]\mathcal{E} = 2\pi k^2 \mathcal{N} ex_0 \int ug(\Delta') d\Delta', \quad (1.32a)$$

$$2 \left[K \frac{\partial}{\partial z} + k \frac{\partial}{\partial ct} \right] \mathcal{E} = 2\pi k^2 \mathcal{N} ex_0 \int vg(\Delta') d\Delta', \quad (1.32b)$$

where $k \equiv \omega/c$ is the vacuum wave vector. We have liberally used extensions of the near-resonance, slowly varying envelope assumptions already introduced for u and v , namely:

$$\begin{aligned} \frac{\partial \mathcal{E}}{\partial z} &\ll K \mathcal{E}, & \frac{\partial \mathcal{E}}{\partial t} &\ll \omega \mathcal{E}, \\ \frac{\partial u}{\partial z} &\ll Ku, \dots \end{aligned} \quad (1.33)$$

and have kept only the largest terms on each side of the equations.

Together with the dipole equations 1.18, which are unchanged by our present concern with a propagation problem, equations 1.32 will form the core of the discussion in the remainder of this chapter. In the following sections we use all four equations to analyze classical pulse characteristics from the "pulse area" point of view, an approach that will be particularly fruitful for the quantum mechanical discussion in Chapter 4.

We devote the remainder of this section to a brief demonstration that our unconventional writing of the dipole equations and the field equations in terms of slowly varying amplitudes u , and v , and \mathcal{E} does *not* lead to

unconventional classical results. Thus we consider the question: what is the self-consistent solution of these four equations 1.18 and 1.32 after a long time has elapsed, in particular, after several relaxation times T ? The answer is the usual expression for the dielectric constant and the associated dispersion relations.

If $t \gg T$, then all dipole transients have died out, and u , v , and $\tilde{\epsilon}$ are all constant in time. The values of u and v are given by equation 1.20 in the limit $t \rightarrow \infty$. Then equation 1.32a immediately gives

$$K^2 - k^2 = k^2 \frac{\omega_p^2}{2\omega} \int \frac{\Delta' g(\Delta') d\Delta'}{\Delta'^2 + T^{-2}}, \quad (1.34a)$$

where $\omega_p = [4\pi\mathcal{N}e^2/m]^{1/2}$ is the so-called plasma frequency of the dielectric. Furthermore, equation 1.32b is equivalent to the simple relation

$$\frac{\partial \tilde{\epsilon}}{\partial z} = -\frac{1}{2} \alpha_c \tilde{\epsilon}, \quad (1.34b)$$

showing that $\tilde{\epsilon}$ decays exponentially with increasing penetration into the dielectric. This familiar result is frequently designated Beer's law.

The classical absorption coefficient α_c entering Beer's law is obviously affected by both homogeneous and inhomogeneous broadening:

$$\alpha_c = \frac{\omega_p^2}{2cT} \int \frac{g(\Delta')}{\Delta'^2 + 1/T^2} d\Delta', \quad (1.35a)$$

and has the two simple limiting forms on resonance: homogeneous broadening dominant ($T \ll T^*$), so that $g(\Delta') \approx \delta(\Delta' - \Delta)$

$$\alpha_c = \frac{\omega_p^2}{2c} \frac{1}{T} \frac{1}{\Delta^2 + 1/T^2} \quad (1.35b)$$

and inhomogeneous broadening dominant ($T^* \ll T$)

$$\alpha_c = \frac{\omega_p^2}{2c} \pi g(0) \approx \frac{\omega_p^2}{2c} T^*. \quad (1.35c)$$

Note that the relation 1.34, and the assumption in equation 1.33 that $\partial \tilde{\epsilon} / \partial z \ll K \tilde{\epsilon}$, together imply $K \gg \alpha_c$. Furthermore the symmetry of the integrands in equations 1.34a and 1.35a, based on the near-resonance approximate symmetry $g(\Delta') \approx g(-\Delta')$, imply that $\alpha_c \gg K - k$ and therefore $K \gg K - k$. It is on this basis that $K = k$ has been used in expressions 1.35

for α_c . Thus the principal effect of the dielectric on the field is to attenuate it gradually. A much smaller effect is to shift its wavelength from $2\pi/k$ to $2\pi/K$.

It is conventional to look at the results for α_c and $K^2 - k^2$ in a slightly different way. Note that equation 1.31 could be rewritten as

$$E(t \gg T, z) = \mathcal{E}_0 [e^{i(\omega t - \tilde{K}z)} + \text{c.c.}] \quad (1.36)$$

in terms of a complex wave vector $\tilde{K} = K - i\alpha_c$, and an arbitrary constant amplitude \mathcal{E}_0 . If we recall that the complex dielectric constant is defined by $\epsilon(\omega) \equiv (\tilde{K}c/\omega)^2$, then

$$\left(\frac{\omega}{c}\right)^2 \epsilon(\omega) = \tilde{K}^2 \approx K^2 - 2iK\alpha_c,$$

where we have neglected a $-\alpha_c^2$ term that makes an insignificant contribution to the real part. It follows directly that the complex dielectric constant may be written as

$$\epsilon(\omega) = 1 + \frac{\omega_p^2}{2\omega} \int \frac{g(\Delta') d\Delta'}{\Delta' + i/T}. \quad (1.37a)$$

In the limit usually considered—that of a purely homogeneously broadened line centered on an atomic resonance ω_a , in which case $g(\Delta') = \delta(\Delta' - \omega + \omega_a)$ —this is the same as the usual dispersion relation

$$\epsilon(\omega) = 1 + \frac{\omega_p^2}{\omega_a^2 - \omega^2 + 2i\omega/T}, \quad (1.37b)$$

which is the standard result (recall equation 1.21).

1.7 THE CLASSICAL “AREA THEOREM”

With an eye on quantum problems, to be discussed in later chapters, we return to the unconventional approach initiated in Section 1.3 and introduce the idea of pulse envelope “area.” We define the classical dimensionless “area” $A(t, z)$ to be:

$$A(t, z) \equiv \kappa \int_{-\infty}^t dt' \mathcal{E}(t', z). \quad (1.38)$$

Here A is essentially the time-integrated electric field envelope function and $\kappa \equiv e/m\omega x_0$, as before.

A picture to guide our classical pulse analysis is sketched in Fig. 1.2. It shows the pulse amplitude as a function of time at the point z in the dielectric. As the term “pulse” indicates, the electric disturbance is finite in extent. The time \bar{t} , close to which the pulse absorption will be analyzed, occurs after the pulse has passed the point of observation z . We label by t_0 the time when the pulse field \mathcal{E} dropped to zero at point z .

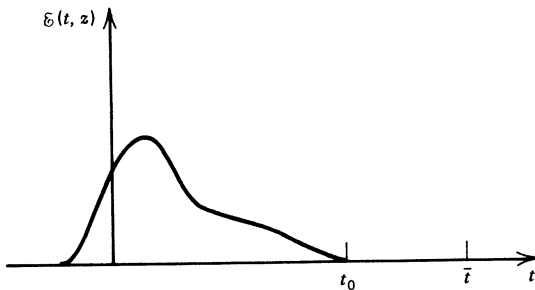


Fig. 1.2 The electric field envelope at position z as a function of time. Time t_0 marks the end of the pulse: at t_0 and for all later times the envelope is zero.

If equation 1.32b is integrated from some time before the pulse arrives, when $\mathcal{E} = 0$, up to \bar{t} when $\mathcal{E} = 0$ again, an equation for $A(\bar{t}, z)$ results:

$$2K \frac{\partial}{\partial z} A(\bar{t}, z) = 2\pi k^2 \frac{\mathcal{N}e^2}{m\omega} \int_{-\infty}^{\bar{t}} \int v(t, z; \Delta') g(\Delta') d\Delta' dt. \quad (1.39)$$

It is easy to show that equations 1.18 imply

$$v(t, z; \Delta) = \frac{-1}{\Delta^2 + T^{-2}} \left[\Delta \dot{u} + \frac{1}{T} \dot{v} + \frac{1}{T} \dot{A} \right], \quad (1.40)$$

so that the time integral in equation 1.39 may be carried out trivially. The result is:

$$2K \frac{\partial A}{\partial z} = -2\pi k^2 \frac{\mathcal{N}e^2}{m\omega} \int d\Delta' \frac{g(\Delta')}{\Delta'^2 + T^{-2}} \left[\Delta' u + \frac{1}{T} v + \frac{1}{T} A \right], \quad (1.41)$$

where all of the variables are now evaluated at time \bar{t} . But at the earlier time t_0 the pulse had already passed the point z , so that from t_0 to \bar{t} the dipoles have been undergoing free oscillation. Thus if we put \mathcal{E} equal to zero and replace t by $\bar{t} - t_0$, equations 1.20 supply the solutions for u and v in equation 1.41. By u_0 and v_0 we must now understand $u(t_0, z; \Delta')$ and $v(t_0, z; \Delta')$. That is, we have:

$$\begin{aligned}\Delta' u + \frac{1}{T} v &= u_0 \left[\Delta' \cos \Delta(\bar{t} - t_0) + \frac{1}{T} \sin \Delta'(\bar{t} - t_0) \right] e^{-(\bar{t} - t_0)/T} \\ &+ v_0 \left[\frac{1}{T} \cos \Delta(\bar{t} - t_0) - \Delta' \sin \Delta'(\bar{t} - t_0) \right] e^{-(\bar{t} - t_0)/T}. \quad (1.42)\end{aligned}$$

In using equation 1.42 to help evaluate equation 1.41 there are two distinct cases of interest, which, for convenience, we label "classical" and "modern." The cases are distinguished by the relationship of the three times in the problem. Two of these times, T and the interval $\bar{t} - t_0$, appear explicitly. The third is T^* , the inhomogeneous lifetime, implied by the finite width of $g(\Delta')$ and defined in relation 1.27.

The two "cases," in which equation 1.42 may be used to evaluate equation 1.41, are these:

$$\text{"classical" case: } \bar{t} - t_0 \gg T^* \gg T; \quad (1.43)$$

$$\text{"modern" case: } T \gg \bar{t} - t_0 \gg T^*. \quad (1.44)$$

The "classical" case, valid for times so long that every dipole's transient response has decayed to zero, has been discussed in the preceding section, albeit from a point of view independent of the pulse "area" concept. It is a simple exercise to show that the pulse "area" approach gives the same results. In this section we devote our attention to the "modern" case. We consider free oscillation times $\bar{t} - t_0$ so short that none of the dipole transients will have damped out (i.e., $\bar{t} - t_0 \ll T$). However, because of the dipole dephasing, which arises from the inhomogeneous broadening, the macroscopic polarization will be completely damped out if $\bar{t} - t_0 \gg T^*$.

Expression 1.41, which describes the change with distance of pulse area, may be simplified by recognizing that the final two terms cancel each other exactly if $t - t_0 \ll T$, as assumed. One may establish this result by integrating the equation of motion 1.18b for $v(t, z; 0)$ for short times and by

recognizing the identity

$$\frac{1}{T} \frac{v(\bar{t}, z; \Delta)}{\Delta'^2 + (1/T)^2} = \pi \delta(\Delta') v(\bar{t}, z; 0), \quad (1.45)$$

which is valid if $T^{-1}[\Delta'^2 + (1/T)^2]^{-1}$ is the most sharply peaked function in the Δ' integration. This is certainly true, in view of the inequalities 1.44.

The evaluation of the remaining term on the right-hand side of equation 1.41 presents some problems. Written in full, with the use of $\Delta' u$ from equation 1.42, it becomes:

$$\int d\Delta' \frac{\Delta'^2 g(\Delta')}{\Delta'^2 + (1/T)^2} \left[u_0 \frac{\cos \Delta'(\bar{t} - t_0)}{\Delta'} - v_0 \frac{\sin \Delta'(\bar{t} - t_0)}{\Delta'} \right] e^{-(\bar{t} - t_0)/T}. \quad (1.46)$$

In the limit $\bar{t} - t_0 \gg T^*$ the trigonometric functions oscillate sufficiently rapidly to give zero integral everywhere except possibly at $\Delta' = 0$. The second term, in fact, has the well-known formal representation

$$\frac{\sin \Delta'(\bar{t} - t_0)}{\Delta'} \rightarrow \pi \delta(\Delta').$$

Thus it would seem that the second term should give no contribution at all, since $\Delta'^2 \delta(\Delta') \equiv 0$. However, since $T \gg \bar{t} - t_0$, the zero at $\Delta' = 0$ of the function $\Delta'^2[\Delta'^2 + (1/T)^2]^{-1}$ is too narrow to have an effect. So we may write

$$- \int v_0 g(\Delta') \frac{\Delta'^2}{\Delta'^2 + (1/T)^2} \frac{\sin \Delta'(\bar{t} - t_0)}{\Delta'} e^{-(\bar{t} - t_0)/T} d\Delta' = -\pi g(0) v(t_0, z; 0), \quad (1.47)$$

where the factor $\exp[-(\bar{t} - t_0)/T]$ is close to unity and has been ignored on the right-hand side. This formally surprising result becomes obvious after a careful appraisal of all of the time inequalities. An illustration is given in Fig. 1.3. The first term in equation 1.46 is less ambiguous and does lead to a zero result. More precisely, the first term is related to the principal part integral of $g(\Delta')/\Delta'$ and so is roughly T^*/T times smaller than the second term, and thus completely negligible.

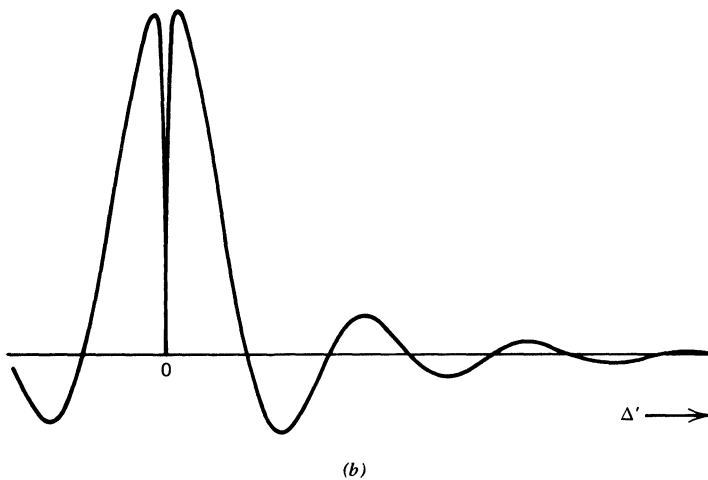
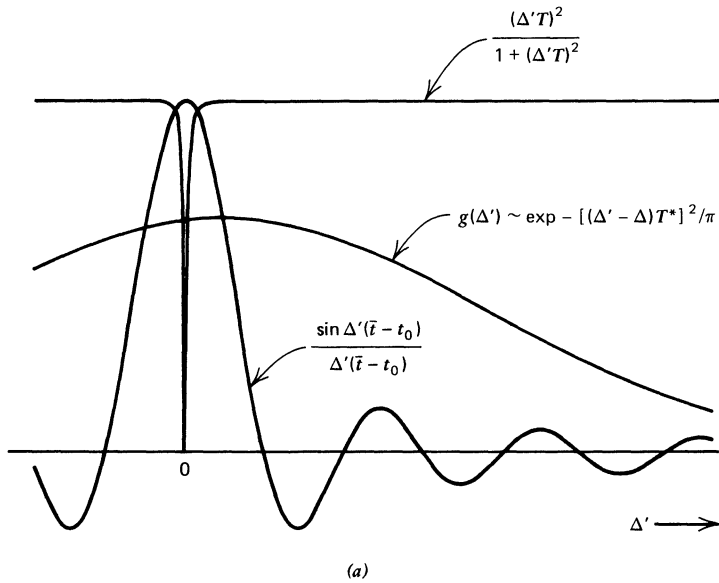


Fig. 1.3 A graphical illustration of the integrand in equation 1.47. The three important functions of Δ' are shown separately in (a), and their product is shown in (b), under the assumption that $g(\Delta')$ is Gaussian and centered somewhat away from $\Delta' = 0$. As the widths of the curves indicate, the “modern” limit is assumed: $T > (\bar{t} - t_0) > T^*$. The product curve (b) shows that, because of the narrowness of the hole at $\Delta' = 0$, it has practically no effect on the area under the curve near $\Delta' = 0$. The integral of the product is therefore proportional to $g(0)$, even though the integrand actually vanishes at $\Delta' = 0$.

Finally, using once more equation 1.18b for times short compared with T , we find the relation

$$v(t_0, z; 0) = -A(t_0, z), \quad (1.48)$$

which connects the pulse area with the on-resonance absorptive part of the dipole amplitude. We may write

$$2K \frac{\partial}{\partial z} A(\bar{t}, z) = -k^2 \frac{\omega_p^2}{2\omega} \pi g(0) A(\bar{t}, z) \quad (1.49)$$

in place of equation 1.41 if we recognize that $A(\bar{t}, z)$ is identically equal to $A(t_0, z)$ since $A(t, z)$ is zero for times after t_0 . Equation 1.49 expresses the classical “area theorem.”

Two important consequences follow from the “area theorem.” First, we have found here the same Beer’s law exponential decay with distance as was implied by relations 1.34b and 1.36:

$$A(\bar{t}, z) = A(\bar{t}, z_0) e^{-\frac{1}{2}\alpha_c(z - z_0)} \quad (1.50)$$

if the same limit $T \gg T^*$ is applied there. But here the result is seen to be independent of the time behavior of the pulse, assuming merely that the pulse is finite in extent; whereas the earlier analysis is valid only after ϵ is constant in time.

Second, we see that the field does not need to interact with a dissipative system to lose energy during propagation. That is, equation 1.49 shows that even if every dipole’s relaxation rate were zero, so that $T = \infty$, the dielectric would still attenuate the field passing through. The physical reason has been mentioned before: the dipoles become excited by the arrival of the pulse as it transfers energy to them and they oscillate in unison at the field frequency. However, after the pulse has gone by, the dipoles revert to their natural frequencies of oscillation. Within a time T^* they are completely out of phase with each other, and generate only a vanishingly small macroscopic polarization density. They may then trade stored energy with each other, but no energy can be radiated away from the dipole system and back into the field.

As a consequence of the wide gap between T and T^* , of the order of 100 nsec in dilute alkali metal vapors for example, quantum optics has seen a variety of ingenious experiments undertaken in the past decade that have

been designed to exploit the energy storage described above. Photon echoes provided the first example of such an experiment. Other effects that have been observed include optical nutation, free induction decay, self-induced transparency, and optical adiabatic inversion. All of these are discussed in the chapters that follow.

1.8 ANOMALOUS CLASSICAL ABSORPTION

To do full justice to recent quantum optical discoveries, it is necessary to point out their largely unexpected implications in the classical domain. We showed in the preceding section the extent to which exponential decay of electric field area is inevitable. The implication that the propagating field energy must necessarily also decay exponentially is false, however. This point is now widely appreciated due to the work of Crisp and others [6, 7]. The explanation is simple and depends on the observation that phase changes of π in the electric field cause the envelope \mathcal{E} to change sign. Thus the integral of \mathcal{E} , that is, the area, may well be zero or nearly so, while the pulse energy, proportional to \mathcal{E}^2 , may be substantial.

A treatment of such anomalous absorption is very easy to give for classical dielectrics. The notation used earlier can be generalized slightly to allow for envelope phase changes. In this section we assume the envelope function \mathcal{E} to be complex:

$$\mathcal{E}(t, z) = |\mathcal{E}(t, z)| e^{i\phi(t, z)}, \quad (1.51)$$

with both modulus and phase varying slowly in space and time. The electric field will be written

$$E(t, z) = 2 \operatorname{Re} [\mathcal{E}(t, z) e^{i(\omega t - kz)}], \quad (1.52)$$

a simple generalization of definition 1.31. Note that the vacuum wave vector $k = \omega/c$ has been used in the exponent, not K . In the present case the true instantaneous wave vector is $k - \partial\phi/\partial z$.

The equations governing the dipoles, as well as the Maxwell wave equation, can be put in complex form very conveniently by use of the complex dipole amplitude

$$r = u + iv \quad (1.53)$$

in place of u and v separately. Then the dipole moment's equations of motion 1.18 may be written:

$$\frac{\partial}{\partial t} r(t, z; \Delta) = \left(i\Delta - \frac{1}{T} \right) r(t, z; \Delta) - i\kappa \tilde{\mathcal{E}}(t, z) \quad (1.54)$$

Maxwell's wave equation 1.31 has the following complex form:

$$-2ik \left[\frac{\partial}{\partial z} + \frac{\partial}{\partial ct} \right] \tilde{\mathcal{E}}(t, z) = -2\pi k^2 \mathcal{N} ex_0 \int d\Delta' g(\Delta') r(t, z; \Delta'). \quad (1.55)$$

Only the largest terms have been retained and the inequalities 1.33 have been used once more to discard higher derivatives of slowly varying quantities.

The simplest method for determining the self-consistent solution of the coupled equations for $r(t, z; \Delta)$ and $\tilde{\mathcal{E}}(t, z)$ is to assume that the time dependence of r and $\tilde{\mathcal{E}}$ is the same:

$$r(t, z; \Delta) = r(\nu, z; \Delta) e^{i\nu t} \quad (1.56a)$$

$$\tilde{\mathcal{E}}(t, z) = e(\nu, z) e^{i\nu t} \quad (1.56b)$$

and to substitute these expressions into equations 1.54 and 1.55. After eliminating r , the resulting equation for $e(\nu, z)$ is linear and of first order

$$\left[\frac{\partial}{\partial z} - i \frac{\nu}{c} + \mathcal{Q}(\nu) \right] e(\nu, z) = 0, \quad (1.57)$$

The explicit expression for $\mathcal{Q}(\nu)$ is:

$$\mathcal{Q}(\nu) = +i \frac{\omega_p^2}{4} \int d\Delta' \frac{g(\Delta')}{\Delta' - \nu + i/T}, \quad (1.58)$$

which may be rewritten in a simpler form:

$$\mathcal{Q}(\nu) = \frac{\omega_p^2}{4} \frac{1}{\frac{1}{\mathfrak{T}} - i(\Delta - \nu)}, \quad (1.59)$$

if $g(\Delta')$ is assumed for convenience to be Lorentzian in shape, centered at the detuning Δ , and with halfwidth $1/T^*$. As in equation 1.28, the total polarization decay rate or approximate total linewidth is denoted: $1/\mathfrak{T} = 1/T + 1/T^*$.

The solution for the field envelope is a simple exponential:

$$e(\nu, z) = e(\nu, 0)e^{-i[\nu/c - i\mathcal{Q}(\nu)]z}. \quad (1.60)$$

What is more important, however, is that the linearity of equations 1.54 and 1.55 allows a completely general solution for $\mathcal{E}(t, z)$ to be synthesized by adding solutions of the exponential type for every frequency ν . In other words, if we recognize that $e(\nu, 0)$ is actually just the ν th Fourier component of the field at $z=0$:

$$e(\nu, 0) = \frac{1}{2\pi} \int dt' \mathcal{E}(t', 0) e^{-i\nu t'} \quad (1.61)$$

it follows that

$$\mathcal{E}(t, z) = \frac{1}{2\pi} \int d\nu \int dt' \mathcal{E}(t', 0) e^{i\nu(t-t')} e^{-i(\nu-\mathcal{Q})z/c} \quad (1.62)$$

an expression essentially the same as one first given by Crisp [6] in a study of pulses with very small area traveling in quantum absorbers.

Whether the pulse absorption implied by the Fourier transform 1.62 is anomalous depends on the length of the pulse τ relative to \mathfrak{T} . Since $1/\tau$ measures the pulse spectral width, frequencies of the order of $\nu \sim 1/\tau$ are the largest ones contributing to the transform. Hence in the “classical” case where $\tau \gg \mathfrak{T}$, it follows that $\nu \mathfrak{T} \ll 1$ for all important frequencies. Thus it is a good approximation to take $\mathcal{Q}(\nu) \approx \mathcal{Q}_0$, independent of ν , where

$$\mathcal{Q}_0 \equiv i \frac{\omega_p^2}{4c} \frac{1}{\Delta + i/\mathfrak{T}}, \quad (1.63)$$

The resulting envelope

$$\mathcal{E}(t, z) = \mathcal{E}\left(t - \frac{z}{c}, 0\right) e^{-\mathcal{Q}_0 z} \quad (1.64)$$

propagates with its initial form and vacuum velocity unchanged, except for the multiplicative Beer’s law damping factor $\exp[-\mathcal{Q}_0 z]$. It is not difficult in the completely monochromatic limit of an infinitely long pulse, when $e(\nu, 0) = \mathcal{E}_0 \delta(\nu - \omega)$, to show that the relation 1.64 is entirely equivalent to the earlier finding (equation 1.36). The complex dielectric constant implied by the envelope solution 1.64 is

$$\epsilon(\omega) = 1 + \frac{\omega_p^2}{2\omega} \frac{1}{\Delta + i/\mathfrak{T}}, \quad (1.65)$$

identical with that derived earlier in equation 1.37a if the same Lorentzian detuning function $g(\Delta')$ is assumed. Obviously, in the “classical” long pulse limit there is nothing anomalous about the behavior of the pulse.

However, pronounced anomalies arise for pulses that satisfy the “super-modern” limit $\tau \lesssim \mathcal{T}$, that is, for pulses shorter than both of the relaxation times T and T^* . In Figs. 1.4 and 1.5 we show the results of Crisp’s numerical integration of the transform 1.62 in the case of Gaussian input pulses.

$$\tilde{\mathcal{E}}(t, 0) = \tilde{\mathcal{E}}_0 e^{-4t^2/\tau^2}$$

with various values of pulse length τ . The negative portions of $\tilde{\mathcal{E}}(t, z)$

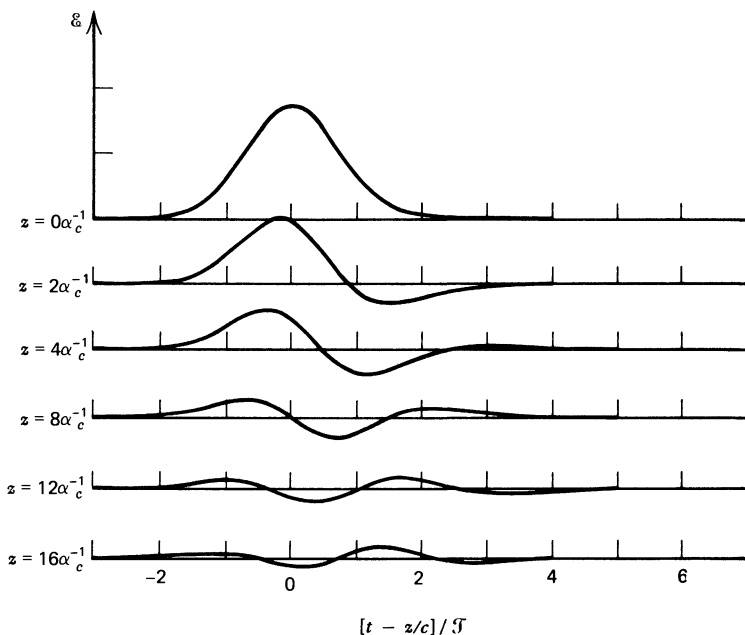


Fig. 1.4 Propagation of a Gaussian pulse of length $\tau = 2\mathcal{T}$. The depth of penetration z is measured in Beer’s law absorption lengths α_c^{-1} . [From M. D. Crisp, *Phys. Rev. A* **1**, 1604 (1970).]

develop very quickly, allowing the pulse area to drop to zero. However, as Fig. 1.6 shows, the corresponding absorption of energy can occur much more slowly.

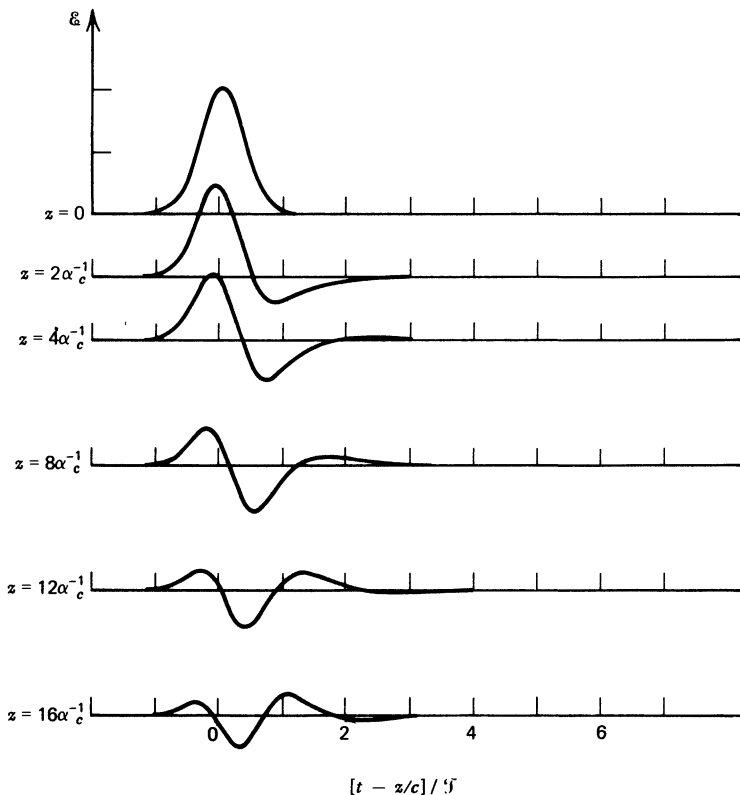


Fig. 1.5 Propagation of a Gaussian pulse of length $\tau = \mathcal{T}$. The depth of penetration z is measured in Beer's law absorption lengths α_c^{-1} . [From M. D. Crisp, *Phys. Rev. A* **1**, 1604 (1970).]

The explanation for these “anomalies” can be given in several guises, the most direct being the following. Only pulses shorter than \mathcal{T} exhibit energy absorption that deviates from Beer's law. These pulses necessarily have spectral widths that exceed the total width $1/\mathcal{T}$ of the dielectric absorption line. Thus major fractions of the pulse energy are concentrated in regions of the spectrum where there is no absorption. It is the wings of the pulse spectrum that have the ability to propagate large distances. There is no real contradiction of Beer's law. It is merely inappropriate to expect Beer's absorption coefficient

$$\alpha_c = \frac{\omega_p^2 \mathcal{T}}{2c}$$

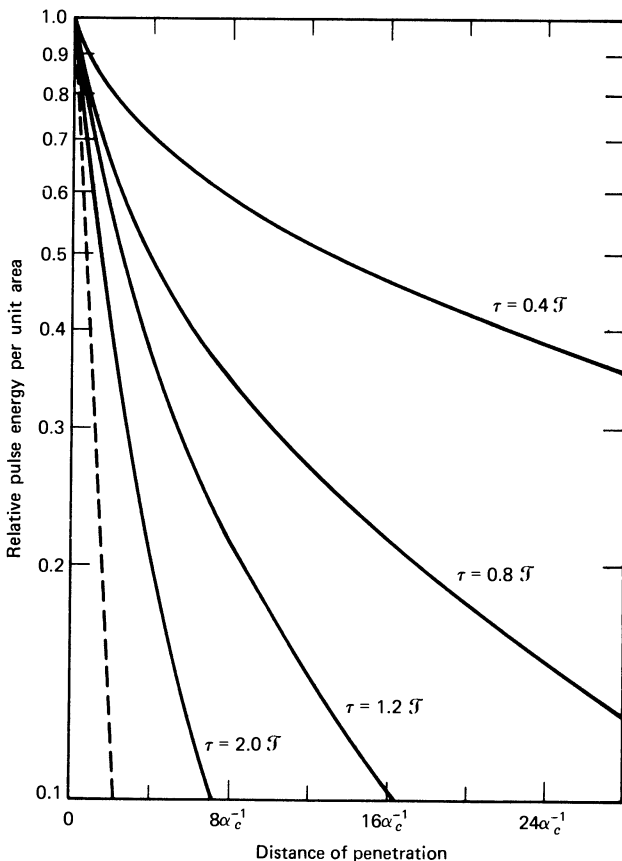


Fig. 1.6 Variation of pulse energy per square centimeter with penetration distance into the absorber for Gaussian pulses of various pulse lengths τ . [From M. D. Crisp, *Phys. Rev. A* **1**, 1604 (1970).]

to apply if the absorption linewidth $1/\mathcal{T}$ is narrower than the pulse spectral width. The situation is quite different in the quantum regime. There one finds strong deviations from Beer's law even for a long pulse whose spectrum lies entirely within the absorption line of the dielectric. We discuss Beer's law and pulse propagation in Chapter 4 from the quantum viewpoint.

References

1. H. A. Lorentz, *The Theory of Electrons*, Dover, New York, 1952, Chap. 4.
2. M. Born and E. Wolf, *Principles of Optics*, Pergamon, Elmsford, N. Y., 1970, 4th edition.

3. I. I. Rabi, *Phys. Rev.* **51**, 652 (1937).
4. E. L. Hahn, *Phys. Rev.* **77**, 297 (1950).
5. R. G. Brewer and R. L. Shoemaker, *Phys. Rev. A* **6**, 2001 (1972).
6. M. D. Crisp, *Phys. Rev. A* **1**, 1604 (1970).
7. F. A. Hopf, G. L. Lamb, Jr., C. K. Rhodes, and M. O. Scully, *Phys. Rev. A* **3**, 758 (1971).

CHAPTER 2

The Optical Bloch Equation

2.1	Introduction	28
2.2	Real Atoms and the Two-Level Atom	29
2.3	Two-Level Atoms and SemiClassical Radiation Theory	34
2.4	The Rotating Wave Approximation	41
2.5	Analogies and Differences Between Classical and Semiclassical Dipole Interactions	46
2.6	The Bloch-Siegert Shift	47
	References	51

2.1 INTRODUCTION

It is impossible to discuss the interaction of collections of atoms with light exactly. It is impossible to treat even one atom's interaction with light exactly. In this chapter we introduce the major approximations that are used repeatedly in Chapters 3, 4, 5, and 6. The principal one is a two-part assumption: that the optical radiation field is very nearly perfectly monochromatic and that it almost exactly coincides in frequency with one of the transition frequencies in the atom under consideration. The two-level atom is the natural product of these assumptions.

A two-level atom is conceptually the same kind of object as a spin-one-half particle in a magnetic field. The basic dynamical equations, which follow from Schrödinger's equation and govern the evolution of two-level atom variables, are practically the same as those appropriate to spins. It also follows that the spin vector formalism of Bloch, developed for magnetic resonance, is immediately applicable to optical resonance problems. To facilitate this application, we follow custom and define a fictitious electric spin vector, or pseudospin vector, whose components are related to the atom's dipole moment and inversion. Schrödinger's equation then determines the vector's time evolution. The equations obeyed by the components of this vector are frequently called the optical Bloch equations.

Further approximations, beyond the two-level atom assumption, have much in common with approximations used in magnetic resonance theory. The most widely used of these is the rotating wave approximation, or

RWA. The attractiveness of the RWA is that its adoption allows the neglect of very complicated effects in the pseudospin dynamics, effects that are associated with oscillations at twice the optical frequency. These very rapid oscillations can lead to secular effects that are, at least in principle, observable. We discuss briefly the most important of these, the Bloch-Siegert frequency shift, and find it to be negligible in optical resonance.

It is clear that a two-level atom has one very important feature, a single resonant frequency, in common with a classical harmonic oscillator. It is also clear on experimental grounds that atoms do behave, in many cases, very much like harmonic oscillators. The usefulness of the classical theory of dispersion rests on this fact. In the fourth and fifth sections of this chapter we show that the only qualitative difference between the radiative interactions of a two-level atom and a classical harmonic oscillator is that the classical dipole moment is coupled directly to the electric field strength, whereas the atomic dipole moment is coupled to the field parametrically. The coupling parameter in the latter case is a variable that may be identified with the degree to which the atom is excited out of its lower level. Under ordinary circumstances, when the atom is nearly in its ground state, the quantum mechanical atom obeys exactly the classical equations of motion.

2.2 REAL ATOMS AND THE TWO-LEVEL ATOM

The energy levels of a real atom depend on the coupling of its various electrons. The number of electrons in the atom tell us which spectroscopic "terms" will occur, and the associated selection rules indicate which pairs of levels are radiatively connected. Usually it is very difficult to predict the absolute energy of these levels. Nonetheless in many real atoms the relative energy spacing of levels within a particular term follow the pattern predicted by theory. For example within a 4F term the relative spacing of the levels labeled $J = \frac{9}{2}, \frac{7}{2}, \frac{5}{2}$, and $\frac{3}{2}$ are in the ratio $\frac{9}{2} : \frac{7}{2} : \frac{5}{2}$ if the term is a perfect example of L - S coupling.

This is clearly not the place to give an extensive account of atomic structure [1], but the energy levels that occur and their relative spacing are important considerations in optical coherent interactions. For many purposes, the ideal atom would be one with only two energy levels. Although no such atom really exists, many coherent resonant interactions do involve

only two of an atom's levels. Thus it is frequently possible to assume, as a good first approximation, that the two-level idealization is valid. It seems desirable therefore to review rapidly the main structural features of simple atoms to clarify the basis for, and possible restrictions on, a two-level assumption. For simplicity we consider an atom obeying Russell-Saunders coupling.

Each electron has associated with it the quantum numbers n , l , m_l , and m_s . Certain groups of electrons, obeying the Pauli principle, come together to form closed shells that are associated with the term 1S_0 , where $L=0$, $S=0$, and $J=0$. Those electrons, called valence electrons, that fall outside the closed shells couple together; as a result a variety of terms arise, depending on the values of L and S that are obtained by summing vectorially the individual l_i and s_i of each of the valence electrons.

As an example, consider sodium, which has the merit of possessing a feature, namely the D lines, that is well known to all physicists and not just to spectroscopists. Here the closed shells are $1s^2 2s^2 2p^6$ and there is one valence electron that in its most tightly bound form is a $3s$ electron. The acquisition of a little energy will however promote the $3s$ electron to $4s, 5s, \dots$, or $3p, 4p, \dots$, or $3d, 4d, \dots$. This single electron has associated with it a doublet structure corresponding to its spin being either "up" or "down." So the sodium ground state consists of a $^2S_{1/2}$ term while the $3p$ electron produces $3p^2P_{3/2}$ and $3p^2P_{1/2}$ levels. The allowed electric dipole transitions between $3p^2P_{3/2} - 3s^2S_{1/2}$ and $3p^2P_{1/2} - 3s^2S_{1/2}$ are the sodium D lines at 5890 \AA and 5896 \AA respectively.

To a zero-order approximation, the absorption spectrum of the D lines would look like two infinitely sharp lines 6 \AA apart. But, as is well known, each line is not perfectly sharp. Each emission or absorption line of the atom has a finite width because of its finite natural radiative lifetime. Effects such as collisions may further shorten the excited state lifetime and so further broaden the line. In this way a lifetime T'_2 may be attributed to each transition and with it an associated homogeneous linewidth $\delta\omega_H \sim 1/T'_2$. Clearly T'_2 is the analogue of T used in the preceding chapter. The need for the prime and the subscript 2 in the case of real atoms will become apparent.

Collisions are usually more important than purely radiative effects and in a dilute gas of $10^{10} - 10^{13} \text{ atoms/cm}^3$ the collision time is of the order of 10^{-7} sec . The Lorentzian-shaped spectral line has a homogeneous linewidth $\delta\omega_H$ of the order of 10^{+8} Hz . The corresponding width in wave-

length is

$$\delta\lambda_H = \lambda \frac{\delta\omega_H}{\omega} \sim 10^{-3} \text{ Å}, \quad (2.1)$$

which is obviously very small compared with $\lambda_{D_1} - \lambda_{D_2} \sim 6 \text{ Å}$.

Furthermore, because of each atom's given velocity, which remains unchanged until its next collision, each atom's Lorentzian line has a definite center frequency ω_0 , which differs more or less from the mean transition frequency $\bar{\omega}_0$ of all the atoms as its velocity component v_z along the interacting field wave vector $\mathbf{k} = \mathbf{z}(\omega/c)$ differs more or less from zero:

$$\omega_0 = \bar{\omega}_0 - \bar{\omega}_0 \left(\frac{v_z}{c} \right). \quad (2.2)$$

If a Maxwell-Boltzmann distribution of velocities is assumed, the full width at halfmaximum of the distribution of center frequencies is given by

$$\delta\omega_0 = 2\omega(2\ln 2)^{1/2} \left(\frac{kT}{Mc^2} \right)^{1/2}, \quad (2.3)$$

where kT is Boltzmann's constant times the absolute temperature and M is the mass of the gas atom. The spectral distribution of all of the Lorentzian lines, each centered on its own ω_0 , is Gaussian, because the velocity distribution is Gaussian. This is shown schematically in Fig. 2.1. The

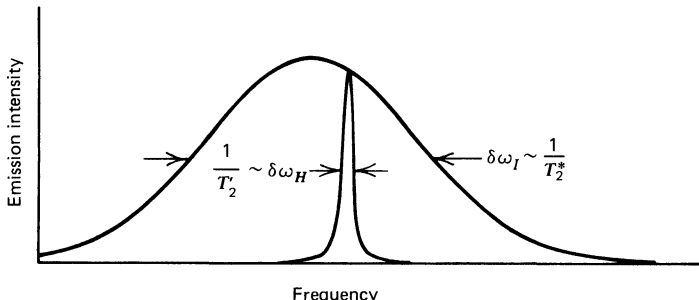


Fig. 2.1 A Lorentzian shows the linewidth associated with homogeneous radiative and collisional damping of gas atoms. Because of the Maxwell-Boltzmann distribution of atomic velocities, and the Doppler effect, there is a Gaussian distribution of such representative Lorentzians over a frequency range much wider than their individual widths. Thus, at ordinary temperatures and pressures, gaseous absorbers are almost purely inhomogeneously broadened, so $\delta\omega_I$ is shown much larger than $\delta\omega_H$.

spectral broadening due to the Doppler effect is inhomogeneous; hence the Doppler width will be denoted by $\delta\omega_I$. Typically $\delta\omega_I$ is much larger than the collision linewidth in gases:

$$\delta\omega_I \sim 10 \text{ GHz} \gg \delta\omega_H \sim 100 \text{ MHz}. \quad (2.4)$$

It is easy to verify, however, that the corresponding inhomogeneous width in wavelength is still very small compared to 6 Å. Consequently, the sodium *D* lines may be independently in or out of resonance with an applied field as long as the field itself does not have a spectral width sufficiently wide to overlap both lines. Considering coherent quasi-monochromatic fields, only sub-picosecond pulses have such a large spectral width.

Of course our discussion is accurate only as far as it goes. In fact there is more structure to be associated with each of the *D*-line levels because sodium has nuclear spin $I = \frac{1}{2}$. The nuclear spin combines with each value of J to produce hyperfine structure. The hyperfine levels are labeled F , where F is the vectorial sum of J and I , and each hyperfine level F is itself $(2F+1)$ -degenerate. This degeneracy may be lifted by an applied magnetic field so that the resultant energy level diagram appropriate to the $3p^2P$ and $3s^2S$ terms is really that shown in Fig. 2.2.

Even if no magnetic field is present and the hyperfine levels are degenerate, care must be taken in the choice of excitation pulse to ensure that the sodium atom may in any sense be thought of as a two-level atom. For example, if one's intention were to carry out an optical experiment on the transition between the $3p^2P_{3/2}(F=2)$ level and the ground state level $3s^2S_{1/2}(F=1)$, one would have to ensure that the spectral width of the optical pulse did not embrace either $3s^2S_{1/2}(F=2)$ or $3p^2P_{3/2}(F=1)$. In other words, the pulse would have to be narrower than 35.5 MHz, which implies a pulse duration longer than about 3×10^{-8} sec. On the other hand, the pulse duration would have to be shorter than the collision time between the atoms, about 10^{-7} sec, if the process is not to be incoherently disturbed.

If such an appropriate pulse, centered on the resonance corresponding to the transition $3p^2P_{3/2}(F=2) - 3s^2S_{1/2}(F=1)$ were available [2], for many purposes the atom would be deemed to be a two-level atom. Even then, as the case of self-induced transparency discussed in Sections 5.2 and 5.3 shows, it turns out that the magnetic degeneracy may not be dismissed so lightly. It might also be well to note that the detailed behavior of any coherent interactions may still depend on dissipative processes such as the

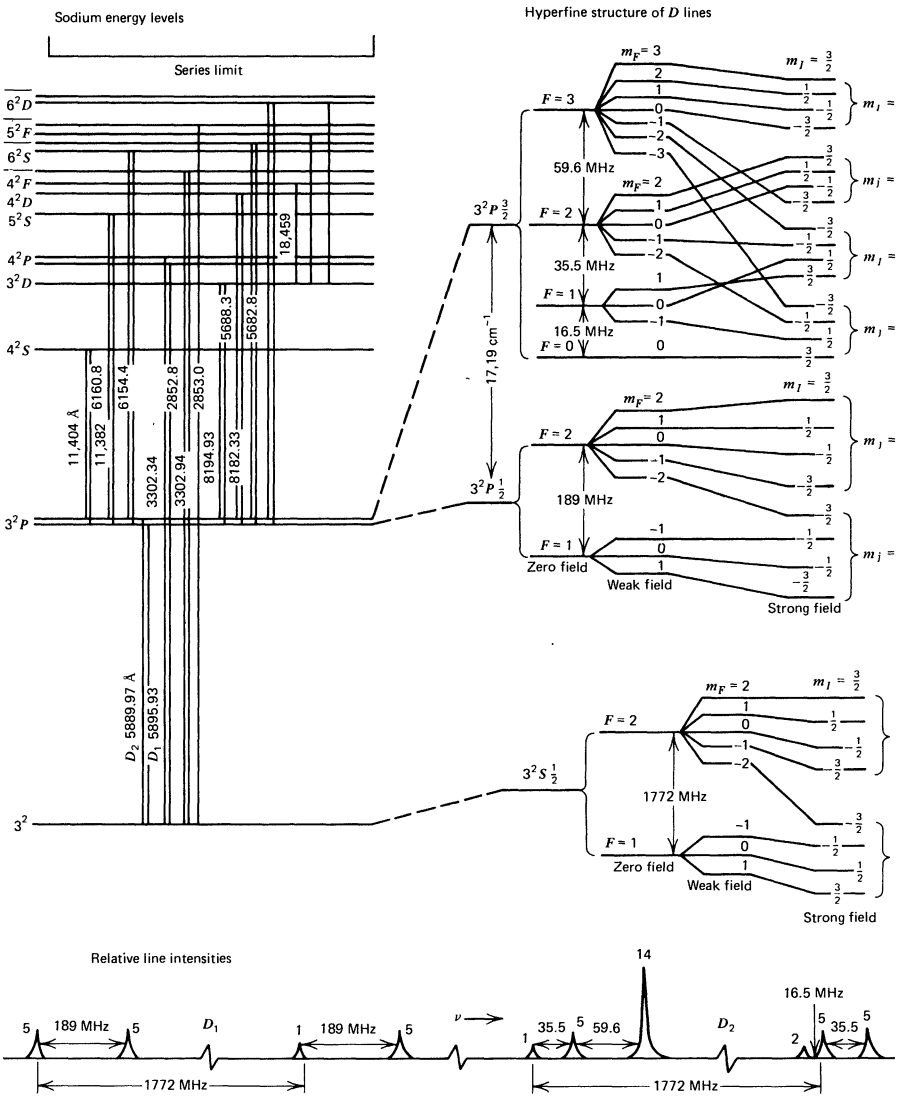


Fig. 2.2 A somewhat simplified diagram of the energy level scheme of sodium, with an expanded representation, not to scale, of the hyperfine structure involved in the D lines. [From F. Schuda and C. R. Stroud, Jr., with permission.]

allowed spontaneous decay from $3p^2P_{3/2}(F=2)$ to $3s^2S_{1/2}(F=2)$, which will contribute a mechanism for removing atoms from the chosen upper level. By no means all elements have hyperfine structure, but the general conditions discussed here must provide the background in deciding if an atom may be thought of as possessing only two levels for the purposes of a particular experiment.

2.3 TWO-LEVEL ATOMS AND SEMICLASSICAL RADIATION THEORY

The semiclassical theory of the interaction of radiation and matter predates quantum electrodynamics. In the areas of resonance and quantum optics it has always been the theory used by most workers. In this section we give a definition of the semiclassical theory in the context of the radiative interactions of a single two-level atom.

We are concerned with electric dipole transitions and can write

$$\hat{\mathcal{H}} = \hat{H}_A - \hat{\mathbf{d}} \cdot \hat{\mathbf{E}}(\mathbf{r}_0) \quad (2.5)$$

for the Hamiltonian of the interacting atom. Obviously $\hat{\mathbf{d}}$ is the atom's dipole moment operator and $\hat{\mathbf{E}}(\mathbf{r}_0)$ is the electric field operator evaluated at \mathbf{r}_0 , the position of the dipole. The unperturbed Hamiltonian \hat{H}_A need not be specified further. It has a discrete spectrum, a part of which is shown in Fig. 2.3. We will continue to use the circumflex $\hat{}$ to denote operators.

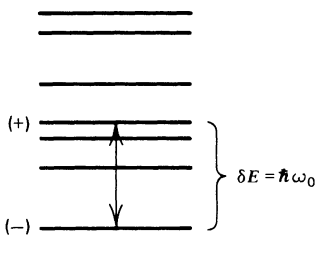


Fig. 2.3 Energy levels of an atom, showing two levels connected by a near-resonant transition.

The electric field is assumed to be quasi-monochromatic with a frequency nearly coincident with the transition frequency connecting two of the atom's energy levels. We take the two levels to be those labeled (+)

and $(-)$ in the figure, and assign to them the energies W_+ and W_- . The corresponding eigenstates of \hat{H}_A will be denoted by $|+\rangle$ and $|-\rangle$.

Only transitions between $|+\rangle$ and $|-\rangle$ will be of interest, so we can concern ourselves exclusively with the two-dimensional Hilbert space spanned by these two state vectors. The matrix elements of the various atomic operators are easily found.

$$\begin{aligned}\langle + | \hat{H}_A | + \rangle &= W_+, & \langle - | \hat{H}_A | - \rangle &= W_-, \\ \langle + | \hat{H}_A | - \rangle &= 0, & \langle - | \hat{H}_A | + \rangle &= 0;\end{aligned}\quad (2.6)$$

and

$$\begin{aligned}\langle + | \hat{\mathbf{d}} | + \rangle &= 0, & \langle - | \hat{\mathbf{d}} | - \rangle &= 0, \\ \langle + | \hat{\mathbf{d}} | - \rangle &= \mathbf{d}_{+-}, & \langle - | \hat{\mathbf{d}} | + \rangle &= (\mathbf{d}_{+-})^*.\end{aligned}\quad (2.7)$$

There are no off-diagonal elements of \hat{H}_A , of course, because $|+\rangle$ and $|-\rangle$ are derived from the beginning to be eigenstates of \hat{H}_A . There are no diagonal elements of $\hat{\mathbf{d}}$ because it is a vector operator and thus has odd parity. The states $|+\rangle$ and $|-\rangle$ are assumed to have definite parity. For the sake of concreteness, it may be worthwhile to compute \mathbf{d}_{+-} in a particularly simple case. If we take $|+\rangle$ and $|-\rangle$ to be the (nlm_l) states (211) and (100) of ordinary atomic hydrogen, then in the coordinate representation \mathbf{d}_{+-} has the form:

$$\mathbf{d}_{+-} = \int \Psi_{211}^*(\mathbf{r}) e \hat{\mathbf{r}} \Psi_{100}(\mathbf{r}) d^3 r. \quad (2.8)$$

This may be written as a product of radial and angular integrals in the usual way. When the actual state functions Ψ_{211} and Ψ_{100} for hydrogen are inserted, these integrals are:

$$\text{radial integral} = \int \frac{1}{(2a_0^2)^{3/2}} e^{-r/2a_0} [er] \frac{2r}{a_0\sqrt{3}} e^{-r/a_0} r^2 dr; \quad (2.9)$$

$$\text{angular integral} = \int Y_{11}^*(\theta, \phi) (\mathbf{x} \sin \theta \cos \phi + \mathbf{y} \sin \theta \sin \phi + \mathbf{z} \cos \theta) Y_{00}(\theta, \phi) d\Omega. \quad (2.10)$$

Both are common integrals and may be performed in many different ways. The results combine to give:

$$\mathbf{d}_{+-} = -\frac{2^7}{3^5} e a_0 (\mathbf{x} - i\mathbf{y}), \quad (2.11)$$

where \mathbf{x} and \mathbf{y} are the Cartesian unit vectors orthogonal to the atom's quantization axis \mathbf{z} . Of course $\Psi_{211}(\mathbf{r})$ and $\Psi_{100}(\mathbf{r})$ are each defined only up to an arbitrary constant phase, so that \mathbf{d}_{+-} actually has a similar imprecision in its definition.

In the general case the dipole matrix elements are complex vectors that might be written simply as

$$\mathbf{d}_{+-} = \mathbf{d}_r + i\mathbf{d}_i; \quad \mathbf{d}_{-+} = \mathbf{d}_r - i\mathbf{d}_i, \quad (2.12)$$

where \mathbf{d}_r and \mathbf{d}_i are real vectors, different for each problem. In the example above

$$\mathbf{d}_r = -\left(\frac{2^7}{3^5}\right)ea_0\mathbf{x}$$

and

$$\mathbf{d}_i = \left(\frac{2^7}{3^5}\right)ea_0\mathbf{y}.$$

In any event, it is clear that the Hermitian operator $\hat{\mathbf{d}}$ can be represented as an off-diagonal matrix in the two-dimensional space, with its matrix elements given by equation 2.12:

$$\hat{\mathbf{d}} \Rightarrow \begin{bmatrix} 0 & \mathbf{d}_r + i\mathbf{d}_i \\ \mathbf{d}_r - i\mathbf{d}_i & 0 \end{bmatrix}. \quad (2.13)$$

It is helpful at this stage to introduce the Pauli shorthand for two-dimensional matrices. Then the dipole moment operator is written in the usual notation:

$$\hat{\mathbf{d}} = \mathbf{d}_r \hat{\sigma}_1 - \mathbf{d}_i \hat{\sigma}_2. \quad (2.14)$$

The operator \hat{H}_A has a similar representation:

$$\hat{H}_A = \frac{1}{2}(W_+ + W_-)\hat{\mathbf{l}} + \frac{1}{2}(W_+ - W_-)\hat{\sigma}_3, \quad (2.15)$$

where $\hat{\mathbf{l}}$ is the 2×2 unit operator.

Either the Schrödinger or Heisenberg equations can be used to determine the time behavior of the atomic system. The simplicity of Pauli

matrix commutators

$$[\hat{\sigma}_1, \hat{\sigma}_2] = 2i\hat{\sigma}_3, \quad \text{et cycl.} \quad (2.16)$$

makes the Heisenberg method unusually straightforward in the present instance, and we adopt that approach. A well-known parallel development in the Schrödinger picture is due to Feynman, Vernon, and Hellwarth [3].

The Heisenberg equation for any operator \hat{O} that is not explicitly time-dependent is

$$i\hbar\dot{\hat{O}} = [\hat{O}, \hat{\mathcal{H}}].$$

In the present case we have

$$\hat{\mathcal{H}} = \frac{1}{2}(W_+ + W_-)\hat{1} + \frac{1}{2}(W_+ - W_-)\hat{\sigma}_3 - (\mathbf{d}_r \cdot \hat{\mathbf{E}})\hat{\sigma}_1 + (\mathbf{d}_i \cdot \hat{\mathbf{E}})\hat{\sigma}_2. \quad (2.17)$$

The three Pauli matrix operators therefore obey the equations:

$$\dot{\hat{\sigma}}_1(t) = -\omega_0\hat{\sigma}_2(t) + \frac{2}{\hbar} [\mathbf{d}_i \cdot \hat{\mathbf{E}}(t)]\hat{\sigma}_3(t), \quad (2.18a)$$

$$\dot{\hat{\sigma}}_2(t) = \omega_0\hat{\sigma}_1(t) + \frac{2}{\hbar} [\mathbf{d}_r \cdot \hat{\mathbf{E}}(t)]\hat{\sigma}_3(t), \quad (2.18b)$$

$$\dot{\hat{\sigma}}_3(t) = -\frac{2}{\hbar} [\mathbf{d}_r \cdot \hat{\mathbf{E}}(t)]\hat{\sigma}_2(t) - \frac{2}{\hbar} [\mathbf{d}_i \cdot \hat{\mathbf{E}}(t)]\hat{\sigma}_1(t), \quad (2.18c)$$

where we have introduced

$$\omega_0 \equiv \frac{W_+ - W_-}{\hbar} \quad (2.19)$$

to stand for the atomic transition frequency, and have also taken the electric field operator in the Heisenberg picture.

Within the two-dimensional space there are conservation laws that follow automatically from the properties of the Pauli matrices. For example, $\hat{\sigma}_1^2 = \hat{\sigma}_2^2 = \hat{\sigma}_3^2 = \hat{1}$. It is instructive to verify that in virtue of equations 2.18 the Pauli matrices, considered as time-dependent operators, continue to obey these relations for all time. The properties of the matrix commutators allow one to show easily, for example, that $\hat{\sigma}_1(t)\hat{\sigma}_1(t) + \hat{\sigma}_1(t)\dot{\hat{\sigma}}_1(t) = 0$.

Thus

$$\left(\frac{d}{dt} \right) \hat{\sigma}_1(t)^2 = 0, \quad \text{so} \quad \hat{\sigma}_1^2(t) = \hat{\sigma}_1^2(0) = \hat{1}.$$

Because of the operator nature of both atom and field variables the dynamical laws embodied in equations 2.18 are quite complex, especially when taken together with the operator Maxwell equations that govern the electric field. No very general solutions are known. Some special cases are examined in Chapter 7. However, for many purposes a related set of equations that is equally complex in every sense except for the operator character of the variables is highly useful. This alternative set of dynamical equations is based on the simple assertion that quantum correlations between field and atom are unimportant.

If quantum correlations can safely be ignored, then operator products such as $\hat{\mathbf{E}}(t)\hat{\sigma}_3(t)$ can be factored in every expectation value:

$$\langle \hat{\mathbf{E}}(t)\hat{\sigma}_3(t) \rangle = \langle \hat{\mathbf{E}}(t) \rangle \langle \hat{\sigma}_3(t) \rangle. \quad (2.20)$$

We define the semiclassical radiation theory of two-level atoms to be the theory resulting from a consistent application of such a factorization to equations 2.18. In addition, if it is necessary to add Maxwell's equations to the complement of dynamical equations, perhaps because the atom or atoms make a significant contribution to $\hat{\mathbf{E}}(t)$ by reradiation, the semiclassical theory will use the expectation value rather than the operator Maxwell equations. In the semiclassical theory $\langle \hat{\mathbf{E}}(t, \mathbf{r}_0) \rangle$ is interpreted to be a purely classical electric field. One important consequence of the restriction of the field variables to expectation values is that the semiclassical theory is not general enough to describe spontaneous emission correctly. Many other radiation reaction effects may, however, be handled easily within the semiclassical theory as we will see in Chapter 4.

In replacing the operator equations 2.18 by their expectation values it is convenient to introduce the notation $s_i(t) \equiv \langle \hat{\sigma}_i(t) \rangle$, or

$$s_i(t) \equiv \langle \hat{\sigma}_i(t) \rangle, \quad i = 1, 2, 3. \quad (2.21)$$

Because there will be no occasion until Chapter 7 to consider operator fields, we continue to use the same symbol $\mathbf{E}(t, \mathbf{r}_0)$ instead of $\langle \hat{\mathbf{E}}(t, \mathbf{r}_0) \rangle$ for the expectation value of the vector electric field operator. Therefore the

three equations for the components of $\mathbf{s}(t)$ may be written:

$$\dot{s}_1(t) = -\omega_0 s_2(t) + \frac{2}{\hbar} [\mathbf{d}_i \cdot \mathbf{E}(t, \mathbf{r}_0)] s_3(t), \quad (2.22a)$$

$$\dot{s}_2(t) = \omega_0 s_1(t) + \frac{2}{\hbar} [\mathbf{d}_r \cdot \mathbf{E}(t, \mathbf{r}_0)] s_3(t), \quad (2.22b)$$

$$\dot{s}_3(t) = -\frac{2}{\hbar} [\mathbf{d}_i \cdot \mathbf{E}(t, \mathbf{r}_0)] s_1(t) - \frac{2}{\hbar} [\mathbf{d}_r \cdot \mathbf{E}(t, \mathbf{r}_0)] s_2(t). \quad (2.22c)$$

These equations represent the general interaction of a two-level atom with an electric field in the semi-classical theory.

Equations 2.22 have a conservation law associated with them that is similar to the operator relation $\hat{\sigma}_1^2 + \hat{\sigma}_2^2 + \hat{\sigma}_3^2 = 3\hat{I}$. By multiplying the expectations $\dot{s}_1, \dot{s}_2, \dot{s}_3$ by s_1, s_2, s_3 respectively and adding the three equations, it is easy to show that

$$s_1^2(t) + s_2^2(t) + s_3^2(t) = \text{constant}. \quad (2.23)$$

It is less obvious that the constant equals unity. To show this, one may take

$$|\psi\rangle = a|+\rangle + b|-\rangle, \quad (2.24)$$

which is sufficiently general to represent any initial state of the two-level atom. Then it is easy to work out

$$s_1(0) = \langle \psi | \hat{\sigma}_1 | \psi \rangle = a^* b + ab^*, \quad (2.25a)$$

$$s_2(0) = \langle \psi | \hat{\sigma}_2 | \psi \rangle = -i(a^* b - ab^*), \quad (2.25b)$$

$$s_3(0) = \langle \psi | \hat{\sigma}_3 | \psi \rangle = |a|^2 - |b|^2, \quad (2.25c)$$

and

$$s_1^2(0) + s_2^2(0) + s_3^2(0) = (|a|^2 + |b|^2)^2.$$

Note that since we require $\langle \psi | \psi \rangle = 1$, then necessarily $|a|^2 + |b|^2 = 1$, which completes the proof that

$$s_1^2(t) + s_2^2(t) + s_3^2(t) = 1. \quad (2.26)$$

Obviously the conservation law in equation 2.26 is another way of saying that the state of the atom remains normalized in time, or, in other words, that probability is conserved.

Before going further it is well to recall the physical significance of the expectation values $s_1(t)$, $s_2(t)$, and $s_3(t)$. Equations 2.21, 2.15, and 2.19 make it clear that $\frac{1}{2}\hbar\omega_0 s_3(t)$ may be called the internal energy of the atom, relative to the average energy $\frac{1}{2}(W_+ + W_-)$ of the two levels under consideration. It is also common to refer to $s_3(t)$ as the inversion. For simplicity $\frac{1}{2}(W_+ + W_-)$ may be defined as the zero of energy and ignored henceforth. Also, equations 2.21 and 2.14 show that $s_1(t)$ and $s_2(t)$ are both manifestations of the atom's dipole moment operator.

For many purposes it is adequate to assume that the states $|+\rangle$ and $|-\rangle$ are connected by a $\Delta m=0$ transition. Then it is useful to adjust the arbitrary phases associated with the states so that \mathbf{d}_i vanishes, and simultaneously denote

$$\frac{2}{\hbar} \mathbf{d}_r \cdot \mathbf{E} \equiv \frac{2d}{\hbar} \mathbf{u}_d \cdot \mathbf{E} \equiv \kappa E. \quad (2.27)$$

That is, the scalar quantity E denotes the component of \mathbf{E} along the unit vector \mathbf{u}_d , and κ has been defined such that

$$\frac{\hbar\kappa}{2} \equiv d, \quad (2.28)$$

where \mathbf{u}_d and d denote the direction and magnitude of the dipole matrix element. $\Delta m = \pm 1$ transitions are discussed briefly in Sec. 4.7.

The semiclassical atomic equations then take a slightly simpler form:

$$\dot{s}_1(t) = -\omega_0 s_2(t), \quad (2.29a)$$

$$\dot{s}_2(t) = \omega_0 s_1(t) + \kappa E(t, \mathbf{r}_0) s_3(t), \quad (2.29b)$$

$$\dot{s}_3(t) = -\kappa E(t, \mathbf{r}_0) s_2(t). \quad (2.29c)$$

It is these equations that will mainly concern us in the next several chapters. They are the electric-dipole analogues of equations that govern spin precession in magnetic resonance [4], and $\mathbf{s}(t)$ can be called the electric dipole "pseudospin" vector. The conservation law 2.26 states that $\mathbf{s}(t)$ is a unit vector. Thus as the two-level atom operators evolve in the course of their interaction with the field, the pseudospin $\mathbf{s}(t)$ traces out an orbit on a unit sphere. A part of one such orbit is shown in Fig. 2.4.

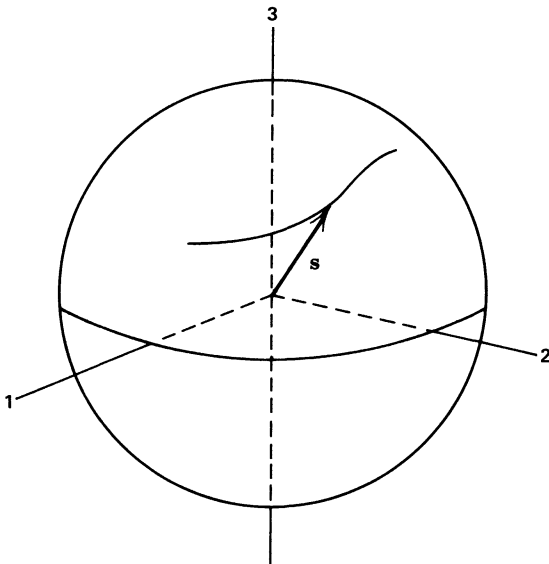


Fig. 2.4 The pseudospin vector \mathbf{s} traces out orbit on the unit sphere.

2.4 THE ROTATING WAVE APPROXIMATION

The pseudospin equations 2.29 can be analyzed much like the corresponding magnetic resonance equations [4, 5]. In particular, they can be rewritten as if they were the equations for the precession of a solid body acted on by a known torque Ω^F , where the superscript F refers to the coordinate system of fixed univectors **1, 2, 3**. The three equations 2.29 are equivalent to the single equation

$$\frac{d}{dt}\mathbf{s}(t) = \boldsymbol{\Omega}^F(t) \times \mathbf{s}(t), \quad (2.30)$$

where the vector \mathbf{s} has components s_1, s_2, s_3 , and the “torque” vector $\boldsymbol{\Omega}^F(t)$ has components:

$$\Omega_1^F(t) = -\kappa E, \quad (2.31a)$$

$$\Omega_2^F(t) = 0, \quad (2.31b)$$

$$\Omega_3^F(t) = \omega_0. \quad (2.31c)$$

The first and third components of the torque vector are clearly responsible for the pseudospin precession.

It is useful to estimate the relative magnitudes of the torque components for typical field strengths E and transition frequencies ω_0 . One very direct way to do this is to determine the field strength required for the two torque components to have equal magnitude: $\hbar\kappa E \approx \hbar\omega_0$. The energy of an optical transition is of order 1 eV. Also, an optical transition dipole moment is typically not very different from the value computed in the preceding section in equation 2.11, so we may take $\hbar\kappa$ to be roughly e times the Bohr radius a_0 . Thus the approximate equality $\hbar\kappa E \approx \hbar\omega_0$ will be satisfied if $E \approx 1V/a_0$, or $E \approx 10^8$ V/cm. Such high field strengths correspond to power densities of the order of 10^{15} W/cm². This power level is attainable with lasers, but is many orders of magnitude larger than that used in any resonance experiment.

There is a simple argument that shows that external fields strong enough to satisfy $\hbar\kappa E \approx \hbar\omega_0$ cannot, in principle, be used in resonance experiments. Electric dipole transitions between low-lying atomic levels have transition energies comparable to the ionization energy. In sodium, for example, the lowest-lying dipole transitions give rise to the D lines, and the relevant levels are separated in energy by about 2 eV, which is roughly two fifths of the $3s^2S_{1/2}$ ionization energy. In hydrogen the corresponding factor is just $3/4$. Thus it is satisfactory to take

$$\hbar\omega_0 \approx \frac{e^2}{a},$$

where e^2/a is approximately the ionization energy of a single valence electron orbiting with radius a around a single charged central core composed of the nucleus and the inner shell electrons. At the same time $\hbar\kappa E \approx eaE$, since ea will be very nearly the transition dipole moment of the same electron. Thus the relation $\hbar\kappa E \approx \hbar\omega_0$ is equivalent to

$$E \approx \frac{e}{a^2}.$$

In other words, for the external field to be strong enough to satisfy $\hbar\kappa E \approx \hbar\omega_0$, it must be as strong as the binding field e/a^2 that holds the electron in its orbit. Obviously it becomes questionable whether the existence of an atom is possible in the presence of such an external field. Certainly, resonant transitions could not be defined.

The consequence is that we may safely take the inequality $\kappa E \ll \omega_0$ to be well-satisfied in every situation of interest in optical resonance. Thus the “torque” vector Ω^F points almost straight along the 3 axis, with a very slight tip in the 1 direction. Precession of the electric dipole “pseudospin” vector $s(t)$ about the “torque” vector $\Omega^F(t)$ may easily be depicted qualitatively as in Fig. 2.5.

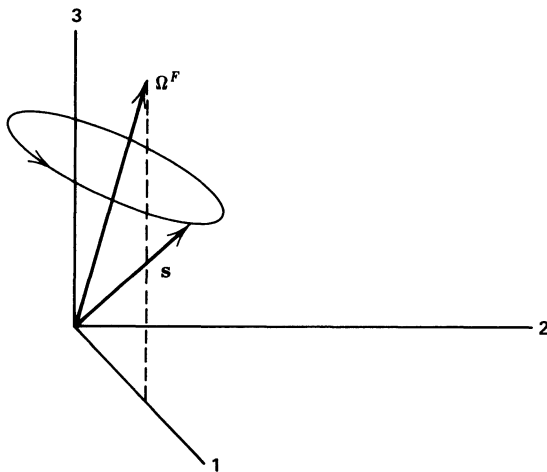


Fig. 2.5 The orbit of the pseudospin unit vector s shown as a precession about the fixed-axis torque vector Ω^F .

The fact that the figure is drawn as shown with $s(t)$ precessing about $\Omega^F(t)$ implies $\Omega^F(t)$ is changing slowly compared with $s(t)$. However $s(t)$ has components oscillating at frequency ω_0 ; and the applied field $E(t)$

$$E(t) = \mathcal{E}(t)[e^{i\omega t} + \text{c.c.}] \quad (2.32)$$

is nearly resonant with the transition in the cases of interest to us. It follows that $\omega \approx \omega_0$, so that $\Omega^F(t)$ is actually changing rapidly, not slowly. The sketch in Fig. 2.5 is therefore inappropriate because $s(t)$ cannot trace a full cycle about $\Omega^F(t)$ before $\Omega^F(t)$ itself changes appreciably.

In magnetic resonance theory the device of changing the coordinate reference frame to one that rotates at the frequency ω has been developed to simplify such situations. The number of rapidly changing variables is reduced thereby, and direct intuitive grasp of the precession is again

possible. The “torque” vector is rewritten as the sum of three “torques”, one Ω_0 along the 3 axis and two much smaller torques that lie entirely in the 1-2 plane:

$$\Omega^F = \Omega^+(t) + \Omega^-(t) + \Omega^0, \quad (2.33)$$

where

$$\Omega^0 = (0, 0, \omega_0), \quad (2.34a)$$

$$\Omega^+ = (-\kappa \hat{\epsilon} \cos \omega t, -\kappa \hat{\epsilon} \sin \omega t, 0), \quad (2.34b)$$

$$\Omega^- = (-\kappa \hat{\epsilon} \cos \omega t, +\kappa \hat{\epsilon} \sin \omega t, 0). \quad (2.34c)$$

Clearly Ω^+ rotates as a right-handed screw as t increases, and Ω^- rotates in the opposite direction. Because $\omega_0 \gg \kappa \hat{\epsilon}$ the natural precession of \mathbf{s} is about the 3 axis. In a coordinate frame following \mathbf{s} and moving to the right at angular velocity ω like a merry-go-round rotating about the 3 axis, the vector Ω^+ is constant, and Ω^- is counter-rotating at angular velocity 2ω . In such a coordinate frame the effect of the “torque” Ω^+ on a spin is steady and cumulative over long times. On the other hand, the effect of the “torque” Ω^- reverses itself $10^{15} - 10^{16}$ times/sec, and is almost completely ineffective. The “rotating wave” approximation consists of ignoring Ω^- for this reason, and writing the pseudospin equations using $\Omega^+ + \Omega^0$ in place of Ω^F . Then it follows that

$$\dot{s}_1 = -\omega_0 s_2 - \kappa \hat{\epsilon} s_3 \sin \omega t,$$

$$\dot{s}_2 = \omega_0 s_1 + \kappa \hat{\epsilon} s_3 \cos \omega t,$$

$$\dot{s}_3 = -\kappa \hat{\epsilon} [s_2 \cos \omega t - s_1 \sin \omega t].$$

It is now necessary to determine what the observer in the rotating frame will see. Any of a number of methods are available to achieve this. As Louisell has shown [5], this problem can be solved by the application of angular momentum algebra and quantum rotation theory. Another approach is to introduce explicitly the appropriate rotation matrix for the vector \mathbf{s} , and define thereby a nearly stationary vector ρ in the rotating

frame with components u, v, w :

$$\begin{bmatrix} u \\ v \\ w \end{bmatrix} = \begin{bmatrix} \cos \omega t & \sin \omega t & 0 \\ -\sin \omega t & \cos \omega t & 0 \\ 0 & 0 & 1 \end{bmatrix} \begin{bmatrix} s_1 \\ s_2 \\ s_3 \end{bmatrix}. \quad (2.35)$$

The equation of motion obeyed by the components of the pseudospin ρ in the rotating frame are:

$$\dot{u} = -(\omega_0 - \omega)v, \quad (2.36a)$$

$$\dot{v} = +(\omega_0 - \omega)u + \kappa \mathcal{E} w, \quad (2.36b)$$

$$\dot{w} = -\kappa \mathcal{E} v, \quad (2.36c)$$

which are the same as the single vector equation

$$\frac{d}{dt} \rho = \Omega \times \rho \quad (2.36d)$$

if the rotating frame torque vector Ω has the components

$$\Omega \equiv (-\kappa \mathcal{E}, 0, \omega_0 - \omega). \quad (2.36e)$$

Equations 2.36 show that, under the RWA, in the rotating frame all of the variables change slowly with time. There are no optical frequencies left in the problem so long as the applied field is near resonance, that is, so long as $|\omega_0 - \omega| \ll \omega_0$, which is what has been supposed.

The physical significance of u , v , and w must be traced back to the basic operators in the Hamiltonian. Clearly $\frac{1}{2}\hbar\omega_0 w$ is the expectation of the atom's unperturbed energy. In other words w is the single atom population difference, which from now on will be called the inversion. Equally clearly, the inverse of the transformation 2.35 shows that u and $-v$ are the components, in units of the transition moment d , of the atomic dipole moment in-phase and in-quadrature with the field E . The third of equations 2.36 confirms this identification by showing explicitly that v is the component effective in coupling to the field to produce energy changes. That is, v is the absorptive component of the dipole moment, while u is the dispersive component.

Because the coordinate transformation 2.35 is merely a rotation, lengths of vectors are preserved. Thus the conservation of probability relation 2.26 now takes the form:

$$u^2(t) + v^2(t) + w^2(t) = 1. \quad (2.37)$$

It is also easy to show directly that this relation is consistent with the equations of motion 2.36 for the pseudospin vector in the rotating coordinate frame.

2.5. ANALOGIES AND DIFFERENCES BETWEEN CLASSICAL AND SEMICLASSICAL DIPOLE INTERACTIONS

Finally it is helpful in developing an intuitive feel for the semiclassical rotating frame equations to note the similarities between them and the classical dipole equations of Chapter 1. In particular, if we set $w = -1$ in equations 2.36 the first two equations are identical to the loss-free version of the classical dipole amplitude equations 1.18.

It is very important that the connection between the equations for quantum and classical dipoles is so close. Because $w(t)$ is the single atom inversion it follows that $w(t) \approx -1$ means the atom is very nearly in its ground state. Thus in all cases where the atom is practically unexcited it must behave classically, exactly as a Lorentzian oscillator. This explains why the Kramers-Heisenberg quantum mechanical dispersion formula [6] looks exactly like the classical Lorentz dispersion formula. The Kramers-Heisenberg optical dispersion formula is found using perturbation theory; hence it is implicit in its derivation that the atomic state is never far from the initial state, which for the problem of dispersion is of course the ground state.

The only distinction between the quantum and classical dipoles is in the constant κ . The classical κ , defined in equation 1.20, is actually a number with arbitrary magnitude, since the classical oscillator amplitude x_0 is unrestricted. On the other hand, there is a definite value associated with κ in the semiclassical theory, since it is defined in terms of d , the magnitude of the atomic dipole matrix element. In this sense the semiclassical equations 2.36 are the natural generalizations of the purely classical equations; and d provides an estimate of the limiting size that ex_0 may take in the classical theory before the quantum theory is called for.

Still another way to contrast the quantum and classical dipole theories is first to note that $u^2 + v^2$ measures the squared amplitude of the dimensionless moment either quantum mechanically or classically. But then only in the quantum theory is there the relation

$$u^2 + v^2 = 1 - w^2$$

which requires the moment to vanish when the dipole's energy is maximum, $w = +1$, as well as minimum, $w = -1$. The most interesting coherent resonant effects are those that take us farthest from the classical or "harmonic oscillator" model of atoms, effects which occur when w is substantially different from -1 .

2.6. THE BLOCH-SIEGERT SHIFT

The reasoning that justifies the rotating wave approximation is not flawless, of course. The RWA is, after all, an approximation. In 1940 Bloch and Siegert showed [7] that the counter-rotating torque Ω^- which the RWA neglects can give rise to a shift in the true resonance frequency of the dipoles. They obtained the first correction to ω_0 due to the action of Ω^- . More recently Shirley [8] has given a more complete expression for the shift. In this section we follow a treatment due to Treacy [9].

Exact resonance between the driving field and a given pseudospin occurs in the RWA when the field frequency ω is identical to the spin's transition frequency ω_0 . To better estimate the resonance frequency we must examine the effect of Ω^- . In the merry-go-round frame rotating to the right about the 3 axis at frequency ω the exact torque, including Ω^- , is

$$\Omega(+\omega) = [-\kappa \hat{e} - \kappa \hat{e} \cos 2\omega t, \kappa \hat{e} \sin 2\omega t, \omega_0 - \omega]. \quad (2.38)$$

When the RWA is invoked, the parts oscillating rapidly at frequency 2ω are dropped, and the rotating-frame equations 2.36 follow. However, some simple features of the exact torque expression 2.38 suggest that a better approximation than the RWA may be possible. For example, it is apparent that if the field is tuned so that $\omega = \frac{1}{3}\omega_0$, then the natural precession about the 3 axis, given by the steady torque component $\omega_0 - \omega$, is to the right at frequency $\frac{2}{3}\omega_0$. At the same time Ω^- contributes a torque that rotates to the left about the 3 axis, but at exactly the same frequency $\frac{2}{3}\omega_0$. Thus the question arises: is there a coordinate frame in which the natural precession

and the rotating part of the torque have not only the same frequency, but also the same direction of rotation?

Inspection of expression 2.38 for the exact torque shows that if there is a coordinate frame answering this description, it must be a counter-rotating frame for which $\omega \approx -\omega_0$, for then the frequency of the rotating part of the torque, 2ω , will nearly equal the natural precession frequency $\omega_0 - \omega \approx 2\omega_0$ in that frame. Of course in such a frame the spin dynamics will be extraordinarily complex, but a derivation of the resonance condition itself may be simply made. The various parts of the exact torque in the counter-rotating frame are sketched in Fig. 2.6. The expression for this

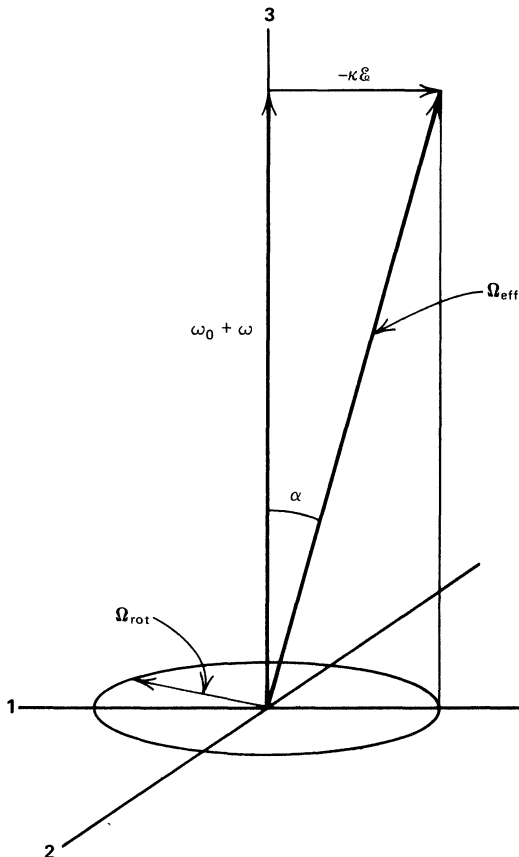


Fig. 2.6 The total torque vector in the counter-rotating frame is shown decomposed into its static part Ω_{eff} and its much smaller rotating part Ω_{rot} .

torque, which we denote by $\Omega(-\omega)$, may be given in two forms:

$$\Omega(-\omega) = [-\kappa \hat{\mathbf{e}}(1 + \cos 2\omega t), -\kappa \hat{\mathbf{e}} \sin 2\omega t, \omega_0 + \omega] \quad (2.39a)$$

and

$$\Omega(-\omega) = \Omega_{\text{eff}} + \Omega_{\text{rot}}. \quad (2.39b)$$

Expression (2.39a) shows that the rotating part of $\Omega(-\omega)$ is given by

$$\Omega_{\text{rot}} = -1\kappa \hat{\mathbf{e}} \cos 2\omega t - 2\kappa \hat{\mathbf{e}} \sin 2\omega t. \quad (2.40a)$$

The static “effective” torque Ω_{eff} is simply the constant part of $\Omega(-\omega)$:

$$\Omega_{\text{eff}} = \mathbf{u}_{\text{eff}} \sqrt{(\kappa \hat{\mathbf{e}})^2 + (\omega + \omega_0)^2}. \quad (2.40b)$$

Here the unit vector \mathbf{u}_{eff} is given by

$$\mathbf{u}_{\text{eff}} = -\mathbf{1} \sin \alpha + \mathbf{3} \cos \alpha, \quad (2.41)$$

and the small angle α is shown in Fig. 2.6.

To determine the resonance condition it is only necessary to repeat an earlier step expressed in equation 2.33. That is, we must separate the time-varying part Ω_{rot} of the torque $\Omega(-\omega)$ into parts rotating with and against the natural precession dictated by the static part of $\Omega(-\omega)$. In this case there is also a part of the time-varying torque that is parallel to \mathbf{u}_{eff} .

For convenience we may introduce a new set of coordinate axes along the unit vectors $\mathbf{1}', \mathbf{2}', \mathbf{3}'$, defined such that $\mathbf{3}' = \mathbf{u}_{\text{eff}}$ and $\mathbf{2}' = \mathbf{2}$. Then \mathbf{u}_{eff} serves as the new polar axis, with $\mathbf{1}'$ and $\mathbf{2}'$ perpendicular to it, and we can write

$$\begin{aligned} \Omega_{\text{rot}} &= -\kappa \hat{\mathbf{e}} \sin \alpha \cos 2\omega t \{\hat{\mathbf{3}'}\}, \\ &\quad -\kappa \hat{\mathbf{e}} \left(\frac{1 + \cos \alpha}{2} \right) \{\mathbf{1}' \cos 2\omega t + \mathbf{2}' \sin 2\omega t\}, \\ &\quad -\kappa \hat{\mathbf{e}} \left(\frac{1 - \cos \alpha}{2} \right) \{\hat{\mathbf{1}}' \cos 2\omega t - \hat{\mathbf{2}}' \sin 2\omega t\}, \end{aligned} \quad (2.42)$$

where each set of braces contains a unit vector. The last two braces represent driving torques perpendicular to the static Ω_{eff} and rotating

about it at frequency $\pm 2\omega$. There are thus two resonance conditions

$$\pm 2\omega = |\Omega_{\text{eff}}| = \sqrt{(\kappa \mathcal{E})^2 + (\omega_0 + \omega)^2} . \quad (2.43)$$

and two solutions

$$\omega = \omega_0 \left[1 + \frac{1}{4} \left(\frac{\kappa \mathcal{E}}{\omega_0} \right)^2 + \dots \right] \quad (2.44a)$$

and

$$\omega = -\frac{1}{3}\omega_0 \left[1 + \frac{3}{4} \left(\frac{\kappa \mathcal{E}}{\omega_0} \right)^2 + \dots \right]. \quad (2.44b)$$

Under the usual condition $\kappa \mathcal{E} \ll \omega_0$ assumed in the expansions above, the first solution is much more important as it corresponds to the right-rotating driving torque, the second term in equation 2.42. The ratio of the amplitude of the left-rotating third term to the amplitude of the right-rotating second term is very small:

$$\frac{1 - \cos \alpha}{1 + \cos \alpha} \approx \left(\frac{\alpha}{2} \right)^2 \approx \frac{1}{4} \left(\frac{\kappa \mathcal{E}}{\omega_0} \right)^2.$$

The second solution and the third term of equation 2.42 correspond to a coupling between atom and field by way of the third subharmonic.

The correction to ω_0 given in solution 2.44a is known as the Bloch-Siegert shift:

$$\delta\omega_{\text{B-S}} = \frac{1}{4} \frac{(\kappa \mathcal{E})^2}{\omega_0} . \quad (2.45)$$

The magnitude of the Bloch-Siegert shift at optical frequencies is very small. For example, a 1 nsec π pulse induces a shift on the order of

$$\delta\omega_{\text{B-S}} = \sim 10^{-10} \omega_0,$$

too small to have been observed. What is interesting is that the Bloch-Siegert shift is a secular effect, albeit a small one, arising from the counter-rotating part of the torque in equation 2.33.

References

1. G. K. Woodgate, *Elementary Atomic Structure*, McGraw-Hill, New York, 1970; H. G. Kuhn, *Atomic Spectra*, 2nd ed., Longmans, London, 1971.
2. T. W. Hänsch, I. S. Shahin, and A. L. Schawlow, *Phys. Rev. Lett.* **27**, 707 (1971); and F. Schuda, M. Hercher, and C. R. Stroud, Jr., *Appl. Phys. Lett.* **22**, 360 (1973).
3. R. P. Feynman, F. L. Vernon, Jr., and R. W. Hellwarth, *J. Appl. Phys.* **28**, 49 (1957).
4. F. Bloch, *Phys. Rev.* **70**, 460 (1946).
5. W. Louisell, *Quantum Statistical Properties of Radiation*, J. Wiley, New York, 1973, Sec. 5.11.
6. W. Heitler, *The Quantum Theory of Radiation*, Oxford University Press, London, 1954.
7. F. Bloch and A. J. F. Siegert, *Phys. Rev.* **57**, 522 (1940); see also A. F. Stevenson, *Phys. Rev.* **58**, 1061 (1940).
8. J. H. Shirley, *Phys. Rev.* **138**, 8979 (1965); see also articles by Cohen-Tannoudji, DuPont-Roc, and Fabre, by Hannaford, Pegg, and Series, and by Stenholm; in *J. Phys. B* **6** (August 1973).
9. E. B. Treacy, in *The Physics of Quantum Electronics* 1969, Optical Sciences Center Technical Report 45, J. B. Mandelbaum and S. F. Jacobs, eds., University of Arizona, 1969, p. 169.

CHAPTER 3

Two-Level Atoms in Steady Fields

3.1 Introduction	52
3.2 π Pulses	53
3.3 The Rabi Solution	56
3.4 Phenomenological Decay Constants	59
3.5 Torrey's Solutions	62
3.6 Optical Nutation	67
3.7 Free Induction Decay	69
3.8 Adiabatic Following	72
References	72

3.1. INTRODUCTION

The simplest interactions are among the most fruitful for very careful study. For in such situations details of the most basic aspects of the theory stand out to be tested. In this chapter we devote our attention to a class of interactions in which the electric field amplitude is steady in time and space. However, we make no assumptions about the strength of the field, allowing the possibility that it might be quite large. In this way a number of nonclassical phenomena may very readily be studied. The Bloch equations in the rotating coordinate system, derived in Chapter 2, can be solved easily and oscillations of the atomic inversion, influenced by detuning and power broadening, are found immediately. These oscillations are the analogues of those in magnetic resonance phenomena described by Rabi more than 30 years ago.

In Section 3.4 incoherent, possibly non-electromagnetic, interactions are introduced into the two-level atom's dynamics. This is done by way of phenomenological relaxation constants, in the same manner in which Bloch incorporated relaxation effects into magnetic resonance theory. These constants are intended to account for the effects of collisions, of natural spontaneous decay, and of all other incoherent line-broadening processes.

The solutions to the Bloch equations with phenomenological decay constants included were given first by Torrey. We reproduce some special cases of his results, and use them to discuss recent experiments on free

induction decay and optical nutation. In the latter case it is apparent that the basic predictions of Rabi concerning inversion oscillation and its consequences are clearly confirmed.

3.2. π PULSES

An important, and historically very early, use of the equations of motion derived in Section 2.4 was to determine the rate of energy absorption by a spin placed in a steady r.f. field. The same calculation can be carried out at optical frequencies, except that the “spin” is really the Bloch vector representing a two-level atom. The Rabi solution [1] of the Bloch vector equations is discussed first because it serves as a simple framework that can be generalized easily to permit the discussion of quite complex interactions of two-level atoms in steady fields.

The Rabi solution is simplest for those atoms exactly at resonance with the laser field. Only two of equations 2.36 then need to be solved, and their solution is found to be a rotation about the **1** axis in the rotating frame. If we define a dimensionless quantity $\theta(t)$ by the relation

$$\theta(t) = \int_{-\infty}^t \kappa \tilde{\mathcal{E}}(t') dt' \quad (3.1)$$

then the solutions to equations 2.36 are:

$$u(t; 0) = u_0, \quad (3.2a)$$

$$v(t; 0) = w_0 \sin \theta(t) + v_0 \cos \theta(t), \quad (3.2b)$$

$$w(t; 0) = -v_0 \sin \theta(t) + w_0 \cos \theta(t), \quad (3.2c)$$

where $u_0 = u(0; 0)$, and so on. The zero in the labels $v(t; 0)$ and $w(t; 0)$ refer to the detuning frequency $\Delta = \omega_0 - \omega$. The quantity $\theta(t)$ may obviously be interpreted as the upward tipping angle of the vector ρ for an on-resonance atom. It is shown in Fig. 3.1.

In the case in which the applied field envelope has the steady value $\tilde{\mathcal{E}}_0$ between t_1 and t_2 , equation 3.1 can be integrated to give:

$$\theta = \kappa \tilde{\mathcal{E}}_0 (t_2 - t_1) = \Omega(0)(t_2 - t_1), \quad (3.3)$$

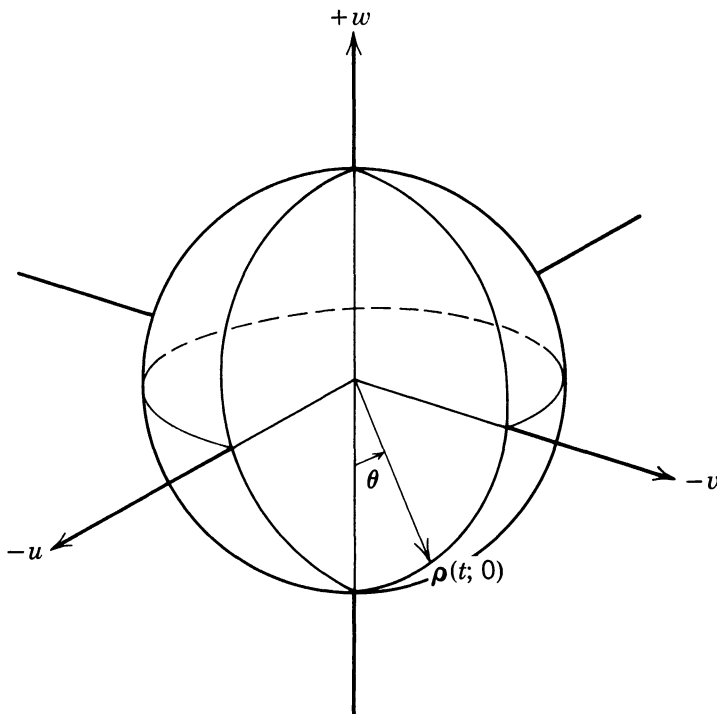


Fig. 3.1 A Bloch vector $\rho(t; 0)$ is shown tipped up by the angle $\theta(t)$ defined in equation 3.1. Notice that θ has direct meaning only for atoms exactly at resonance with the field. Thus θ lies in the v - w plane. It is measured positive in counterclockwise rotations about the $-u$ axis in our definition.

where $\Omega(0) = \kappa \mathcal{E}_0$ is called the Rabi frequency on resonance.

The Rabi frequency gives the rate at which transitions are coherently induced between the two atomic levels. If the atom is initially in its ground state, so that $w_0 = -1$ and $v_0 = 0$, then after a time δt such that $\kappa \mathcal{E}_0 \delta t = \pi$, equation 3.2c shows that $w = +1$, and the atom is in its upper state. Another way of saying the same thing is to point out that a coherent light wave in the form of a square pulse, as shown in Fig. 3.2, will just exactly invert a ground-state atom if the pulse is a “ π pulse,” if $\kappa \mathcal{E}_0(t_2 - t_1) = \pi$. This terminology has literal significance for true spins. A “ π pulse” of magnetic radiation turns a spin from alignment to antialignment with a static magnetic field.

The quantity $\kappa \mathcal{E}_0(t_2 - t_1)$, as well as giving the net tipping angle θ due to the pulse action, is exactly the area under the curve in Fig. 3.2, in

agreement with the definition made in Chapter 1 of pulse envelope area:

$$A(t) = \kappa \int_{-\infty}^t \mathcal{E}(t') dt' = \theta(t), \quad (3.4)$$

with the understanding that κ is now taken in its quantum form. It is remarkable and very helpful in picturing the effect of pulses on atoms to

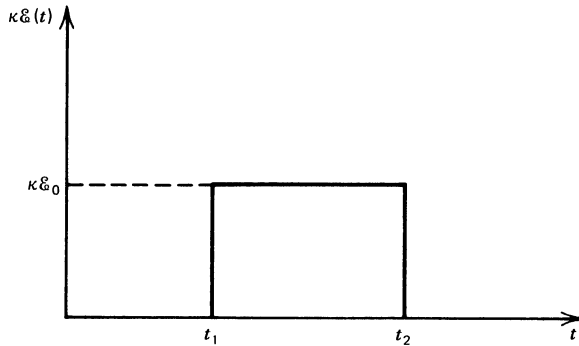


Fig. 3.2 The envelope function times κ for a square pulse. The area under the solid curve is the pulse area.

realize that envelope area can be translated directly into an atomic parameter as obvious as θ , the angle through which the pulse tips the Bloch vector of the on-resonance atoms. Resonant pulses with areas of π , 2π , 3π , and so on, are obviously particularly important in the theory, as they have the power to invert the atomic population 1, 2, 3, and so on, times.

That the solutions 3.2 are the result of a rotation can be shown in another way. If the rotating frame equations 2.36 are also written as a single vector precession equation:

$$\frac{d\rho}{dt} = \Omega \times \rho \quad (3.5)$$

where the rotating frame Bloch vector ρ and torque Ω are

$$\rho = (u, v, w) \quad (3.6)$$

and

$$\Omega = (-\kappa \mathcal{E}, 0, \Delta), \quad (3.7)$$

then equation 3.5 may be written in full:

$$\frac{d}{dt} \begin{bmatrix} u \\ v \\ w \end{bmatrix} = \begin{bmatrix} 0 & -\Delta & 0 \\ +\Delta & 0 & \kappa \mathcal{E} \\ -0 & -\kappa \mathcal{E} & 0 \end{bmatrix} \begin{bmatrix} u \\ v \\ w \end{bmatrix}. \quad (3.8)$$

When the on-resonance atoms are considered and Δ is set equal to zero, equation 3.8 shows that the precession is about the **1** axis only.

3.3. THE RABI SOLUTION

The general solution of equation 3.5, valid for any detuning Δ , is also a rotation. In the most general case, the precession about Ω cannot be unraveled analytically. If, however, the problem is confined to the Rabi case in which \mathcal{E} has the steady value \mathcal{E}_0 , then a solution is possible. In the off-resonance Rabi case, the “torque” vector Ω in the rotating frame is a constant vector in the **1**-**3** plane, as sketched in Fig. 3.3. In this case, a solution to equations 2.36 or 3.5 is accomplished by two successive rotations. The first is about the **2** axis through the angle χ shown in Fig. 3.3 and defined by

$$\tan \chi = \frac{\Delta}{\kappa \mathcal{E}_0}. \quad (3.9)$$

This rotation puts Ω onto the **1** axis. The Bloch vector ρ is, of course, also

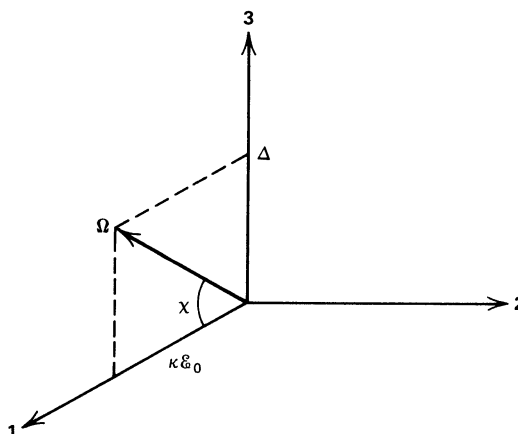


Fig. 3.3 The torque vector in the rotating frame is constant and lies in the **1**-**3** plane. The angle χ is defined in equation 3.9.

affected by the coordinate rotation, becoming $\rho' = (u', v', w')$, where

$$\begin{bmatrix} u \\ v \\ w \end{bmatrix} = \begin{bmatrix} \cos \chi & 0 & \sin \chi \\ 0 & 1 & 0 \\ -\sin \chi & 0 & \cos \chi \end{bmatrix} \begin{bmatrix} u' \\ v' \\ w' \end{bmatrix}. \quad (3.10)$$

When this relationship is used, the equivalent of equation 3.8 is:

$$\frac{d}{dt} \begin{bmatrix} u' \\ v' \\ w' \end{bmatrix} = \begin{bmatrix} 0 & 0 & 0 \\ 0 & 0 & \Omega(\Delta) \\ 0 & -\Omega(\Delta) & 0 \end{bmatrix} \begin{bmatrix} u' \\ v' \\ w' \end{bmatrix}. \quad (3.11)$$

As may readily be seen, the pseudospin ρ' is now precessing about the new **1** axis with frequency $\Omega(\Delta)$:

$$\Omega(\Delta) = \sqrt{\Delta^2 + (\kappa \mathcal{E}_0)^2}. \quad (3.12)$$

The frequency $\Omega(\Delta)$ is clearly the Rabi frequency generalized to account for detuning. A second rotation, specifically a counter-rotation about the **1** axis through the angle $-\Omega(\Delta)t$ will lead to a coordinate frame in which the pseudospin vector $\rho'' = (u'', v'', w'')$ is stationary, where (u'', v'', w'') is given by:

$$\begin{bmatrix} u' \\ v' \\ w' \end{bmatrix} = \begin{bmatrix} 1 & 0 & 0 \\ 0 & \cos \Omega t & -\sin \Omega t \\ 0 & \sin \Omega t & \cos \Omega t \end{bmatrix} \begin{bmatrix} u'' \\ v'' \\ w'' \end{bmatrix}. \quad (3.13)$$

At any time, equations 3.10 and 3.13 may be used to relate (u'', v'', w'') with (u, v, w) . However, at time $t=0$, the transformation 3.13 is particularly simple and (u'', v'', w'') may be identified with the initial Bloch vector (u_0, v_0, w_0) where:

$$u_0 \equiv u(0; \Delta), \quad v_0 \equiv v(0; \Delta), \quad w_0 = w(0; \Delta).$$

When this form for (u'', v'', w'') is combined with equations 3.10 and 3.13, we find the desired solution relating (u, v, w) and (u_0, v_0, w_0) :

$$\begin{bmatrix} u \\ v \\ w \end{bmatrix} = \begin{bmatrix} \cos \chi & 0 & \sin \chi \\ 0 & 1 & 0 \\ -\sin \chi & 0 & \cos \chi \end{bmatrix} \begin{bmatrix} 1 & 0 & 0 \\ 0 & \cos \Omega t & -\sin \Omega t \\ 0 & \sin \Omega t & \cos \Omega t \end{bmatrix} \times \begin{bmatrix} \cos \chi & 0 & -\sin \chi \\ 0 & 1 & 0 \\ \sin \chi & 0 & \cos \chi \end{bmatrix} \begin{bmatrix} u_0 \\ v_0 \\ w_0 \end{bmatrix}. \quad (3.14)$$

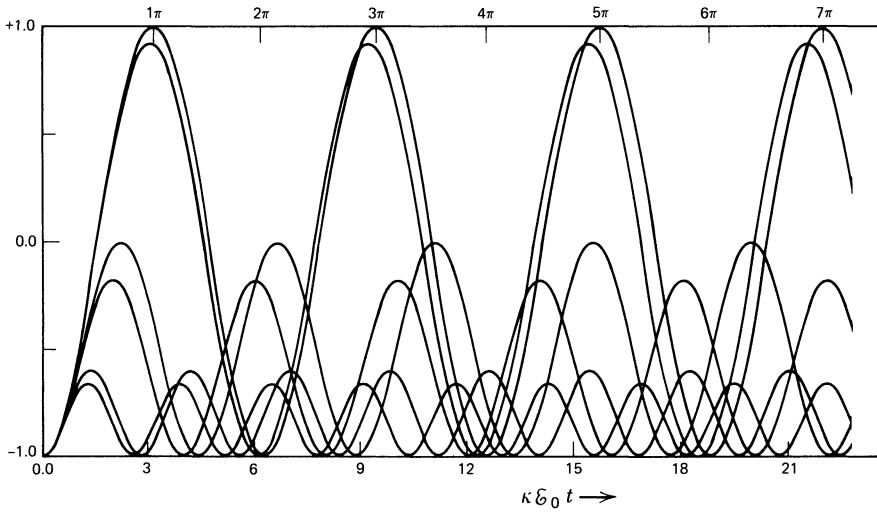
This product of transformations is equivalent to a single very complicated rotation:

$$\begin{bmatrix} u \\ v \\ w \end{bmatrix} = \begin{bmatrix} \frac{(\kappa \tilde{\varepsilon}_0)^2 + \Delta^2 \cos \Omega t}{\Omega^2} & \frac{-\Delta}{\Omega} \sin \Omega t & \frac{-\Delta \kappa \tilde{\varepsilon}_0}{\Omega^2} (1 - \cos \Omega t) \\ \frac{\Delta}{\Omega} \sin \Omega t & \cos \Omega t & \frac{\kappa \tilde{\varepsilon}_0}{\Omega} \sin \Omega t \\ \frac{-\Delta \kappa \tilde{\varepsilon}_0}{\Omega^2} (1 - \cos \Omega t) & \frac{-\kappa \tilde{\varepsilon}_0}{\Omega} \sin \Omega t & \frac{\Delta^2 + (\kappa \tilde{\varepsilon}_0)^2 \cos \Omega t}{\Omega^2} \end{bmatrix} \begin{bmatrix} u_0 \\ v_0 \\ w_0 \end{bmatrix}, \quad (3.15)$$

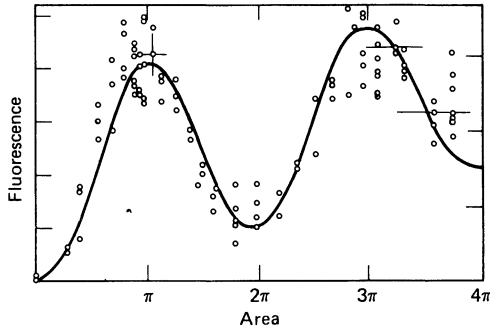
where, by Ω , we understand the generalized Rabi frequency defined in relation 3.12. It is straightforward to verify directly that relation 3.15 expresses a rotation by showing that the lengths of the initial and final vectors are the same: $u^2 + v^2 + w^2 = u_0^2 + v_0^2 + w_0^2$.

The solution for the inversion is worth writing explicitly:

$$\begin{aligned} w(t; \Delta) &= -u_0 \frac{\Delta \kappa \tilde{\varepsilon}_0}{[\Delta^2 + (\kappa \tilde{\varepsilon}_0)^2]} \left[1 - \cos \sqrt{\Delta^2 + (\kappa \tilde{\varepsilon}_0)^2} t \right] \\ &\quad - v_0 \frac{\kappa \tilde{\varepsilon}_0}{\sqrt{\Delta^2 + (\kappa \tilde{\varepsilon}_0)^2}} \sin \sqrt{\Delta^2 + (\kappa \tilde{\varepsilon}_0)^2} t \\ &\quad + w_0 \frac{\Delta^2 + (\kappa \tilde{\varepsilon}_0)^2 \cos \sqrt{\Delta^2 + (\kappa \tilde{\varepsilon}_0)^2} t}{[\Delta^2 + (\kappa \tilde{\varepsilon}_0)^2]}. \end{aligned} \quad (3.16)$$



(a)



(b)

Fig. 3.4 (a) The Rabi solution, showing the inversion as a function of time, and the effects of detuning. The highest curve shows the inversion of an atom exactly on resonance, and the curve lying only slightly below it is detuned from resonance by 0.2 times the on-resonance Rabi frequency $\kappa\hat{\varepsilon}_0$. The next lower pair of curves are for atoms detuned by 1.0 and 1.2 times $\kappa\hat{\varepsilon}_0$; and the bottom pair of curves are for atoms detuned by 2.0 and 2.2 times $\kappa\hat{\varepsilon}_0$. Notice that the relative detuning $0.2\kappa\hat{\varepsilon}_0$ within each pair has a much greater influence on the atoms whose absolute detunings are larger. At the time $\kappa\hat{\varepsilon}_0 t = 5\pi$ the two curves in the lowest pair have gotten completely out of phase, while the two curves in the highest pair have drifted apart a negligible amount. The presence of substantial inhomogeneous broadening, so that $1/T_2^* \gg \kappa\hat{\varepsilon}_0$, would allow relatively very few atoms to experience complete inversion or to remain in phase with each other. Note that the atoms exactly on resonance reach complete inversion for driving pulse areas that are odd multiples of π , that is, $\kappa\hat{\varepsilon}_0 t = \pi, 3\pi, 5\pi$, and so on. (b) The degree of inversion in a system of atoms experiencing Rabi oscillation may be monitored by detecting the atoms' fluorescence. An example is shown in which the variation of fluorescence intensity and therefore of inversion, as a function of input pulse area, is evident. [From H. M. Gibbs, *Phys. Rev. A* **8**, 446 (1973)].

Necessarily, it is found that as $\Delta \rightarrow 0$ in the limit of zero detuning, expression 3.16 reproduces the earlier result 3.2:

$$w(t; 0) = w_0 \cos(\kappa \mathcal{E}_0 t) - v_0 \sin(\kappa \mathcal{E}_0 t). \quad (3.17)$$

It is common to see expression 3.16 specialized to the case of an atom initially in its ground state where $u_0 = v_0 = 0$ and $w_0 = -1$:

$$w(t; \Delta) = -1 + \frac{2(\kappa \mathcal{E}_0)^2}{(\kappa \mathcal{E}_0)^2 + \Delta^2} \sin^2 \sqrt{(\kappa \mathcal{E}_0)^2 + \Delta^2} \frac{t}{2}. \quad (3.18)$$

The behavior of the inversion for several values of Δ for a given value of $\kappa \mathcal{E}_0$ is sketched in Fig. 3.4. Note that if the system is tuned closely enough to exact resonance so that $\Delta < \kappa \mathcal{E}_0$, then appreciable inversion occurs with each cycle.

3.4. PHENOMENOLOGICAL DECAY CONSTANTS

In the discussion of the classical problems associated with resonant pulse interactions, the role of various dipole decay times was important. Such decay times must be incorporated into the quantum discussion, too. This may be done in almost exactly the same way. The dipole oscillations must damp out in the absence of a driving field. The equations for the expectation values in the rotating frame may be modified very simply to allow for this feature:

$$\dot{u} = -\Delta v - \frac{u}{T'_2}, \quad (3.19a)$$

$$\dot{v} = \Delta u - \frac{v}{T'_2} + \kappa \mathcal{E} w, \quad (3.19b)$$

$$\dot{w} = -\frac{w - w_{\text{eq}}}{T_1} - \kappa \mathcal{E} v. \quad (3.19c)$$

These are the optical analogues of the semphenomenological equations first proposed by Bloch [2] for nuclear spins.

One difference between equation 3.19 and the corresponding classical equations 1.18 and 1.19 has already been noted in Section 2.4: there is an extra variable, w , the inversion. Because there are interactions, such as collisions in a gas or phonon scattering in a solid, which can disturb the

dipole oscillations of the resonant atom without disturbing its energy, the inversion w can decay at a different rate from u and v . It is customary to allow for this possibility, following Bloch, by assigning a decay time T_1 to the inversion that differs from the dipole moment decay time T'_2 . Furthermore, incoherent energy input due to contact with a thermal reservoir at finite temperature, a broad-band flash lamp, an electronic discharge, or other source, may keep the inversion above a certain value, even when the resonant field amplitude \mathcal{E} is zero. In equation 3.19c this equilibrium value, toward which the inversion relaxes when $\mathcal{E} = 0$, has been denoted by w_{eq} .

In the theory of magnetic resonance T_1 and T'_2 are called longitudinal and transverse homogeneous lifetimes because they govern the decay of those components of a magnetic spin which are, respectively, parallel with and perpendicular to the static component of the magnetic Zeeman field, conventionally chosen to lie along the 3 axis. The prime on T'_2 serves to distinguish the transverse moment lifetime due to incoherent interactions that affect all atoms homogeneously, such as collisions, radiative decay, and “spin”-exchange, from the lifetime due to inhomogeneous effects, which we denote by T_2^* . The most common origin of an inhomogeneous lifetime T_2^* is the Doppler effect, which assigns each atom its own individual effective resonant frequency according to its velocity. In solids, random local strain fields have the same effect. The consequent random distribution of resonant frequencies and the resulting dephasing of the individual dipole moments in a macroscopic collection of atoms lead to macroscopic polarization damping even if homogeneous T'_2 -type damping is absent, just as in the case of classical oscillators. The expression

$$\frac{1}{T_2} \equiv \frac{1}{T'_2} + \frac{1}{T_2^*} \quad (3.20)$$

defines the total transverse decay time T_2 . The classical analogue was denoted by \mathfrak{T} in Chapter 1.

The addition of damping terms to the Bloch equations makes them noticeably more complicated as well as more realistic. In the presence of a steady field, however, they remain linear first-order equations with constant coefficients. Therefore, they can be solved explicitly, so long as \mathcal{E} is constant. In agreement with the notation of the preceding section, we denote this constant value by \mathcal{E}_0 .

3.5. TORREY'S SOLUTIONS

In 1949, Torrey [3] gave detailed solutions to equations 3.19, using Laplace transform techniques. With some slight notational changes, Torrey's solutions may be written as

$$\Gamma(t) = Ae^{-at} + \left[B \cos st + \frac{C}{s} \sin st \right] e^{-bt} + D, \quad (3.21)$$

where Γ stands for either u , v , or w . Depending on which one Γ denotes, the constant coefficients A , B , C , D take different values, while a , b , and s depend only on Δ , $\kappa \mathcal{E}_0$, T_1 , and T'_2 . Clearly the undamped solutions 3.15 are special cases in which $a = b = 0$ and $A + D = 0$.

The longtime steady-state solution D for each variable is easily found by putting $\dot{u} = \dot{v} = \dot{w} = 0$, and solving the resulting algebraic equations. The results are:

$$u(\infty; \Delta) = -w_{\text{eq}} \frac{(\Delta T'_2)(\kappa \mathcal{E}_0 T'_2)}{1 + (\Delta T'_2)^2 + T_1 T'_2 (\kappa \mathcal{E}_0)^2}, \quad (3.22a)$$

$$v(\infty; \Delta) = w_{\text{eq}} \frac{\kappa \mathcal{E}_0 T'_2}{1 + (\Delta T'_2)^2 + T_1 T'_2 (\kappa \mathcal{E}_0)^2}, \quad (3.22b)$$

$$w(\infty; \Delta) = w_{\text{eq}} \frac{1 + (\Delta T'_2)^2}{1 + (\Delta T'_2)^2 + T_1 T'_2 (\kappa \mathcal{E}_0)^2}. \quad (3.22c)$$

In the limit of very long T_1 and T'_2 , when it is scarcely proper to speak of steady-state solutions at all, there is nevertheless a shadow of the undamped solutions 3.15 in these results. If we put $T_1 = T'_2 = \infty$ and do not admit incoherent external energy input, so that $w_{\text{eq}} = -1$, then equations 3.22 reproduce the time-independent parts of solution 3.15 if $w_0 = -1$ and $u_0 = v_0 = 0$.

Some of the features of the Torrey solutions, particularly the secular determinant that determines the three rates a , b , and s , are worth deriving here. The Laplace transform approach follows naturally from the identity:

$$x(t) = x_0 + \int_0^t dt' \dot{x}(t'), \quad (3.23)$$

where $x_0 \equiv x(0)$. If we let $\mathcal{L}_\lambda[x]$ denote the Laplace transform of $x(t)$ with parameter λ ,

$$\mathcal{L}_\lambda[x] \equiv \int_0^\infty e^{-\lambda t} x(t) dt,$$

then, since

$$\mathcal{L}_\lambda[1] = \frac{1}{\lambda},$$

we find that

$$\mathcal{L}_\lambda[x] = \frac{1}{\lambda} x_0 + \int_0^\infty dt e^{-\lambda t} \int_0^t dt' \dot{x}(t').$$

However, the order of the t and t' integrations may be interchanged, so that the second term in the equation immediately above becomes

$$\int_0^\infty dt' \dot{x}(t') \int_{t'}^\infty dt e^{-\lambda t} = \frac{1}{\lambda} \int_0^\infty dt' e^{-\lambda t'} \dot{x}(t'),$$

which is exactly the same as $(1/\lambda) \mathcal{L}_\lambda[\dot{x}]$. Thus the basic identity 3.23 is equivalent to the Laplace transform relation:

$$\lambda \mathcal{L}_\lambda[x] = x_0 + \mathcal{L}_\lambda[\dot{x}]. \quad (3.24)$$

If, as in the case of the Bloch equations, only first-order differential equations are to be solved, the Laplace transform identity 3.24 is valuable because it turns differential equations for the time-dependent variables into algebraic equations for their transforms.

The successive substitution of u , v , and w for x in relation 3.24 and the use of equations 3.19a, b, and c in turn for \dot{u} , \dot{v} , and \dot{w} lead to three algebraic equations:

$$\lambda \mathcal{L}_\lambda[u] = u_0 - \frac{1}{T'_2} \mathcal{L}_\lambda[u] - \Delta \mathcal{L}_\lambda[v], \quad (3.25a)$$

$$\lambda \mathcal{L}_\lambda[v] = v_0 - \frac{1}{T'_2} \mathcal{L}_\lambda[v] + \Delta \mathcal{L}_\lambda[u] + \kappa \mathcal{E}_0 \mathcal{L}_\lambda[w], \quad (3.25b)$$

$$\lambda \mathcal{L}_\lambda[w] = w_0 - \frac{1}{T'_1} \mathcal{L}_\lambda[w] + \frac{1}{T'_1} \frac{w_{eq}}{\lambda} - \kappa \mathcal{E}_0 \mathcal{L}_\lambda[v]. \quad (3.25c)$$

The vanishing of the determinant of the coefficients of equations 3.25 gives the secular equation whose roots are the eigenfrequencies of the problem, that is, the negatives of the Torrey rate constants a , b , and s . The secular equation is:

$$\left(\lambda + \frac{1}{T'_2}\right) \left[\left(\lambda + \frac{1}{T'_2}\right) \left(\lambda + \frac{1}{T_1}\right) + (\kappa \mathcal{E}_0)^2 \right] + \Delta^2 \left(\lambda + \frac{1}{T_1}\right) = 0. \quad (3.26)$$

In the most general case, no simple factorizations occur, and a cubic equation must be solved.

As Torrey [3] has pointed out, however, in three special situations of interest, equation 3.26 has relatively simple solutions. These three cases are:

1. *Strong Collisions.* If collisions cause energy decay whenever they cause dipole phase interruption, it is sensible to take $T_1 = T'_2$. Then equation 3.26 has the roots:

$$\lambda = -\frac{1}{T'_2}, \quad -\frac{1}{T'_2} \pm i \sqrt{\Delta^2 + (\kappa \mathcal{E}_0)^2}.$$

Thus, in the notation of solution 3.21, strong collisions imply

$$a = b = \frac{1}{T'_2},$$

$$s = \sqrt{\Delta^2 + (\kappa \mathcal{E}_0)^2}.$$

Detailed solutions in this case have also been given by Jaynes [4], using a two-dimensional matrix method that reduces greatly the complexity of the calculations.

2. *Exact Resonance.* When $\Delta = 0$, the cubic equation 3.26 has the roots:

$$\lambda = -\frac{1}{T'_2}, \quad -\frac{1}{2} \left(\frac{1}{T_1} + \frac{1}{T'_2} \right) \pm i \sqrt{(\kappa \mathcal{E}_0)^2 - \frac{1}{4} \left(\frac{1}{T_1} - \frac{1}{T'_2} \right)^2},$$

which implies that

$$a = \frac{1}{T'_2},$$

$$b = \frac{1}{2} \left(\frac{1}{T_1} + \frac{1}{T'_2} \right),$$

and

$$s = \sqrt{(\kappa \mathcal{E}_0)^2 - \frac{1}{4} \left(\frac{1}{T_1} - \frac{1}{T'_2} \right)^2}.$$

3. Intense External Field. If the external field is intense enough so that $\kappa \mathcal{E}_0 T'_2 \gg 1$, then it is also true that $\kappa \mathcal{E}_0 T_1 \gg 1$, and *a fortiori* true that $\kappa \mathcal{E}_0 \gg \left(\frac{1}{T'_2} - \frac{1}{T_1} \right)$. Thus we temporarily denote the difference between transverse and longitudinal decay rates by γ :

$$\gamma \equiv \frac{1}{T'_2} - \frac{1}{T_1},$$

and rewrite equation 3.26 in terms of T'_2 and γ :

$$\left(\lambda + \frac{1}{T'_2} \right) \left[\Delta^2 + (\kappa \mathcal{E}_0)^2 + \left(\lambda + \frac{1}{T'_2} \right)^2 - \gamma \left(\lambda + \frac{1}{T'_2} \right) \right] = \gamma \Delta^2. \quad (3.27)$$

If $\kappa \mathcal{E}_0$ is very large compared to γ , equation 3.27 has two kinds of root. The first of these follows from the assumption that $(\lambda + 1/T'_2)^2$ is small compared with $\Delta^2 + (\kappa \mathcal{E}_0)^2$, in which case it is natural to rearrange equation 3.27 into the form:

$$\left(\lambda + \frac{1}{T'_2} \right) = \frac{\gamma \Delta^2}{\left[\Delta^2 + (\kappa \mathcal{E}_0)^2 \right] \left[1 + \frac{\left(\lambda + \frac{1}{T'_2} \right) \left(\lambda + \frac{1}{T'_2} - \gamma \right)}{\Delta^2 + (\kappa \mathcal{E}_0)^2} \right]},$$

and solve by simple iteration. This root is

$$\lambda \approx -\frac{1}{T'_2} + \gamma \frac{\Delta^2}{\Delta^2 + (\kappa \tilde{\varepsilon}_0)^2} + O\left[\left(\frac{\gamma}{\kappa \tilde{\varepsilon}_0}\right)^3\right].$$

The second kind of root occurs if $(\lambda + 1/T'_2)^2$ is as large as $\Delta^2 + (\kappa \tilde{\varepsilon}_0)^2$, but has the opposite sign, so that the bracket in equation 3.27 is small, on the order of γ . Then an alternative rearrangement is natural:

$$\left(\lambda + \frac{1}{T'_2}\right)^2 + \Delta^2 + (\kappa \tilde{\varepsilon}_0)^2 = \gamma \left(\lambda + \frac{1}{T'_2}\right) \left[1 + \frac{\Delta^2}{\left(\lambda + \frac{1}{T'_2}\right)^2}\right].$$

To first order in γ the factor $(\lambda + 1/T'_2)^2$ on the right-hand side may be replaced by $-\left[\Delta^2 + (\kappa \tilde{\varepsilon}_0)^2\right]$. This gives a simple quadratic equation for $(\lambda + 1/T'_2)$, whose solutions are the second and third intense-field roots:

$$\lambda = -\frac{1}{T'_2} + \frac{\frac{1}{2}\gamma(\kappa \tilde{\varepsilon}_0)^2}{\Delta^2 + (\kappa \tilde{\varepsilon}_0)^2} \pm i \sqrt{\Delta^2 + (\kappa \tilde{\varepsilon}_0)^2} + O\left[\left(\frac{\gamma}{\kappa \tilde{\varepsilon}_0}\right)^2\right].$$

Thus in an intense coherent field satisfying

$$\kappa \tilde{\varepsilon}_0 \gg \gamma = \frac{1}{T'_2} - \frac{1}{T_1}$$

the three rates contributing to the various terms in the Torrey solution 3.21 are:

$$a = \frac{1}{T'_2} - \left(\frac{1}{T'_2} - \frac{1}{T_1}\right) \frac{\Delta^2}{\Delta^2 + (\kappa \tilde{\varepsilon}_0)^2} + O\left[\left(\frac{\gamma}{\kappa \tilde{\varepsilon}_0}\right)^3\right],$$

$$b = \frac{1}{T'_2} - \frac{1}{2} \left(\frac{1}{T'_2} - \frac{1}{T_1}\right) \frac{(\kappa \tilde{\varepsilon}_0)^2}{\Delta^2 + (\kappa \tilde{\varepsilon}_0)^2} + O\left[\left(\frac{\gamma}{\kappa \tilde{\varepsilon}_0}\right)^3\right],$$

$$s = \sqrt{\Delta^2 + (\kappa \tilde{\varepsilon}_0)^2} + O\left[\left(\frac{\gamma}{\kappa \tilde{\varepsilon}_0}\right)^2\right].$$

It is interesting to check this last set of expressions for a , b , and s against the first two sets derived. The strong collision limit is defined by $\gamma \equiv 0$, and the leading terms in the intense field roots exactly reproduce the strong collision roots derived in (1). At resonance, when $\Delta = 0$, the intense-field roots are seen to be the lowest-order terms in an expansion in powers of γ of the exact on-resonance roots derived in case 2.

Torrey has given explicitly the coefficients A , B , and C that occur in the solution 3.21. They are very complicated functions of the parameters Δ , $\kappa\mathcal{E}_0$, T_1 , T'_2 , and w_{eq} . Instead of treating the exact solutions of the damped Bloch equations further, we go on to a discussion of some observations of coherent transient effects, effects whose existence is implied by the solution given in equation 3.21.

3.6. OPTICAL NUTATION

The pseudospin vector \mathbf{s} responds to the rotating torque $\Omega^0 + \Omega^+$ in a very complicated way, even in the absence of damping. This is shown clearly by the Rabi solution 3.15 for the Bloch vector $\rho = (u, v, w)$, the rotating frame equivalent of \mathbf{s} . However, those vectors ρ very near to resonance undergo motion that is relatively easy to visualize. In the limit $\Delta \rightarrow 0$, the solution 3.15 reduces to the equation 3.2, which shows that the on-resonance ρ 's merely go up and down in the 2-3 plane at the frequency $\kappa\mathcal{E}_0$. In the original nonrotating coordinate frame, the corresponding motion of the vectors \mathbf{s} is a rapid precession at frequency ω about the 3 axis, upon which the much slower up-and-down motion is superimposed. In the language appropriate to spinning tops, the slow up-and-down motion of the vector is termed nutation.

Spin nutation was recognized very early in magnetic resonance. Because the up-and-down motion of the spin takes it partially out of its ground state with every nutation, its ability to absorb radiation is impaired and then restored at the frequency $\kappa\mathcal{E}_0$. Tang and Statz [5] were the first to suggest that the effect should be observable with optical pulses. They argued that a step-function light pulse traveling through an amplifying medium would develop an oscillatory intensity modulation at its leading edge while the way in which the sinusoid damped out would give information about the relaxation processes. The principal requirement for the observation of the effect is that the frequency of the anticipated modulation, the Rabi frequency, must be of the order of or greater than the linewidth of the transition.

Another way of understanding what is taking place is to imagine an intense coherent light pulse driving the on-resonance atoms successively from the lower state, to a coherent superposition state, to the upper state, back to the coherent superposition state with its large electric dipole moment, back to the lower state, and so on. The cycle repeats but is subject to damping by relaxation processes in the medium. The oscillation in population difference reacts back on the field, and amplitude-modulates the light. Off resonance, the atoms do not actually reach the upper state but otherwise undergo essentially the same behavior. This is just the behavior discussed in Section 3.3 and shown in Fig. 3.4, and the frequency at which the modulation occurs is the generalized Rabi frequency given by equation 3.12:

$$\Omega(\Delta) = \sqrt{\Delta^2 + (\kappa \mathcal{E})^2} .$$

Of course, it is necessary at least that $\Omega(\Delta) > 1/T_2'$ in order that a few population oscillations occur before damping destroys the effect. Consequently there is an easily estimated minimum value for the size of the field. Also, for the effect to be seen, the pulse duration must be several times $1/\kappa \mathcal{E}_0$; that is, it must be a many- π pulse.

Hocker and Tang [6] observed optical nutation using an absorption band in gaseous SF₆ and a pulse from a 10.6- μ CO₂ laser. They observed amplitude modulation on the leading edge of the pulse when the pressure of the SF₆ was sufficiently high. Although the modulation was not obviously sinusoidal, the power level required for observation, about 200 W/cm², agreed approximately with the theoretical value of 160 W/cm². More recently, by using cw CO₂ laser radiation and by pulsed Stark-shifting of molecular transitions in C¹³H₃F and NH₂D, Brewer and Shoemaker [7] have observed a variety of coherent transient phenomena, optical nutation among them.

The Brewer-Shoemaker technique is relatively straightforward. Since it allows the observation of a wide range of transient optical resonance effects, it deserves a brief discussion. A typical experiment involves three steps. In the first step, a spectrally very narrow cw laser irradiates and saturates a small portion of an inhomogeneously broadened atomic absorption line. (Saturation phenomena are discussed in some detail in Chapter 6.) In the second step, a static electric field is switched on very abruptly, causing a sudden Stark shifting and/or splitting of the resonance

line. The third step consists of monitoring the radiation emitted by the saturated and Stark-shifted absorber, usually by beating it against the very narrow cw laser signal that has remained on throughout the experiment.

In any experiment of this type, there are two groups of molecules that play major roles. They are, on the one hand, the molecules originally on resonance and saturated by the laser, which find themselves far out of resonance after the Stark field is turned on; on the other hand, the molecules with the opposite experience: originally far off resonance and unexcited, but exactly on resonance after the Stark shift. To this second group of molecules, it appears as if the laser itself has suddenly been turned on when the Stark field is applied. As a consequence, they begin to absorb the laser light, and their Bloch vectors begin to rotate according to the Rabi prescription (equation 3.15), with $u_0 = v_0 = 0$ and $w_0 = -1$ because they were in their ground states initially. In other words, they undergo nutation and give rise to a modulation of the transmitted laser beam, as shown in Fig. 3.5. When the Stark field is turned off, the laser beam is again modulated, this time because of the nutation of the molecules in the first group which are suddenly returned to resonance by the second Stark field switching. The modulation due to nutation does not continue indefinitely in either case, of course, because the homogeneous lifetimes, T_1 and T'_2 , limit the nutation. This is clearly shown in equation 3.21. The bracketed oscillating term is damped out at the rate $b \neq 0$.

3.7. FREE INDUCTION DECAY

It is also interesting to consider the evolution of the molecules in the first group after the Stark field is turned on. They were originally excited by the cw laser field. We show in equation 3.22c what degree of inversion is to be expected in these molecules after a lengthy exposure to the laser. If $T_1 = T'_2$, and $w_{\text{eq}} = -1$, the inversion is:

$$w(t \gg T'_2; \Delta) = - \frac{\Delta^2 + (1/T'_2)^2}{\Delta^2 + (\kappa \mathcal{E}_0)^2 + (1/T'_2)^2},$$

which can be substantially different from -1 , almost zero in fact (see Fig. 6.3), for the exactly on-resonance molecules if the steady laser field strength \mathcal{E}_0 is sufficiently large in relation to $1/T'_2$.

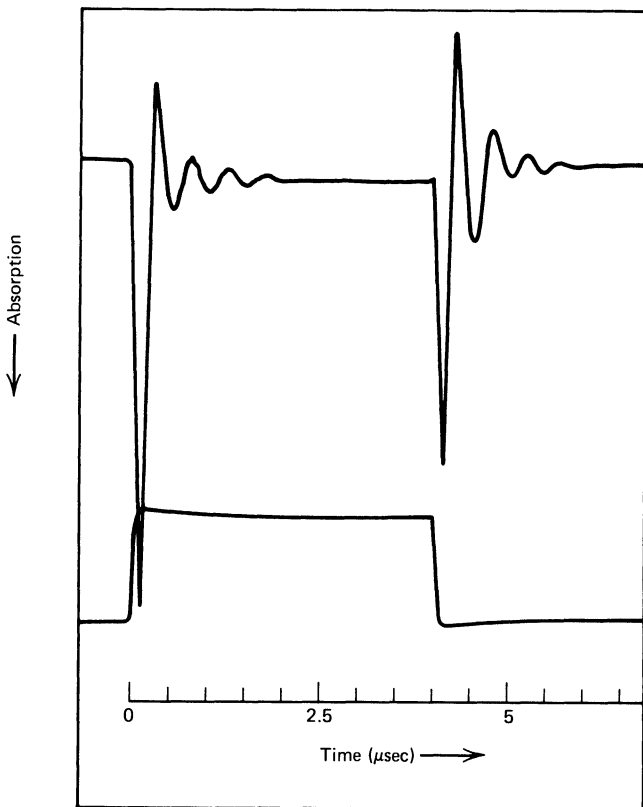


Fig. 3.5 Damped optical nutation oscillations observed by Stark-field switching. [From R. G. Brewer and R. L. Shoemaker, *Phys. Rev. Lett.* **27**, 631 (1971).]

When these molecules are Stark-shifted far out of resonance, they begin to radiate freely within a band of frequencies centered at $\omega + \delta\omega_s$, where ω is the laser frequency and $\delta\omega_s$ is the amount of the Stark shift. The width of the band will be the same as the bandwidth originally excited by the cw excitation, which is the smaller of $1/T_2^*$ and $[(\kappa\mathcal{E}_0)^2 + (1/T_2')^2]^{1/2}$. If, as in the Brewer-Shoemaker experiments, the absorption line is mainly Doppler-broadened, and if $\kappa\mathcal{E}_0 \gg 1/T_2'$ so that nutation may be observed, the excited bandwidth is approximately $\kappa\mathcal{E}_0$. Thus the signal radiated by these originally excited molecules will have a lifetime of no more than approximately $1/\kappa\mathcal{E}_0$, because the molecular dipoles within the bandwidth $\kappa\mathcal{E}_0$ will be completely out of phase and unable to radiate after that time. This termination of the free radiation by dephasing is called free induction decay. Brewer and Shoemaker have observed exactly this effect in NH_2D

gas. They detect the rapid beat at the frequency $\delta\omega_s$ between the laser and the molecular radiation, and plot the result as in Fig. 3.6. Note that the beats decay in roughly the same time that the overall signal decays. This is in accordance with the explanation outlined above, because the overall signal decay is due to the modulation of the transmitted laser amplitude by the nutation of the second group of molecules, which occurs at frequency $\kappa\tilde{\epsilon}_0$. The decay of the beats themselves is a manifestation of so-called free-induction decay, observed very early in magnetic resonance studies [8]. It is due, in both magnetic and optical resonance, to the dephasing of a group of freely precessing dipoles, the dephasing taking place before T_1 - and T_2' -type decay can operate. In this sense, free-induction decay is anomalously rapid.

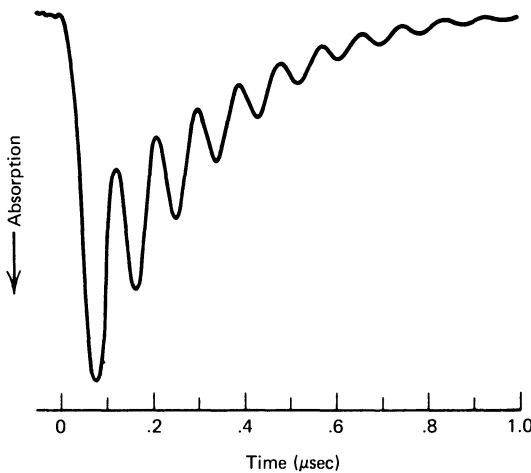


Fig. 3.6 Optical free induction decay in NH_2D at 10.6μ following the application of a step-function Stark field. [From R. G. Brewer and R. L. Shoemaker, *Phys. Rev. A* **6**, 2001 (1972).]

Finally, we may remark that it is not accidental that both optical nutation and free-induction decay have magnetic analogues. Coherent optical transient effects will naturally mirror similar magnetic transient phenomena so long as the same Bloch equations underlie each. The solutions given by Torrey [3] to the Rabi problem, some of which we quoted in the preceding section, should be adequate for optical resonance studies of two-level atoms that use steady saturating laser fields. It is mainly when wave propagation effects become important that optical

resonance ceases to be a high-frequency copy of magnetic resonance. In the following chapter, we begin a study of these propagation effects.

3.8. ADIABATIC FOLLOWING

It is obvious that the addition of damping terms to the Bloch equations makes them more complicated as well as more realistic. The exact solutions found by Torrey and discussed in Section 3.5 are those applicable to the case of a constant field envelope. Under certain conditions it is possible to lift the restriction that \mathcal{E} be constant, and find approximate solutions to the damped Bloch equations. These solutions are valid if \mathcal{E} varies slowly enough, “adiabatically” in a sense, and the term “adiabatic following” may be used to describe collectively the associated experimental phenomena [9].

Although analytic solutions exist to the adiabatic following problem, it is instructive first to use the vector model in the no-damping limit of the optical Bloch equations to understand physically what is happening. As shown in equation 3.5 the loss-free optical Bloch equations may be written as a single vector precession equation:

$$\frac{d\rho}{dt} = \Omega \times \rho, \quad (3.32)$$

where the Bloch vector ρ is

$$\rho = (u, v, w) \quad (3.33a)$$

and the torque Ω is

$$\Omega(t) = (-\kappa \mathcal{E}(t), 0, \Delta). \quad (3.33b)$$

The precession equation has the interpretation that the Bloch vector ρ is precessing about the torque vector at a precession frequency $\Omega(\Delta, t) = |\Omega|$:

$$\Omega(\Delta, t) = \sqrt{(\kappa \mathcal{E}(t))^2 + \Delta^2}, \quad (3.34)$$

as shown in Fig. 3.7, under the assumption that $\Delta = \omega_0 - \omega$ is negative, for definiteness. When the amount off resonance $|\Delta|$ is large enough, say several inhomogeneous linewidths $1/T_2^*$, it is usually a good approximation to assume that $\Omega(\Delta)$ is much greater than the rate of change of \mathcal{E} . In room temperatures gases, for example, T_2^* is of the order of 0.1 nsec, so that only picosecond pulses can provide coherent fields that change on the

scale of $\frac{1}{2} - \frac{1}{10} \times T_2^*$. Of course, if the response of ρ to the applied field $\mathcal{E}(t)$ is to be a coherent precession, then the action of \mathcal{E} must be brief compared to the relaxation times T_1 and T_2' which have been omitted from equation 3.32. Thus the duration τ of the applied field and the magnitude of the detuning $|\Delta|$ can be assumed to satisfy

$$|\Delta|^{-1} < T_2^* < \tau < T_2', T_1. \quad (3.35)$$

Here the pulse is assumed to be smooth, and τ is defined loosely by $\mathcal{E}/\tau \sim d\mathcal{E}/dt$.

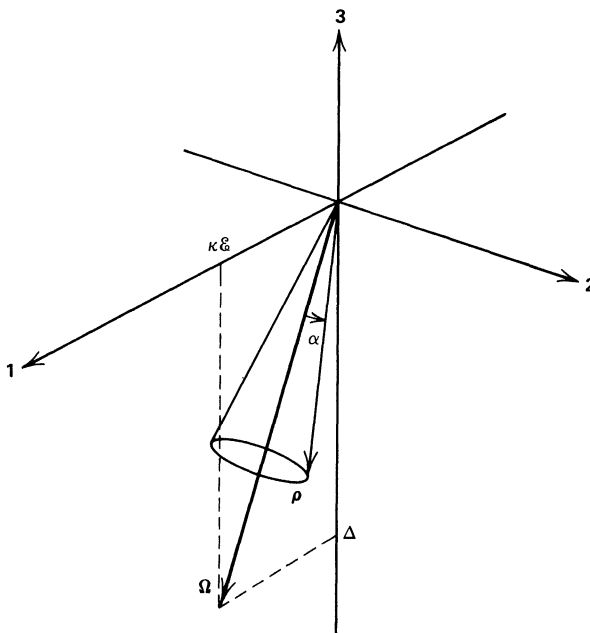


Fig. 3.7 Precession of Bloch vector ρ in a narrow cone about the rotating frame torque vector Ω .

Under these conditions the torque vector $\Omega(t)$ changes its direction very slowly compared with the rate $|\Omega|$ at which ρ precesses about it. Under this condition the Bloch vector may be said to be adiabatically following $\Omega(t)$. If the resonant atoms are in their ground states prior to the arrival of the pulse, then ρ initially points straight down along the 3 axis. Because $|\Delta|$ has been assumed to be large, Ω also is initially almost vertical. Thus it is a

good approximation to assume that the precessing Bloch vector remains nearly parallel to the torque Ω as Ω moves adiabatically. The smallness of the angle α in Fig. 3.7 suggests that a simple geometrical derivation may be made of the Bloch vector components. In the limit $\alpha=0$ one easily finds:

$$u = \frac{-\kappa\hat{\epsilon}}{\sqrt{(\kappa\hat{\epsilon})^2 + \Delta^2}}, \quad (3.36a)$$

$$v = 0, \quad (3.36b)$$

$$w = \frac{\Delta}{\sqrt{(\kappa\hat{\epsilon})^2 + \Delta^2}}. \quad (3.36c)$$

Of course ρ cannot be exactly parallel to Ω , as equations 3.36 would indicate, because then $\Omega \times \rho = 0$, and $d\rho/dt$ would also vanish identically. The principal failing of a purely geometrical picture of adiabatic following is that it is hard to obtain the finite corrections of order α to solution 3.36b.

The first example of adiabatic following to be investigated experimentally was adiabatic inversion, a concept familiar from magnetic resonance [10]. Treacy pointed out [11] that if $\Delta = \omega_0 - \omega$ could be made to change adiabatically from a large negative value ($\omega \approx \omega_0 + 10/T_2^*$, say) to a large positive value ($\omega \approx \omega_0 - 10/T_2^*$), then w would follow adiabatically, going from $w \approx -1$ to $w \approx +1$ in the process. That is, a ground state population could be adiabatically inverted. The detuning Δ is a function of time if the field frequency ω or the atomic frequency ω_0 is a function of time. Loy has recently demonstrated optical adiabatic inversion [12] by using the Brewer-Shoemaker method to modulate ω_0 in NH₃ vapor.

A more complete and systematic solution of the Bloch equations in the adiabatic following limit has been developed by Crisp [13]. Starting from the Bloch equations 3.19, which have phenomenological damping terms included, Crisp combines the u and v equations as in the classical analysis of Section 1.7. The Bloch equations then take the form:

$$\frac{d}{dt}(u - iv) = -\left(\frac{1}{T'_2} + i\Delta\right)(u - iv) - i\kappa\hat{\epsilon}w, \quad (3.37a)$$

$$\frac{d}{dt}w = -\frac{1}{T'_1}(w - w_{eq}) - \kappa\hat{\epsilon}v. \quad (3.37b)$$

Equation 3.37a is a linear first-order differential equation for the complex dipole amplitude $u - iv$, and can be integrated exactly:

$$u(t) - iv(t) = \int_{-\infty}^t [-i\kappa \hat{\mathcal{E}}(t')] w(t') e^{-[1/T'_2 + i\Delta](t-t')} dt'. \quad (3.38)$$

Here we have invoked the assumption that the atoms were all in their ground states at $t = -\infty$, requiring $w(-\infty) = 1$ and the vanishing of the other two components, $u(-\infty)$ and $v(-\infty) = 0$. A shift in the integration variable to $s \equiv t - t'$ allows a somewhat simpler expression for the solution:

$$u(t) - iv(t) = \int_0^\infty [i\kappa \hat{\mathcal{E}}(t-s)] w(t-s) e^{-[1/T'_2 + i\Delta]s} ds. \quad (3.39)$$

The adiabatic following assumption, that $\hat{\mathcal{E}}(t)$ and the Bloch vector's components vary slowly on the scale of Δ^{-1} , can now be utilized. Crisp [13] points out that a Taylor expansion of $\kappa \hat{\mathcal{E}}(t-s)w(t-s)$:

$$\kappa \hat{\mathcal{E}}(t-s)w(t-s) = \sum_{n=0}^{\infty} \frac{(-1)^n s^n d^n}{n!} \frac{d^n}{dt^n} [\kappa \hat{\mathcal{E}}(t)w(t)]$$

allows the integral 3.39 to be evaluated as follows:

$$u(t) - iv(t) = \frac{-i}{\frac{1}{T'_2} + i\Delta} \sum_{n=0}^{\infty} \frac{(-1)^n}{\left[\frac{1}{T'_2} + i\Delta \right]^n} \frac{d^n}{dt^n} [\kappa \hat{\mathcal{E}}(t)w(t)]. \quad (3.40)$$

Although the solution 3.40 is found only in terms of an infinite series, it may be expected to be highly useful. If the adiabatic following approximation is valid, the quantity $\kappa \hat{\mathcal{E}}(t)w(t)$ varies very little in the time $|1/T'_2 + i\Delta|^{-1}$, and the series converges rapidly.

On the assumption of rapid convergence, an adequate solution for $u(t)$ and $v(t)$ is given by

$$u(t) - iv(t) = \frac{-i}{\frac{1}{T'_2} + i\Delta} \left\{ \kappa \hat{\mathcal{E}}(t)w(t) - \frac{1}{\frac{1}{T'_2} + i\Delta} \frac{d}{dt} [\kappa \hat{\mathcal{E}}(t)w(t)] \right\}. \quad (3.41)$$

If the field is tuned far from resonance so that $|1/T'_2 + i\Delta|$ is large enough,

then the first term alone may be used to substitute for v in equation 3.37b. Crisp has pointed out that the result is a well-known rate equation for the inversion:

$$\dot{w} = -\frac{1}{T_1}(w - w_{eq}) - \frac{(\kappa \mathcal{E})^2 T'_2}{1 + \Delta T'_2} w. \quad (3.42)$$

We comment further on this equation in Chapter 6.

Closer to resonance, when the second term in solution 3.41 must also be kept, the vector picture formulas given in equations 3.36 are recovered in two steps. In the first step, equation 3.37b is used to obtain

$$\frac{d}{dt}(\kappa \mathcal{E} w) = -(\kappa \mathcal{E})^2 v + w \frac{d}{dt}(\kappa \mathcal{E}) \quad (3.43)$$

when the basic adiabatic following inequality 3.35 is used to justify neglecting the term proportional to $1/T_1$. This result, together with equation 3.41, is equivalent to

$$u \approx -\left(\frac{\kappa \mathcal{E}}{\Delta}\right) w$$

$$v \approx \left[\frac{d}{dt}(\kappa \mathcal{E}) \right] \left[\Delta^2 + (\kappa \mathcal{E})^2 \right]^{-1} w$$

when inequality 3.35 is invoked again to discard $1/T'_2$ in comparison to Δ . The second step uses inequality 3.35, as well as the results above for u and v , to conclude $u \gg v$ and $u^2 + w^2 \approx 1$. It is then simple to solve directly for w , and then for u and v :

$$u = -\frac{\kappa \mathcal{E}}{\sqrt{\Delta^2 + (\kappa \mathcal{E})^2}}, \quad (3.44a)$$

$$v = \frac{\Delta}{\sqrt{\Delta^2 + (\kappa \mathcal{E})^2}} \frac{d(\kappa \mathcal{E})/dt}{\left[\Delta^2 + (\kappa \mathcal{E})^2\right]}, \quad (3.44b)$$

$$w = \frac{\Delta}{\sqrt{\Delta^2 + (\kappa \mathcal{E})^2}}. \quad (3.44c)$$

The results for u and w are the same found geometrically, and the result for v is new. As Grischkowsky has pointed out [9], v may be obtained from the geometrical picture if the first Bloch equation 3.19a is solved for v in the limit $T_2' \rightarrow \infty$, and the geometrical result 3.36a is used to find u .

If the field and atoms are still closer to resonance with one another, so that even higher terms in the series 3.40 are required for satisfactory convergence, the present analysis becomes very complicated, essentially because ρ can no longer be considered to be following Ω adiabatically. Adiabatic following may be viewed as a regime of coherent interactions intermediate between the regimes of two distinct theories of such interactions: classical linear dispersion theory on the one hand and the quantum optical nonlinear theory on the other. In the next chapter we discuss some of the very nonclassical effects predicted to occur when the adiabatic following approximation fails because the atoms and field are very nearly exactly on resonance, that is, when ω falls within the inhomogeneous atomic absorption line of the atoms.

Recent interest in the abiotic following regime of coherent interactions is almost entirely due to the experimental work of Grischkowsky and his colleagues. Reference must be made to their papers for an adequate appreciation of the elegant experiments already undertaken and reported [9].

References

1. I. I. Rabi, *Phys. Rev.* **51**, 652 (1937).
2. F. Bloch, *Phys. Rev.* **70**, 460 (1946).
3. H. C. Torrey, *Phys. Rev.* **76**, 1059 (1949).
4. E. T. Jaynes, *Phys. Rev.* **98**, 1099 (1955).
5. C. L. Tang and H. Statz, *Appl. Phys. Lett.* **10**, 145 (1968).
6. G. B. Hocker and C. L. Tang, *Phys. Rev. Lett.* **21**, 591 (1969).
7. R. G. Brewer and R. L. Shoemaker, *Phys. Rev. Lett.* **27**, 631 (1971); *Phys. Rev. A* **6**, 2001 (1972).
8. E. L. Hahn, *Phys. Rev.* **77**, 297 (1950).
9. D. Grischkowsky, *Phys. Rev. Lett.* **24**, 866 (1970); D. Grischkowsky and J. A. Armstrong, *Phys. Rev. A* **6**, 1566 (1972); D. Grischkowsky, *Phys. Rev. A* **7**, 2096 (1973); D. Grischkowsky, E. Courtens, and J. A. Armstrong, *Phys. Rev. Lett.* **31**, 422 (1973).
10. A. Abragam, *The Principles of Nuclear Magnetism*, Oxford University Press, London, 1961, pp. 65-66.
11. E. B. Treacy, *Phys. Lett.* **27A**, 421 (1968). See also E. B. Treacy and A. J. DeMaria, *Phys. Rev. Lett.* **29A**, 369 (1969) for experimental results.
12. M. M. T. Loy, *Phys. Rev. Lett.* **32**, 814 (1974).
13. M. D. Crisp, *Phys. Rev. A* **8**, 2128 (1973).

CHAPTER 4

Pulse Propagation

4.1 Introduction	78
4.2 Maxwell's Equation	78
4.3 Bloch Vector Behavior	81
4.4 The McCall-Hahn "Area Theorem"	85
4.5 Self-Induced Transparency	89
4.6 Phase-Modulation Effects	101
4.7 Circularly Polarized Light	107
References	109

4.1 INTRODUCTION

Electric dipole transitions in atoms typically produce radiation in the optical region of the spectrum. Consequently, almost every experiment involving electric dipoles and radiation must take account of the transport of radiation through the dipole medium. This is not true for magnetic transitions, and magnetic resonance phenomena, because typical magnetic dipole radiation has wavelengths of the order of millimeters or much larger. For this reason we find in this chapter, where the propagation of radiation is studied, new phenomena unknown in magnetic resonance studies.

The nonlinear "area theorem" of McCall and Hahn is the central element in these new phenomena. The area theorem generalizes and supplants Beer's law of linear absorption and leads to the existence of effects such as lossless propagation in an absorbing medium, the well-defined breakup of large pulses into smaller ones, and pulse compression by coherent absorption.

4.2 MAXWELL'S EQUATION

As in the classical case, we restrict attention to electric dipole radiation propagating along the z axis. The one-dimensional wave equation

$$\left[\frac{\partial^2}{\partial z^2} - \frac{1}{c^2} \frac{\partial^2}{\partial t^2} \right] E(t, z) = \frac{4\pi}{c^2} \frac{\partial^2}{\partial t^2} P(t, z) \quad (4.1)$$

is sufficient for the wide variety of effects to be considered. The polarization density is defined in the classical way except that $ex(t, z)$ must be replaced by $d\langle \sigma_1(t, z) \rangle$:

$$P(t, z) = \mathcal{N}d[\langle \sigma_1(t, z) \rangle]_{av}.$$

Here $[\dots]_{av}$ denotes an average over all dipoles within dz of z at time t . This average has a concrete and by now familiar expression if inhomogeneous broadening is present. In terms of the slowly varying amplitudes $u(t, z; \Delta)$ and $v(t, z; \Delta)$, we have

$$P(t, z) = \mathcal{N}d \int g(\Delta') [u \cos(\omega t - Kz) - v \sin(\omega t - Kz)] d\Delta'. \quad (4.2)$$

This differs from the classical expression 1.30 only by the replacement of ex_0 by d . Exactly the same form will be taken for $E(t, z)$ as in equation 1.31:

$$E(t, z) = \mathcal{E}(t, z)[e^{i(\omega t - Kz)} + c.c.]. \quad (4.3)$$

By substituting equations 4.2 and 4.3 into the wave equation 4.1 and after invoking the assumption of slowly varying amplitudes, we find the classical in-phase and in-quadrature equations again:

$$[K^2 - k^2]\mathcal{E}(t, z) = 2\pi k^2 \mathcal{N}d \int u(t, z; \Delta') g(\Delta') d\Delta', \quad (4.4a)$$

$$2 \left[K \frac{\partial}{\partial z} + k \frac{\partial}{\partial ct} \right] \mathcal{E}(t, z) = 2\pi k^2 \mathcal{N}d \int v(t, z; \Delta') g(\Delta') d\Delta', \quad (4.4b)$$

consistent with the interpretation of E as a completely classical field in semiclassical radiation theory.

Of course, from this point on, very little will be the same as in the classical analysis. The quantum dipole envelope functions obey the nonlinear optical Bloch equations given in Chapter 3:

$$\dot{u} = -\Delta v - \frac{u}{T'_2}, \quad (4.5a)$$

$$\dot{v} = \Delta u - \frac{v}{T'_2} + \kappa \mathcal{E} w, \quad (4.5b)$$

$$\dot{w} = -\kappa \mathcal{E} v - \frac{(w - w_{eq})}{T_1}, \quad (4.5c)$$

and u , v , and w are strongly restricted by the probability conservation law,

$$u^2 + v^2 + w^2 = \text{constant},$$

which is valid over time intervals short compared with T_1 and T'_2 . If T_1 and T'_2 are both much longer than the interval during which an experiment might be carried out, damping may be ignored altogether, and equation 2.37,

$$u^2 + v^2 + w^2 = 1, \quad (4.6)$$

may be used for the conservation of probability.

The energy of the combined macroscopic system consisting of dielectric absorber and radiation field is also a conserved quantity if the damping rates $1/T_1$ and $1/T'_2$ are small enough to be ignored. In that case, the in-quadrature Maxwell equation 4.4b and equation 4.5c for the atomic inversion may be combined to derive

$$\frac{c}{2\pi} \frac{\partial \mathcal{E}^2}{\partial z} + \frac{1}{2\pi} \frac{\partial \mathcal{E}^2}{\partial t} + \frac{\partial U}{\partial t} = 0, \quad (4.7)$$

where the matter energy density is

$$U = \mathcal{N} \frac{\hbar\omega}{2} \int d\Delta' g(\Delta') w(t, z; \Delta'). \quad (4.8)$$

Obviously relation 4.7 is simply the energy-flux conservation relation 1.5, expressed in terms of envelope functions.

At the end of Section 2.4, following the derivation of the pseudospin equations 2.36, we remarked that it is the constraint 4.6 that expresses what is perhaps the sharpest distinction between classical and semiclassical theories. A classical linear oscillator can oscillate with arbitrary amplitude, larger and larger if more and more energy is fed in. The quantum mechanical two-level atom, on the other hand, can store energy only up to an amount $\hbar\omega_0$. By the same token there is a finite largest expectation value of the dipole moment for a two-level atom. Thus the field equations beginning with 4.2 contain the definite-valued parameter d instead of the arbitrary classical ex_0 . These limits on the ranges of energies and moments available to the atom have direct physical consequences, of course, coherent and incoherent saturation effects being among the most obvious. In the following sections we begin an examination of coherent saturation phenomena.

4.3 BLOCH VECTOR BEHAVIOR

With Q -switched and mode-locked lasers it is relatively simple to create light pulses that last only a few nanoseconds, or even only a few picoseconds. When working with dilute gases or cooled solids, many materials are available in which T'_2 is much longer than a few nanoseconds. An atom in such a material undergoes practically no damping during its brief interaction with nanosecond and picosecond pulses. The dynamical evolution of the dipole variables can then be studied as if the damping terms were not present. In the absence of damping the optical Bloch equations reduce to:

$$\dot{u} = -\Delta v, \quad (4.9a)$$

$$\dot{v} = \Delta u + \kappa \mathcal{E} w, \quad (4.9b)$$

$$\dot{w} = -\kappa \mathcal{E} v, \quad (4.9c)$$

and the conservation law 4.6 holds exactly.

Before going further it is useful to point out the range of pulse lengths that are compatible with the approximations made so far. In order to ignore damping the duration of the pulse τ must be short enough to satisfy $\tau < T_1, T'_2$. On the other hand, the validity of the slowly varying envelope Maxwell equations 4.5 rests on τ being long enough to satisfy $\tau \gg 1/\omega$. In a wide variety of optically resonant materials both restrictions can be met if τ falls between 10^{-8} and 10^{-13} sec. Thus there is a range of about 5 orders of magnitude over which τ can vary without seriously invalidating our basic equations.

Ordinarily the on-resonance atoms experience the most dramatic effects in any interaction. Thus we look first at the Bloch equations exactly on resonance, remembering that \mathcal{E} is now time-dependent. The most common initial condition, in which all atoms are in their ground states, leads to $u(t, z; \Delta=0)=0$ for all time. In that case the optical Bloch equations reduce to a pair solved already:

$$\dot{v} = \kappa \mathcal{E} w, \quad (4.10)$$

$$\dot{w} = -\kappa \mathcal{E} v. \quad (4.11)$$

The solutions have been given in equations 3.1:

$$v(t, z; 0) = -\sin \theta(t, z), \quad (4.12)$$

$$w(t, z; 0) = -\cos \theta(t, z), \quad (4.13)$$

where the Bloch vector tipping angle is identical with the pulse “area” in the familiar way,

$$\theta(t, z) = \kappa \int_{-\infty}^t \mathcal{E}(t', z) dt', \quad (4.14)$$

except that now a dependence on position has been allowed for.

Because $\mathcal{E}(t, z)$ is time-dependent, the Rabi solutions of Chapter 3 cannot be expected to be relevant here. However, it may be reasonable to expect that the off-resonance dipoles respond to \mathcal{E} in the same way as the resonant dipoles, but perhaps with a detuning-dependent reduction in amplitude. Thus we assume the validity of the simple factorization

$$v(t, z; \Delta) = v(t, z; 0) F(\Delta), \quad (4.15)$$

where $F(\Delta)$ is called the dipole “spectral response” function. Surprisingly, with the aid of this factorization assumption it is not very difficult to solve the Bloch equations completely. Note first of all that equation 4.9c is immediately integrable if $\dot{\theta}$ is substituted for $\kappa \mathcal{E}$, and v is expressed in terms of θ by using equations 4.12 and 4.15. The result is

$$w(t, z; \Delta) = -F(\Delta) \cos \theta + F(\Delta) - 1. \quad (4.16)$$

Only $u(t, z; \Delta)$ is still unknown as a function of θ but that barrier can easily be overcome. Both equations 4.9a and 4.9b can be solved for $\Delta \dot{u}$. These two relations for $\Delta \dot{u}$, when equated, give an equation for θ alone:

$$\ddot{\theta} = \frac{\Delta^2 F(\Delta)}{1 - F(\Delta)} \sin \theta,$$

an equation familiar from the theory of the pendulum. What is more, the coefficient of $\sin \theta$ cannot depend on Δ , because neither $\ddot{\theta}$ nor $\sin \theta$ depend on Δ . By convention this coefficient is labeled $1/\tau^2$. Then the equation is simply

$$\ddot{\theta} - \frac{1}{\tau^2} \sin \theta = 0, \quad (4.17)$$

and θ has the full range of elliptic function solutions typical of pendulum problems [1].

Only one of the pendulum solutions to the Bloch-vector tipping angle equation 4.18 can be made to fit the boundary conditions appropriate to a

single pulse. Both \mathcal{E} and $\dot{\mathcal{E}}$ must vanish at $t = \pm\infty$, so that $\dot{\theta}$ and $\ddot{\theta}$ must satisfy the same conditions. Such restrictions imply a nonoscillating pendulum, a situation that is possible only if the pendulum was balanced vertically in the infinite past and then falls and swings once completely over to end up just balanced vertically again in the infinite future. The associated solution for θ is:

$$\theta(t, z) = 4 \tan^{-1} \left[\exp \left(\frac{t - t_0}{\tau} \right) \right], \quad (4.18)$$

and the electric field envelope corresponding to such θ behavior is the famous hyperbolic secant pulse of McCall and Hahn [2]:

$$\mathcal{E}(t, z) = \left(\frac{2}{\kappa\tau} \right) \operatorname{sech} \frac{t - t_0}{\tau}. \quad (4.19)$$

The z dependences of θ and \mathcal{E} are obviously still hidden in t_0 . The parameter τ is clearly the pulse length and deserves its position as a primary characteristic of the solution. The dipole spectral response function can be found in terms of the pulse length and the detuning:

$$F(\Delta) = \frac{1}{1 + (\Delta\tau)^2}, \quad (4.20)$$

and is obviously Lorentzian.

The analytic solutions for the atomic variables may also be determined explicitly. They are most easily derived by use of the relation $\cos(\theta/2) = -\tanh[(t - t_0)/\tau]$. It is then found that [2]

$$u = \frac{2\Delta\tau}{1 + (\Delta\tau)^2} \operatorname{sech} \left(\frac{t - t_0}{\tau} \right), \quad (4.21a)$$

$$v = \frac{2}{1 + (\Delta\tau)^2} \operatorname{sech} \left(\frac{t - t_0}{\tau} \right) \tanh \left(\frac{t - t_0}{\tau} \right), \quad (4.21b)$$

$$w = -1 + \frac{2}{1 + (\Delta\tau)^2} \operatorname{sech}^2 \left(\frac{t - t_0}{\tau} \right). \quad (4.21c)$$

It is also simple to verify that the probability conservation law is exactly fulfilled: $u^2 + v^2 + w^2 = 1$. Thus solutions for the coupled Bloch variables u ,

v , and w are relatively easily found. The trajectory on the unit sphere of the Bloch vector corresponding to these solutions is shown in Fig. 4.1. The several curves depict vectors with different detunings Δ . Only the on-resonance vectors have no projection on the u axis, corresponding to a dipole exactly in quadrature with the electric field.

However, the solution 4.19 for the electric field envelope is more remarkable. Without introducing Maxwell's equations, in any form, the dependence on time of the electric field amplitude has been determined. This shows the strength of the constraints that the nonlinearities of the quantum dipole equations impose on the phenomena of resonance optics.

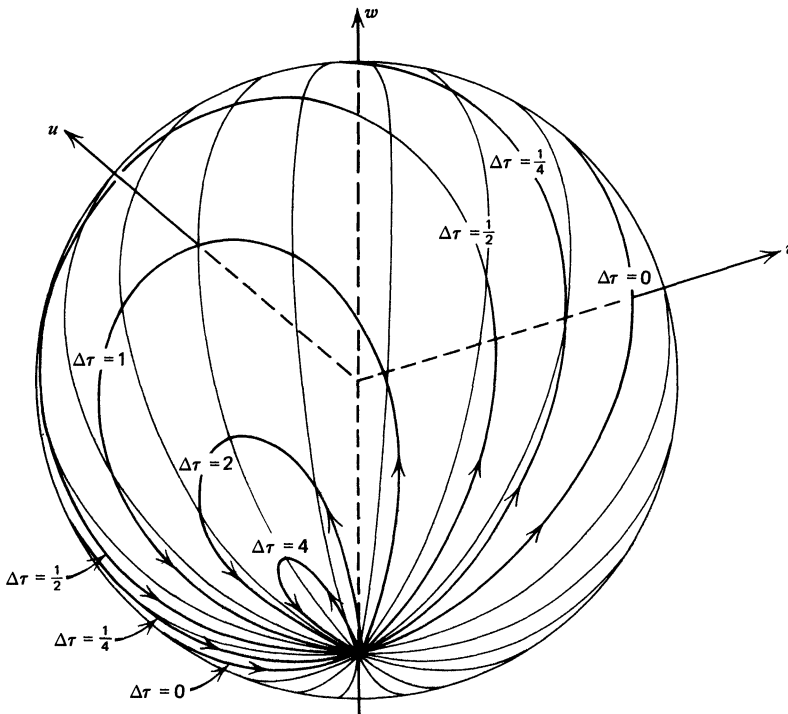


Fig. 4.1 Bloch vector trajectories on the unit sphere corresponding to the solutions to the Bloch equations given in equations 4.21. The different trajectories correspond to Bloch vectors with different detunings, and the labels give the value of $\Delta\tau$. In every case the vector is being driven by the 2π sech pulse given in equation 4.19; and τ is the pulse length. [From S. L. McCall and E. L. Hahn, *Phys. Rev.* **183**, 457 (1969).]

The unposed question is: what is the relation between Maxwell's equations and the unique one-pulse solution 4.19 that the atomic equations imply? To answer the question, one could simply substitute equations 4.19 and 4.21 into Maxwell's equations directly. However, a much more revealing and deeper approach is to attack Maxwell's equations independently of these specific solutions, and instead ask what general forms of pulse evolution are possible. This approach will lead directly to the quantum mechanical “area theorem” of McCall and Hahn [2].

4.4 THE MCCALL-HAHN “AREA THEOREM”

In Section 1.6 the idea of electric field envelope “area” was used to re-derive Beer’s law of absorption for electric fields in dielectrics. Moreover, there was some advantage to the “area” approach if the electric field consisted of an arbitrary pulse instead of a steady field. The area approach showed that an exponential absorption law was still valid, even if the individual dipole damping time was very long compared with an observation time, the case that we labeled “modern,” but that absorption then arose from polarization decay due to inhomogeneous dephasing effects rather than from individual dipole damping.

We make use of these classical insights in this section, and derive a quantum mechanical “area theorem,” one that is both qualitatively and quantitatively different from the classical theorem. The situation to be studied is conceptually the same as that of the “modern” case in Chapter 1. To emphasize this fact, Fig. 1.2 is reproduced as Fig. 4.2.

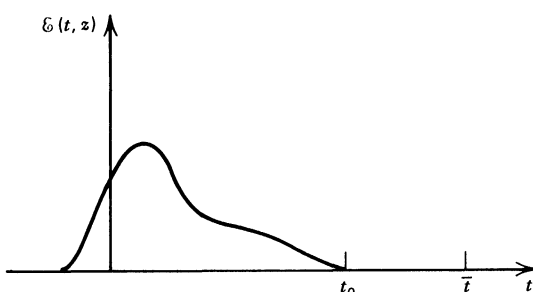


Fig. 4.2 The electric field envelope at position z as a function of time. Time t_0 marks the end of the pulse: at t_0 and for all later times the envelope is zero.

After defining envelope area as in equation 1.38,

$$A(t, z) = \kappa \int_{-\infty}^t \mathcal{E}(t', z) dt', \quad (4.22)$$

the first step is the integration of the in-quadrature Maxwell equation 4.4b from $t = -\infty$ up to the time \bar{t} that occurs after the pulse has passed the point of observation z . The quantum mechanical result is:

$$\frac{\partial A(\bar{t}, z)}{\partial z} = \frac{\pi \mathcal{N} \hbar \kappa^2}{2K} k^2 \int d\Delta g(\Delta) \int_{-\infty}^{\bar{t}} v(t, z; \Delta) dt,$$

in obvious analogy to the classical expression 1.39. The time integral, as well as the consequent detuning integral, are done exactly as in the classical treatment. Despite the appearance of w in the quantum equation for v , the result is

$$\frac{\partial A}{\partial z} = \frac{\pi \mathcal{N} \hbar \kappa^2}{K} k^2 \pi g(0) v(t_0, z; 0), \quad (4.23)$$

which is the counterpart to the classical equations 1.48 and 1.49. It is obtained if the pulse is substantially shorter than T'_2 . To obtain exactly the classical result it is only necessary to make the replacement $\kappa d \rightarrow e^2/m\omega$, which is valid in the classical regime.

However, at this point quantum nonlinearities enter the picture. In contrast to the classical situation, the absorptive part of the on-resonance dipole amplitude is a nonlinear function of θ , and thus of area:

$$v(t_0, z; 0) = -\sin A(t_0, z). \quad (4.24)$$

Because $\mathcal{E}(t, z) = 0$ for all $t > t_0$, $A(\bar{t}, z)$ is exactly the same as $A(t_0, z)$. The “area theorem” first derived by McCall and Hahn in 1967 [2] is thus an immediate consequence of the combined equations 4.23 and 4.24:

$$\frac{\partial}{\partial z} A(\bar{t}, z) = -\frac{1}{2} \alpha \sin A(\bar{t}, z). \quad (4.25)$$

The absorption coefficient α is

$$\alpha = \frac{4\pi^2 \mathcal{N} \omega d^2 g(0)}{\hbar c}, \quad (4.26)$$

if we recall $d = \frac{1}{2}\hbar\kappa$ and ignore the small distinction between K and k . It should be remarked that there is no consistent expression for α in the optical resonance literature. This is because different definitions of "the" dipole moment d are occasionally encountered. In Section 4.7 we comment further on this point.

It is common to call α the reciprocal Beer's absorption length, and α can be recognized as the quantum analog of the reciprocal absorption length α_c of Chapter 1. In fact if we merely insert the identity $2d^2/\hbar = \kappa d$ into the relation 4.26 defining α and then make the classical replacement $\kappa d \rightarrow e^2/m\omega$, α is found to be identical to α_c as given in equation 1.35c. This is

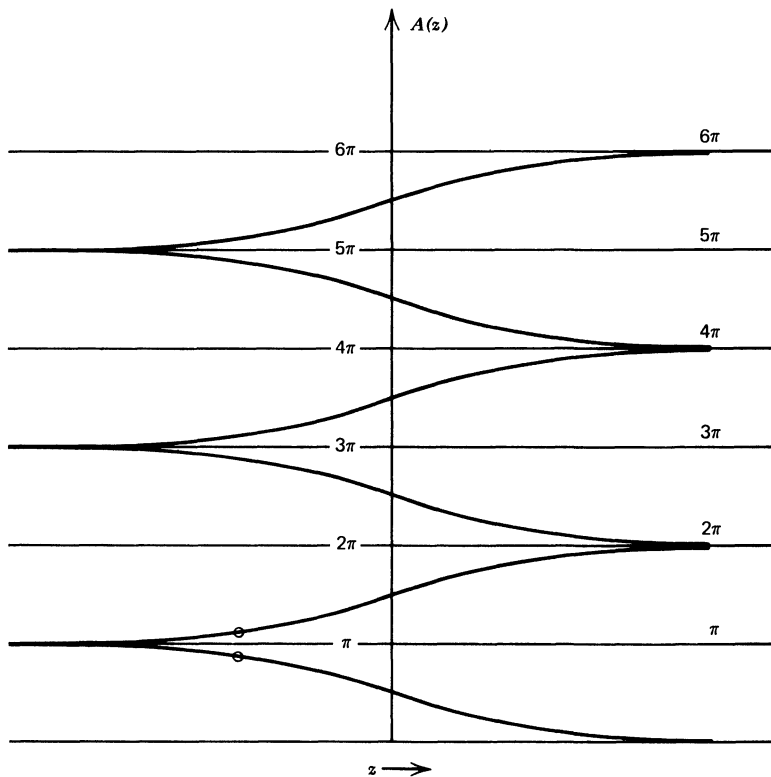


Fig. 4.3 The McCall-Hahn quantum optical area theorem. Several branches of the solution to equation 4.25 are shown by plotting envelope area against distance of penetration of the pulse into the medium. The value of z that corresponds to the entry face of the absorber is determined by the input area of the pulse. The location of the entry face in the case of 0.9π and 1.1π pulses is shown by the circles on the lower two curves.

to be expected. In the limit of weak fields the area is small and $\sin A \approx A$, so that in this limit the quantum area theorem becomes a linear relation

$$\frac{\partial}{\partial z} A(t, z) = -\frac{1}{2} \alpha A(t, z) \quad (\text{weak field}). \quad (4.27)$$

At the same time, in the limit of weak fields the atom is never excited far from its ground state. As we showed in Section 2.5, an atom near to its ground state obeys purely classical equations. Thus the coefficient α in the quantum area theorem *must* be the same as the coefficient α_c in Chapter 1, and we can hereafter understand the classical area theorem to be the quantum area theorem taken in the limit of weak fields.

In contrasting the quantum and classical area theorems 4.25 and 4.27 it is apparent that when $A \gtrsim \pi$, there are significant new features in the quantum expression. Most important, if $A = n\pi$, for any n , the pulse envelope area suffers no attenuation in propagation, since $\partial A / \partial z = 0$. The areas that are even multiples of π are more stable than those that are odd multiples. This is shown in Fig. 4.3. With increasing penetration of the pulse into the absorber, the area tends toward even multiples of π .

Gibbs and Slusher [3] have used the implications of the third branch of the area curve shown in Fig. 4.3 in a successful attempt to compress and amplify strong pulses by sending them through an *absorbing* medium. If a strong pulse with $A = 3\pi$ is injected into the medium, Fig. 4.3 shows that it will tend toward $A = 2\pi$ as it propagates. However, if the pulse is shorter than about 10 nsec, which is relatively easy to accomplish, there are no effective energy-loss mechanisms available to it. That is, it does not interact with any given group of atoms long enough for either T_1 or T'_2 to be effective. Thus it will have approximately the same energy, no matter what the area. Some justification for this approximation comes from the numerical computations due to McCall and Hahn [2] that show that the energy loss rate of a 3π pulse is on the order of $\frac{1}{10}$ the rate α which enters the area theorem and classical Beer's law decay. As a consequence it is approximately true that $W_{3\pi} = W_{2\pi}$, where the energies of the original 3π pulse and of its eventual 2π successor may be written, roughly, as

$$W_{3\pi} \propto \hat{\mathcal{E}}_{3\pi}^2 \tau_{3\pi}, \quad (4.28)$$

$$W_{2\pi} \propto \hat{\mathcal{E}}_{2\pi}^2 \tau_{2\pi},$$

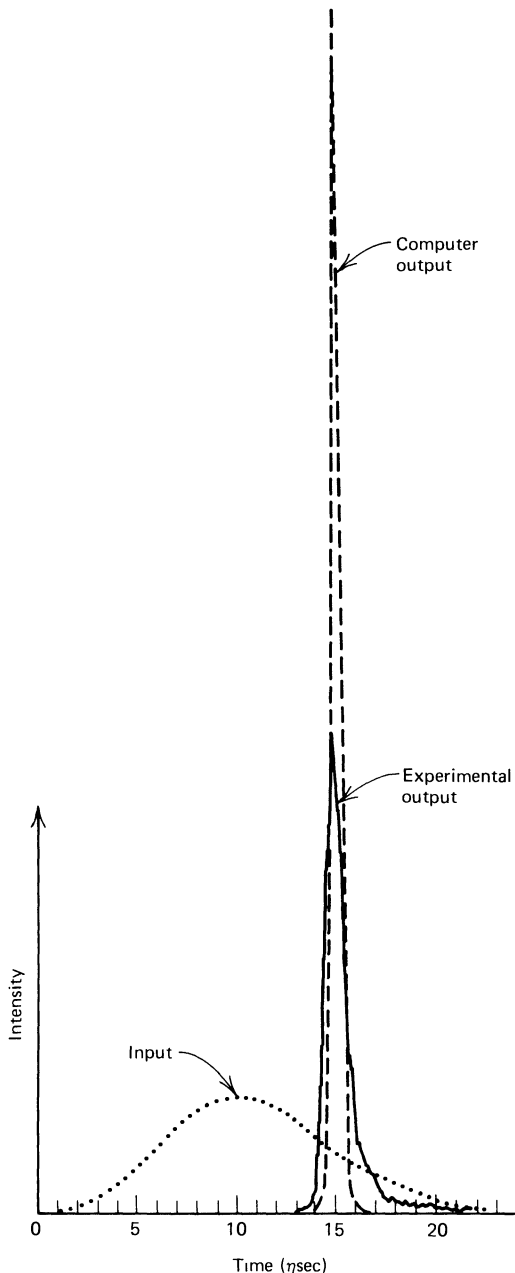


Fig. 4.4 Optical pulse compression and peak amplification by propagation in a passive absorber. The solid and dashed curves are the experimental and theoretical output pulses, and the dotted curve is the input pulse with area 3.5π . [From H. M. Gibbs and R. E. Slusher, *Appl. Phys. Lett.* **18**, 505 (1971).]

where $\tau_{3\pi}$ and $\tau_{2\pi}$ are the lengths of the pulse in its 3π and 2π forms. But $(\kappa \tilde{\mathcal{E}}_{2\pi})\tau_{2\pi} = 2\pi$, and $(\kappa \tilde{\mathcal{E}}_{3\pi})\tau_{3\pi} = 3\pi$, if the pulses are reasonably smooth. The relations hold exactly, of course, for square pulses. Thus equating $W_{3\pi}$ and $W_{2\pi}$, we may write

$$3\pi \tilde{\mathcal{E}}_{3\pi} = 2\pi \tilde{\mathcal{E}}_{2\pi}.$$

What is more, it is easy to establish that

$$\tau_{2\pi} = \frac{4}{9}\tau_{3\pi}, \quad (4.29)$$

which shows that the 3π pulse has become substantially shorter as well as more intense in its evolution toward 2π . The very real practical possibilities of such pulse shortening are shown in Fig. 4.4.

Since pulse area and dipole turning angle θ are identical, it is clear that a $2\pi n$ pulse is merely one that returns the dipole exactly to its original state. That such pulses should be particularly stable against disruption by interaction with the atoms is also clear. If such a pulse returns the dipole exactly to its original state, then the dipole can take no energy from the pulse.

Finally, it should be remarked that the stable long-lived pulses implied by the quantum area theorem are quite different from those discussed in Section 1.7. Indeed the area theorem derived here depends on the dephasing of the atomic dipole moments in the interval between T_2^* and T_2' . Here there is no assumption that the pulse is extremely short, whereas $\tau < T_2^*$ and $\tau < T_2'$ were both required in Chapter 1.

4.5 SELF-INDUCED TRANSPARENCY

A novel consequence of the nonlinear interaction of the field with the resonant atoms was observed by McCall and Hahn in computer solutions of the coupled Maxwell and optical Bloch equations and subsequently confirmed experimentally by them [2]. The nature of the effect is easily understood qualitatively. The quantum mechanical area theorem shows that slowly varying optical pulses with area equal to an integer multiple of 2π will be "stable." What McCall and Hahn inferred from their numerical results was that not only the area, but also the shape appeared to be stable after the pulse had propagated through a few Beer's absorption lengths of

resonant absorber, but before the pulse had propagated for times as long as either T_1 or T'_2 . These pulses behaved as if the medium were transparent; and McCall and Hahn named the phenomenon "self-induced transparency" to call attention to the fact that it is the special 2π property of the pulse itself which makes the medium "transparent" to it. Such anomalous pulse behavior is shown in Fig. 4.5.

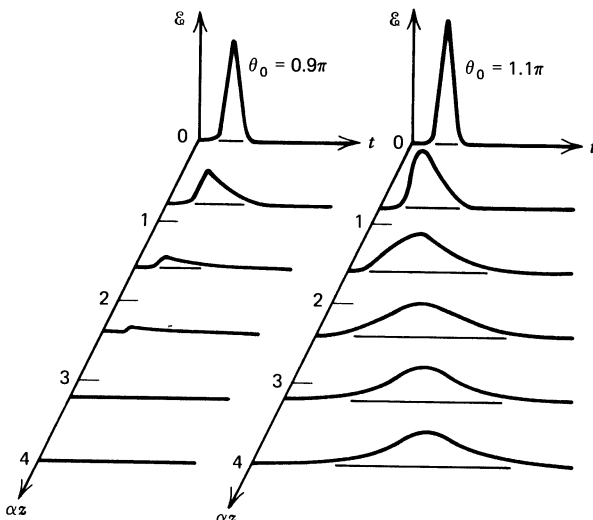


Fig. 4.5 Pulse area plots showing the anomalous behavior predicted by the area theorem. A pulse with input area slightly below π is rapidly attenuated as it evolves toward zero area, whereas a pulse with input area slightly above π is attenuated relatively little as it evolves toward 2π area and a sech shape. [From S. L. McCall and E. L. Hahn, *Phys. Rev.* **183**, 457 (1969).]

We now demonstrate that a 2π pulse which is both area-stable and shape-stable is indeed a solution of the lossless coupled Maxwell and optical Bloch equations. If a pulse is to have a constant shape, it must look the same to any observer, and can therefore be called a steady-state pulse. The simplest way to ensure the steady-state property is to require the field and dipole envelope functions to depend on time and space only through the "local time" coordinate $\xi = t - z/V$, where V is the constant pulse velocity. If this is the case, the partial derivatives appearing in equation

4.4b can be converted to ordinary derivatives with respect to ξ :

$$\frac{\partial}{\partial t} \rightarrow \frac{d}{d\xi} \quad \text{and} \quad \frac{\partial}{\partial z} \rightarrow -\left(\frac{1}{V}\right) \frac{d}{d\xi}.$$

If a dot (\cdot) now stands for a ξ derivative rather than a time derivative, then only the in-quadrature Maxwell equation changes in appearance:

$$[K^2 - k^2] \dot{\mathcal{E}}(t, z) = +2\pi k^2 \mathcal{N} d \int u(t, z; \Delta') g(\Delta') d\Delta', \quad (4.30a)$$

$$2\left(\frac{K}{V} - \frac{k}{c}\right) \dot{\mathcal{E}}(t, z) = -2\pi k^2 \mathcal{N} d \int v(t, z; \Delta') g(\Delta') d\Delta'. \quad (4.30b)$$

The solution of equations 4.30, together with the lossless atomic equations 4.9 can be accomplished in several ways. The most commonly used techniques all involve the use of the factorization assumption 4.15. We follow the methods used by Matulic and Eberly [4].

The energy flow conservation relation 4.7 takes an especially simple form in the case of steady-state pulses, because both sides of the relation are exact derivatives with respect to ξ , allowing it to be integrated once. By making use of the factorization 4.15 as well as the convenient shorthand definition

$$\frac{1}{\mu^2} \equiv \frac{\pi(\omega/c)^2 \mathcal{N}(d/\kappa)}{K/V - k/c} \int F(\Delta') g(\Delta') d\Delta', \quad (4.31)$$

we find the following conservation relation between atomic inversion $w(\xi; \Delta)$ and the field energy flux $\mathcal{E}^2(\xi)$:

$$w(\xi; \Delta) = w_0(\Delta) + \frac{1}{2} \mu^2 F(\Delta) \mathcal{E}^2(\xi). \quad (4.32)$$

Here the constant $w_0(\Delta)$ is clearly the value taken by the inversion when the field vanishes. A second integral of the combined Maxwell and optical Bloch equations is also easy to derive. Elimination of $v(\xi; \Delta)$ between equations 4.9a and 4.9c, together with the use of the energy conservation relation 4.32 derived above, leads to

$$u(\xi; \Delta) = u_0(\Delta) + \frac{\Delta}{\kappa} \mu^2 F(\Delta) \mathcal{E}(\xi). \quad (4.33)$$

This is a relation between \mathcal{E} and the in-phase dipole amplitude that has strong resemblances to the purely classical relation 1.20a.

Both integrations 4.32 and 4.33 of the Bloch equations 4.5 are exact only in the limits $T_1 \rightarrow \infty$ and $T'_2 \rightarrow \infty$. For finite T_1 and T'_2 these relations will be in error by amounts of the order of t/T_1 and t/T'_2 , where t is the integration time. In all cases of interest the integration time will be effectively bounded by the time duration of the excitation, that is, by the pulse length τ . Therefore, as anticipated, we are constrained to consider pulses that are sufficiently short for both $\tau/T_1 \ll 1$ and $\tau/T'_2 \ll 1$ to be valid.

The next step is to obtain an equation for the field envelope itself. This is done by differentiating equation 4.30b once with respect to ζ , and then using the second Bloch equation to replace \dot{v} by $\Delta u + \kappa \mathcal{E} w$. Then u and w may be expressed entirely in terms of powers of \mathcal{E} and various constants by repeated use of the conservation relations 4.32 and 4.33. The resulting equation itself has an obvious first integral. If we assume that the atoms are initially in their ground states, then at $\zeta = -\infty$ it follows that $u = v = 0$ and $w = -1$. Similarly, it is certainly true of any physical pulse that $\mathcal{E}(-\infty) = 0$ and $\dot{\mathcal{E}}(-\infty) = 0$. Taking account of these initial conditions, the envelope equation in its simplest form becomes

$$\dot{\mathcal{E}}^2 = \left(\frac{\kappa}{2}\right)^2 \mathcal{E}^2 [M^2 - \mathcal{E}^2], \quad (4.34)$$

where the constant M is given by

$$M^2 = \left(\frac{4}{\kappa^2}\right) \left[\frac{\kappa^2}{\mu^2 F - \Delta^2} \right]. \quad (4.35)$$

Although it is possible to integrate equation 4.34, many of the properties of its solution are transparent when it is considered graphically. A graphical analysis leads, for example, to an easy understanding of the physical meaning of the constant M .

In Fig. 4.6 we show $\dot{\mathcal{E}}^2$ plotted as a function of \mathcal{E}^2 . The physically possible values of \mathcal{E}^2 lie between 0 and M^2 , since $\dot{\mathcal{E}}^2$ must certainly be positive. We see that M is the maximum value of \mathcal{E} . Moreover, it may be shown that for very weak fields equation 4.34 predicts exponential growth of \mathcal{E} at the rate $\frac{1}{2}\kappa M$. Thus M not only fixes the eventual maximum intensity of the pulse, but also controls the rate at which the maximum is reached. This dual role for M will be seen to be equivalent to a restriction on the area of the pulse. By convention the weak-field growth rate of the

field envelope is denoted by $1/\tau$. Thus it follows that $M^2 = 4/\kappa^2\tau^2$; and then the definition 4.35 and the condition $F(0) = 1$ allow μ^2 and $F(\Delta)$ to be found separately:

$$F(\Delta) = \frac{1}{1 + (\Delta\tau)^2} \quad (4.36)$$

and

$$\mu^2 = \kappa^2\tau^2. \quad (4.37)$$

Finally the explicit solution for the envelope function

$$\mathcal{E}(\zeta) = \frac{2}{\kappa\tau} \operatorname{sech} \left(\frac{\zeta}{\tau} \right) \quad (4.38)$$

follows from these parameter evaluations and from a straightforward integration of equation 4.34.

It is simple to show that the area of the envelope in equation 4.38 is 2π , independent of both κ and τ . As mentioned above, this is a consequence of

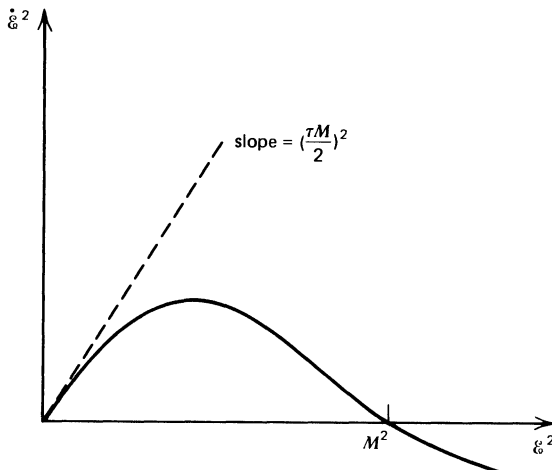


Fig. 4.6 A phase-plane plot of equation 4.34 for the steady-state pulse envelope. The same parameter M determines both the maximum value of the envelope and the weak-field growth rate $\dot{\mathcal{E}}/\mathcal{E}$, and thus fixes the pulse area. [Adapted from R. A. Marth, D. A. Holmes, and J. H. Eberly, *Phys. Rev. A* **9**, 2733, (1974).]

the fact that the maximum amplitude $2/\kappa\tau$ and the small-field growth rate $1/\tau$ involve τ in the same way.

The envelope solution 4.38 is exactly the same as that found earlier in equation 4.19, except that the variable of integration now is $\zeta = t - z/V$. The expression found here for $F(\Delta)$ is also the same as found previously. Furthermore, it is easy to verify that the solutions for u , v , and w are the same expressions given in relations 4.21. Thus the integration of the time-dependent Bloch equations in Section 4.3 is consistent with the integration here of the space- and time-dependent coupled Maxwell and Bloch equations, under the condition that the pulse and its interaction travel at a constant fixed velocity V . It is interesting to look carefully at the expression for the velocity of the 2π sech pulse. From relation 4.37 and the definition 4.31 it follows that:

$$\frac{1}{V} = \frac{1}{c} + \frac{\pi \mathcal{N} \hbar \omega \kappa^2}{2c} \int \frac{g(\Delta') d\Delta'}{\Delta'^2 + (1/\tau)^2}.$$

Here we have used a result derived below, namely that to a good approximation $K \approx k = \omega/c$. It is usually most convenient to use the absorption coefficient α defined in equation 4.26 to express the velocity more simply:

$$\frac{1}{V} - \frac{1}{c} = \frac{\alpha}{2\pi g(0)} \int \frac{g(\Delta') d\Delta'}{\Delta'^2 + (1/\tau)^2}. \quad (4.39)$$

When the pulse length τ is substantially longer than $T_2^* \approx \pi g(0)$, the integral in equation 4.39 may be approximated by assuming that $g(\Delta')$ is sufficiently smooth and broad to be evaluated at the origin and removed from the integral. In that case one finds

$$\frac{c}{V} = 1 + \frac{1}{2} \alpha c \tau, \quad (4.40)$$

an exceptionally simple relationship between the pulse length and pulse velocity. Since $c\tau$ can be of the order of several meters, much longer than the medium's absorption length α^{-1} , the velocity of the pulse in the medium can be very much smaller than c . This effect has been verified experimentally, and is discussed in Chapter 5. Equation 4.40 shows that the delay suffered by a 2π pulse, because of the difference between V and c , in

traveling through a length L of absorber is given by

$$\tau_d = \frac{L}{V} - \frac{L}{c} = \frac{1}{2}(\alpha L)\tau. \quad (4.41)$$

It is easy, given the solutions already found for \mathcal{E} and u , to establish that the in-phase Maxwell equation 4.30a is also satisfied by the 2π -sech pulse of equation 4.38 if the carrier wave vector K satisfies

$$\frac{K^2 - k^2}{2k} = \frac{\alpha}{2\pi g(0)} \int \frac{\Delta' g(\Delta') d\Delta'}{\Delta'^2 + (1/\tau)^2}.$$

In the ordinary case $g(\Delta')$ is a very broad smooth function so that the integrand is approximately an odd function. Consequently, the integral is very small, and to within first order in small quantities the dispersion relation for K reduces to the expression:

$$K - k = \frac{\alpha}{2\pi g(0)} \int \frac{\Delta' g(\Delta') d\Delta'}{\Delta'^2 + (1/\tau)^2}. \quad (4.42)$$

The earlier approximation $K \approx k$, used in arriving at equation 4.39, is therefore justified.

In summary, self-induced transparency may be characterized as the phenomenon of short coherent pulses traveling anomalously long distances, at anomalously low velocities, through resonant absorbers. It is interesting that so much of the phenomenon is superficially a classical one. For example, neither the velocity formula 4.39 nor the dispersion relation 4.42 involve \hbar directly. It is only in the expression 4.38 for the pulse envelope itself that evidence of the nonclassical and nonlinear foundation of the effect is seen. The constant κ has a real meaning only in the nonlinear quantum theory of dipole oscillators.

It should be pointed out that we have exhibited only a steady-state 2π pulse, whereas the area theorem makes no great distinction between 2π and 4π and other $2n\pi$ pulses, or between steady-state and nonsteady-state pulses. It can be shown [4] that there are, in fact, no steady-state single-pulse solutions to the inhomogeneously broadened absorber problem other than the 2π sech pulse of equation 4.38. However, two other types of pulses have been investigated. On the one hand, Arecchi et al. [5], Crisp [6], and Eberly [7] have shown that infinite pulse-train solutions are possible. These have an area of $2\pi\infty$, and the envelope shape is determined by

certain elliptic functions. This is a natural consequence of the fact that the basic field equation, in either of the forms 4.17 or 4.34, is also the equation for a pendulum, for which the solutions are well-known to be elliptic functions. Physically such solutions correspond to a continual exchange of energy from a steady optical wave to the atoms and back, in the way that a pendulum that can rotate all the way over its pivot point continually exchanges kinetic energy for potential energy, and vice versa, as it rotates.

An entirely different type of self-induced transparency pulse has also been investigated, initially by G. L. Lamb, Jr. [8]. Lamb's methods are powerful enough to obtain analytic descriptions of non-shape-preserving propagating lossless pulses. His work describes pulse excitations with total envelope area equal to 4π or 6π , for example. In such cases the electric envelope splits up into discrete pieces, each with area 2π , but with different pulse lengths, amplitudes, and velocities. Thus a whole range of possibilities may be studied, including the "scattering" of one pulse by another as two pulses moving with different velocities pass through one another.

In Fig. 4.7 we show such a collision process, beginning at the point where two pulses have coalesced into a single pulse. The analytic expression for the combined envelope of these pulses, given by Lamb in an extensive review [8] of pulse propagation, is

$$\kappa \hat{\mathcal{E}}(t, z) = \left(\frac{\tau_1^2 - \tau_2^2}{\tau_1^2 + \tau_2^2} \right) \frac{\frac{2}{\tau_1} \operatorname{sech} \left(\frac{\xi_1}{\tau_1} \right) + \frac{2}{\tau_2} \operatorname{sech} \left(\frac{\xi_2}{\tau_2} \right)}{1 - \frac{2\tau_1\tau_2}{\tau_1^2 + \tau_2^2} \left[\tanh \frac{\xi_1}{\tau_1} \tanh \frac{\xi_2}{\tau_2} - \operatorname{sech} \frac{\xi_1}{\tau_1} \operatorname{sech} \frac{\xi_2}{\tau_2} \right]}, \quad (4.43)$$

where τ_1 and τ_2 are the widths of the two colliding pulses and ξ_1 and ξ_2 are the "local times" $t - z/V_1$ and $t - z/V_2$. The two velocities are related to the two pulse lengths by expressions similar to equation 4.40. As the two pulses move apart after the collision, the total envelope $\hat{\mathcal{E}}(t, z)$ splits into two separate steady-state envelopes:

$$\hat{\mathcal{E}}(t, z) \rightarrow \frac{2}{\kappa\tau_1} \operatorname{sech} \left(\frac{\xi_1}{\tau_1} \pm \phi \right) + \frac{2}{\kappa\tau_2} \operatorname{sech} \left(\frac{\xi_2}{\tau_2} \mp \phi \right),$$

each with area 2π . Here the relative phase ϕ depends on the pulse lengths

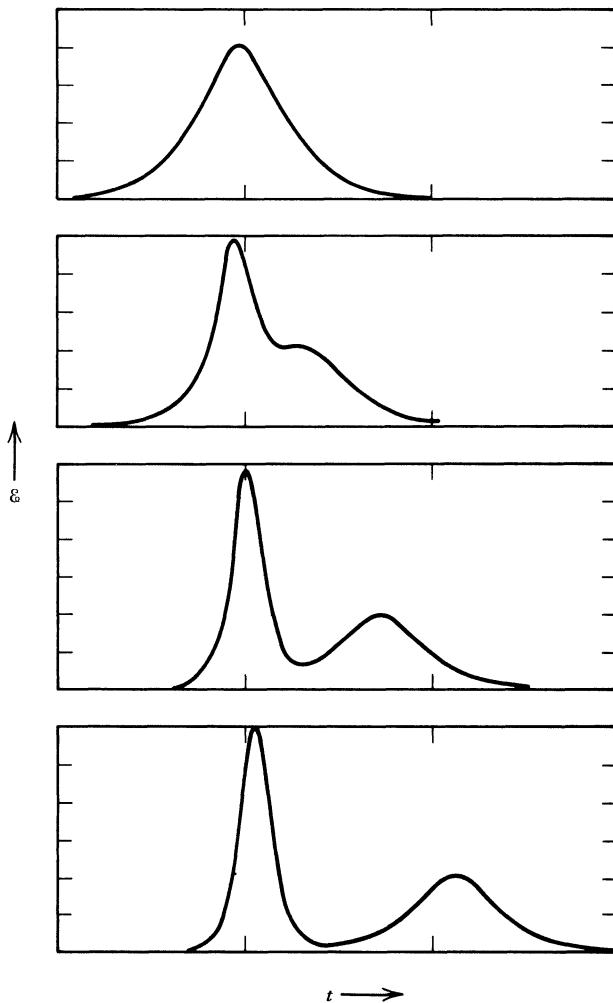


Fig. 4.7 Breakup of a 4π pulse into two 2π pulses. The envelope amplitude is shown as a function of time for four different positions in the absorber. Note the peak height growth during the course of breakup. [By permission of G. L. Lamb, Jr.]

in a relatively simple way:

$$\phi = 2 \left(\frac{\tau_2}{\tau_1} + \frac{\tau_1}{\tau_2} \right)^{-1}.$$

We also show in Fig. 4.8 three pulses in the process of moving away from a point of collision.

It should be pointed out that the conventional view of the processes shown in Figs. 4.7 and 4.8 is not that they are collisions, but that they exemplify pulse "breakup" of 4π and 6π pulses respectively. This view is closer to current experimental practice, and may be said to be verified in the work of Gibbs and Slusher, which is discussed in the next chapter.

It is interesting that out of a number of possible zero-area pulses [8], called $0\text{-}\pi$ pulses, there is one that does not seem to be interpretable in terms of a collision or a breakup. Figure 4.9 shows this pulse evolving in

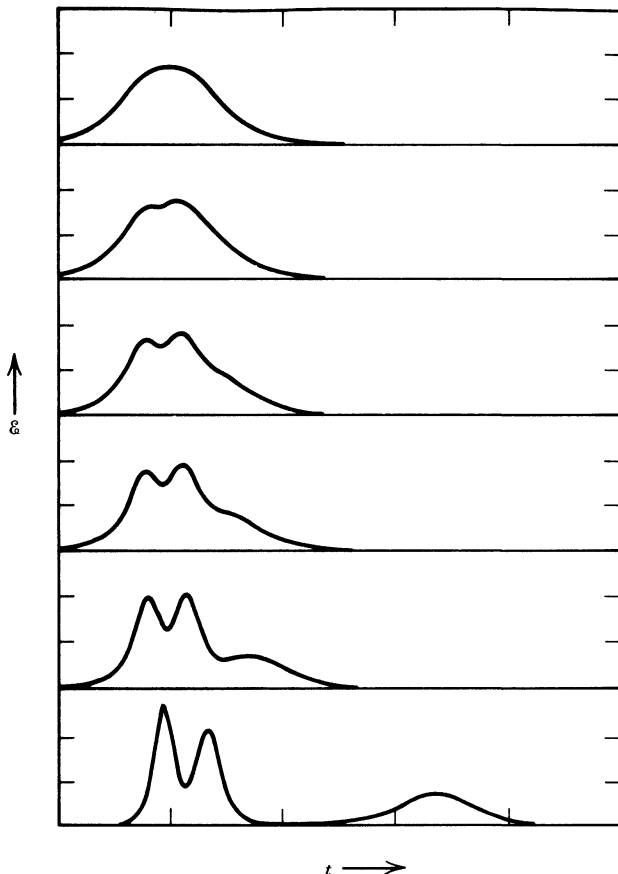


Fig. 4.8. Breakup of a 6π pulse into three 2π pulses. The envelope amplitude is shown as a function of time for six different positions in the absorber. Again note the peak height growth during the course of breakup. [From G. L. Lamb, Jr., *Rev. Mod. Phys.* **43**, 99 (1971).]

time. It might be called a "bound state" of two stable pulses, say with areas $+2\pi$ and -2π . The stability of such a "bound state" pulse, as well as the quantized areas observed in other pulses: $A = \pm 2n\pi$, have led to some speculation concerning nonlinear particle wave equations, and the possibility that elementary particle stability may be explained by nonlinear fundamental interactions. Some discussion of this point, as well as earlier references, may be found in a study of the so-called sine-Gordon equation by Rubinstein [9].

Finally it must be mentioned that very recent progress has allowed nonsteady-state solutions to the slowly varying optical pulse equations to

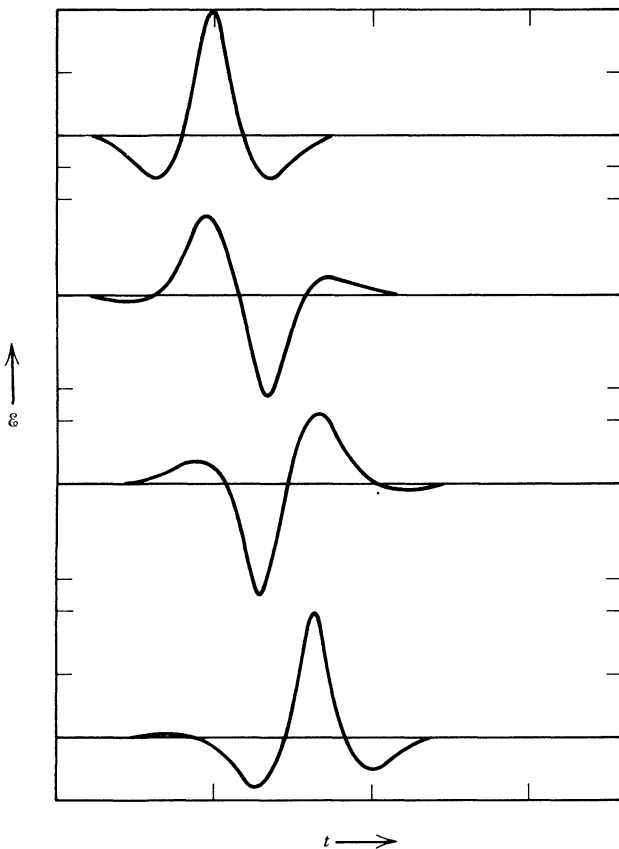


Fig. 4.9 A "bound state" 0π pulse that does not experience breakup. [From G. L. Lamb, Jr., *Rev. Mod. Phys.* **43**, 99 (1971).]

be obtained for an arbitrary number N of 2π pulses. A solution conjectured by Gibbon and Eilbeck [10] has been confirmed by them with Caudrey and Bullough [11]. Equally interesting is the remarkable discovery of solutions to the initial-value problem for a broad class of nonlinear evolution equations by Ablowitz, Kaup, Newell, and Segur [12]. The technique of inverse scattering is used to find the solutions. The existence of one method that successfully treats such nonlinear evolution equations as the Korteweg-de Vries equations, the sine-Gordon equation, and the Benney-Newell equation, in addition to the optical pulse equation, hints at important similarities in widely scattered branches of physics which are only beginning to be exploited. Undoubtedly advances in this field will continue to be made rapidly.

4.6 PHASE MODULATION EFFECTS

Some modifications arise to the earlier equations if we take a more general expression than formerly for the field

$$E(t, z) = \mathcal{E}(t, z)[e^{i(\omega t - Kz + \phi(t, z))} + \text{c. c.}], \quad (4.44)$$

where $\phi(t, z)$ is a phase function that is slowly varying in the same sense that $\mathcal{E}(t, z)$ has been assumed to be slowly varying. As before, the vacuum wave vector ω/c will be denoted by k . The instantaneous wave vector can now be identified as $K - \partial\phi/\partial z$, and is not necessarily a constant. There is also the possibility of a non-constant instantaneous field frequency, which may be denoted by $\omega(t)$:

$$\omega(t) = \omega + \frac{\partial}{\partial t} \phi(t, z), \quad (4.45)$$

leading to the possibility of frequency modulation phenomena that were formerly excluded.

The basic Bloch equations are not affected by this change until the rotating frame is chosen. Usually it is most convenient to work in the frame rotating at the field's instantaneous frequency. In that case the

Bloch equations for the rotating frame variables acquire new nonlinearities:

$$\dot{u} = -(\Delta - \dot{\phi})v, \quad (4.46a)$$

$$\dot{v} = (\Delta - \dot{\phi})u + \kappa \mathcal{E} w, \quad (4.46b)$$

$$\dot{w} = -\kappa \mathcal{E} v, \quad (4.46c)$$

and of course become considerably more difficult to analyze. The presence of a frequency-modulated field does not, however, affect probability conservation for the atom, and it may be verified easily that $u^2 + v^2 + w^2 = 1$, as before.

In addition to the changes in the Bloch equations, the second-order Maxwell wave equation has a more general slowly varying in-phase part. Specifically one finds for the Maxwell equations

$$\mathcal{E} \left[K^2 - k^2 - 2K \frac{\partial \phi}{\partial z} - 2k \frac{\partial \phi}{\partial ct} \right] = 2\pi k^2 \mathcal{N} d \int u g(\Delta') d\Delta', \quad (4.47)$$

$$\left[K \frac{\partial}{\partial z} + k \frac{\partial}{\partial ct} \right] \mathcal{E} = 2\pi k^2 \mathcal{N} d \int v g(\Delta') d\Delta'. \quad (4.48)$$

It is enough to mention three problems in which phase modulation plays a role. In the first of these the effect on the on-resonance atoms of a strong externally prescribed field is required. This is a variant of the Rabi problem; we are uninterested in the radiation emitted by the atoms, but merely ask for the response of the atoms to an applied field. Thus only equations 4.46 with $\Delta = 0$ are relevant, and we ignore the Maxwell equations.

Without presenting an answer of any generality to this question, we may simply observe that a “natural” solution follows if the impressed external field has a sech envelope and a tanh frequency sweep. Given that much, it is simple to construct a complete solution. If the magnitude of the frequency sweep is denoted by $2\delta\omega$, then

$$\dot{\phi} = -\delta\omega \tanh \frac{t - t_0}{\tau}, \quad (4.49a)$$

$$u = \frac{-\delta\omega\tau}{\sqrt{1 + (\delta\omega\tau)^2}} \operatorname{sech} \frac{t - t_0}{\tau}, \quad (4.49b)$$

$$v = \frac{-1}{\sqrt{1 + (\delta\omega\tau)^2}} \operatorname{sech} \frac{t - t_0}{\tau}, \quad (4.49c)$$

$$w = \tanh \frac{t - t_0}{\tau}, \quad (4.49d)$$

$$\mathcal{E} = \left(\frac{1}{\kappa\tau} \right) \sqrt{1 + (\delta\omega\tau)^2} \operatorname{sech} \frac{t - t_0}{\tau}. \quad (4.49e)$$

An interesting aspect of solutions 4.49 is that they provide an analytically exact extension of well-known approximate results in the context of adiabatic inversion. It is not surprising that this result should have some relation to adiabatic inversion. Adiabatic inversion is achieved in magnetic resonance by slowly changing the magnitude of the static \mathbf{z} component of the magnetic field so that the effective field changes sign, thus inverting all of the spins that are following the effective field. But inspection of the rotating frame torque vector 2.41 shows that it is as effective to frequency-modulate the driving field, that is, to put time dependence into ω , as it is to vary ω_0 .

The adiabatic changes implied by the solution 4.49 are sketched in Fig. 4.10. The atomic inversion w is shown on the same time axis with the driving field amplitude $\mathcal{E}(t, z)$, and the instantaneous frequency shift $\dot{\phi}(t, z)$. The heavy lines in the plots of \mathcal{E} and $\dot{\phi}$ show the constant-amplitude field and linear frequency sweep usually assumed in approximate treatments. It is important to realize that the analyticity of our exact solution eliminates all adiabatic restrictions. That is, because the solutions are infinitely smooth, the dipoles are effectively warned by the very weak leading edges of the pulse's amplitude and phase functions that an inverting pulse is coming. Thus the inversion process really is a slow one, having been started long before the pulse peak arrives, even though the main peak is made as short and sharp as desired. This could be a valuable experimental consideration if inhomogeneous broadening must be overcome. Treacy has given a short discussion [13] of complications due to T_2^* effects.

It is also interesting that solutions are valid for arbitrarily small or zero frequency modulation. If $\delta\omega \rightarrow 0$, then \mathcal{E} becomes a standard π pulse. That is, the area of the envelope in equation 4.49 is

$$A = \int \kappa \mathcal{E}(t, z) dt = \pi \sqrt{1 + (\delta\omega\tau)^2},$$

which reduces to $A = \pi$ as $\delta\omega \rightarrow 0$. A π pulse would naturally be expected to invert the atoms. On the other hand, if the frequency modulation were substantial enough so that $\delta\omega\tau = \sqrt{3}$, then $A = 2\pi$. In this case, the solutions no longer appear so readily understandable. We have discovered a 2π pulse that merely inverts the atoms, and does not return them to their ground states.

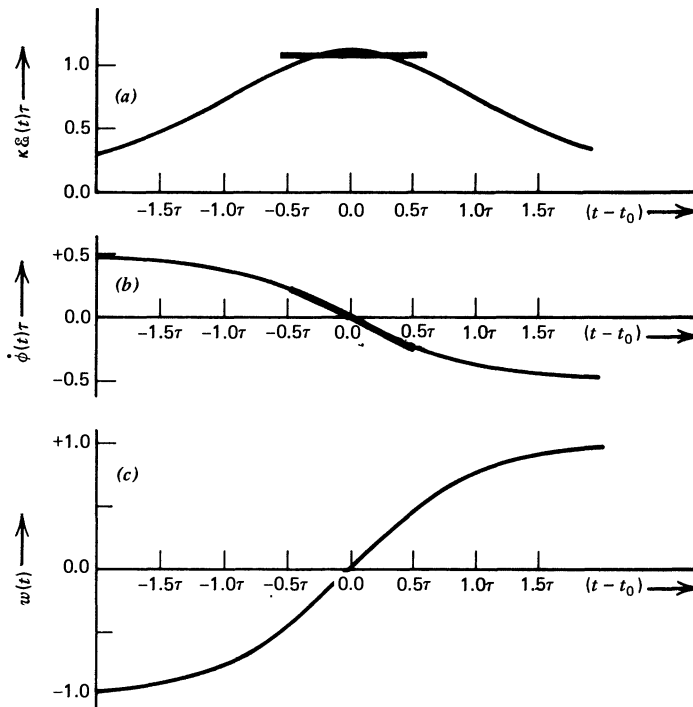


Fig. 4.10 Graphs of the solutions 4.49 showing “nonadiabatic” inversion by a chirped sech pulse.

The explanation is fairly simple. In the presence of frequency modulation, the identity between pulse area and dipole turning angle is no longer true. The most dramatic consequence, in principle, of this lack of identity is the failure of the area theorem. As soon as frequency modulation of the driving field is permitted, the usual area theorem cannot be derived, and there is no known replacement for it. This leads us to the second problem involving frequency modulation.

The knowledge that frequency modulation effects invalidate the derivation of the area theorem casts some doubt on the generality of the solution obtained in Section 4.5 for the lossfree 2π pulse of self-induced transparency. Such a pulse may seem to be only a mathematical fiction, arising physically only in the unlikely event that a pulse was absolutely free of frequency modulation.

It can be established [14], however, that within the approximations used in Section 4.5 no frequency modulation is possible in a self-consistent shape-preserving pulse. The important approximation made in Section 4.5 is the neglect of second derivative terms in writing the slowly varying envelope in-phase and in-quadrature Maxwell equations. Within that slowly varying restriction the only steady-state possibility for the field phase is in fact $\phi(t, z) = \text{constant}$, and $\dot{\phi}$ vanishes identically, allowing the area theorem to hold.

As in the preceding section, derivatives with respect to $\xi = t - z/V$ will be denoted by a dot (\cdot). After changing to the ξ variable, we differentiate the in-phase Maxwell equation 4.47 once more. The i that results from the differentiation may be eliminated by using equation 4.46a; and the factorization assumption 4.15 may be used to simplify the integration over detunings Δ' , with the result:

$$2\mathcal{E}\dot{\phi} + \ddot{\phi} = \left(\bar{\Delta} - \frac{K-k}{V^{-1}-c^{-1}} \right) \dot{\mathcal{E}}, \quad (4.50)$$

where we have used the very good approximation $(K^2 - k^2)/2K \approx K - k$ and the abbreviation

$$\bar{\Delta} = \frac{\int \Delta' F(\Delta') g(\Delta') d\Delta'}{\int F(\Delta') g(\Delta') d\Delta'}. \quad (4.51)$$

The phase equation 4.50 is a linear first-order equation for $\dot{\phi}$, and \mathcal{E} is its integrating factor. The solution

$$\dot{\phi} = \frac{1}{2} \left[\bar{\Delta} - \frac{K-k}{V^{-1}-c^{-1}} \right] \quad (4.52)$$

shows immediately that $\dot{\phi}$ is a constant. By convention, the pulse frequency shift is taken to be zero where there is no pulse, namely at $t = -\infty$. Therefore, because $\dot{\phi}(-\infty) = 0$, equation 4.52 shows that $\dot{\phi}(\xi) = 0$ for all

values of ζ . In other words, no frequency modulation is possible in a slowly varying steady-state pulse. Note that this result is more general than it first appears. The conclusion that $\dot{\phi}=0$, when applied to equation 4.52 leads to the expression

$$\frac{K-k}{V^{-1}-c^{-1}} = \frac{\int \Delta' F(\Delta') g(\Delta') d\Delta'}{\int F(\Delta') g(\Delta') d\Delta'},$$

which is exactly the ratio of results 4.41 and 4.39 for $K-k$ and $1/V-1/c$.

Finally, in a third and very recent development, Lamb has incorporated phase modulation effects into his optical pulse equations. He finds [15], in agreement with Matulic [14], that slowly varying 2π pulses are not

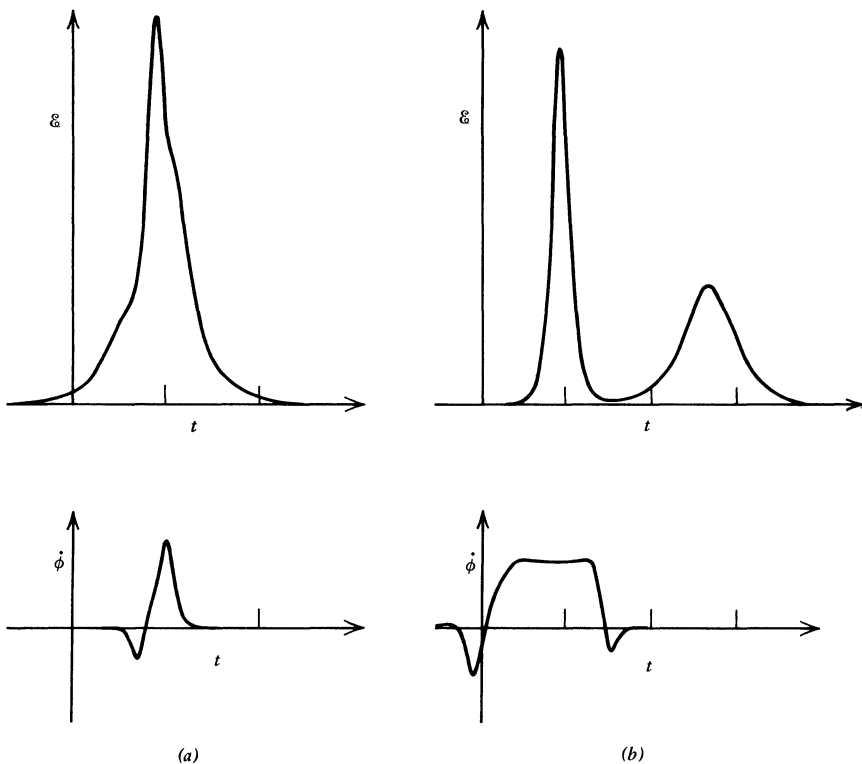


Fig. 4.11 Envelope amplitude and rate of change of phase of a 4π pulse: (a) initially and (b) at a later position in the absorber. The scales are different in each case. [From G. L. Lamb, Jr., *Phys. Rev. Lett.* **31**, 196 (1973).]

frequency-modulated. However, Lamb shows that the collision of two 2π pulses that have different carrier frequencies leads to a 4π pulse that can be frequency-modulated. An example of such a collision, or breakup, is shown in Fig. 4.11.

4.7 CIRCULARLY POLARIZED LIGHT

Certain convenience attaches to the use of circularly polarized light in optical resonance. For example, the optical Bloch equations 2.36 are then exact. No rotating wave approximation need be made in order to derive them. Unfortunately, caution must be exercised in translating formulas derived for linear polarization into their circularly polarized counterparts. This is because there is no consistent definition given for "the" dipole moment d in the literature. Slusher and Gibbs [16, Appendix D] have examined this point carefully.

However such a translation is readily possible if several elementary points are consistently observed. As an illustration we sketch below a derivation of the Bloch equations and the slowly varying envelope Maxwell equations for circularly polarized light and a $|\Delta M|=1$ transition.

A suitable definition for the envelope of a circularly polarized light wave is

$$\mathbf{E}_c(t, z) = (\sqrt{2}) \mathcal{E} [\mathbf{x} \cos(\omega t - Kz) + \mathbf{y} \sin(\omega t - Kz)]. \quad (4.54)$$

The presence of the $\sqrt{2}$ is to ensure that the wave carries the same energy as the linearly polarized wave defined by equation 4.3:

$$\mathbf{E}(t, z) = \mathcal{E} \mathbf{x} [e^{i(\omega t - Kz)} + \text{c. c.}], \quad (4.55)$$

which is the definition we have consistently chosen in this book. The factor $\sqrt{2}$ is, however, placed in parentheses because it is frequently not used in the literature (see [2], e.g.).

The precise written form of Maxwell's equations and of the optical Bloch equations depend on the envelope definition. However, the form of the Bloch equations depends only on the matrix elements of the product $\mathbf{d} \cdot \mathbf{E}$. For a $|\Delta M|=1$ transition, \mathbf{d}_{+-} is a number times the vector $\mathbf{x} \pm i\mathbf{y}$. This is shown, for example, in equation 2.11. Thus we define the quantity d

for a $|\Delta M|=1$ transition by

$$\mathbf{d}_{+-} = d \frac{\mathbf{x} - i\mathbf{y}}{(\sqrt{2})}. \quad (4.56)$$

The factor $\sqrt{2}$ is included so that $\mathbf{d}_{+-} \cdot \mathbf{d}_{-+} = d^2$, consistent with equations 2.27 and 2.28 and with the remainder of the book. Again the $\sqrt{2}$ is placed in parentheses to show that in many treatments it is ignored. Clearly, if both $(\sqrt{2})$'s in definitions 4.54 and 4.56 are retained, as we would prefer, or if both are discarded, as in the work of McCall and Hahn [2], the product $\mathbf{d}_{+-} \cdot \mathbf{E}$ remains the same and equals $d \mathcal{E} \exp[-i(\omega t - Kz)]$. Therefore either approach leads to the same optical Bloch equations, which in the rotating frame are the same as the equations 2.29 with the same definition 2.28 for κ .

The Maxwell equations are another matter because field envelope and dipole moment appear on opposite sides of the equations. The polarization density $P(t, z)$ is defined in terms of the expectation of the dipole moment operator. Because \mathbf{d}_{+-} is complex for a $|\Delta M|=\pm 1$ transition, the corresponding operator form for $\hat{\mathbf{d}}$ involves $\hat{\sigma}_2$ as well as $\hat{\sigma}_1$:

$$\hat{\mathbf{d}} \Rightarrow \begin{pmatrix} 0 & \mathbf{d}_{+-} \\ \mathbf{d}_{-+} & 0 \end{pmatrix} = \frac{d}{(\sqrt{2})} (\mathbf{x}\hat{\sigma}_1 + \mathbf{y}\hat{\sigma}_2). \quad (4.57)$$

Here the definition 4.56 as well as the Hermitian property $\mathbf{d}_{-+} = (\mathbf{d}_{+-})^*$ have both been used. Thus, in the notation of definitions 2.21 and 2.35,

$$\begin{aligned} \langle \hat{\mathbf{d}} \rangle = & \frac{d}{(\sqrt{2})} \{ u [\mathbf{x} \cos(\omega t - Kz) + \mathbf{y} \sin(\omega t - Kz)] \\ & + v [-\mathbf{x} \sin(\omega t - Kz) + \mathbf{y} \cos(\omega t - Kz)] \}, \end{aligned} \quad (4.58)$$

where it is obvious that u and v still have the significance assigned to them throughout the book: u is the amplitude of the part of $\langle \hat{\mathbf{d}} \rangle$ in-phase with \mathbf{E}_c and v is the in-quadrature amplitude.

The two slowly varying Maxwell equations that follow from \mathbf{E}_c as given in equation 4.54 and from $\mathbf{P} = \mathcal{N} \langle \hat{\mathbf{d}} \rangle$, with $\langle \hat{\mathbf{d}} \rangle$ given immediately above,

are

$$[K^2 - k^2](\sqrt{2}) \mathcal{E}(t, z) = 4\pi k^2 \mathcal{N} \frac{d}{(\sqrt{2})} u(t, z; \Delta), \quad (4.59a)$$

$$2 \left[K \frac{\partial}{\partial z} + k \frac{\partial}{\partial ct} \right] (\sqrt{2}) \mathcal{E}(t, z) = 4\pi k^2 \mathcal{N} \frac{d}{(\sqrt{2})} v(t, z; \Delta). \quad (4.59b)$$

These are identical with equations 4.4, apart from the inclusion of inhomogeneous broadening, only if both factors $(\sqrt{2})$ are retained. If both are discarded, the McCall-Hahn forms for these equations are obtained. This difference has no physical consequences, of course, since it arises from a difference in conventions regarding definitions of "the" envelope function \mathcal{E} and "the" dipole moment d . Obviously, however, caution must be exercised in comparing results of different authors, if they involve d or \mathcal{E} explicitly.

References

1. See any advanced mechanics textbook, or P. F. Byrd and M. D. Friedman, *Handbook of Elliptic Integrals*, Springer-Verlag, Berlin, 1954, p. 7, example V.
2. S. L. McCall and E. L. Hahn, *Phys. Rev.* **183**, 457 (1969); *Phys. Rev. Lett.* **18**, 908 (1967).
3. H. M. Gibbs and R. E. Slusher, *Appl. Phys. Lett.* **18**, 505 (1971).
4. L. Matulic and J. H. Eberly, *Phys. Rev. A* **6**, 822, 1258E (1972). See also R. A. Marth, D. A. Holmes, and J. H. Eberly, *Phys. Rev. A* **9**, 2733 (1974).
5. F. T. Arecchi, V. DeGiorgio, and C. G. Someda, *Phys. Lett.* **27A**, 588 (1968).
6. M. D. Crisp, *Phys. Rev. Lett.* **22**, 820 (1969).
7. J. H. Eberly, *Phys. Rev. Lett.* **22**, 760 (1969).
8. G. L. Lamb, Jr., *Phys. Lett.* **25A**, 181 (1967); *Rev. Mod. Phys.* **43**, 99 (1971). For a recent extension of these results, see T. W. Barnard, *Phys. Rev. A* **7**, 373 (1973).
9. J. Rubenstein, *J. Math. Phys.* **11**, 258 (1970).
10. J. D. Gibbon and J. C. Eilbeck, *J. Phys. A* **5**, L122 (1972).
11. P. J. Caudrey, J. D. Gibbon, J. C. Eilbeck, and R. K. Bullough, *Phys. Rev. Lett.* **30**, 237 (1973).
12. M. J. Ablowitz, D. J. Kaup, A. C. Newell, and H. Segur, *Phys. Rev. Lett.* **31**, 125 (1973).
13. E. B. Treacy, in *The Physics of Quantum Electronics* 1969, Optical Sciences Center Technical Report 45, J. B. Mandelbaum and S. F. Jacobs, eds., University of Arizona, 1969, pp. 183–187.
14. L. Matulic, *Optics Comm.* **2**, 249 (1970).
15. G. L. Lamb, Jr., *Phys. Rev. Lett.* **31**, 196 (1973).
16. R. E. Slusher and H. M. Gibbs, *Phys. Rev. A* **5**, 1634 (1972).

CHAPTER 5

Pulse Propagation Experiments

5.1 Introduction	110
5.2 Self-Induced Transparency	110
5.3 Effects of Degeneracy	117
5.4 Incoherent Saturation and Pulse Delay	121
5.5 π Pulses in Mode-Locked Lasers	126
References	128

5.1 INTRODUCTION

The observation of the remarkable phenomenon of self-induced transparency by McCall and Hahn in a ruby absorber inspired related experimental efforts on a wide scale. In this chapter we mention some of this work and describe some of the realities that hamper experimental work with $n\pi$ pulses—realities omitted from the idealistic theoretical treatment of the preceding chapter. These include the occasional appearance of a third energy level that interacts fairly strongly with the light; the frequent presence of level degeneracies in the resonant absorber; and the inevitable occurrence of incoherent relaxation phenomena, especially those associated with T_2' .

If a third energy level is close to the two resonant levels some doubt is cast on the validity of the two-level atom model that underlies all of the theory. For degenerate absorbers there is no known area theorem, with the consequence that only 0π pulses in degenerate media enjoy most of the advantages given to all $2n\pi$ pulses in nondegenerate absorbers. As for T_2' , its principal effect is to blur the distinction between coherent $n\pi$ pulse phenomena and incoherent saturation or bleaching.

5.2 SELF-INDUCED TRANSPARENCY

Even in their original paper [1] proposing a theory of self-induced transparency McCall and Hahn offered confirming experimental evidence that the effect existed. Their very difficult pioneering experiment required some compromises and not all the experimental parameters met the theoretical ideal. They realized that their light pulse entered the sample

with a nonuniform intensity distribution, but felt that any small portion of the wavefront could be assumed to obey the predictions of the plane-wave model for short distances. They anticipated, too, that the more intense portions of the beam would exhibit shorter pulse delays, and the less intense portions would exhibit longer ones. Significantly, they found delays equivalent to increases in optical path length of about 100 sample lengths.

In the McCall-Hahn experiment the absorber was a liquid-helium-cooled ruby rod while a *Q*-switched liquid-nitrogen-cooled ruby laser provided the short input pulse. The laser was designed to work on the $\bar{E}(2E) \rightarrow 4A_2(\pm\frac{3}{2})$ transition which, by thermal tuning, was made resonant with the $4A_2(\pm\frac{1}{2}) \rightarrow \bar{E}(2E)$ transition in the cold sample. With this arrangement they demonstrated that although weak light, well below the onset of nonlinear transmission, was attenuated by more than 10^5 , intense light was transmitted unattenuated. This self-induced transparency diminished with increasing temperature and disappeared at 40°K where the very rapid relaxation between the levels $2\bar{A}(2E)$ and $\bar{E}(2E)$ imposed the condition $T'_2 < \kappa$, and irreversible relaxations destroyed the prepared states of the atoms involved.

In light of experience with high-power lasers and saturated absorption, it might appear that the nonlinear transmission observed in self-induced transparency could be interpreted as a "hole-burning" or "bleaching" effect, in which the absorption profile is totally saturated by the leading edge of the pulse. The nature of incoherent saturation is discussed in detail in Section 5.4. A more nearly ideal experiment demonstration of self-induced transparency was not achieved until gaseous absorbers were investigated.

Patel and Slusher [2] were the first to present results for a gaseous absorber. They demonstrated delay times of about 0.2 μ sec in SF₆, and found output pulses that appeared more symmetric than the input pulses produced from a CO₂ laser. They showed, too, that their output pulse intensity always exceeded the corresponding maximum input pulse tail intensity over a major fraction of its duration and presented this as an argument that it was self-induced transparency that had been observed. However, their work was questioned, particularly by Rhodes, Szöke, and Javan [3], because of the questions of level degeneracy in the SF₆ and of bleaching or incoherent saturation. In a subsequent work Patel [4] argued against the idea that incoherent bleaching was the explanation of the results by showing that the optical delay was intensity-dependent and, indeed, that at higher SF₆ pressures the delay began to decrease after

passing a maximum. For our purposes the precise interpretation of the SF₆ results with respect to level degeneracy is peripheral. Clear-cut experiments in nondegenerate systems have now been performed, and we discuss the effects of degeneracy separately in Section 5.3.

Gibbs and Slusher [5] have described detailed experiments on the propagation of coherent optical pulses in dilute Rb vapor, a nondegenerate resonant absorber. Their input optical pulse came from a ²⁰²Hg II laser and had an entirely coherent frequency profile; that is, its spectral width was due to the finite extent in time of the pulse envelope and not to phase or frequency instabilities within the envelope. It was also known that the pulse was free of chirping. The pulse was passed through an aperture to ensure that the wavefront was sensibly plane and of uniform intensity.

The laser light was produced using a hollow cathode discharge tube pulsed at 160 pulses/sec. Then a 5 to 10 nsec portion of the 1 μ sec laser pulse was selected by means of a Pockels cell and passed into a 1 to 10 mm long cell of ⁸⁷Rb absorbing atoms at a vapor density of 10¹¹ to 10¹³ atoms/cm³. At zero magnetic field the relevant absorption line in rubidium is at 7947.64 Å. Slusher and Gibbs used a 74.5 kOe magnetic field to Zeeman-tune the transition to coincidence with the laser light at 7944.66 Å. Finally, only weak focusing of the laser light was required to obtain pulses with areas of several π .

As an absorber rubidium possesses many attractive features; one of the most important is that the use of the magnetic tuning not only puts the rubidium into resonance with the laser, but also selects a single transition between a pair of nondegenerate magnetic sublevels and picks out a discrete transition from those that arise because of the different values of M_F . In other words, the use of the magnetic field allows a simple two-level absorption with a unique dipole moment.

In the Slusher-Gibbs experiments the rubidium was homogeneously distributed through the absorption cell, and a high absorption coefficient could be achieved in a very short length of medium. The inverse Doppler width of the transition was 0.8 nsec while the pulse length τ was 7 nsec, long enough to ensure that all frequency components of the pulse were uniformly absorbed. The natural lifetime of the upper level was 28 nsec, long compared with τ .

Using this near-perfect combination of pulse and absorber, Slusher and Gibbs observed nonlinear transmission. Their input 2π pulse did not enjoy 100% transmission, presumably only because the input pulse was not a hyperbolic secant in shape and had to be reshaped by the medium. Large pulse delays were observed, corresponding to energy leaving the pulse,

coherently exciting the atoms, and returning to the trailing edge of the pulse with no loss but with a delay occasioned by the temporary and coherent storage of pulse energy in the atoms. The delays observed were substantially in agreement with the theoretical prediction 4.41, and corresponded to pulse velocities as much as 3 orders of magnitude slower than c . Pulse breakup also occurred very much in agreement with the prediction of the area theorem (see Fig. 5.1).

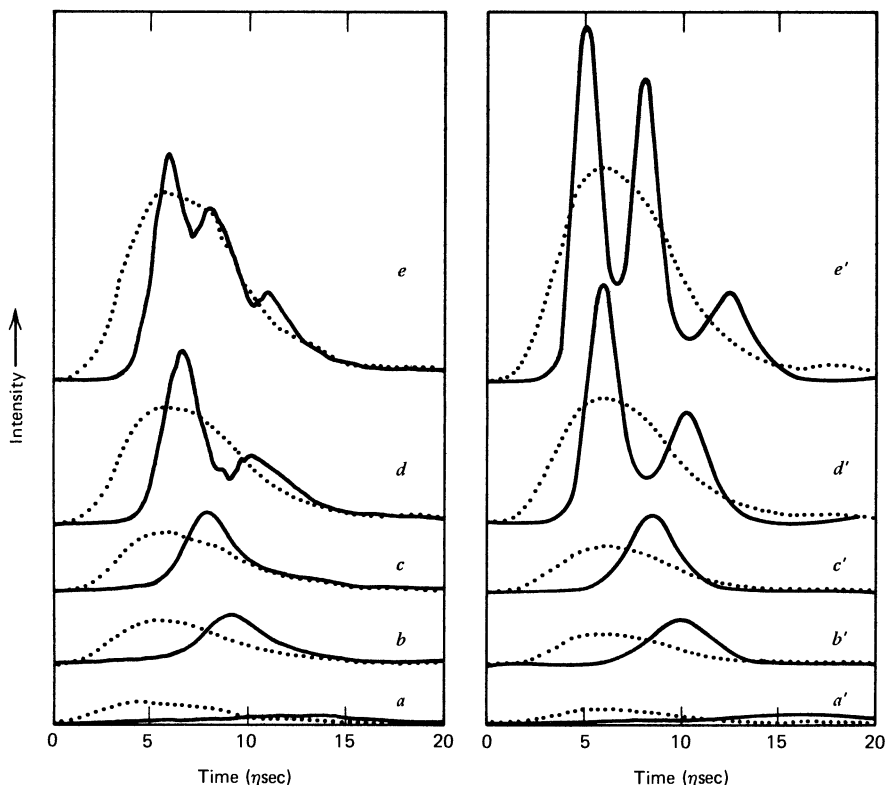


Fig. 5.1 Input and output pulse shapes for both experimental and theoretical pulses. The dotted curves depict input pulses, and the full curves depict the corresponding output pulses after propagation through five Beer's lengths of absorber. Experimental curves *a* through *e* appear as the gun barrel points in Fig. 5.2, and denote pulses with areas of slightly less than 2π , between 2π and 3π , slightly less than 5π , and approximately 6π , respectively. Theoretical curves *a'* through *e'* appear as the peace symbol points in Fig. 5.2, and denote pulses with areas of 6.28, 8.7, 10.5, 17.5, and 23, respectively. These areas are for sech input pulses, and probably underestimate the actual pulse areas because of a failure to account for the long pulse tails. Nevertheless, pulse breakup of the pulses with areas above 3π , and the absence of breakup of the pulses with smaller areas, is in excellent agreement with the predictions of the theory. [From R. E. Slusher and H. M. Gibbs, *Phys. Rev. A* 5, 1634 (1972), and erratum, *ibid.* 6, 1255 (1972).]

The observation of a dip in the output versus input intensity plot in the range 2π to 3π shown in Fig. 5.2 may be attributed to 4π pulses coherently exciting and deexciting the atoms twice. In other words, part of the pulse is absorbed and reemitted at a slightly later time. Evidence was produced to show that in some instances the peak of the output intensity exceeded the peak of the input intensity, although clearly the total output energy was less than the total input energy. Again this can only be explained by a coherent interaction between light and atomic dipoles; no theory of incoherent saturation can be made to predict such a result.

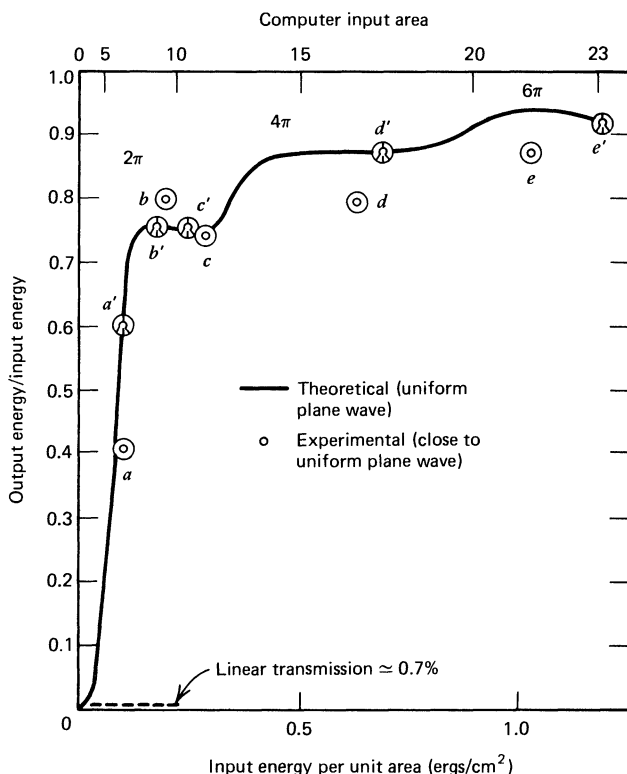


Fig. 5.2 Nonlinear transmission accompanying self-induced transparency in Rb vapor. The pulse shapes for the gun barrel and peace symbol points are shown in Fig. 5.1. The theoretical curve does not show perfect transparency even at areas of 2π , 4π , and 6π , because the actual losses due to collisional and radiative damping that are present in Rb vapor were allowed for in the numerical calculation of the curve. [From R. E. Slusher and H. M. Gibbs, *Phys. Rev. A* **5**, 1637 (1972), and erratum, *ibid.* **6**, 1255 (1972).]

By changing the magnitude of the magnetic field the rubidium absorber could be detuned from resonance. It was found that the transmitted pulse shapes were identical to those on resonance, provided that the density was increased to give the same αL as during the on-resonance measurements. No significant pulling of the off-resonance 2π pulse toward the line center appeared. The only observable shift occurred at the lowest input areas when, as a consequence of the higher absorption coefficient for those frequency components of the pulse near the resonance, the shift was some 10 to 20 MHz away from the resonance. More recent work on frequency pulling has been reported by Diels and Hahn[6].

According to a computer calculation of McCall and Hahn, a pulse with an area just less than 3π will be reshaped by self-induced transparency into a propagating pulse of area 2π with an amplified peak, and with its width narrowed. This phenomenon was discussed semi-quantitatively at the end of Section 4.4. A lens may be used to increase the intensity in a 2π pulse, while obviously lessening the beam width, and so enlarge its envelope area to 3π . This in turn may be used to produce a 2π pulse of yet greater height and narrower width in a second absorption cell. A compression of an order of magnitude has been reported by Gibbs and Slusher [7].

The beautiful experimental work of Gibbs and Slusher leaves no doubt about the validity of the theory developed by McCall and Hahn for the coherent coupling between a coherent pulse and the dipole moments of an ensemble of atoms. However, another piece of work that should be mentioned is that of Asher and particularly of Asher and Scully [8], who investigated the effect on self-induced transparency of the phase relaxation time T'_2 by warming a ruby sample from 5 to 60°K. As T'_2 approached τ , because of the warming, the transmission and pulse delay were both reduced, particularly for near- π pulses, but considerably less so for pulses with area greater than 2π . These results are once again consistent with computer solutions in the case where T'_2 approaches τ . The plot of energy out/energy in against input energy shown in Fig. 5.3 is an excellent example of the rapid rise from linear absorption to near transparency. It may be seen that changing the input by a factor of 20 changes the transmission by a factor of 10,000 in the region near the transparency threshold area of π .

The experimental work described so far is for the so-called broad-line limit in which the inhomogeneous spectral width of the absorber is much greater than the frequency width of the input pulse, that is, $T_1, T'_2 > \tau > T_2^*$.

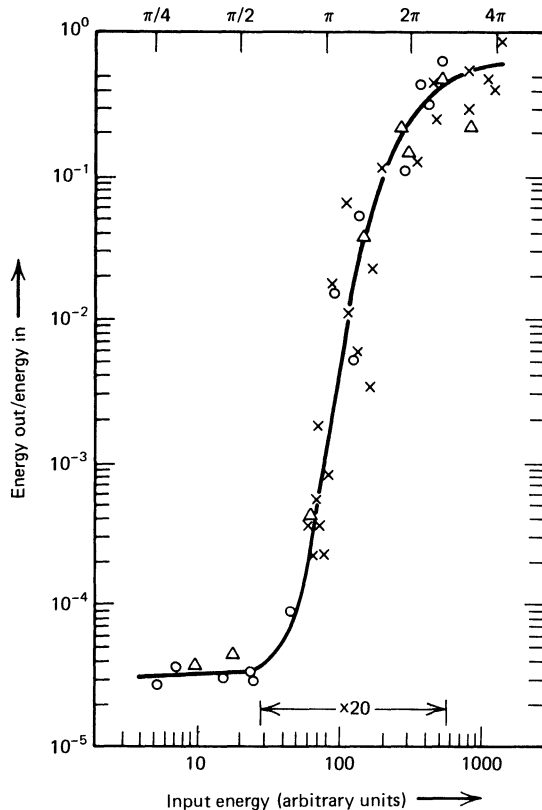


Fig. 5.3 Energy transmission ratio observed in pulse propagation in a ruby absorber, showing the very steep nonlinear threshold behavior at the onset of self-induced transparency. The curve is a fit to the experimental points. [From I. M. Asher and M. O. Scully, *Optics Comm.* 3, 395 (1971).]

There is also a sharp-line limit where $T_1, T_2, T_2^* > \tau$ for which the hyperbolic secant is still the steady-state pulse form even if the sharp line is not in resonance with the center frequency of the pulse. In truth, it is exactly because the steady-state sech solution remains the same for each homogeneous component without regard to its detuning Δ that the full inhomogeneously broadened line also supports a hyperbolic secant steady-state pulse. The sharp-line limit has been investigated by Gibbs and Slusher [9] using an atomic beam of rubidium perpendicular to the optical pulse direction. The rubidium Doppler width is only 30 MHz compared to the

120 MHz of the incident pulse. Both pulse breakup and pulse shaping were found to occur for input areas in the range π to 6π .

5.3 EFFECTS OF DEGENERACY

In experiments of the kind discussed in this chapter, two types of degeneracy can mask or influence the behavior of the self-induced transparency process. A pulse has well-defined envelope area only if the absorber has a unique dipole moment. This is clear from the role played by $\kappa = 2d/\hbar$ in the defining relation 4.40:

$$A(t, z) = \kappa \int_{-\infty}^t \mathcal{E}(t', z) dt' = \frac{2d}{\hbar} \int_{-\infty}^t \mathcal{E}(t', z) dt', \quad (5.1)$$

If the absorber were degenerate in the sense that several of its absorption lines overlapped, each possessing a unique dipole moment, it is unlikely that self-induced transparency could occur unless, absurdly coincidentally, the ratios of the dipole moments involved were integers.

However, it is always true that the medium is degenerate in the sense that each level J is $(2J+1)$ degenerate in the absence of a magnetic field. This is the spatial degeneracy arising from the quantization of the z component of the angular momentum: $M = J, J-1, J-2, \dots, -J$. Such degeneracy does not occur in nuclear magnetic resonance because there the magnetic field has already lifted any spatial degeneracy. But for optical transitions spatial degeneracy undoubtedly can be an obstacle to a simple interpretation of resonant pulse propagation experiments, especially since separating the individual transitions by more than the inhomogeneous width would usually require unrealistically high magnetic fields.

In the presence of spatial degeneracy electric dipole matrix elements are best written labeled with the appropriate magnetic quantum number:

$$\mathbf{d}_{M+-} = \langle +, J' M' | \hat{\mathbf{d}} | -, JM \rangle. \quad (5.2)$$

Electric dipole transitions permit nonzero matrix elements only in the cases where

$$\Delta J = J' - J = -1, 0, 1. \quad (5.3)$$

If we consider only incident electric fields linearly polarized along the

quantization axis, it also follows that

$$\Delta M = M' - M = 0, \quad (5.4)$$

and the only transitions that occur are π transitions. The relevant matrix elements that remain may be simply written as

$$\langle +, J+1, M | \hat{\mathbf{d}}_z | -, J, M \rangle = \sqrt{\frac{(J+1)^2 - M^2}{(J+1)^2}} \| \hat{\mathbf{d}}_{J+1,J} \|, \quad (5.5a)$$

$$\langle +, J, M | \hat{\mathbf{d}}_z | -, J, M \rangle = \frac{M}{J} \| \hat{\mathbf{d}}_{J,J} \|, \quad (5.5b)$$

$$\langle +, J-1, M | \hat{\mathbf{d}}_z | -, J, M \rangle = \sqrt{\frac{J^2 - M^2}{J^2}} \| \hat{\mathbf{d}}_{J-1,J} \|, \quad (5.5c)$$

where the double-bar symbol is related to the dipole moment's reduced matrix element and is independent of M . It then follows immediately that certain transitions will behave as though there were no degeneracy. For example, if $J=0$ and $J'=1$, then M can only be zero and

$$\langle +, 1, 0 | \hat{\mathbf{d}} | -, 0, 0 \rangle = \sqrt{\frac{1^2 - 0^2}{1^2}} \| \hat{\mathbf{d}}_{1,0} \| = \| \hat{\mathbf{d}}_{1,0} \|.$$

Similarly if $J=1$ and $J'=0$, then M can again only be zero and

$$\langle +, 0, 0 | \hat{\mathbf{d}} | -, 1, 0 \rangle = \| \hat{\mathbf{d}}_{0,1} \|.$$

However, the only other transition for which this happy state of affairs occurs is $J=J'=1$, although it should be noted that all $\Delta J=0$ transitions have integrally related dipole moments. Similar examination of the relevant dipole moments shows that the transitions

$$J = \frac{1}{2} \Rightarrow \frac{1}{2},$$

$$J = \frac{3}{2} \Rightarrow \frac{1}{2},$$

$$J = \frac{1}{2} \Rightarrow \frac{3}{2},$$

have π components that behave as though in a two-level atom. Of course all σ transitions must be excluded by careful choice of the polarization of the input pulse.

There is also another situation in which the degeneracy of the levels is immaterial. It is revealed by a careful reexamination of the area theorem, taking account of degeneracy. Just as the classical polarization density was generalized to include dependence on z as well as t and to account for inhomogeneous broadening through the introduction of the lineshape function $g(\Delta)$, so the expression 4.2 may be generalized to include degenerate levels. This is accomplished simply by summing the polarization over all the electric dipole transitions between the magnetic states of the two-level atom:

$$P(t, z) = \mathcal{N} \sum_M d_M \int g(\Delta'_M) [u_M \cos(\omega t - Kz) - v_M \sin(\omega t - Kz)] d\Delta'_M. \quad (5.6)$$

When degeneracy is allowed for in this way, the corresponding generalization of the in-quadrature Maxwell equation 4.6 may be written as

$$\frac{\partial \mathcal{E}}{\partial z} + \frac{1}{c} \frac{\partial \mathcal{E}}{\partial t} = \pi k \mathcal{N} \sum_M d_M \int v_M g(\Delta'_M) d\Delta'_M, \quad (5.7)$$

from which an immediate generalization of the area theorem 4.25 may be derived. As relation 5.1 suggests, when d is not unique, it is useful to define $\kappa_M = 2d_M/\hbar$ and to use

$$\phi(z) = \int_{-\infty}^t \mathcal{E}(t', z) dt'$$

instead of area as the primary variable. It follows that $\phi(z)$ satisfies the relation

$$\frac{\partial \phi(z)}{\partial z} = \frac{\pi^2 \mathcal{N} \hbar \omega g(0)}{2c} \sum \kappa_M \sin(\kappa_M \phi), \quad (5.8)$$

which embraces the area theorem 4.25 as a special case. However, the nonintegrally related values of κ_M make it impossible to pick a set of ϕ 's for which $\partial \phi / \partial z$ vanishes for a degenerate system. However, there is always one such value of ϕ , namely zero. If ϕ is zero, the right-hand side of equation 5.8 always vanishes, independent of the κ_M 's; hence the time integral of $\mathcal{E}(t, z)$ does not change with increasing penetration into the absorber. Thus an inhomogeneously broadened degenerate absorber can still support propagation for anomalously long distances, even without obeying an area theorem, if the electric field E has one or several phase

reversals so that \mathcal{E} changes sign often enough to give it a vanishing time integral.

It is also informative to consider pulses traveling in degenerate absorbers that are homogeneously broadened. The area of pulses in such media may be governed by very complicated restrictions. However, the integrated envelope of sufficiently long pulses will decay according to Beer's law:

$$\phi(z) = \phi(0)e^{-\frac{1}{2}\alpha z}.$$

This does not need to imply, however, that the pulse energy also obeys Beer's law. If we define

$$S(z) = \frac{c}{2\pi} \int_{-\infty}^{\infty} \mathcal{E}^2(t, z) dt \quad (5.9)$$

as a measure of pulse energy, then it is easy to show that the atoms in a homogeneously broadened on-resonance line act to modify $S(z)$ in the following manner:

$$\frac{\partial}{\partial z} S(z) = -\mathcal{V} \frac{\hbar\omega}{2} \sum_M [1 - \cos(\kappa_M \phi(z))]. \quad (5.10)$$

This attenuation law is a direct consequence of a time integration of the energy flux relation 4.7 combined with the expression 4.13 for the on-resonance inversion. Again we find that if field phase reversals allow $\phi=0$ while $\mathcal{E} \neq 0$, propagation proceeds without energy decay. Note that this result is quite different from the similar classical result derived in Section 1.7. In this case there need be no assumption that the pulse length is much shorter than both T_2' and T_2^* .

Unfortunately, experiments to date with CO₂ laser pulses in SF₆ vapor, a multiply degenerate absorber, have involved only finite area pulses, and there has been more than one interpretation advanced for the observations. Although intensity-dependent pulse delays and dramatic pulse steepening and reshaping have been observed, there may remain a question concerning the extent to which these effects arise from self-induced transparency alone, or from incoherent and saturation processes. A number of workers [10] have discussed these points extensively. Very recently experimental observation of 0π pulse transparency has been reported [11], and the effects of degeneracy have been studied systematically using a cw dye laser and an atomic absorber [11].

5.4 INCOHERENT SATURATION AND PULSE DELAY

The preceding sections have mentioned the danger of self-induced transparency being confused with incoherent saturation. The possibility of confusion is a real one because a small part of a sufficiently strong incoherent pulse can stimulate enough transitions to excite nearly half of the atoms in the lower level of a two-level absorber to the upper level, and saturate the absorption line. The rest of the pulse will then be transmitted completely unattenuated as if the absorber were transparent. The transmitted pulse will also undergo a delay because the leading part of the pulse will be used up saturating the medium, effectively moving the center of gravity of the pulse backward. Of course, in self-induced transparency qualitatively similar effects occur.

With these similarities in mind Smith and Allen [10] have examined pulse transmission in lead vapor, and have analyzed their experimental results from the point of view of both coherent and incoherent theories. They have found (see Fig. 5.4) that lead vapor laser pulse transmission through a lead vapor cell shows a rapid rise through several orders of magnitude from a small value at low input intensities to nearly 100% as the input intensity reaches a threshold. Not only is the shape of the transmission curve appropriate to self-induced transparency but, as Fig. 5.5 shows, the observed pulse delay changes slightly with αL and with input intensity. It is easy to interpret such results as qualitative evidence for self-induced transparency. However, in the case of these lead vapor data, semiquantitative comparisons with the theory of self-induced transparency are easily made. The threshold for self-induced transparency in the lead vapor system should be about 1.4 W/cm^2 for the 12 nsec pulses used, while the threshold observed in Fig. 5.4 corresponds to approximately 250 W/cm^2 . In addition, the pulse delay associated with self-induced transparency should be appreciably greater than that shown in Fig. 5.5; for example, when $\alpha L = 11.0$ the delay should be nearly 65 nsec, rather than 5 nsec as observed.

It is well known that, to a certain degree, it is possible to describe pulse propagation with rate equations that ignore coherence in the interaction between pulse and absorber. A common form for such equations is:

$$\frac{\partial n_2}{\partial t} = -\sigma(n_2 - n_1)g(t, z) - \frac{n_2}{T_1} \quad (5.11)$$

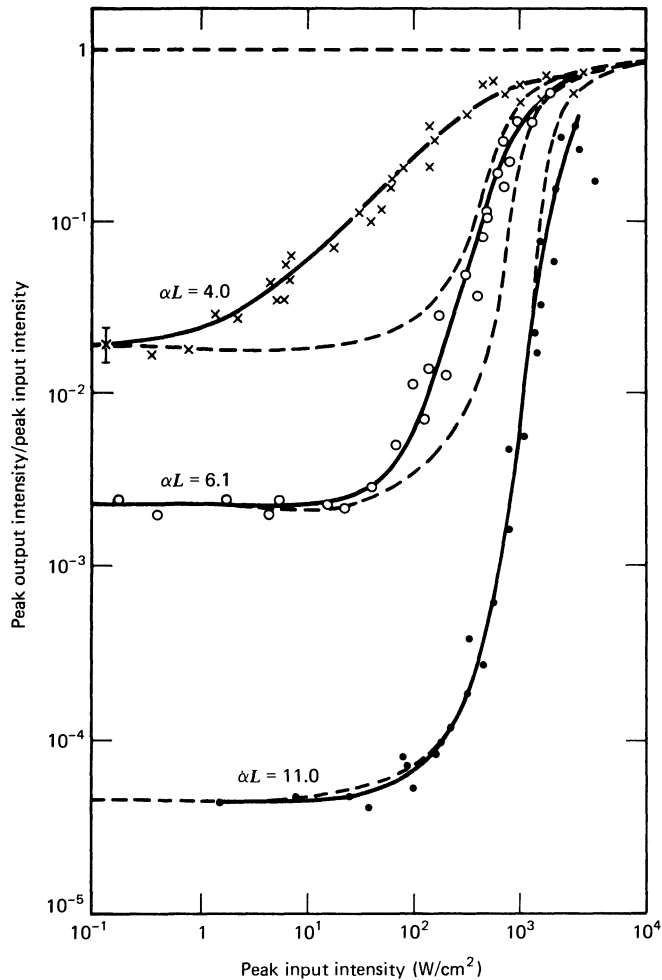


Fig. 5.4 Peak intensity transmission ratio observed in pulse propagation through 4.0, 6.1, and 11.0 Beer's lengths of Pb vapor. The solid lines are fits to the experimental data, and the dashed lines express the predictions of Selden's theory [12]. [From K. W. Smith and L. Allen, *Optics Comm.* **8**, 166 (1973).]

and

$$\frac{\partial \mathcal{I}}{\partial z} = \sigma(n_2 - n_1)\mathcal{I}(t, z), \quad (5.12)$$

where $\mathcal{I}(t, z)$ is the normalized photon flux, n_2 and n_1 are the number

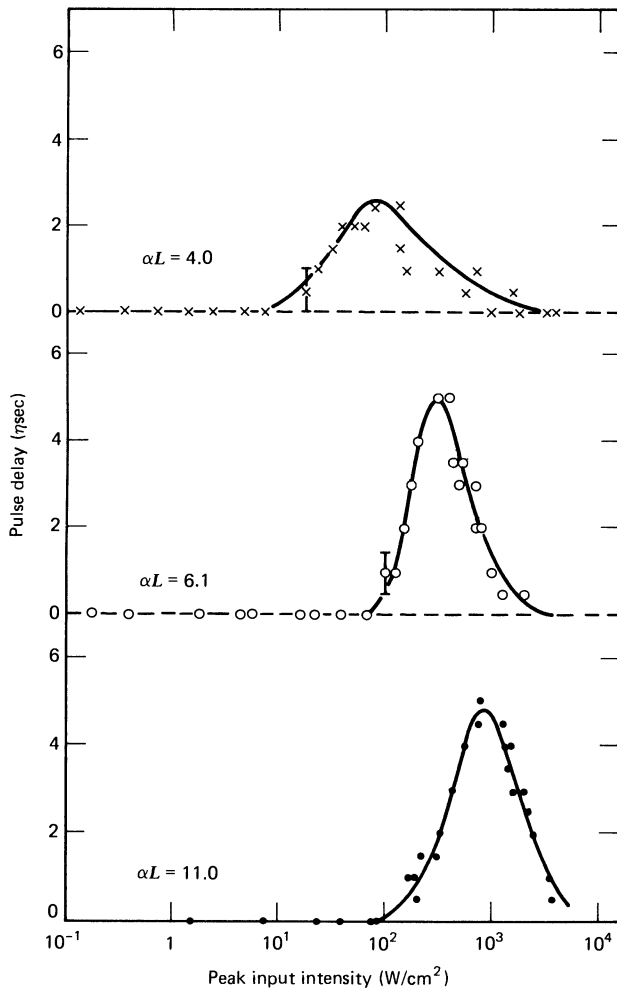


Fig. 5.5 Pulse delay times observed in pulse propagation through 4.0, 6.1, and 11.0 Beer's lengths of Pb vapor, as a function of peak input intensity. The solid lines are fits to the experimental data. [From K. W. Smith and L. Allen, *Optics Comm.* **8**, 166 (1973).]

densities of atoms in the upper and lower levels, and σ is the absorption cross-section per atom. These equations are perfectly adequate to describe incoherent bleaching. A discussion of the way in which such rate equations relate to the optical Bloch equations will be given in Chapter 6; but here these easily recognizable equations will be used without further elaboration.

Gires and Combaud [12] developed a rate equation approach to the incoherent optical saturation of a resonant absorber, and Selden [12] has solved the equations in terms of a time-varying transmittance. The rate equation theory shows that saturation introduces pulse distortion and a pulse delay that rises with incident intensity to a maximum and then decreases with further increase of intensity. High intensity pulses are transmitted with little distortion or attenuation, but pulses of intermediate intensity suffer a reduction in pulse width and a delay, in addition to suffering some attenuation.

This incoherent theory has been applied by Smith and Allen to their lead vapor results. Although the theory was developed for a homogeneous absorber while the lead system is inhomogeneous, the agreement when αL is largest is very good. It is less good for the smaller values of αL . This is reasonable on the grounds that at the high intensities necessary for the $\alpha L = 11.0$ case to show transmission, the hole burned in the absorber may well be so wide that the absorber very nearly behaves homogeneously. The incoherent saturable absorber theory predicts pulse narrowing by a factor of about 0.5 and a delay of approximately 4 nsec, while the equivalent observed values are 0.6 and 3 to 5 nsec.

It may be argued that incoherent bleaching and self-induced transparency are more closely linked than is generally supposed. The experimental results in lead are unambiguously due to incoherent bleaching and not self-induced transparency because collisions with energetic electrons remaining in the lead absorber plasma tube drastically shorten the coherence time of the absorber. However, there may well be occasions when the distinction between coherent and incoherent processes is not so clear-cut. We discuss some reasons for a possible blurring of this distinction in the following paragraphs.

The threshold for *incoherent* bleaching in the rate equation theory occurs when the stimulated absorption rate $\mathcal{I}\sigma$ just equals the incoherent decay rate $1/T_1$ of the absorber. The corresponding incoherent threshold of the power density is

$$\mathcal{P}_{\text{incoh}} = \hbar\omega \mathcal{I}_{\text{incoh}} \approx \frac{\hbar\omega}{\sigma T_1}. \quad (5.13)$$

The threshold for the onset of *coherent* bleaching, that is, for self-induced transparency, is achieved when the coherent pulse has envelope area equal approximately to π . In other words, if τ is the coherent pulse length,

threshold corresponds roughly to $\kappa \mathcal{E} \tau \approx \pi$. Thus the threshold power density for coherent bleaching is

$$\mathcal{P}_{\text{coh}} = \frac{c}{2\pi} \mathcal{E}_{\text{coh}}^2 \approx \frac{\pi c}{2\kappa^2 \tau^2}. \quad (5.14)$$

The relation between these two threshold power densities is easily worked out using the identity

$$\mathcal{N}\sigma = \alpha, \quad (5.15)$$

where \mathcal{N} is the total number density of absorber atoms and α is the Beer's law absorption coefficient given in equation 4.26. The result for an inhomogeneously broadened absorber is

$$\mathcal{P}_{\text{incoh}} = \frac{\tau^2}{T_1 T_2^*} \mathcal{P}_{\text{coh}}, \quad (5.16)$$

if factors of order unity are ignored.

Consequently the power threshold for incoherent bleaching can easily be comparable with or smaller than the threshold for self-induced transparency, especially in systems with relatively long-lived coherence that satisfy $T_1, T_2 \gg \tau$. In view of this possibility it appears that the shape of a transmission curve, such as that in Fig. 5.4, and its position with respect to input intensity are both poor indicators of self-induced transparency. The only unchallengeable evidence for self-induced transparency is the existence of sufficiently large pulse delays that vary as $\frac{1}{2}\alpha L\tau$ and, completely unambiguously, pulse breakup into separate 2π pulses, or peak amplification of 3π pulses [see Sec. 4.4].

Courtens and Szöke provide an elegant argument [13] with respect to the implications of pulse delay. They demonstrate, in the limit where the optical carrier frequency ω is displaced far away from resonance ω_0 , that the self-induced transparency values for the envelope propagation velocity and the propagation vector reduce to those of linear dispersion theory. They show that if $(\delta \mathcal{E} / \mathcal{E})(\tau_d / \tau) > 1$, where τ_d is the pulse delay, then the pulse is attenuated more than it is delayed, and it always remains under the initial pulse envelope. Only when the product of the ratios is smaller than unity will the peak of the pulse move beyond the input tail after it has propagated through sufficient length of medium. They compute the small signal absorption constant far from resonance and find $(\delta \mathcal{E} / \mathcal{E})(\tau_d / \tau) = \tau / T'_2$. But the condition that $\tau / T'_2 < 1$ is precisely that required to obtain

transparency. Thus the observation of a pulse delay beyond the input pulse tail is not sufficient evidence of transparency. Finally, McCall and Hahn [1] and Hopf and Scully [14] have investigated the variation of delay time with pulse area in the coherent case and demonstrate that the effect of finite T_1 and T'_2 is to lessen the delay. Viewed as a whole, incoherent saturation and pulse delay manifest themselves as an apparent limit of the coherent case; the intensities involved are comparable and the pulse delays are compatible as T'_2 approaches τ .

5.5 π PULSES IN MODE-LOCKED LASERS

The cw gas laser provides another instance in which coherent and incoherent phenomena are intertwined. The basic lasing process is reasonably well described by rate equations, and laser threshold is accurately predicted in this way. However agreement with careful experimental work is found only in a theory that takes careful account of atomic coherence. The first example of such a theory of optical pulses in inverted media was presented by Arecchi and Bonifacio [15].

In a free running cw gas laser the frequencies of the axial modes are displaced from the passive cavity resonances because of the effects of intermode competition and the dispersion characteristics of the medium providing the gain. In some circumstances the mode frequencies and phases may be simply related one to another in such a way that the modes are said to be self-locked [16]. Then the output of the laser is no longer cw but consists of a train of pulses of periodicity $c/2L$, where L is the length of the cavity, and of pulse width $nc/2L$, where n is the number of longitudinal modes so "locked."

Fox and Smith [17] suggested that a mode-locked laser pulse traveling back and forth in the cavity could well be a π pulse. If a pulse were to last longer than the time required to drive the population from the upper level to the lower, then the medium would amplify the first part of the pulse and attenuate the last part, thus shortening the pulse. Conversely, if the pulse were shorter than the time required, it would be lengthened. A self-consistent pulse amplified without distortion ought therefore to have the intensity and duration required for a π pulse.

Equation 3.18 shows that the effect of a coherent stimulating field on an

atom is to drive the inversion according to

$$w = 1 - \frac{2(\kappa\mathcal{E})^2}{(\kappa\mathcal{E})^2 + \Delta^2} \sin^2 \frac{1}{2} \sqrt{(\kappa\mathcal{E})^2 + \Delta^2} t, \quad (5.17)$$

assuming the atom to be in its upper level at $t=0$, provided that t is short compared with the time scale of any incoherent processes. Thus a pulse of incident radiation of length

$$\tau = \pi [(\kappa\mathcal{E})^2 + \Delta^2]^{-1/2} \quad (5.18)$$

will cause a maximum change of population. If \mathcal{E} is known experimentally, equation 5.1 allows the duration required of a π pulse to be predicted. Fox and Smith showed good experimental agreement with theory, provided that $\Delta/2\pi$ was taken as 275 MHz. Their explanation for this was that the system behaved as if all atoms were removed by some average frequency separation from that of the stimulating field. Obviously in reality the pulse is the result of the interaction of a number of modes and the above mentioned single mode theory is a very approximate one.

Furthermore, a neon absorber cell placed in a He-Ne laser cavity can be arranged to cause a continuous train of optical pulses [18]. In explanation one may argue that either the loss cell is bleached and so produces pulsing in the same way that saturable dyes do in locking solid-state lasers, or that a π pulse from the laser tube inverts the loss medium, reflects from the mirror, reinverts the loss medium, and so emerges without sustaining any net loss. This would, of course, suppose that a π pulse could be transmitted through either an absorber or an amplifier without loss, or at least that whatever small losses there might be would be made up by the gain of the amplifying medium.

It has also been found [19] in a similar experiment that the pulse repetition frequency of the order of $c/2L$ expected from a laser cavity of length L varies as $I^{-1/3}$, where I is the peak intensity of the pulse, and that, as $c/2L$ changes, the pulse width also changes approximately as $I^{-1/3}$, suggesting that $I\tau^3$ is a constant, at least in some regimes. Furthermore the measured frequency $c/2L$ differs from the value implied by the size of the cavity, suggesting an effective pulse velocity of less than c , apparent evidence of pulse delay. McCall and Hahn have shown [20] that their coherent pulse theory, described in Chapter 4, may be applied to

traveling-wave laser amplifiers. When limited to signals small enough so that pulse breakup is unlikely, their work may be expected to be relevant in the present case, and indeed agrees quantitatively with the data [18, 19].

Interestingly, the Lamb theory of the laser [21] may be used as well to comment on π pulses and mode-locking. Allen and co-workers have shown [22] that the Lamb theory can be solved rigorously for the case of three locked axial modes, and that the solutions are well-verified experimentally for both the He-Ne 6328 Å and 1.15 μm lasers. However, in locked three-mode pulses in these lasers, no preferred value for pulse envelope area θ is found [23]. Similarly $I\kappa^3$ varies considerably with $c/2L$. However, for constant $c/2L$, in going from one locking regime to another by shifting the center of the gain curve slightly with respect to the mode resonances, both θ and $I\tau^3$ are very nearly constant, which is consistent with the data mentioned above. That the three-mode case seems incompatible with the π pulse picture is not altogether surprising. The pulse duration in such a system would be well in excess of the dipole relaxation times involved. In the other experimental work cited here pulse durations of the order of 10^{-10} sec occur, and the language of π pulse propagation may well be appropriate. One sees, however, that π pulses are not the inevitable consequence of mode-locking. Of course this is not surprising either. The pulse envelope area in a real laser is not in any sense a good constant of the system. The shape of the mode in the cavity means that the beam cross-section and thus the field vary from point to point along the length of the cavity, so that a unique envelope area cannot be realized.

References

1. S. L. McCall and E. L. Hahn, *Phys. Rev. Lett.* **18**, 908 (1967); *Phys. Rev.* **183**, 457 (1969).
2. C. K. N. Patel and R. E. Slusher, *Phys. Rev. Lett.* **19**, 1019 (1967).
3. C. K. Rhodes, A. Szöke, and A. Javan, *Phys. Rev. Lett.* **21**, 1151 (1968).
4. C. K. N. Patel, *Phys. Rev. A* **1**, 979 (1970).
5. H. M. Gibbs and R. E. Slusher, *Phys. Rev. Lett.* **24**, 638 (1970); R. E. Slusher and H. M. Gibbs, *Phys. Rev. A* **5**, 1634 (1972) and *A* **6**, 1255E (1972); R. E. Slusher, in *Progress in Optics*, E. Wolf, ed., North-Holland, Amsterdam, 1974, Vol. 12.
6. J. C. Diels and E. L. Hahn, *Phys. Rev. A* **8**, 1084 (1973).
7. H. M. Gibbs and R. E. Slusher, *Appl. Phys. Lett.* **18**, 505 (1971).
8. I. M. Asher, *Phys. Rev. A* **5**, 349, (1972); I. M. Asher and M. O. Scully, *Optics Comm.* **3**, 395 (1971).
9. H. M. Gibbs and R. E. Slusher, *Phys. Rev. A* **6**, 2326 (1972).

10. J. P. Gordon, C. H. Wang, C. K. N. Patel, R. E. Slusher, and W. J. Tomlinson, *Phys. Rev.* **179**, 294 (1969); C. K. Rhodes and A. Szöke, *Phys. Rev.* **184**, 25 (1969); P. K. Cheo and C. H. Wang, *Phys. Rev. A* **1**, 225 (1970); F. A. Hopf, G. L. Lamb, Jr., C. K. Rhodes, and M. O. Scully, *Phys. Rev. A* **3**, 758 (1971); G. L. Lamb, Jr., *Rev. Mod. Phys.* **43**, 99 (1971); A. Zembrod and Th. Gruhl, *Phys. Rev. Lett.* **27** 287 (1971); K. W. Smith and L. Allen, *Optics Comm.* **8**, 166 (1973).
11. H. P. Grieneisen, J. Goldhar, N. A. Kurnit, and A. Javan, *Appl. Phys. Lett.* **21**, 559 (1972); and G. J. Salamo, H. M. Gibbs, and G. G. Churchill, *Phys. Rev. Lett.* **33**, 273 (1974).
12. F. Gires and F. Combaud, *J. de Phys.* **26**, 325 (1965); and A. C. Selden, *Br. J. Appl. Phys.* **18**, 743 (1967).
13. E. Courtens and A. Szöke, *Phys. Lett.* **28A**, 296 (1968).
14. F. A. Hopf and M. O. Scully, *Phys. Rev. B* **1**, 50 (1970).
15. F. T. Arecchi and R. Bonifacio, *I.E.E.E. Journ. Quantum Electronics* **1**, 169 (1965). See also J. A. Armstrong and E. Courtens, *ibid.* **4**, 411 (1968), and *ibid.* **5**, 249 (1969).
16. L. Allen and D. G. C. Jones, in *Progress in Optics*, E. Wolf, ed., North-Holland, Amsterdam, 1971, Vol. 9, p. 181.
17. A. G. Fox and P. W. Smith, *Phys. Rev. Lett.* **18**, 826 (1967).
18. A. G. Fox, S. E. Schwarz, and P. W. Smith, *Appl. Phys. Lett.* **12**, 371, (1968).
19. A. Frova, M. A. Duguay, C. G. B. Garrett, and S. L. McCall, *J. Appl. Phys.* **40**, 3969 (1969).
20. S. L. McCall and E. L. Hahn, *Phys. Rev. A* **2**, 861 (1970).
21. W. E. Lamb, Jr., *Phys. Rev.* **134**, 1429 (1964).
22. D. G. C. Jones, M. D. Sayers, and L. Allen, *J. Phys. A* **2**, 95 (1969); M. D. Sayers and L. Allen, *Phys. Rev. A* **1**, 1730 (1970).
23. L. Allen, *Phys. Rev. Lett.* **27**, 1115 (1971).

CHAPTER 6

Saturation Phenomena

6.1	Introduction	130
6.2	Rate Equations	131
6.3	Induced Transition Rate in a Monochromatic Field	133
6.4	The Rate Equation Limit of the Bloch Equations	134
6.5	The Rate Equation Limit of the Maxwell Equations	137
6.6	Saturation and Nonlinear Spectroscopy	139
6.7	Saturated Absorption	142
6.8	Propagating Wave Attenuation and Amplification	143
6.9	Dispersion in Saturated Media and Self-Focusing	151
	References	151

6.1 INTRODUCTION

It is only possible to observe coherent effects such as optical nutation and self-induced transparency if the time scale associated with the interaction of the resonant radiation field with the atoms is shorter than the atomic relaxation times T_1 and T_2' . However, this restriction does not limit the range of interesting and important resonant interactions. In this chapter we take up the question of incoherent resonance phenomena occurring over times that may be much longer than T_2' , or even much longer than both T_2' and T_1 .

Traditionally incoherent optical effects are described by simple detailed-balance rate equations similar to those mentioned in Section 5.4. We show that such equations are merely a special case of the coherent Bloch equations by deriving them from the Bloch equations in a quasi-steady-state limit. In the same limit Maxwell's wave equation also reduces to a rate equation.

By solving the Bloch equations exactly instead of perturbatively in the steady-state limit the influence of saturation on absorption is clearly evident. The possibility of holeburning and its use in high-precision spectroscopy are natural consequences. The effects of propagation are also easily investigated in the steady-state limit, and field amplification is discussed briefly. The field rate equation shows the successive occurrence of exponential growth, linear growth, and finally saturation, in the course of the amplification process. Dispersive effects that are typical of

amplifiers, including self-focusing and the existence of a phase velocity greater than c , are briefly mentioned.

6.2 THE RATE EQUATION APPROXIMATION

Many problems in optical physics can be analyzed very straightforwardly using rate equations. Although almost any differential equation could be called a “rate” equation, the term is usually reserved for first-order equations that arise from simple balancing arguments. Thus the famous Einstein derivation of the Planck distribution function used rate equations; in that instance Einstein’s equations followed from the idea that at thermal equilibrium the number of atoms undergoing absorption just balances the number undergoing emission. Lamb [1] has demonstrated that for a laser well above threshold a rate equation approach leads to results not far from those of a much more sophisticated theory. Both amplified spontaneous emission and many-atom cooperative phenomena can be treated by rate equations [2,3]; and discussions of saturation effects are often given in rate equation form.

The rate equations frequently assumed to describe a two-level atom are

$$\dot{n}_2 = -R(n_2 - n_1) - \frac{n_2}{T_1}, \quad (6.1)$$

$$\dot{n}_1 = +R(n_2 - n_1) + \frac{n_2}{T_1}, \quad (6.2)$$

where R expresses the rate of stimulated emission and absorption due to an applied field and n_1 and n_2 are the level population densities. The equations are obviously sensible. The first one says that the upper level population changes for three reasons, at three different rates: at the rate $-Rn_2$ because of induced emission, at the rate $+Rn_1$ because of absorption of radiation by lower level atoms, and at the rate $-n_2/T_1$ because of natural decay independent of the inducing field. The sum of these must equal the total rate $d\dot{n}_2/dt$. A similar argument leads to the second equation with one change. The term $+n_2/T_1$ represents atoms being added to the first-level population because of decay from the second level. There is no term to represent decay from the first level because the two-level model assumes that there is no other level lower than the first. In a real atom the lower of the two resonant levels under consideration is

often not the actual ground level of the atom, so that there really are levels lower than the first resonant level to which it can decay. The absence of such decay processes is one of the flaws of the two-level model for resonant interactions.

The “closed-system” assumption that keeps atoms within the two-level model is reflected in the rate equations by the existence of a simple conservation law. The sum of equations 6.1 and 6.2 shows that $n_1 + n_2$ is constant. This “conservation of atoms” law is equivalent to probability conservation. As before, the constant total density $n_1 + n_2$ of resonant atoms will be denoted by \mathcal{N} . The population density difference $n_2 - n_1$ is usually termed the atomic inversion density, and the single-atom inversion w is related to it by $n_2 - n_1 = \mathcal{N}w$. Thus the relations

$$n_1 = \frac{\mathcal{N}}{2}(1-w), \quad (6.3a)$$

$$n_2 = \frac{\mathcal{N}}{2}(1+w), \quad (6.3b)$$

can be used to transform the original rate equations 6.1 and 6.2 into a single equation for the inversion:

$$\dot{w} = -2Rw - \frac{(w+1)}{T_1}. \quad (6.4)$$

The question of interest is: what connection can this equation for the inversion have with the inversion equation 3.19c derived from the Heisenberg equations for the atom?

$$\dot{w} = -\frac{w - w_{eq}}{T_1} - \kappa \mathcal{E} v. \quad (3.19c)$$

The Heisenberg equations, and thus also the Bloch equations, are frequently termed coherent equations, meaning that they incorporate details of the atom-field interaction that depend on dipole phase and electric field strength. Equations that depend only on dipole magnitude, atomic inversion, and field intensity, such as the rate equations 6.1 and 6.2, are termed incoherent equations. We now show that under some circumstances the extra phase information contained in the Bloch equations becomes lost or irrelevant, thus reducing the Bloch equations to incoherent

rate equations. It is convenient first to derive an expression for the induced transition rate constant R appearing in the rate equations.

6.3 INDUCED TRANSITION RATE IN A MONOCHROMATIC FIELD

In the presence of an almost monochromatic field the correct expression for the induced transition rate R differs from the one usually quoted [4], which is derived for a light source with a very broad spectrum. The probability of an induced transition due to a monochromatic field with frequency ω is given by the expression [5]

$$p = \frac{2\pi\omega}{\hbar\gamma} n(\omega) |\boldsymbol{\epsilon} \cdot \mathbf{d}_{+-}|^2 \frac{\sin^2 \frac{1}{2}(\omega_0 - \omega)t}{[\frac{1}{2}(\omega_0 - \omega)]^2}, \quad (6.5)$$

where $n(\omega)$ is the number of photons with frequency ω and $\boldsymbol{\epsilon}$ is the field polarization vector. However, in a real atom the transition frequency ω_0 is uncertain within its collision- or otherwise-broadened homogeneous linewidth. Consequently it is necessary to average expression 6.5 over all frequencies ω_0 about the line center frequency $\bar{\omega}_0$.

For a Lorentzian line the density of states is given by

$$\rho(\omega_0) = \frac{1}{\pi T'_2} \frac{1}{(\omega_0 - \bar{\omega}_0)^2 + (1/T'_2)^2}.$$

The relation

$$\frac{\sin^2 \frac{1}{2}(\omega_0 - \omega)t}{(\omega_0 - \omega)^2} \rightarrow \frac{\pi}{2} t \delta(\omega_0 - \omega), \quad (6.6)$$

which is valid after a sufficiently long time t , allows the sum over states to be carried out explicitly. If we assume for simplicity that the field frequency is tuned to the center of the homogeneous line, so that $\omega = \bar{\omega}_0$, then

$$R = \int \frac{dp}{dt} \rho(\omega_0) d\omega_0 = \frac{4\pi^2}{\hbar^2} \left(\frac{\hbar \omega n(\omega)}{\gamma} \right) |\boldsymbol{\epsilon} \cdot \mathbf{d}_{+-}|^2 \frac{T'_2}{\pi} \quad (6.7)$$

expresses the total induced transition rate.

The expression 6.7 for the transition rate is more familiarly written in terms of \mathcal{E} instead of $n(\omega)$. The connection between \mathcal{E} and n is readily

established to be

$$\frac{\hbar\omega n(\omega)}{cV} \Rightarrow \frac{2\mathcal{E}^2}{4\pi} \quad (6.8)$$

by recognizing that each side of the correspondence states the field energy density. Thus, in terms of the semiclassical envelope function, \mathcal{E} the induced transition rate may be written as

$$R = \frac{T'_2(\kappa\mathcal{E})^2}{2}. \quad (6.9)$$

6.4 THE RATE EQUATION LIMIT OF THE BLOCH EQUATIONS

The expression for R derived above allows the inversion rate equation 6.4 to be written explicitly as follows:

$$\dot{w} = -\frac{Iw}{T_1} - \frac{(w+1)}{T_1}, \quad (6.10)$$

where the “dimensionless intensity”

$$I = (\kappa\mathcal{E})^2 T_1 T'_2 \quad (6.11)$$

has been used.

It is simple to show that with few assumptions this rate equation may also be derived from the optical Bloch equations 3.19:

$$\dot{u} + \frac{u}{T'_2} = -\Delta v, \quad (6.12a)$$

$$\dot{v} + \frac{v}{T'_2} = \Delta u + \kappa\mathcal{E} w, \quad (6.12b)$$

$$\dot{w} + \frac{w - w_{eq}}{T_1} = -\kappa\mathcal{E} v. \quad (6.12c)$$

If T'_2 is very short, then u and v will quickly reach the quasi-steady-state

values

$$u = -\kappa \mathcal{E} T'_2 \frac{\Delta T'_2}{1 + (\Delta T'_2)^2} w, \quad (6.13a)$$

$$v = \kappa \mathcal{E} T'_2 \frac{1}{1 + (\Delta T'_2)^2} w. \quad (6.13b)$$

Under these circumstances the inversion obeys the simple equation:

$$\dot{w} = -\frac{\mathcal{L} I w}{T_1} - \frac{(w - w_{eq})}{T_1}, \quad (6.13c)$$

where \mathcal{L} is the Lorentzian factor

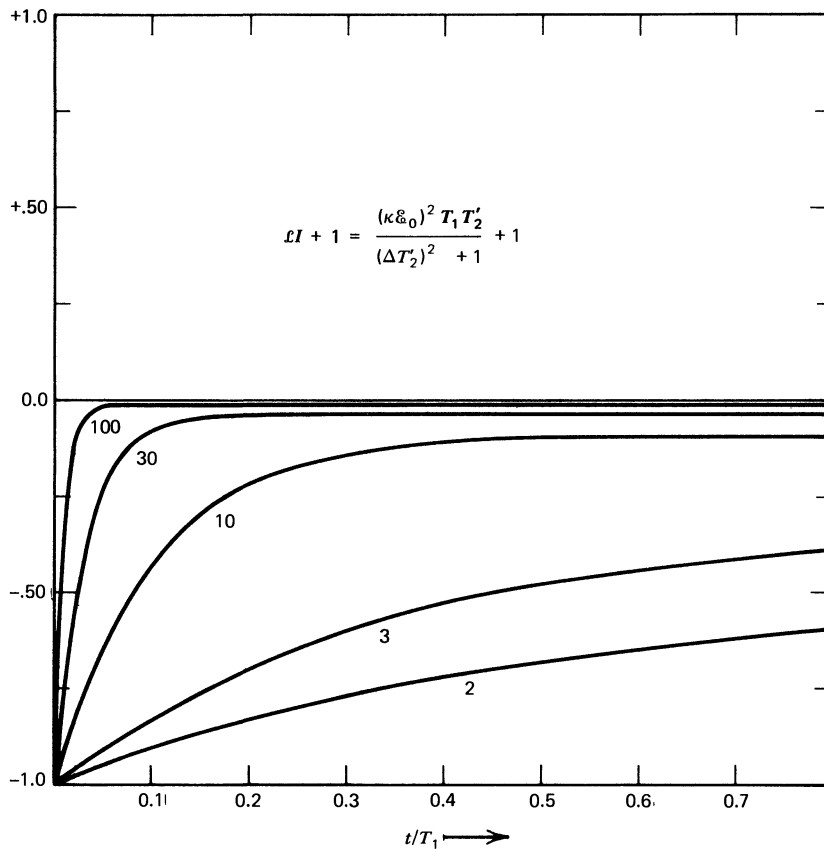
$$\mathcal{L} = \frac{1}{[1 + (\Delta T'_2)^2]}, \quad (6.14)$$

and I is defined in equation 6.11. A comparison of the third quasi-steady-state Bloch equation 6.13c with the rate equation 6.10 shows them to be identical on resonance, if I itself is the only energy input so that $w_{eq} = -1$. Thus the population rate equations 6.1 and 6.2 may be regarded merely as a special case of the optical Bloch equations, obtained in the limit of very rapid dipole phase interruption, when T'_2 is the shortest of all of the incoherent relaxation rates.

The general rate equation 6.13c closely resembles the equation of motion for the population difference found in semiclassical laser theory. It is readily solved explicitly if I is a constant in time:

$$w(t; \Delta) = \frac{w_{eq}}{[\mathcal{L} I + 1]} + \left[w(0; \Delta) - \frac{w_{eq}}{\mathcal{L} I + 1} \right] \exp \left\{ -\frac{(\mathcal{L} I + 1)}{T_1} t \right\} \quad (6.15)$$

where $w(0; \Delta)$ is the initial value of $w(t; \Delta)$. The solution is plotted in Fig. 6.1. Several features of solution 6.15 are obvious in the figure. The decay rate is influenced both by detuning and by the field strength and can be substantially greater than $1/T_1$, particularly for the on-resonant atoms. Far enough from resonance, $w(t; \Delta)$ is independent of I . The steady-state value of w differs from w_{eq} in a way that depends on Δ and I . Section 6.6 is devoted to some consequences of this dependence.



(a)

Fig. 6.1 The inversion as a function of time, given by equation 6.15, for an atom in its ground state exposed to a steady coherent external field, in the rate equation limit: $(T_1)^{-1}$, $d/dt \ll (T_2)^{-1}$. The inversion depends on field strength and detuning through the parameter $\mathcal{L}I+1$ which labels the curves. (a) There is assumed no incoherent energy source for the atoms, so $w_{eq} = -1$. Very strong coherent fields drive w to 0. (b) An incoherent energy source is assumed to be present and strong enough so that $w_{eq} = +\frac{1}{2}$. Only weak coherent fields permit relaxation of w toward $+\frac{1}{2}$, while strong coherent fields drive the inversion to zero, as in (a).

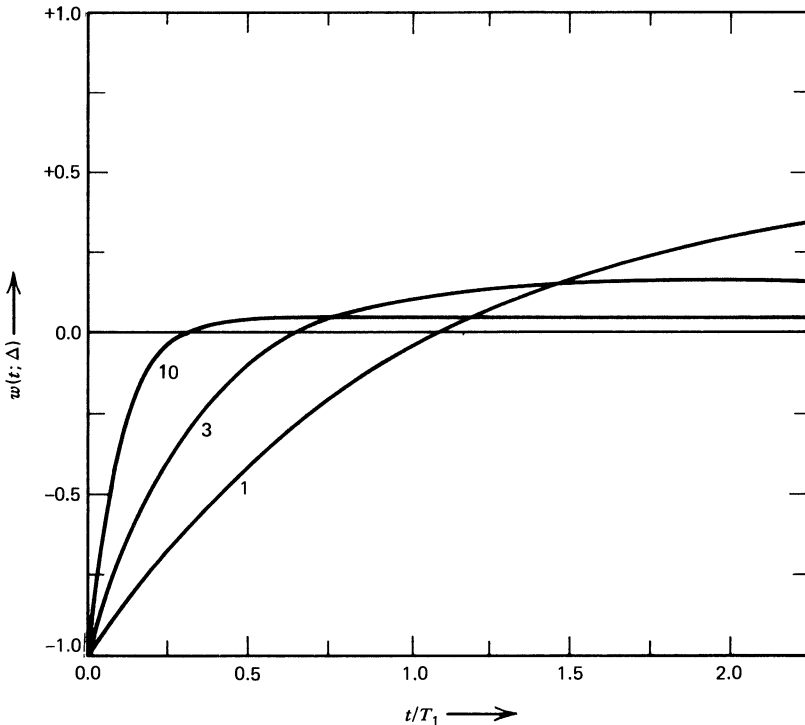


Fig. 6.1 (Continued)

(b)

6.5 THE RATE EQUATION LIMIT OF THE MAXWELL EQUATIONS

In the general case, the field intensity I is of course not constant, but obeys an equation of motion of its own. This equation of motion must ultimately derive from Maxwell's equations, but it is most frequently given in the form of a rate equation. For example, the Gires-Combaud rate equation 5.12, in the present notation, states that the intensity obeys the law:

$$\frac{\partial \mathcal{I}}{\partial z} = \mathcal{N} \sigma \mathcal{I} w. \quad (6.16)$$

It is interesting to trace the way in which such a rate equation follows from Maxwell's equations, in particular from the absorptive equation 4.4b that we derived directly from the Maxwell wave equation 4.1.

Under the quasi-steady-state assumption introduced above, we may use equation 6.13b for v in the Maxwell equation 4.4b. Multiplication of both

sides by $\kappa^2 T_1 T'_2 \mathcal{E}$ in order to introduce the dimensionless intensity I leads to

$$\left[\frac{\partial}{\partial z} + \frac{1}{c} \frac{\partial}{\partial t} \right] I(t, z) = -\alpha(t, z; w) I(t, z), \quad (6.17)$$

where $\alpha(t, z; w)$ is the generalized inversion-dependent quantum mechanical absorption coefficient:

$$\alpha(t, z; w) = -\frac{4\pi^2 \mathcal{N} \omega d^2}{\hbar c} \int \frac{1}{\pi T'_2} \frac{g(\Delta')}{(\Delta')^2 + (1/T'_2)^2} w(t, z; \Delta') d\Delta'. \quad (6.18a)$$

As in the classical expression 1.35a, we have put $K = k$ in writing α .

There are several interesting special cases of formula 6.18a. The most obvious is the classical expression 1.35a, to which it reduces in the appropriate limits. This may be shown by making the familiar replacement $2d^2/\hbar = \kappa d \rightarrow e^2/m\omega$, and considering weak excitation of the absorber, so that $w(t, z; \Delta) \rightarrow -1$. Clearly both homogeneous and inhomogeneous types of broadening contribute to the quantum expression for α , just as they do to the classical absorption coefficient.

If inhomogeneous broadening is dominant, and if $\mathcal{L}I \lesssim 1$ so that w is not strongly Δ' -dependent, the Lorentzian acts like a delta function in formula 6.18a, allowing the integral to be carried out approximately:

$$\alpha(t, z; w) \xrightarrow{T'_2 \ll T_2} -\frac{4\pi^2 \mathcal{N} \omega d^2}{\hbar c} g(0) w(t, z; 0). \quad (6.18b)$$

This expression reproduces α , the absorption coefficient 4.26 associated with the area theorem, when $w = -1$.

Finally, if homogeneous broadening is dominant, then $g(\Delta')$ is very narrow relative to the Lorentzian and may be treated like a delta function in formula 6.18. If $g(\Delta')$ is centered at a value of detuning given by Δ , then we find

$$\alpha(t, z; w) \xrightarrow{T'_2 \gg T_2} -\frac{4\pi^2 \mathcal{N} \omega d^2}{\hbar c} \frac{1}{\pi T'_2} \frac{1}{\Delta^2 + (1/T'_2)^2} w(t, z; \Delta), \quad (6.18c)$$

in which case we recognize $-\alpha(t, z; w)$ as $\mathcal{N}w$ times the product of the

off-resonance single-atom absorption cross-section $\sigma(\Delta)$:

$$\sigma(\Delta) = \frac{4\pi^2\omega d^2}{\hbar c} \frac{1}{\pi T'_2} \frac{1}{\Delta^2 + (1/T'_2)^2}. \quad (6.19)$$

It is clear that this is the appropriate form for α to allow us to recognize the basic intensity rate equation 6.17 as a simple generalization of the Gires-Combaud on-resonance equation 6.16. When the field being absorbed is exactly on resonance and steady in time, so that $\Delta=0$, and $\partial I/\partial t=0$, then equations 6.16 and 6.17 are identical.

Thus we reach the same conclusions regarding the Maxwell field equations as we reached regarding the atomic Bloch equations in Section 6.4: they are no better than familiar rate equations if collisions or other incoherent dipole interruptions cause the homogeneous relaxation time T'_2 to be substantially shorter than all other response and relaxation times.

6.6 SATURATION AND NONLINEAR SPECTROSCOPY

In a wide class of experiments the steady-state values taken by u , v , and w , after all of their temporal oscillations have been damped out, are of particular interest. It is possible to imagine having to describe an experiment in which $\mathcal{E}(t, z)$ has settled down to the steady value $\mathcal{E}_0(z)$ after a time much longer than T_1 or T'_2 . This is easy to do in the optical regime where T_1 and T'_2 are usually shorter than 1 μ sec. The Bloch equations may be used to analyze such experiments. The steady-state value of the inversion follows immediately from equation 6.15 in the long-time limit:

$$w(\infty; \Delta) = \frac{w_{\text{eq}}}{1 + \mathcal{L}I}. \quad (6.20)$$

The corresponding solutions to the dispersive and absorptive parts of the dipole moment, which will be required below, have been given in equations 3.22. They may be rederived by replacing w in equations 6.13a and 6.13b by $w(\infty; \Delta)$ given immediately above:

$$u(\infty; \Delta) = -w_{\text{eq}}\Delta T'_2 \frac{\mathcal{L}}{1 + \mathcal{L}I} \kappa \mathcal{E}_0 T'_2 \quad (6.21a)$$

and

$$v(\infty; \Delta) = w_{\text{eq}} \frac{\mathcal{L}}{1 + \mathcal{L}I} \kappa \mathcal{E}_0 T'_2. \quad (6.21b)$$

These solutions for u and v are identical with the long-time limits of the classical solutions 1.20a and 1.20b except for the factor $-w_{\text{eq}}/1 + \mathcal{L}I$. Because I is proportional to \mathcal{E}_0^2 this factor introduces into the solutions an important nonlinearity. In Fig. 6.1 the effect of this nonlinearity on the inversion may clearly be seen. The stronger the field is made, the more likely it is that the inversion is driven to zero. In other words, the driving field is causing each atom to make transitions back and forth between its two energy levels so rapidly that its effective energy on the average is just the mean of $+\frac{1}{2}\hbar\omega_0$ and $-\frac{1}{2}\hbar\omega_0$, namely zero. The field-atom interaction is said to be saturated.

In the absence of any incoherent input of energy, w_{eq} is equal to -1 . For such a two-level atom the steady-state inversion has the form

$$w(\infty; \Delta) = -\frac{1 + (\Delta T'_2)^2}{1 + (\Delta T'_2)^2 + I}, \quad (6.22)$$

where we have used equations 6.14 and 6.19. This expression shows how the energy stored in the system depends on the intensity of the incident field. For a given detuning, the steady-state inversion becomes increasingly less negative as I increases. The width at half height $\delta(w_{1/2})$ of the profile of w versus Δ increases as a function of intensity:

$$\delta(w_{1/2}) = \frac{1}{T'_2} [1 + I]^{1/2} = \frac{1}{T'_2} \left[1 + T_1 T'_2 (\kappa \mathcal{E}_0)^2 \right]^{1/2}, \quad (6.23)$$

showing power broadening. In Fig. 6.2, $w(\infty; \Delta)$ is shown plotted against $\Delta T'_2$ for several values of I . Finally, it should be pointed out that w is negative for all finite values of \mathcal{E}_0 . An incoherently saturating field can never produce a positive inversion.

An important implication of expression 6.22 for the steady-state inversion is that the atoms nearest to resonance with the steady external field \mathcal{E}_0 are not pure absorbers, since they have been stimulated by \mathcal{E}_0 partially out of their ground states. The consequence for an inhomogeneously broadened absorption line can be quite dramatic. A weak probe beam used to scan the line will experience anomalously low absorption in the neighborhood of the saturating field frequency as shown in Fig. 6.3 in the next

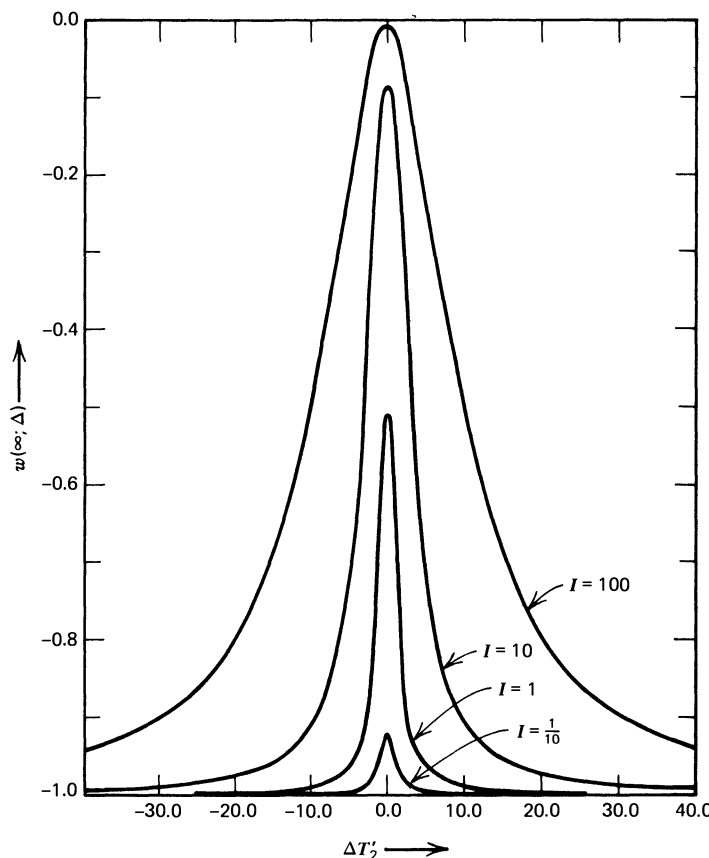


Fig. 6.2 The steady-state inversion of an atom exposed to a steady coherent field, in the rate equation limit, as a function of detuning. The three curves correspond to coherent fields with dimensionless intensities $I = \frac{1}{10}, 1, 10, 100$. The curves are taken from equation 6.22.

section. In effect, the saturating field \mathcal{E}_0 burns a hole in the absorption line. Furthermore, the width of the hole depends, as equation 6.23 shows, on the relaxation times T_1 and T'_2 . Thus information about homogeneous linewidths, usually inaccessible buried within the much wider inhomogeneous line, may be obtained using this method. Some of the most dramatic possibilities for nonlinear spectroscopy arise in connection with tunable saturating and probing laser sources. Hänsch, Shahin, and Schawlow have made a direct optical determination [6] of the Lamb shift in hydrogen, for example. An extensive theoretical discussion, with many references to early work, has been given by Shirley [7].

6.7 SATURATED ABSORPTION

It is possible to calculate the power absorbed from the saturating field by the medium. The work per unit volume done on the atoms in time dt by the driving field through its interaction with the atomic dipole moments is given by

$$dU = E \frac{dP}{dt} dt. \quad (6.24a)$$

The power absorbed per unit volume follows directly from the use of relations 4.2 and 4.3:

$$\left(\frac{dU}{dt} \right) = -2\mathcal{E}_0 \mathcal{N} \omega d \int d\Delta' g(\Delta') [u(t, z; \Delta') \cos(\omega t - Kz) \sin(\omega t - Kz) + v(t, z; \Delta') \cos^2(\omega t - Kz)], \quad (6.24b)$$

where small terms such as \dot{u} and \dot{v} have been ignored compared with ωu and ωv .

Although the two terms in equation 6.24b contribute roughly equally to the instantaneous rate of energy absorption, only the second term has a nonzero average over times longer than an optical cycle or two. Thus, as expected, only the in-quadrature or absorptive part $v(t, z; \Delta')$ of the dipole moment leads to steady power flow into the absorber. The average value, per atom, of this steady power flow may be written as

$$\mathcal{P} = -\frac{\hbar\omega}{2} \frac{w_{eq}}{T_1} \int d\Delta' g(\Delta') \frac{\mathcal{L}I}{1 + \mathcal{L}I}, \quad (6.25a)$$

where equation 6.21b has been used for $v(t, z; \Delta')$, and $\cos^2(\omega t - kz)$ has been replaced by its average value $\frac{1}{2}$. It may be seen that when the atom is actually an absorber, that is, when w_{eq} is negative, the power absorbed is positive.

An expression equivalent to equation 6.25a was derived for magnetic resonance absorption by Bloch [8] in the limit of zero inhomogeneous broadening. In order to obtain the optical expression analogous to that of Bloch we need only replace $g(\Delta')$ by $\delta(\Delta - \Delta')$:

$$\mathcal{P} \xrightarrow{T_2 \ll T_2^*} -\frac{\hbar\omega}{2} \frac{w_{eq}}{T_1} \frac{T_1 T_2' (\kappa \mathcal{E}_0)^2}{1 + (\Delta T_2)^2 + T_1 T_2' (\kappa \mathcal{E}_0)^2}.$$

Power broadening appears naturally in \mathcal{P} , just as in the magnetic resonance case. For fields sufficiently strong that $T_1 T'_2 (\kappa \mathcal{E}_0)^2 \gg 1 + (\Delta T'_2)^2$, the saturation maximum is determined solely by the single-atom spontaneous emission power $\hbar\omega/T_1$ and by the equilibrium level of the inversion. The greatest value of the absorption is reached, of course, when the inversion is least: $w_{\text{eq}} = -1$.

The “hole-burning” mentioned in Section 6.6 is contained in expression 6.25a. This is apparent if the incident saturating beam’s power flow, given by $c \mathcal{E}_0^2/2\pi$, is factored out:

$$\mathcal{P} = \frac{c \mathcal{E}_0^2}{2\pi} \int \sigma(\Delta') \left[\frac{-w_{\text{eq}}}{1 + \mathcal{L}I} \right] g(\Delta') d\Delta'. \quad (6.25b)$$

Here $\sigma(\Delta')$ is the single-atom absorption cross-section given in equation 6.19; it is the off-resonance generalization of the σ appearing in the rate equations 5.12 and 6.16. The importance of equation 6.25b is that it shows that power absorption is directly attributable to the single-atom absorption cross-section $\sigma(\Delta')$ only if a *saturated* inhomogeneous lineshape function

$$g_{\text{sat}}(\Delta') = (-w_{\text{eq}}) \frac{g(\Delta')}{1 + \mathcal{L}I} \quad (6.26)$$

is used to account for inhomogeneous broadening. When a saturated inhomogeneous lineshape function is invoked, the fraction of atoms having detuning Δ' within the detuning range $d\Delta'$ is effectively $g_{\text{sat}}(\Delta')d\Delta'$, smaller than $g(\Delta')d\Delta'$ by the factor $(-w_{\text{eq}})[1 + \mathcal{L}I]^{-1}$.

We show this effective reduction in the number of resonant atoms, due to saturation, in Fig. 6.3. Of course the total number of resonant atoms in the vicinity of the “hole” in Fig. 6.3 is not actually reduced. Those atoms at exact resonance with the external field, the ones for which $\Delta=0$, simply do not do their fair share of work in absorbing the field. They frequently find themselves excited into their upper level, ready to emit instead of absorb. In contrast, atoms in the inhomogeneous line far from resonance, atoms for which $\Delta \gg 1/T'_2$, are rarely excited far from their lower level and behave as normal absorbers.

6.8 PROPAGATING WAVE ATTENUATION AND AMPLIFICATION

To discuss wave attenuation and amplification Maxwell’s equations must be combined with the Bloch equations. The simplest situation, and the one

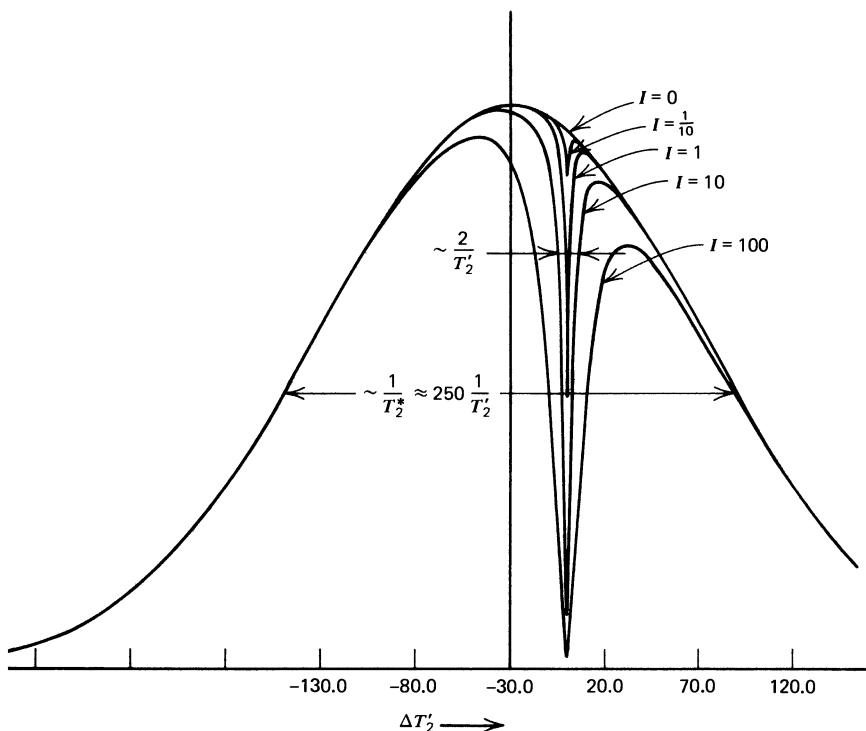


Fig. 6.3 “Hole burning,” or the effective reduction in the number of absorber atoms under an inhomogeneously broadened absorption line in the presence of coherent external fields of various strengths. The curves correspond to the values 0, $\frac{1}{10}$, 1, 10, and 100 for the dimensionless intensity I .

closest to the familiar classical case, occurs when the pulse envelope \mathcal{E} is effectively constant over many lifetimes T_1 and T'_2 which are in turn much shorter than T_2^* . In this case the intensity rate equation 6.17 simplifies considerably. The time derivative on the left-hand side may be ignored, and $\alpha(t, z; w)$ replaced by expression 6.18c. The inversion may be replaced by its asymptotic limit given in equation 6.20. The equation governing the attenuation of the pulse may then be written as

$$\frac{\partial}{\partial z} I(z) = \alpha(\Delta) \left[\frac{w_{eq}}{1 + \mathcal{L} I(z)} \right] I(z), \quad (6.27)$$

where $\alpha(\Delta)$ is the single-atom small-signal absorption coefficient, equal to $\mathcal{N}\sigma(\Delta)$:

$$\alpha(\Delta) = \frac{4\pi^2 \mathcal{N} \omega d^2}{\hbar c} \frac{1}{\pi T'_2} \frac{1}{\Delta^2 + (1/T'_2)^2}. \quad (6.28)$$

The classical absorption formula appropriate to homogeneously broadened absorbers is easily recovered from equation 6.27 by taking the small-signal limit ($\mathcal{L}I \ll 1$) and by ignoring incoherent energy inputs ($w_{eq} = -1$). Then equation 6.27 reduces to the familiar Beer's law:

$$\frac{\partial}{\partial z} I(z) = -\alpha(\Delta)I(z),$$

completely equivalent to equation 1.34b.

In a normal absorber $w_{eq} = -1$, and so the intensity is attenuated with increasing z . However, if by some means the resonant atoms are prepared in their excited states with higher probability than in their ground states, then $w_{eq} > 0$ and $I(z)$ grows with increasing penetration into the medium: the light beam is amplified.

Arbitrarily high amplification is predicted by equation 6.27 if $w_{eq} > 0$. In practice, the medium that acts as host for the resonant atoms begins to interact with the field, if the intensity is high enough. Such an interaction is usually very nonresonant and weak and to a good approximation leads merely to ordinary linear absorption. Therefore the equation that realistically describes cw electric fields in amplifying resonant media is a simple generalization of equation 6.27:

$$\frac{\partial}{\partial z} I(z) = -\beta I(z) + \alpha(\Delta) \left[\frac{w_{eq}}{1 + \mathcal{L}I(z)} \right] I(z), \quad (6.29)$$

where β is the small-signal absorption coefficient of the host medium. In most cases equation 6.29 is interesting only if $\beta \ll \alpha(\Delta)$, because only then is substantial amplification possible. Of course $\alpha(\Delta) \rightarrow 0$ when $\Delta \gg 1/T'_2$, so we may conclude immediately that strong amplification of a pulse that is detuned from resonance by many absorption linewidths is highly improbable.

Furthermore, even for $\alpha(\Delta) \gg \beta$, $I(z)$ eventually saturates. The limiting

value of the intensity, defined by $\partial I / \partial z = 0$, is easily found to be

$$I(\infty) = \left(\frac{w_{\text{eq}}\alpha(\Delta)}{\beta} - 1 \right) [1 + (\Delta T'_2)^2]. \quad (6.30)$$

Icsevgi and Lamb [9] have carried out the integration of equation 6.29. However, the general behavior of $I(z)$ is obvious, even without integrating the equation. Some curves of intensity versus distance of propagation are sketched in Fig. 6.4. There are three distinct regions of pulse growth. In the beginning $I(z)$ is small and both $\mathcal{L}I$ and βI can be ignored. At this stage pulse growth is exponential, and the growth rate is $w_{\text{eq}}\alpha(\Delta)$. Next, especially near to resonance, $\mathcal{L}I$ begins to play some role but $-\beta I$ is still negligible. In this second stage growth is only linear, at the rate $w_{\text{eq}}\alpha(\Delta)/\mathcal{L}$. Finally, the third stage is one of saturation. As $I(z)$ grows large enough so that $-\beta I$ has some influence, the growth rate gradually decreases to zero. At larger distances into the medium the propagation of the pulse involves only the transfer to the host medium of the energy of the inversion in the resonant medium through the absorption coefficient β .

It is useful to define a dimensionless gain ratio r by the ratio of the amplification rate $w_{\text{eq}}\alpha(\Delta)$ to the attenuation rate β :

$$r \equiv \frac{w_{\text{eq}}\alpha(\Delta)}{\beta}. \quad (6.31)$$

Equation 6.30 shows that amplification will not be possible if $r < 1$, so that the value $r = 1$ defines the threshold value of the inversion w_{eq} necessary to sustain amplification.

Icsevgi and Lamb [9] remark that it is possible to derive, via perturbation theory, an analogue to equation 6.29, which we have derived by way of a nonperturbative integration of the Bloch equations. The result, through third-order perturbation theory, corresponds to a small-signal expansion of equation 6.29 in powers of $\mathcal{L}I$:

$$\frac{\partial}{\partial z} I = (w_{\text{eq}}\alpha(\Delta) - \beta)I - w_{\text{eq}}\alpha(\Delta)\mathcal{L}I^2. \quad (6.32)$$

This truncated small-signal equation is not unphysical. It also predicts saturation at a finite value of I :

$$I_{\text{pert}}(\infty) = \frac{1}{r}(r-1)[1 + (\Delta T'_2)^2]. \quad (6.33)$$

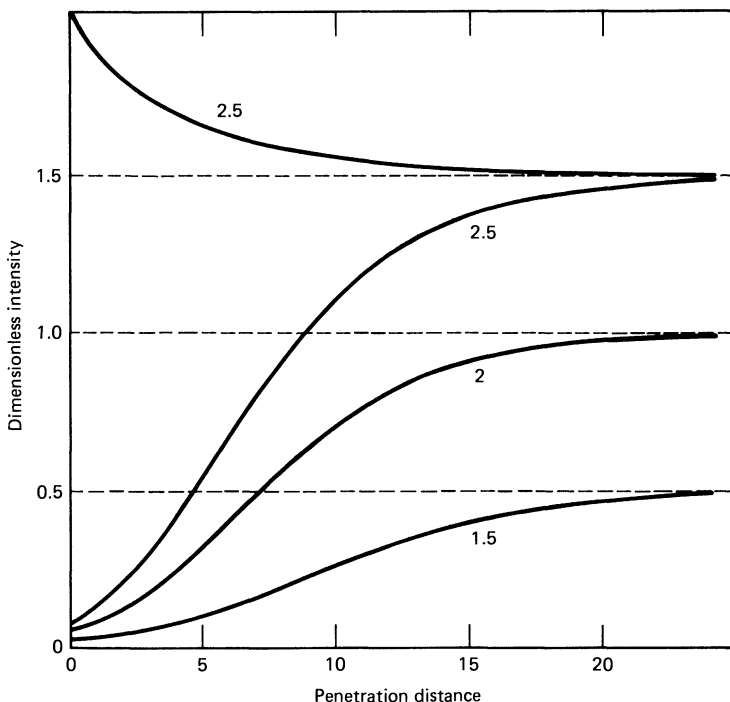


Fig. 6.4 Amplification of a cw signal for various values of the parameter $r/\beta W_{eq}$ as a function of penetration distance into the amplifier. Several possible values of input intensity are shown. [From A. Icsevgi and W. E. Lamb, Jr., *Phys. Rev.* **185**, 517 (1969).]

This is smaller than the exact value given in equation 6.30, but only by the factor $1/r$ which is unity at threshold.

It is possible to discuss amplification much more generally than we have done. If the traveling wave is actually a pulse, short in time compared with T_1 and T'_2 , all of the atomic and field variables have time dependences that cannot be ignored. For a discussion of amplification in a wide variety of possible situations the reader is referred to Icsevgi and Lamb [9]. Reviews with many early references have been given by Arecchi et al. [10] and G. L. Lamb [10].

6.9 DISPERSION IN SATURATED MEDIA AND SELF-FOCUSING

Dispersive characteristics of the propagation process, as opposed to absorptive ones, may be studied using the in-phase Maxwell equation. If we

again assume for simplicity a homogeneous line, detuned by amount Δ from the steady carrier frequency ω , then the dispersion relation

$$K^2 - k^2 = 2\pi k^2 \mathcal{N} d \left[\frac{u(z; \Delta)}{\mathcal{E}_0(z)} \right], \quad (6.34)$$

which follows from equation 4.4a in the limit $g(\Delta') \rightarrow \delta(\Delta' - \Delta)$, is z -dependent. It may be written in a more familiar form if equation 6.21a is used to eliminate the ratio $u(z; \Delta)/\mathcal{E}_0(z)$. The result is:

$$K^2 - k^2 = k^2 \left(\frac{4\pi \mathcal{N} d^2}{\hbar} \right) \frac{\Delta}{\Delta^2 + (1/T_2')^2} \left[\frac{-w_{eq}}{1 + \mathcal{L} I(z)} \right]. \quad (6.35)$$

This expression should be compared directly with its classical counterpart. Except for the final bracketed factor, equation 6.35 is identical to the classical relation 1.34a, with the understanding that once again the replacement $\kappa d \rightarrow e^2/m\omega$ must be made.

It is the final factor in the dispersion relation 6.35 that is interesting, because this factor contains the z dependence through the intensity $I(z)$. This dependence on position and intensity of the wave-vector K is a manifestation of the quantum dipole's inability to respond in proportion to the field strength. That this nonproportionality sets in only for relatively high intensities is to be expected. We have already seen in Section 2.4 that a weakly excited quantum dipole behaves entirely classically, in which case u is strictly proportional to \mathcal{E}_0 . In the small-signal limit, when $\mathcal{L} I \ll 1$, the z dependence is insignificant.

However, if $w_{eq} > 0$ and the intensity grows as the field propagates, the z dependence may become a prominent feature of the dispersion relation. In that case it is convenient to define a local phase velocity $v_{ph} = \omega/K$ and a local index of refraction $n(z) = c/v_{ph}(z)$. The resulting expression for the index is therefore:

$$n^2(z) = 1 + \frac{4\pi \mathcal{N} d^2}{\hbar} \frac{\Delta}{\Delta^2 + (1/T_2')^2} \left[\frac{-w_{eq}}{1 + \mathcal{L} I(z)} \right]. \quad (6.36)$$

In Fig. 6.5 the relation between $n(z)$ and I is sketched. Note that if the medium is an amplifier, as the figure assumes, the index is always smaller

than unity and the carrier wave velocity is greater than the speed of light in vacuum. This is typical of amplifiers, and has been pointed out repeatedly in the recent literature [11]. There is no contradiction with causality or the special theory of relativity. As DaCosta shows [12], any feature of a pulse, such as the arrival of its leading edge or a discontinuity in its amplitude, which could carry information, will travel no faster than c .

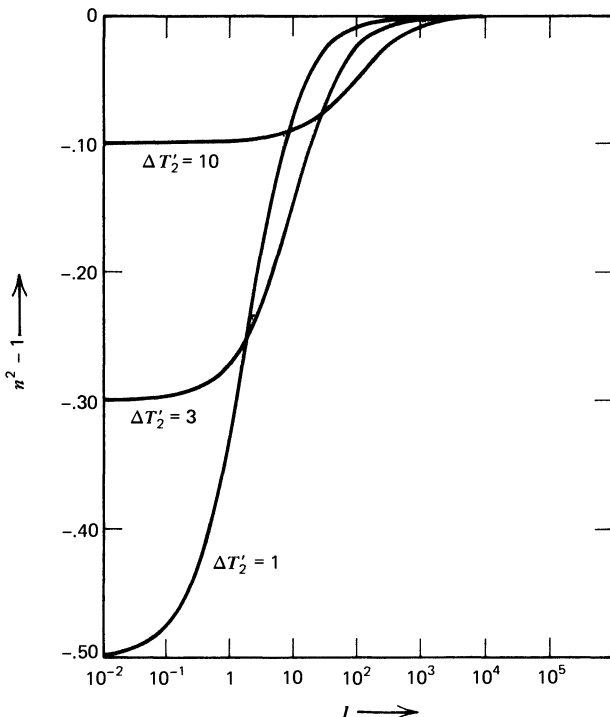


Fig. 6.5 Index of refraction in an amplifier. The figure depicts equation 6.36 and shows that n^2 approaches unity rapidly as I grows in the course of amplification. The three curves for $\Delta T'_2 = 1, 3$, and 10 show that the dependence on I is weaker for absorbers detuned further from resonance.

Kelley and Javan [13, 14] have pointed out that self-focusing is a possible consequence of the nonlinear relation 6.36 between n and I . Like the absorptive relation 6.29, this relation can be developed as a series of

powers of $\mathcal{L}I$:

$$n^2 = 1 + \frac{4\pi \mathcal{N}d^2}{\hbar} \frac{\Delta}{\Delta^2 + (1/T_2')^2} (-w_{eq})[1 - \mathcal{L}I + \dots]. \quad (6.37)$$

Self-focusing can occur because a light beam is ordinarily more intense along its axis than at its edges. Thus a medium with an index of refraction of the form

$$n = n_0 + \delta n, \quad (6.38)$$

where δn is directly proportional to I , will have a higher index at the beam axis, and a lower phase velocity there than on the beam edges. The medium therefore behaves as a convex lens. A gradual convergence of the beam toward the axis is the consequence. A quantitative analysis [13] shows that a beam of input diameter D comes to a focus in a distance Z_f , where

$$Z_f = \frac{1}{4}D \left(\frac{n_0}{\delta n} \right)^{1/2}. \quad (6.39)$$

In the present case, where the I -dependence of n is due to the saturation of the resonant transition, inspection of equation 6.37 allows the following identifications:

$$n_0^2 = 1 + \frac{\alpha(\Delta)\lambda}{2\pi} (-w_{eq})\Delta T_2' \quad (6.40)$$

and

$$2n_0\delta n = -\frac{\alpha(\Delta)\lambda}{2\pi} \frac{(-w_{eq})\Delta T_2'}{\left[1 + (\Delta T_2')^2\right]} I. \quad (6.41)$$

Here we have introduced the transition wavelength $\lambda = 2\pi\omega/c$, and have used the small-signal absorption coefficient $\alpha(\Delta)$ appropriate to a homogeneously broadened absorber, given in equation 6.28:

$$\alpha(\Delta) = \frac{4\pi \mathcal{N}\omega d^2}{\hbar c} \frac{T_2'}{1 + (\Delta T_2')^2}.$$

Expression 6.41 shows that δn is positive only when $w_{eq}\Delta$ is positive. Consequently self-focusing can be achieved when a light beam saturates an amplifying medium ($w_{eq} > 0$) whose resonance frequency is higher than that of the light ($\Delta > 0$), or when a light beam saturates an absorber ($w_{eq} < 0$) whose resonance frequency lies below that of the light ($\Delta < 0$). In all other cases defocusing occurs.

In dilute gaseous absorbers the nonlinear coefficient δn can be quite significant, causing self-focusing within 10–100 cm for input beams 10–100 microns in diameter. In recent experiments, using sodium vapor and a tunable laser, Bjorkholm and Ashkin [15] have made observations of self-focusing in accord with the steady-state Javan-Kelley analyses.

References

1. W. E. Lamb, Jr., *Phys. Rev.* **134**, 1429 (1964).
2. L. Allen and G. I. Peters, *Phys. Rev. A* **8**, 2031 (1973).
3. J. H. Eberly, *Am. J. Phys.* **40**, 1374 (1972).
4. For example, see L. I. Schiff, *Quantum Mechanics*, McGraw-Hill, New York, 1968, 3rd ed., pp. 401–405; W. Louisell, *Radiation and Noise in Quantum Electronics*, McGraw-Hill, New York, 1964, Secs. 5.4 and 5.5.
5. W. Louisell, *Quantum Statistical Properties of Radiation*, Wiley, New York, 1973, Sec. 5.2, case 1.
6. T. W. Hänsch, I. S. Shahin, and A. L. Schawlow, *Nature* **235**, 63 (1972); see also T. W. Hänsch, I. S. Shahin, and A. L. Schawlow, *Phys. Rev. Lett.* **27**, 707 (1971); and T. W. Hänsch, M. H. Nayfeh, S. A. Lee, S. M. Curry, and I. S. Shahin, *Phys. Rev. Lett.* **32**, 1336 (1974).
7. J. H. Shirley, *Phys. Rev. A* **8**, 347 (1973).
8. F. Bloch, *Phys. Rev.* **70**, 460 (1946); see also G. E. Pake, *Am. J. Phys.* **18**, 438 (1950).
9. A. Icsevgi and W. E. Lamb, Jr., *Phys. Rev.* **185**, 517 (1969).
10. F. T. Arecchi, G. L. Masserini, and P. Schwendimann, *Rev. Nuov. Cim.* **1**, 181 (1969); G. L. Lamb, Jr., *Rev. Mod. Phys.* **43**, 99 (1971).
11. N. G. Basov et al., *Sov. Phys. Dokl.* **10**, 1039 (1966); N. G. Basov, R. V. Ambartsumyan, V. S. Zuev, P. G. Kryukov, and V. S. Letokhov, *Sov. Phys. J.E.T.P.* **23**, 16 (1966); F. A. Hopf and M. O. Scully, *Phys. Rev.* **179**, 399 (1969); A. Icsevgi and W. E. Lamb, Jr., Ref. 9.
12. R. C. T. DaCosta, *J. Math. Phys.* **11**, 2799 (1970).
13. P. L. Kelley, *Phys. Rev. Lett.* **15**, 1005 (1965).
14. A. Javan and P. L. Kelley, *I.E.E.E. Journ. Quant. Electron.* **2**, 470 (1966).
15. J. E. Bjorkholm and A. Ashkin, *Phys. Rev. Lett.* **32**, 129 (1974).

Quantum Electrodynamics and Spontaneous Emission

7.1 Introduction	152
7.2 Basic Equations of Motion	153
7.3 Atomic Inversion Oscillation, the Quantum Electrodynamic Rabi Problem	157
7.4 Single-Atom Spontaneous Emission	162
7.5 Quantum Electrodynamic Perturbation Theory	170
References	172

7.1 INTRODUCTION

For the most part optics is insensitive to the finest details of the electromagnetic field. The possibility that quantization of the radiation field has important consequences is usually deliberately overlooked in both experimental and theoretical work. There are, however, two situations in which field quantization cannot be ignored. The first situation is encountered when one discovers an optical problem, almost no matter how idealistically stated, which can be solved exactly within the framework of a quantized field theory. Such problems are rare enough to have an importance of their own, virtually independent of their relevance to possible experimental work. The second situation arises when an optical interaction causes an observed effect that cannot be quantitatively accounted for except by a quantized field theory.

In this chapter we discuss problems of both of these types. The best example of the first type was provided by Jaynes and Cummings who showed that a single two-level atom obeyed solvable equations of motion when interacting with a single-mode quantized radiation field. The results in this case are particularly interesting because they are very closely related to those of the semiclassical Rabi problem, discussed at length in Chapter 3. The second type of problem arises in treatments of spontaneous emission, especially in connection with the radiative frequency shift, or Lamb shift, associated with the emission. Both of these problems are discussed in the following sections after a brief review of very elementary quantum electrodynamics. The approach that we have followed in

the first six chapters, which concentrates wherever possible on the dynamical variables themselves rather than on probability amplitudes, is easily extended to handle quantized fields. Because in quantum electrodynamics the electric field amplitude becomes an operator, some care is required with commutation relations and the relative ordering of operators. For the sake of comparison with the usual perturbation theory approach to radiative frequency shifts, the last section is devoted to a standard calculation of the same Lamb shift calculated by Heisenberg equation methods in Section 7.4.

7.2 BASIC EQUATIONS OF MOTION

The interaction of a single electron with the electromagnetic radiation field is described by the nonrelativistic Hamiltonian:

$$\hat{H} = \frac{1}{2m} \left(\hat{\mathbf{p}} - \frac{e}{c} \hat{\mathbf{A}} \right)^2 + \Phi(\mathbf{r}) + \sum_{\lambda} \hbar \omega_{\lambda} \hat{a}_{\lambda}^{\dagger} \hat{a}_{\lambda}. \quad (7.1)$$

The potential $\Phi(\mathbf{r})$ acts to bind the electron to the nucleus. The atom itself, in the absence of the field, has properties determined by

$$\hat{H}_A = \frac{1}{2m} \hat{p}^2 + \Phi(\mathbf{r}), \quad (7.2)$$

which we simply call the atomic Hamiltonian. We choose to work in the radiation gauge in which the vector potential $\hat{\mathbf{A}}$ is purely transverse, and also assume that all longitudinal electric fields are already incorporated in $\Phi(\mathbf{r})$.

The field Hamiltonian

$$\hat{H}_F = \sum_{\lambda} \hbar \omega_{\lambda} \hat{a}_{\lambda}^{\dagger} \hat{a}_{\lambda} \quad (7.3)$$

has been written in standard form with the zero-point energy discarded by an appropriate choice of origin for the energy scale. In the Heisenberg picture the photon creation and destruction operators \hat{a}_{λ} and $\hat{a}_{\lambda}^{\dagger}$ obey the canonical equal-time commutation relation appropriate to bosons:

$$[\hat{a}_{\lambda}(t), \hat{a}_{\lambda'}^{\dagger}(t)] = \delta_{\lambda\lambda'}. \quad (7.4)$$

We define the usual photon number states to be the eigenstates of the number operator at $t=0$. The familiar properties of these states may be summarized as follows:

$$\hat{a}_\lambda(0)|n_\lambda\rangle = \sqrt{n_\lambda} |n_\lambda - 1\rangle; \quad \hat{a}_\lambda^\dagger(0)|n_\lambda\rangle = \sqrt{n_\lambda + 1} |n_\lambda + 1\rangle. \quad (7.5)$$

The vector potential $\hat{\mathbf{A}}$, which couples atom and field, may be expressed in terms of the same \hat{a}_λ and \hat{a}_λ^\dagger operators:

$$\hat{\mathbf{A}}(t, \mathbf{r}) = \sum_{\lambda} \left(\frac{2\pi\hbar c^2}{\omega_{\lambda} \mathcal{V}} \right)^{1/2} [\mathbf{u}_{\lambda}(\mathbf{r}) \hat{a}_{\lambda}(t) + \mathbf{u}_{\lambda}^*(\mathbf{r}) \hat{a}_{\lambda}^\dagger(t)],$$

where λ indexes *both* the polarization *and* the wave vector \mathbf{k}_{λ} of the λ th mode. As usual, $\mathbf{u}_{\lambda}(\mathbf{r})$ is one of a complete set of mode functions appropriate to the cavity within which the radiation is quantized. The mode functions are orthonormal over the cavity volume \mathcal{V} :

$$\int_{\mathcal{V}} \mathbf{u}_{\lambda}(\mathbf{r}) \cdot \mathbf{u}_{\lambda'}^*(\mathbf{r}) d^3r = \delta_{\lambda\lambda'}. \quad (7.6)$$

They are also solenoidal or “transverse” functions: $\nabla \cdot \mathbf{u}_{\lambda}(\mathbf{r}) = 0$. In many commonly encountered cases there is no actual physical cavity in the problem, and the \mathbf{u}_{λ} 's are simply taken to be the mode functions appropriate to a large imaginary cubical box with volume \mathcal{V} and periodic boundary conditions. In such cases

$$\mathbf{u}_{\lambda}(\mathbf{r}) = (\mathcal{V})^{-\frac{1}{2}} \boldsymbol{\epsilon}_{\lambda} e^{i\mathbf{k}_{\lambda} \cdot \mathbf{r}}, \quad (7.7)$$

where $\boldsymbol{\epsilon}_{\lambda}$ is either one of the two unit polarization vectors orthogonal to \mathbf{k}_{λ} , and the vector potential takes the familiar form:

$$\hat{\mathbf{A}}(t, \mathbf{r}) = \sum_{\lambda} \mathbf{g}_{\lambda} [\hat{a}_{\lambda}(t) e^{i\mathbf{k}_{\lambda} \cdot \mathbf{r}} + \hat{a}_{\lambda}^\dagger e^{-i\mathbf{k}_{\lambda} \cdot \mathbf{r}}], \quad (7.8)$$

where for convenience we have defined

$$\mathbf{g}_{\lambda} \equiv \sqrt{\frac{2\pi\hbar c^2}{\omega_{\lambda} \mathcal{V}}} \boldsymbol{\epsilon}_{\lambda}. \quad (7.9)$$

In deriving the Heisenberg equations of motion for the atomic electron we restrict attention to near-resonant situations in which only one atomic

transition need be considered. The consequences of this restriction are just the same as in Chapter 2. The state space of the atom is two-dimensional, and the atomic operators can be represented by combinations of the 2×2 Pauli matrices. For later convenience we deviate slightly from the approach of Section 2.3. The first deviation is to drop the term $(e^2/2mc^2) \times \hat{A}^2$ from the Hamiltonian 7.1 and use only $(e/mc)\hat{\mathbf{A}} \cdot \hat{\mathbf{p}}$ as the interaction Hamiltonian. The interaction Hamiltonians $-\hat{\mathbf{d}} \cdot \hat{\mathbf{E}}$ and $-(e/mc) \times \hat{\mathbf{A}} \cdot \hat{\mathbf{p}} + (e^2/2mc^2)\hat{A}^2$ differ in the dipole approximation by a gauge transformation. The best-known discussion of these points is due to Power and Zienau [1].

The second deviation is to follow Dicke [2] and use the operators $\hat{R}_i = \frac{1}{2}\hat{\sigma}_i$ ($i = 1, 2, 3$), to represent the atomic operators. This is merely a notational device intended as a reminder that we are treating electric rather than magnetic dipole transitions. The factor of $\frac{1}{2}$ serves to give the \hat{R} 's the convenient commutation relations of angular momentum components:

$$[\hat{R}_1, \hat{R}_2] = i\hat{R}_3.$$

These two changes, $(e/mc)\hat{\mathbf{A}} \cdot \hat{\mathbf{p}}$ for $\hat{\mathbf{d}} \cdot \hat{\mathbf{E}}$, and \hat{R} 's for $\hat{\sigma}$'s, lead to the following effective two-level Hamiltonian:

$$\hat{\mathcal{H}} = \hbar\omega_0\hat{R}_3 + 2\left(\frac{\omega_0 d}{c}\right)\hat{R}_2\hat{A} + \sum_{\lambda} \hbar\omega_{\lambda}\hat{a}_{\lambda}^{\dagger}\hat{a}_{\lambda}. \quad (7.10)$$

In deriving equation 7.10 we have used the well-known relations between momentum and coordinate matrix elements:

$$\langle + | \frac{e\hat{\mathbf{p}}}{m} | - \rangle = \frac{i}{\hbar} \langle + | [\hat{H}_A, e\hat{\mathbf{r}}] | - \rangle = i\omega_0 \hat{\mathbf{d}}_{+ -}. \quad (7.11)$$

As in Chapter 2, $|+\rangle$ and $|-\rangle$ are the upper and lower states of our atom, ω_0 is the transition frequency separating the states, and $\hat{\mathbf{d}}_{+ -} = \langle + | e\hat{\mathbf{r}} | - \rangle$ is the dipole moment matrix element. In addition, we have chosen the phases of the states such that $\hat{\mathbf{d}}_{+ -} = +d\mathbf{u}_d$, where d is real and \mathbf{u}_d is a unit vector in the direction of $\hat{\mathbf{d}}_{+ -}$. Finally, the scalar \hat{A} is intended to denote the scalar product of $\hat{\mathbf{A}}$ with \mathbf{u}_d , evaluated at \mathbf{r}_0 , the position of the dipole:

$$\hat{A} = \hat{\mathbf{A}} \cdot \mathbf{u}_d = \sum_{\lambda} g_{\lambda} [\hat{a}_{\lambda} e^{i\mathbf{k}_{\lambda} \cdot \mathbf{r}_0} + \hat{a}_{\lambda}^{\dagger} e^{-i\mathbf{k}_{\lambda} \cdot \mathbf{r}_0}] \quad (7.12)$$

where the scalar quantity g_λ is defined to be

$$g_\lambda \equiv \mathbf{g}_\lambda \cdot \mathbf{u}_d = \sqrt{\frac{2\pi\hbar c^2}{\omega_\lambda \epsilon_0}} \epsilon_\lambda \cdot \mathbf{u}_d, \quad (7.13)$$

the projection of \mathbf{g}_λ along the dipole matrix element.

The Heisenberg equations for the atomic operators are easily derived:

$$\dot{\hat{R}}_1 = -\omega_0 \hat{R}_2 + 2\left(\frac{\omega_0 d}{\hbar c}\right) \hat{A} \hat{R}_3, \quad (7.14a)$$

$$\dot{\hat{R}}_2 = \omega_0 \hat{R}_1, \quad (7.14b)$$

$$\dot{\hat{R}}_3 = -2\left(\frac{\omega_0 d}{\hbar c}\right) \hat{A} \hat{R}_1. \quad (7.14c)$$

The operator equations 7.14 are not so different from equations 2.29, which we derived from the $\hat{\mathbf{d}} \cdot \hat{\mathbf{E}}$ interaction, as they might seem. In equation 7.14 one may introduce $\kappa = 2d/\hbar$, and make the canonical transformation $\hat{R}_1 \rightarrow -\tilde{\hat{R}}_2$, $\hat{R}_2 \rightarrow \tilde{\hat{R}}_1$, $\hat{R}_3 \rightarrow \tilde{\hat{R}}_3$. The identification of $-(\omega_0/c)\hat{A}$ with \hat{E} , which is valid near resonance, shows that the resulting equations for $\tilde{\hat{R}}_1, \tilde{\hat{R}}_2, \tilde{\hat{R}}_3$ are exactly those given in equations 2.29 for $\hat{\sigma}_1, \hat{\sigma}_2, \hat{\sigma}_3$.

In this chapter the radiation field is accorded full operator status. No decorrelation, such as that invoked in Chapter 2 to define the approximate semiclassical theory, is introduced. The field mode operators obey the equation:

$$\dot{\hat{a}}_\lambda = -i\omega_\lambda \hat{a}_\lambda - 2i\left(\frac{\omega_0 d}{\hbar c}\right) g_\lambda^*(\mathbf{r}_0) \hat{R}_2, \quad (7.15)$$

where

$$g_\lambda(\mathbf{r}_0) \equiv g_\lambda e^{i\mathbf{k}_\lambda \cdot \mathbf{r}_0}. \quad (7.16)$$

We leave as an instructive exercise the problem of working backward from equations 7.12 and 7.15 to recover the familiar Maxwell wave equation [3]:

$$\left[\nabla^2 - \frac{1}{c^2} \frac{\partial^2}{\partial t^2} \right] \hat{\mathbf{A}}(t, \mathbf{r}) = -\frac{4\pi}{c} \hat{\mathbf{J}}^T(t, \mathbf{r}), \quad (7.17)$$

where $\hat{\mathbf{J}}^T(t, \mathbf{r})$ is the transverse part of the current $\hat{\mathbf{J}}(t, \mathbf{r})$, which arises from the oscillations of the quantum dipole at \mathbf{r}_0 :

$$\hat{\mathbf{J}}(t, \mathbf{r}) = -2d\mathbf{u}_d \omega_0 \hat{R}_2(t) \delta^3(\mathbf{r} - \mathbf{r}_0). \quad (7.18)$$

Finally, a remark about the ordering of the operators in equations 7.10 and 7.14 is appropriate. The field operators commute with all of the atomic operators at all equal times because the field and atomic operators refer to distinct degrees of freedom of the combined system. Thus products of operators, such as $\hat{A}(t, \mathbf{r}_0)\hat{R}_3(t)$, may be written in several equivalent ways. The range of possibilities is suggested by the relations:

$$\begin{aligned} \sum_{\lambda} g_{\lambda} (\hat{a}_{\lambda} + \hat{a}_{\lambda}^{\dagger}) \hat{R}_3 &= \sum_{\lambda} g_{\lambda} (\hat{a}_{\lambda} \hat{R}_3 + \hat{R}_3 \hat{a}_{\lambda}^{\dagger}) \\ &= \sum_{\lambda} g_{\lambda} \hat{R}_3 (\hat{a}_{\lambda} + \hat{a}_{\lambda}^{\dagger}) = \sum_{\lambda} g_{\lambda} (\hat{a}_{\lambda}^{\dagger} \hat{R}_3 + \hat{R}_3 \hat{a}_{\lambda}), \end{aligned}$$

all of which are valid if the time arguments associated with the various Heisenberg operators are the same.

In the following sections, for reasons of convenience, we adopt “normal” ordering with respect to the field operators. That is, at the outset of any calculation we assume that operator products have been written so that any field mode destruction operators appear on the right-hand side of the product and any field mode creation operators appear on the left-hand side. For example, only the last of the four orderings above is “normal” with respect to \hat{a}_{λ} and $\hat{a}_{\lambda}^{\dagger}$. Naturally, one’s freedom to change orderings in midcalculation is limited because different operators may acquire differing time arguments and because the interaction of the field with the atom may make the separation of different degrees of freedom difficult at a time other than the initial instant. It is clear that any ordering could be adopted at the outset. The second ordering above is frequently called “antinormal” with respect to \hat{a}_{λ} and $\hat{a}_{\lambda}^{\dagger}$, and it or any other could be used consistently without changing the results.

7.3 ATOMIC INVERSION OSCILLATION, THE QUANTUM ELECTRODYNAMIC RABI PROBLEM

The interaction of a single dipole with a monochromatic radiation field presents an important theoretical problem in electrodynamics. It is an unrealistic problem in the sense that experiments are not done with single atoms or single-mode fields. However, as a model for real atom-field problems it is very useful, particularly because it has exact solutions. In Sections 1.3 and 3.2 we have shown that exact solutions are possible in the contexts of the classical Lorentz oscillator and the quantum mechanical

two-level atom, when either of these interact with a monochromatic classical radiation field.

In this section we show that even in quantum electrodynamics, where the field is quantized, an exact solution is possible. This is interesting and important for several reasons. Obviously, the exact solution of any nontrivial problem has intrinsic theoretical interest. But in this case, in addition, the quantum electrodynamic solution allows a rare and direct comparison with the corresponding semiclassical solution. Furthermore, the presence of spontaneous emission in the quantized theory adds a new element to the problem.

The basic Hamiltonian is given in equation 7.10. After eliminating all but one of the field modes, and relabeling the coupling constant, equation 7.10 can be written as

$$\hat{\mathcal{H}} = \hbar\omega_0\hat{R}_3 + \hbar\omega\hat{a}^\dagger\hat{a} + \frac{i}{2}\hbar q(\hat{R}_+ - \hat{R}_-)(\hat{a} + \hat{a}^\dagger). \quad (7.19)$$

We have replaced \hat{R}_2 by the appropriate combination of the usual atomic raising and lowering operators

$$\hat{R}_\pm \equiv \hat{R}_1 \pm i\hat{R}_2, \quad (7.20)$$

and have located the single atom at the origin. The constant q obviously has dimensions of frequency, and is given by

$$q = -2\left(\frac{\omega_0 d}{\hbar c}\right)\left(\frac{2\pi\hbar c^2}{\omega V}\right)^{\frac{1}{2}} \boldsymbol{\epsilon} \cdot \mathbf{u}_d. \quad (7.21)$$

It is appropriate now to make the quantum electrodynamic equivalent of the rotating wave approximation as in Chapter 2. The rotating wave approximation (RWA) consists in discarding terms that oscillate at roughly twice the highest frequencies of interest, which in this case are ω and ω_0 . In the absence of interaction between atom and field the behavior of the operators in equation 7.19 is easily seen to be

$$\begin{aligned} \hat{R}_3(t) &= \hat{R}_3(0), \\ \hat{R}_\pm(t) &= \hat{R}_\pm(0)e^{\pm i\omega_0 t}, \\ \hat{a}(t) &= \hat{a}(0)e^{-i\omega t}, \\ \hat{a}^\dagger(t) &= \hat{a}^\dagger(0)e^{i\omega t}. \end{aligned} \quad (7.22)$$

Since the electromagnetic field-dipole coupling is a weak one, we expect these time dependences to be only slightly modified even when the atom and field interact. Thus operator product terms such as $\hat{R}_+ \hat{a}^\dagger$ and $\hat{R}_- \hat{a}$ give rise to oscillations at the frequencies $\pm(\omega_0 + \omega)$. Under the RWA these terms are discarded from equation 7.19, leaving the effective Hamiltonian:

$$\hat{\mathcal{H}}^{\text{RWA}} = \hbar\omega_0 \hat{R}_3 + \hbar\omega \hat{a}^\dagger \hat{a} + \frac{i}{2} \hbar q (\hat{R}_+ \hat{a} - \hat{a}^\dagger \hat{R}_-). \quad (7.23)$$

An early solution of the quantum electrodynamic problem posed by the RWA Hamiltonian above was given by Jaynes [4] and by Jaynes and Cummings [5]. We approach the problem very differently, perhaps more straightforwardly, by working in the Heisenberg picture.

The RWA interaction involves only operators that interchange one unit of excitation between atom and field. For example, $\hat{R}_+ \hat{a}$ acts to decrease the photon number by one and simultaneously raise the atom's energy one notch. For this reason, the number of excitations contained in the system is constant. Therefore the excitation number operator $\hat{N} = \hat{R}_3 + \hat{a}^\dagger \hat{a}$ is a constant and consequently must commute with $\hat{\mathcal{H}}^{\text{RWA}}$. This is easily verified. Obviously $\hat{\mathcal{H}}^{\text{RWA}}$ is itself a constant within the rotating wave approximation.

In light of these remarks it proves useful to write $\hat{\mathcal{H}}^{\text{RWA}}$ as follows:

$$\hat{\mathcal{H}}^{\text{RWA}} = \frac{1}{2} \hbar \bar{\omega} \hat{N} + \frac{1}{2} \hbar \Delta (\hat{R}_3 - \hat{a}^\dagger \hat{a}) + \frac{i}{2} \hbar q (\hat{R}_+ \hat{a} - \hat{a}^\dagger \hat{R}_-), \quad (7.24)$$

where

$$\bar{\omega} \equiv (\omega_0 + \omega) \quad \text{and} \quad \Delta \equiv (\omega_0 - \omega). \quad (7.25)$$

It is then easy to find the following Heisenberg equation for the atom energy:

$$\ddot{\hat{R}}_3 = -\frac{1}{2} q^2 (2\hat{N} + 1) \hat{R}_3 + 2iq\Delta (\hat{R}_+ \hat{a} - \hat{a}^\dagger \hat{R}_-).$$

Some rearrangement, and use of the relation (7.24), leads to the simple equation:

$$\left[\frac{d^2}{dt^2} + \hat{\Omega}^2 \right] \hat{R}_3(t) = \Delta \left[\hat{\omega}^{\text{RWA}} - \frac{1}{2} \hat{N} (\bar{\omega} - \Delta) \right], \quad (7.26)$$

where $\hbar\hat{\omega}^{\text{RWA}} = \hat{\mathcal{H}}^{\text{RWA}}$ and the energy oscillation frequency $\hat{\Omega}$ is given by

$$\hat{\Omega}^2 = \Delta^2 + q^2(\hat{N} + \frac{1}{2}). \quad (7.27)$$

Clearly $\hat{\Omega}$ is the quantum electrodynamic expression for the Rabi frequency. It governs the rate of oscillation of the atomic inversion.

The right-hand side of equation 7.26 involves only constant operators, so that the solution is found easily. To compare the quantum electrodynamic solution with the semiclassical solution, given in equation 3.18, we first take the expectation value of equation 7.26 in the state $|n, m\rangle$, which is an eigenstate of both $\hat{a}^\dagger \hat{a}$ and \hat{R}_3 at $t=0$:

$$\hat{a}^\dagger(0)\hat{a}(0)|n, m\rangle = n|n, m\rangle, \quad n = 0, 1, 2, \dots,$$

$$\hat{R}_3(0)|n, m\rangle = m|n, m\rangle, \quad m = +\frac{1}{2} \text{ or } -\frac{1}{2}.$$

Then, since $\langle \hat{\omega}^{\text{RWA}} \rangle = m\omega_0 + n\omega$, and $\langle \hat{N} \rangle = (n+m)$, the solution may be written as

$$\langle \hat{R}_3(t; \Delta) \rangle = \langle \hat{R}_3(0; \Delta) \rangle \times \left[1 - \frac{2q^2(n+m+\frac{1}{2})}{\Delta^2 + q^2(n+m+\frac{1}{2})} \sin^2 \frac{1}{2}\Omega_{nm}t \right], \quad (7.28)$$

where

$$\Omega_{nm}^2 \equiv \Delta^2 + q^2(n+m+\frac{1}{2}). \quad (7.29)$$

In the presence of the n -photon field the atom is driven from its ground state to a superposition of excited and ground states and back again. Only exact-resonance atoms, those for which $\Delta=0$, actually reach the excited state. This is qualitatively the same behavior as that of a semiclassical two-level atom exposed to a near-resonance constant-amplitude classical field. It is interesting that the relation between the semiclassical result, given earlier in equation 3.18, is even quantitatively practically identical with equation 7.28 above. Note that the expectation of \hat{E}^2 in the chosen initial state is

$$\frac{1}{4\pi} \langle \hat{E}^2 \rangle = \frac{n\hbar\omega}{cV} \quad (7.30a)$$

in the first approximation, whereas the corresponding classical average is

$$[E^2]_{av} = [(2\mathcal{E}_0 \cos \omega t)^2]_{av} = 2\mathcal{E}_0^2. \quad (7.30b)$$

Thus the relation between semiclassical and quantized field parameters is

$$(\kappa \mathcal{E}_0)^2 \leftrightarrow nq^2. \quad (7.31)$$

The closeness of the correspondence between equation 3.18 and 7.28 is especially evident when it is recalled that the inversion $w(t; \Delta)$ is related to the energy operator $\hat{R}_3(t; \Delta)$ by $w(t) = \langle \hat{\sigma}_3 \rangle = 2\langle \hat{R}_3 \rangle$.

Equation 7.28 shows the importance of spontaneous emission in the quantized field theory if the initial atomic state is not the ground state. If the atom is initially in its excited state so that $\langle \hat{R}_3(0; \Delta) \rangle = +\frac{1}{2}$ and if the initial field is the vacuum so that $n=0$, the quantum electrodynamic solution 7.28 shows that the atom's energy oscillates at the Rabi frequency $(\Delta^2 + q^2)^{1/2}$:

$$2\langle \hat{R}_3(t; \Delta) \rangle \Big|_{\substack{m=\frac{1}{2}, \\ n=0}} = 1 - \frac{2q^2}{\Delta^2 + q^2} \sin^2 \sqrt{\Delta^2 + q^2} \frac{t}{2}. \quad (7.32)$$

On the other hand, the corresponding zero-field semiclassical result, which may be obtained from equation 3.18 by putting $\mathcal{E}_0=0$ and $w_0=+1$, is not oscillatory at all:

$$w(t, \Delta) = w_0 = +1. \quad (7.33)$$

And finally, if there is initially no excitation of either atom or field ($m=-\frac{1}{2}, n=0$), naturally there are no oscillations in either the quantum or the semiclassical theories.

To compare the result 7.28 with that first found by Jaynes and Cummings, we may recall that the relation $p_{+-}(t) = \frac{1}{2} - \langle \hat{R}_3(t) \rangle_{n\frac{1}{2}}$ gives the connection between the energy expectation and the probability p_{+-} that the atom has made the transition from upper to lower state. Then equation 7.28 is equivalent to

$$p_{+-}(t) = \frac{(n+1)q^2}{(\omega_0 - \omega)^2 + (n+1)q^2} \sin^2 \sqrt{(\omega_0 - \omega)^2 + q^2} \frac{t}{2}, \quad (7.34)$$

which is exactly their result.

Finally, a few closing remarks are in order concerning the Hamiltonian $\hat{\mathcal{H}}^{\text{RWA}}$ and the Jaynes-Cummings approach to the quantum electrodynamic Rabi problem. First, when only one radiation mode may be excited, the atom and the mode simply trade energy back and forth. This is an obvious

consequence of the oscillatory solution 7.28 for \hat{R}_3 and the fact that $\hat{R}_3 + \hat{a}^\dagger \hat{a}$ is a constant. However, a many-mode, one-atom problem can also be solved almost exactly in the RWA. It forms the basis of the theory of spontaneous emission and natural line broadening due originally to Weisskopf and Wigner [6]. Similarly the “inverse” problem posed by many atoms and one field mode can serve as a basis for a model of quantum electrodynamic field attenuation ([7], Secs. 7.1–7.3; [8]) if there are assumed to be enough atoms with different resonant frequencies to provide a broad continuous atomic absorption line.

Some work has also been done on the situations that arise when a finite number of atoms interact with a single-mode quantized field. The basic difficulty in this case is that the computational problems become unmanageable, even though algorithms to obtain exact solutions are known [9].

Lastly, we should point out an important basic difference between the quantum problem solved in equation 7.28 and the semiclassical problem solved in equation 3.18 with which it has been compared. The quantum treatment automatically takes account of radiation reaction: if the atom gains energy, the field must lose energy, and vice versa. This feature is absent from our treatment in Chapter 3. Jaynes and Cummings [5] have also supplied a semiclassical solution that includes the effects of radiation reaction. Instead of trigonometric oscillations, as in equations 3.57 and 7.28, they find oscillatory elliptic functions. The differences are discussed at length in their paper.

7.4 SINGLE-ATOM SPONTANEOUS EMISSION

We now apply the Heisenberg operator equations 7.14 and 7.15 to the simplest of all quantum electrodynamic situations involving an atomic source current and all of the modes of the radiation field. Consider one two-level atom in its upper level, with all field modes empty of photons. It is well-known, of course, that the atom will emit a photon and decay to the lower level spontaneously. Because a continuum of modes is available to the emitted photon we expect real decay, in contrast to the behavior exhibited by the Jaynes-Cummings atom in the preceding section. In that case the atom simply traded its excitation periodically back and forth with the single field mode available to it.

A proper theory of spontaneous emission should lead to expressions for

a decay rate, or lifetime, of the excited system as well as an approximate radiative lineshape. The first satisfactory theory given was due to Weisskopf and Wigner [6]. The Weisskopf-Wigner treatment leads to the correct expressions for lifetime and lineshape, but fails to give an adequate picture of the line shift that accompanies the decay. The approach that we adopt [10] has the advantage of leading to the correct value of the shift as well as giving the correct lifetime and lineshape.

Equation 7.15 for $\hat{a}_\lambda(t)$ is simpler than the atomic equations 7.14 because it contains no operator products. It may be integrated formally:

$$\hat{a}_\lambda(t) = \hat{a}_\lambda^v(t) - \left(\frac{\omega_0 d}{\hbar c} \right) g_\lambda^*(\mathbf{r}_0) \int_0^\infty dt' [\hat{R}_+(t') - \hat{R}_-(t')] G_\lambda(t-t'), \quad (7.35)$$

where $\hat{a}_\lambda^v(t)$ is the free field or "vacuum part" of the solution:

$$\hat{a}_\lambda^v(t) = \hat{a}_\lambda(0) e^{-i\omega_\lambda t} \quad (7.36)$$

and $G_\lambda(t, t')$ is the retarded Green's function:

$$G_\lambda(t, t') = (\lim \epsilon \rightarrow 0^+) \begin{cases} 0, & \text{if } t < t' \\ e^{-i(\omega_\lambda - i\epsilon)(t-t')}, & \text{if } t > t' \end{cases}. \quad (7.37)$$

There is little point in maintaining a specific symbol \mathbf{r}_0 for the position of the single atom. It is set equal to zero hereafter.

It is not possible to go further with an exact solution of the Heisenberg equations 7.14 and 7.15. However, as far as the atom is concerned, spontaneous radiative decay is a very slow process, requiring many millions of cycles of dipole oscillation, on the average, before it is complete. Thus we assume that $\hat{R}_\pm(t)$ may be written as $\hat{S}_\pm(t) \exp(\pm i\omega_0 t)$, where $\hat{S}_\pm(t)$ is an unknown operator whose time variation compared with $\exp(\pm i\omega_0 t)$ is slow enough to permit its removal from the integral in equation 7.35. The remaining integration involves only exponentials and can be performed easily. For example, the last term in equation 7.35 leads to

$$\lim_{\epsilon \rightarrow 0} \hat{S}_-(t) e^{-i(\omega_\lambda - i\epsilon)t} \frac{e^{i(\omega_\lambda - \omega_0 - i\epsilon)t} - 1}{i(\omega_\lambda - \omega_0 - i\epsilon)} = \hat{R}_-(t) \lim_{\epsilon \rightarrow 0^+} \frac{1 - e^{-i(\omega_\lambda - \omega_0 - i\epsilon)t}}{i(\omega_\lambda - \omega_0 - i\epsilon)}. \quad (7.38)$$

After a suitably long time the limit becomes simply

$$\frac{1}{i(\omega_\lambda - \omega_0 - i\epsilon)} = -i \frac{P}{\omega_\lambda - \omega_0} + \pi\delta(\omega_\lambda - \omega_0) \equiv -i\xi^*(\omega_\lambda - \omega_0). \quad (7.39)$$

Here P and δ denote principal part and delta function as usual. The zeta function is defined following Heitler [11]. It will prove useful as an abbreviation, especially in the sections that follow.

The lowering operator for the λ th mode can now be conveniently written as

$$\hat{a}_\lambda(t) = \hat{a}_\lambda^v(t) + \hat{a}_\lambda^s(t), \quad (7.40)$$

where the homogeneous term or “vacuum part” $\hat{a}_\lambda^v(t)$ is given in equation 7.36 and the “source part” $\hat{a}_\lambda^s(t)$ follows from our approximate evaluation of the integral in equation 7.35:

$$\hat{a}_\lambda^s(t) = i\left(\frac{\omega_0 d}{\hbar c}\right) g_\lambda^* \left[\hat{R}_+(t) \xi^*(\omega_\lambda + \omega_0) - \hat{R}_-(t) \xi^*(\omega_\lambda - \omega_0) \right]. \quad (7.41)$$

The designation “source part” for $\hat{a}_\lambda^s(t)$ serves to emphasize that the contribution of the second term in equation 7.35 is the analogue of the inhomogeneous or source term in the well-known retarded solution

$$\mathbf{A}(t, \mathbf{r}) = \frac{1}{c} \int \frac{[\mathbf{J}^T(t, \mathbf{r}')]_{\text{ret}}}{|\mathbf{r} - \mathbf{r}'|} d^3 r' \quad (7.42)$$

of the wave equation 7.17 familiar from classical electrodynamics.

The expression 7.41 may also be called a Markovian source field because the approximation used in deriving it results in an $\hat{a}_\lambda^s(t)$ that depends entirely on atomic operators with the same time argument t . This implies that the system’s memory of the earlier times $t' < t$ in the integral in equation 7.35 is very poor. Note that later times $t' > t$ are excluded by the choice of the retarded time solution: $G_\lambda(t - t')$ vanishes if $t' > t$.

To obtain a complete understanding of the behavior of the atom undergoing spontaneous emission, the integration of the field operator equation 7.15 must be followed by an integration of the atomic operator equations 7.14a to 7.14c as well. It is not clear how this might be done explicitly. Fortunately, so long as we remain interested only in first approximations to expressions for the lifetime, lineshape, and line shift of the atomic transition it is unnecessary to integrate the atomic equations in operator form.

For the purposes of this chapter it is sufficient to find the vacuum expectation value of the dipole moment operators, rather than the operators themselves. In working out the expectation values of $\hat{R}_1(t)$, $\hat{R}_2(t)$, and $\hat{R}_3(t)$, we will be careful to avoid any decorrelation approximation, such as that which leads to semiclassical theory. As a first step, before computing expectation values, we will work out the only operator products, $\hat{A}\hat{R}_3$ and $\hat{A}\hat{R}_1$, that appear in the atomic equations. The definition of \hat{A} in terms of \hat{a}_λ and \hat{a}_λ^\dagger , the understanding that operator products are to be taken in normally ordered form, and the approximate integration of the \hat{a}_λ equation together lead to the complicated expressions:

$$\begin{aligned} \hat{A}\hat{R}_1 &= \sum_\lambda g_\lambda \left\{ \hat{a}_\lambda^{v\dagger} \hat{R}_1 + \hat{R}_1 \hat{a}_\lambda^v \right\} \\ &+ \frac{\pi}{2} \left(\frac{\omega_0 d}{\hbar c} \right) \sum_\lambda g_\lambda^2 \left\{ \delta(\omega_\lambda - \omega_0) - \delta(\omega_\lambda + \omega_0) \right\} \\ &+ \pi \left(\frac{\omega_0 d}{\hbar c} \right) \sum_\lambda g_\lambda^2 \left\{ \delta(\omega_\lambda - \omega_0) + \delta(\omega_\lambda + \omega_0) \right\} \hat{R}_3, \end{aligned} \quad (7.43)$$

and

$$\begin{aligned} \hat{A}\hat{R}_3 &= \sum_\lambda g_\lambda \left\{ \hat{a}_\lambda^{v\dagger} \hat{R}_3 + \hat{R}_3 \hat{a}_\lambda^v \right\} \\ &+ \frac{i}{2} \left(\frac{\omega_0 d}{\hbar c} \right) \sum_\lambda g_\lambda^2 \left\{ \xi^*(\omega_\lambda + \omega_0) - \xi(\omega_\lambda - \omega_0) \right\} \hat{R}_+ \\ &+ \frac{i}{2} \left(\frac{\omega_0 d}{\hbar c} \right) \sum_\lambda g_\lambda^2 \left\{ \xi^*(\omega_\lambda - \omega_0) - \xi(\omega_\lambda + \omega_0) \right\} \hat{R}_-. \end{aligned} \quad (7.44)$$

Here we have used the relations

$$\hat{R}_3(t)\hat{R}_\pm(t) = \pm \frac{1}{2}\hat{R}_+(t), \quad \hat{R}_\pm(t)\hat{R}_\mp(t) = \frac{1}{2} \pm \hat{R}_3(t) \quad (7.45)$$

and

$$[\xi(x) - \xi^*(x)] \pm [\xi(y) - \xi^*(y)] = -2\pi i [\delta(x) \pm \delta(y)] \quad (7.46)$$

in order to simplify the right-hand sides of the equations.

Notice that the first terms in the expressions for both $\hat{A}\hat{R}_3$ and $\hat{A}\hat{R}_1$ are written explicitly normally ordered. This is necessary, having started with normal ordering, because the vacuum and source parts of the field do not

separately commute with \hat{R}_1 or \hat{R}_3 , even though the total mode operators \hat{a}_λ and \hat{a}_λ^\dagger as well as the field \hat{A} itself do commute, at equal times, with all of the atomic operators.

Having determined $\hat{A}\hat{R}_1$ and $\hat{A}\hat{R}_3$ exactly, within the approximation implied by equation 7.41, we may now take vacuum expectation of equations 7.14. By vacuum expectation, denoted simply by the brackets $\langle \dots \rangle$, we mean an expectation value computed in the state $|\psi\rangle = |\text{vacuum}\rangle |\Phi\rangle$, where $|\Phi\rangle$ is an arbitrary state of the two-level atom, and $|\text{vacuum}\rangle$ is the no-photon state. To be precise, $|\text{vacuum}\rangle$ satisfies $a_\lambda^v(0)|\text{vacuum}\rangle = 0$. Taking the energy equation first, we find:

$$\frac{d}{dt} \langle \hat{R}_3(t) \rangle = -\frac{1}{\tau_1} \left\{ \frac{1}{2} + \langle \hat{R}_3(t) \rangle \right\}, \quad (7.47)$$

where $1/\tau_1$ is the product of the coefficients appearing in equations 7.43 and 7.14c:

$$\frac{1}{\tau_1} = 2\pi \left(\frac{\omega_0 d}{\hbar c} \right)^2 \sum_{\lambda} g_{\lambda}^2 [\delta(\omega_{\lambda} - \omega_0) \pm \delta(\omega_{\lambda} + \omega_0)]. \quad (7.48)$$

The advantage of having chosen normal ordering to work with is evident in the details of the step from equation 7.14c to equation 7.47.

The vacuum expectation of the terms involving the vacuum parts of the field operators are all zero, because of the ordering itself and not because of any decorrelation. We have used only the free field operator property $\hat{a}_{\lambda}^v(t)|\text{vacuum}\rangle = 0$ and its adjoint $\langle \text{vacuum} | \hat{a}_{\lambda}^{v\dagger}(t) \rangle = 0$, which follow from equations 7.5 and 7.36, to determine

$$\langle \hat{a}_{\lambda}^{v\dagger}(t) \hat{R}_1(t) \rangle = \langle \hat{R}_1(t) \hat{a}_{\lambda}^v(t) \rangle = 0. \quad (7.49)$$

It should be noted that equation 7.49 would not hold if any other ordering were to be adopted. For example, antinormal ordering would give rise to the expressions

$$\langle \Phi | \langle \text{vacuum} | \hat{R}_1 \hat{a}_{\lambda}^{v\dagger} | \text{vacuum} \rangle | \Phi \rangle = \langle \Phi | \langle \text{vacuum} | \hat{R}_1 | 1_{\lambda} \rangle | \Phi \rangle e^{i\omega_{\lambda} t}. \quad (7.50a)$$

But it is not possible then to go further. It is not true that the right side of equation 7.50a can be reduced to

$$\langle \text{vacuum} | 1_{\lambda} \rangle \langle \Phi | \hat{R}_1 | \Phi \rangle e^{i\omega_{\lambda} t}, \quad (7.50b)$$

because $\hat{R}_1(t)$ cannot be removed from the photon matrix element except

at $t=0$. For later times, as equation 7.14a suggests, $\hat{R}_1(t)$ will not be a purely atomic operator. The interaction term $2(\omega_0 d/\hbar c)A\hat{R}_3$ in equation 7.14a ensures that the atomic dipole moment operator $\hat{R}_1(t)$ will be made up, at least partly, of photon operators, for $t>0$. Of course, if antinormal ordering had been invoked for the source parts as well as the vacuum parts of the field, compensating changes in the source terms would lead eventually to the same result found in equation 7.47. This may be verified by explicit computation [12, 13].

The value of $1/\tau_1$, which equation 7.47 shows to be the atom's energy decay rate, may be worked out easily in the continuum limit of the mode sum. The replacement

$$\frac{1}{\sqrt{\lambda}} \sum_{\text{pol}} \rightarrow \frac{1}{(2\pi)^3} \int d^3k \sum_{\text{polarizations}} \quad (7.51)$$

transforms the mode sum into an integral over wave vectors plus a polarization sum. By using the identity

$$\sum_{\text{pol}} [\epsilon(k) \cdot \mathbf{u}_d]^2 = 1 - (\mathbf{u}_k \cdot \mathbf{u}_d)^2, \quad (7.52)$$

the angular integral is easily carried out:

$$\int [1 - (\mathbf{u}_k \cdot \mathbf{u}_d)^2] d\Omega(\hat{k}) = \frac{8\pi}{3}. \quad (7.53)$$

The remaining integral over frequencies is trivial on account of the delta functions, leading finally to the expression

$$\frac{1}{\tau_1} = \frac{4}{3} \frac{\omega_0^3 d^2}{\hbar c^3}. \quad (7.54)$$

In other words $1/\tau_1$ is exactly the Einstein A coefficient, as it should be. Thus the atomic lifetime is found correctly. The subscript 1 on τ_1 is intended as a twofold reminder. First, τ_1 is the basic energy decay rate of which T_1 is the phenomenological counterpart in Chapters 3 to 6. Second, τ_1 refers only to single-atom decay. Its many-atom analog τ_N is discussed in Chapter 8.

The decay of the atom's energy is obviously exponential in time. Explicit integration of equation 7.47 yields the decay law:

$$\langle \hat{R}_3(t) \rangle = -\frac{1}{2} + \left\{ \langle \hat{R}_3(0) \rangle + \frac{1}{2} \right\} e^{-t/\tau_1}, \quad (7.55)$$

which is valid for arbitrary initial excitation $\langle \hat{R}_3(0) \rangle$. As expected, no matter what value $\langle \hat{R}_3 \rangle$ has initially, it eventually and monotonically reaches its ground state value of $-\frac{1}{2}$. The exponential nature of the decay correctly suggests that the lineshape is Lorentzian. If desired, a more thorough derivation of the lineshape is possible [10] via an investigation of the dipole correlation function $\langle \hat{R}_+(t+\tau) \hat{R}_-(t) \rangle$. The result confirms a Lorentzian shape with full width at halfmaximum equal to $1/\tau_1$, as expected for the natural lineshape.

Next consider the equation for $\hat{R}_+ = \hat{R}_1 + i\hat{R}_2$, the “positive frequency” part of the dipole moment operator R_1 . Its vacuum expectation value equation is

$$\frac{d}{dt} \langle \hat{R}_+(t) \rangle = i\omega_0 \langle \hat{R}_+(t) \rangle + 2 \left(\frac{\omega_0 d}{\hbar c} \right) \langle \hat{A}(t) \hat{R}_3(t) \rangle. \quad (7.56)$$

Upon inserting the expression for $\hat{A}\hat{R}_3$ found in equation 7.44 into equation 7.56 the normally ordered vacuum parts vanish, leaving the relatively simple equation

$$\frac{d}{dt} \langle R_+(t) \rangle = i \left(\omega_0 + \delta + \frac{i}{2\tau_1} \right) \langle R_+(t) \rangle - i \left(\delta - \frac{i}{2\tau_1} \right) \langle R_-(t) \rangle. \quad (7.57)$$

Here the lifetime τ_1 is that given in equation 7.48 and 7.54 and the parameter δ is determined, in the continuum limit of the mode sums, by

$$\delta = - \frac{8\pi}{3\hbar c} \left(\frac{\omega_0 d}{2\pi c} \right)^2 \int_0^{Kc} \left\{ \frac{P}{\omega - \omega_0} - \frac{1}{\omega + \omega_0} \right\} \omega d\omega, \quad (7.58)$$

where P indicates the principal part of the integral and a fictitious upper limit Kc has been supplied in order to cut off the evident ultraviolet divergence.

The second term on the right-hand side of equation 7.57 may be taken account of by first finding the equation satisfied by $\langle \hat{R}_- \rangle$ analogous to equation 7.57, and then solving the two linear coupled first-order equations exactly. However, to a first approximation, the effects of $\langle \hat{R}_- \rangle$ in equation 7.57 are negligible and may be ignored altogether. Thus the solution

$$\langle \hat{R}_+(t) \rangle = \langle \hat{R}_+(0) \rangle e^{i(\omega_0 + \delta)t} e^{-t/2\tau_1} \quad (7.59)$$

may be taken for the dynamical behavior of the dipole expectation value.

The real and imaginary parts of equation 7.59 are, of course, $\langle \hat{R}_1(t) \rangle$ and $\langle \hat{R}_2(t) \rangle$.

Clearly equation 7.59 states an expected conclusion. The dipole oscillates rapidly and decays in amplitude slowly. A new element, however, is provided by δ . The role of δ is obviously that of a shift in the transition line center. Such a shift, present in the vacuum state of the field, may be called the Lamb shift of the two-level atom. The expression 7.58 for the shift has several interesting features. First, it does not agree with the shift given by the familiar Weisskopf-Wigner approach ([7], Sec. 5.6) to spontaneous emission. This is because of the term $1/(\omega_\lambda + \omega_0)$ in the integrand. Second, again because of the same term, the leading divergence of δ is not linear in the cutoff K , but merely logarithmic, as it must be in a correct nonrelativistic calculation. Third, δ is exactly the same as the completely mass-renormalized frequency shift which can be calculated in second-order nonrelativistic perturbation theory. In other words, the Heisenberg operator technique reaches the correct conclusion, in first approximation, as regards all three parameters: lifetime, lineshape, and lineshift.

In addition, the results show that the conventional "explanation" of spontaneous decay, that vacuum fluctuations "stimulate" the atom to emit spontaneously, need not be adopted. This approach shows, in fact, that the vacuum part of the field, $\hat{a}_\lambda^v(t)$, plays no obvious or exclusive role in determining either the frequency shift δ or the decay rate $1/\tau_1$.

A natural interpretation of these results, based on the old idea of radiation reaction instead of vacuum fluctuations, may be preferred. It is seen in the transition from equations 7.14 through 7.43 and 7.44 to equations 7.55 and 7.59 that the vacuum part of the field makes no direct contribution, and that the total Lamb shift and decay rate come entirely from the source part of the field in interaction with the atom. In very classical language, it is not the presence of vacuum fields but of the dipole's own source field that modifies the atom's characteristics in such a way as to produce a finite decay rate, and a shift of the noninteracting natural transition frequency.

However, the interpretation one uses can almost be made a matter of personal preference. Senitzky [12] and Milonni, Ackerhalt, and Smith [13] have shown that, to a large degree, the interpretation of a calculation that seems most natural is predetermined by the rule of ordering employed. For example, normal ordering emphasizes the role of atomic source field

reaction to the exclusion of vacuum fluctuations. On the other hand, the use of symmetric ordering ensures that the Lamb shift δ arises entirely from vacuum fluctuations. As Fain and Khanin [14] have emphasized, however, there is no ordering in which the lifetime τ_1 can arise solely from vacuum fluctuations. This is essentially because atomic reactions (atom fluctuations) are needed to prevent spontaneous absorption processes. As we have shown, normal ordering does allow both the lifetime τ_1 and the shift δ to arise solely from radiation reaction.

7.5 QUANTUM ELECTRODYNAMIC PERTURBATION THEORY

For completeness, we conclude this chapter with a brief review of the traditional perturbation treatment of radiative level shifts. More extensive discussions are available [15]. To compare the perturbation theory result with that computed by Heisenberg equation integration, we consider again the same fictitious two-level atom.

In second-order stationary state perturbation theory the shift in the energy of the state $|a\rangle$, due to a perturbing term \hat{V} in the Hamiltonian, is

$$\delta E_a = - \sum_{b \neq a} \frac{\langle a | \hat{V} | b \rangle \langle b | \hat{V} | a \rangle}{E_b - E_a}. \quad (7.60)$$

In the case of the two-level atom the perturbation arises from the interaction of the atom with the quantized radiation field. As equation 7.10 shows:

$$\hat{V} = 2 \left(\frac{\omega_0 d}{c} \right) \hat{R}_2(0) \hat{A}(0), \quad (7.61)$$

where the operators $\hat{R}_2(0)$ and $\hat{A}(0)$ are now time-independent, as they must be, in the Schrödinger picture. The state $|a\rangle$ is one of the two atom-photon states

$$|\text{vacuum}\rangle |\pm\rangle,$$

whereas $|b\rangle$ is one of the states

$$|1_\lambda\rangle |\pm\rangle.$$

We want to find the energy shifts δE_\pm of the atom in its upper (+) and

lower ($-$) states while the field is in its vacuum state.

For example, δE_+ , reduces easily to

$$\delta E_+ = - \left(\frac{\omega_0 d}{c} \right)^2 \sum_{\lambda} \frac{|\langle + | \hat{R}_+(0) | - \rangle|^2 |\langle \text{vacuum} | g_{\lambda} \hat{a}_{\lambda}(0) | 1_{\lambda} \rangle|^2}{\hbar(\omega_{\lambda} - \omega_0)}, \quad (7.62)$$

which, after performing the polarization sum and the angular integration, reduces to

$$\delta E_+ = - \frac{8\pi}{3c} \left(\frac{\omega_0 d}{2\pi c} \right)^2 \int_0^{Kc} \frac{1}{\omega - \omega_0} \omega d\omega. \quad (7.63)$$

The integral diverges linearly with K as $K \rightarrow \infty$. However, the argument is usually made that the leading contribution to the integral, which is independent of ω_0 and thus independent of whatever binding forces created the atom, should be subtracted off and ignored. This subtraction is justified on the grounds that the subtracted term represents an intrinsic property of the free electron and not any feature of the bound system. To effect the subtraction, we may use the identity

$$\frac{\omega d\omega}{\omega - \omega_0} = \left[1 + \frac{\omega_0}{\omega - \omega_0} \right] d\omega \quad (7.64)$$

and then discard the 1. The remaining integral diverges “only” logarithmically, a harmless sort of divergence expected in nonrelativistic bound-state calculations [15]. The discarded linearly divergent integral may be completely concealed in a mass renormalization of the electron, and has no observable consequences.

The energy of the lower atomic state $|-\rangle$ is also shifted by the interaction \hat{V} . Note that this is due to the presence in \hat{V} of counter-rotating terms, a result related to the result of Section 2.6, where the presence of the counter-rotating wave led to the Bloch-Siegert frequency shift. The lower state energy shift is

$$\delta E_- = - \frac{8\pi}{3c} \left(\frac{\omega_0 d}{2\pi c} \right)^2 \int_0^{Kc} \frac{\omega d\omega}{\omega + \omega_0}, \quad (7.65)$$

which can also be renormalized by subtracting the part of the integrand which is independent of ω_0 .

However, an atom with only two energy levels is so unrealistically simple that there is actually no need for renormalization. The only observable aspect of the energy level shifts in equations 7.63 and 7.65 is the resonance frequency shift obtained from their difference. The linearly divergent parts of δE_+ and δE_- cancel in the difference, leaving the properly logarithmically divergent result:

$$\frac{(\delta E_+ - \delta E_-)}{\hbar} = -\frac{8\pi}{3\hbar c} \left(\frac{\omega_0 d}{2\pi c} \right)^2 \int_0^{Kc} \left\{ \frac{P}{\omega - \omega_0} - \frac{1}{\omega + \omega_0} \right\} \omega d\omega, \quad (7.66)$$

which we see to be the same as the formula for the frequency shift δ given in expression 7.58. Thus perturbation theory and the Markovian Heisenberg equation integration yield the same frequency shift, in first approximation, as they should.

References

1. E. A. Power and S. Zienau, *Phil. Trans. Roy. Soc.* **251**, 427 (1959); see also Z. Fried, *Phys. Rev. A* **8**, 2835 (1974).
2. R. H. Dicke, *Phys. Rev.* **93**, 99 (1954).
3. W. H. Louisell, *Quantum Statistical Properties of Radiation*, Wiley, New York, 1973, Sec. 4.9.
4. E. T. Jaynes, Microwave Laboratory Report No. 502, Stanford University, 1958.
5. E. T. Jaynes and F. W. Cummings, *Proc. I. E. E.* **51**, 89 (1963).
6. V. Weisskopf and E. Wigner, *Z. Phys.* **63**, 54 (1930).
7. W. H. Louisell, *Radiation and Noise in Quantum Electronics*, McGraw-Hill, New York, 1964.
8. B. R. Mollow, *Phys. Rev.* **168**, 1896 (1968).
9. M. Tavis and F. W. Cummings, *Phys. Rev.* **170**, 379 (1968); *ibid.* **188**, 692 (1969). Recent work has been devoted to the interesting question of thermodynamic phase transitions in N two-level-atom systems. See K. Hepp and E. Lieb, *Ann. Phys.* **76**, 360 (1973); Y. K. Wang and F. K. Hioe, *Phys. Rev. A* **7**, 831 (1973); L. M. Narducci, M. Orszag, and R. A. Tuft, *Collect. Phen.* **1**, 113 (1973).
10. (a) J. R. Ackerhalt, P. L. Knight and J. H. Eberly, *Phys. Rev. Lett.* **30**, 456 (1973); (b) J. R. Ackerhalt and J. H. Eberly, *Phys. Rev. D* **10**, 3350 (1974); (c) P. A. M. Dirac, *Phys. Rev.* **139**, B684 (1965).
11. W. Heitler, *The Quantum Theory of Radiation*, 3rd ed., Oxford University Press, London, 1954, Sec. 8.
12. I. R. Senitzky, *Phys. Rev. Lett.* **31**, 954 (1973).

13. P. W. Milonni, J. R. Ackerhalt, and W. A. Smith, *Phys. Rev. Lett.* **31**, 958 (1973); and P. W. Milonni and W. A. Smith, *Phys. Rev. A* (1975).
14. V. M. Fain and Ya. I. Khanin, *Quantum Electronics*, Vol 1, M.I.T. Press, Cambridge, Mass., 1969, p. 211. See also comments by V. L. Ginsburg, *Sov. Phys. Dokl.* **24**, 131 (1939), especially p. 134; and by G. S. Agarwal, *Phys. Rev. A* **10**, 717 (1974).
15. Introductory treatments of radiative level shifts are found in: H. A. Bethe and E. E. Salpeter, *Quantum Mechanics of One and Two-Level Atoms*, Springer-Verlag, Berlin, 1957, Sec. 19; E. A. Power, *Introductory Quantum Electrodynamics*, Longmans, Green, London, 1964, Chap. 9.; J. D. Bjorken and S. D. Drell, *Relativistic Quantum Mechanics*, McGraw-Hill New York, 1965, Sections 4.4 and 8.7; W. Heitler, Ref. 11; and W. H. Louisell, Ref. 3.

CHAPTER 8

***N*-Atom Spontaneous Emission and Superradiant Decay**

8.1 Introduction	174
8.2 Many-Atom Operator Equations and Field Operator Solution	174
8.3 <i>N</i>-Atom Spontaneous Emission	176
8.4 Superradiance	181
8.5 Some Restrictive Considerations	189
References	194

8.1. INTRODUCTION

Einstein's identification of the importance of spontaneous contributions to the process of light emission by atoms marked the beginning of quantum electrodynamics. Dirac's later quantization of the radiation field variables could be accepted almost immediately as a correct step because it led directly to Einstein's values for the A and B coefficients. The traditional view of spontaneous emission has held that it contributes a random and incoherent stochastic character to the emission process. In this chapter we discuss the question of coherent spontaneous emission arising from many atoms emitting collectively. If the number of atoms emitting is N , the intensity of the fluorescence would ordinarily be expected to be proportional to N . Dicke was the first to emphasize that even the incoherent quantum electrodynamic event of spontaneous emission could give rise to a fluorescent output proportional to N^2 instead of to N . This phenomenon, which has come to be called superradiance, has classical and semiclassical counterparts. The following sections treat superradiance semiquantitatively along the lines developed for the one-atom emission problem of the preceding chapter. Some restrictive conditions that arise from the smallness of the optical wavelength compared to the size of realizable samples are emphasized in the last two sections.

8.2. MANY-ATOM OPERATOR EQUATIONS AND FIELD OPERATOR SOLUTION

If the quantum system under consideration has several or many atoms, the basic QED Hamiltonian given in equation 7.10 must be modified. If the

possibility of inhomogeneous broadening is ignored, at least temporarily, the appropriate N -atom Hamiltonian is

$$\hat{\mathcal{H}} = \sum_{l=1}^N \left[\hbar\omega_0 \hat{R}_{l3} + 2 \left(\frac{\omega_0 d}{c} \right) \hat{A}_l \hat{R}_{l2} \right] + \sum_{\lambda} \hbar\omega_{\lambda} \hat{a}_{\lambda}^{\dagger} \hat{a}_{\lambda}. \quad (8.1)$$

That is, $\hat{\mathcal{H}}$ is merely the sum of the field Hamiltonian plus N individual atom and interaction Hamiltonians indexed by the label l .

The vector potential \hat{A}_l with which the l th atom's dipole interacts is, in general, a function of \mathbf{r}_l , the l th atom's position:

$$\hat{A}_l = \sum_{\lambda} [g_{\lambda}(\mathbf{r}_l) \hat{a}_{\lambda} + g_{\lambda}^*(\mathbf{r}_l) \hat{a}_{\lambda}^{\dagger}]. \quad (8.2)$$

Here the \mathbf{r}_l dependence of $g_{\lambda}(\mathbf{r}_l)$ is as given in equations 7.13 and 7.16:

$$g_{\lambda}(\mathbf{r}_l) \equiv \sqrt{\frac{2\pi\hbar c^2}{\omega_{\lambda} \epsilon_0}} \cdot \mathbf{\epsilon} \cdot \mathbf{u}_d e^{i\mathbf{k}_{\lambda} \cdot \mathbf{r}_l}. \quad (8.3)$$

It accounts for the arbitrary positions of the N atoms with respect to each other.

The many-atom counterparts of the one-atom equations 7.14 and 7.15 are simply derived from the Hamiltonian immediately above:

$$\dot{\hat{R}}_{l+}(t) = i\omega_0 \hat{R}_{l+}(t) + 2 \left(\frac{\omega_0 d}{\hbar c} \right) \hat{R}_{l3}(t) \hat{A}_l(t), \quad (8.4)$$

$$\dot{\hat{R}}_{l3}(t) = - \left(\frac{\omega_0 d}{\hbar c} \right) [\hat{R}_{l+}(t) + \hat{R}_{l-}(t)] \hat{A}_l(t), \quad (8.5)$$

$$\dot{\hat{a}}_{\lambda} = -i\omega_{\lambda} \hat{a}_{\lambda} - \left(\frac{\omega_0 d}{\hbar c} \right) \sum_{l=1}^N g_{\lambda}^*(\mathbf{r}_l) [\hat{R}_{l+}(t) - \hat{R}_{l-}(t)]. \quad (8.6)$$

Radiation reaction is evident in these many-atom equations: each atom is driven by the total field \hat{A} , and each field mode is driven by the total dipole moment. This coupling means that each atom is partially driven by itself through its own source field, partially by the source field of all the other atoms, and partially by the external field present. In the case of zero applied field, the external field is the same as the vacuum field.

The source field contribution to $\hat{a}_\lambda(t)$ will be the same as in the one-atom case, except that the right-hand side of equation 7.41 must now be summed over all atoms:

$$\hat{a}_\lambda^s(t) = i \left(\frac{\omega_0 d}{\hbar c} \right) \sum_{l=1}^N g_\lambda^*(\mathbf{r}_l) \left[\hat{R}_{l+}(t) \xi^*(\omega_\lambda + \omega_0) - \hat{R}_{l-}(t) \xi^*(\omega_\lambda - \omega_0) \right], \quad (8.7)$$

where the ξ functions have the same meaning as in relation 7.39. The vacuum field contribution to $\hat{a}_\lambda(t)$ has the same value as before:

$$\hat{a}_\lambda^v(t) = \hat{a}_\lambda(0) e^{-i\omega_\lambda t}, \quad (8.8)$$

since it is completely independent of the atoms.

8.3. *N*-ATOM SPONTANEOUS EMISSION

In the absence of applied fields, each excited atom in a large collection will decay spontaneously to its ground state. However, it is misleading to rely exclusively on the conclusions of Section 7.4, which show that a single atom decays monotonically and exponentially to its ground state. This does not necessarily apply to an ensemble of atoms because, as Section 8.2 shows, each excited atom may be substantially influenced during its decay by the fields of all of the other atoms.

The consequences of many-atom effects for *N*-atom spontaneous decay are easily explored, at least semiquantitatively, by working out the time-dependent rate at which the photon number in a given mode increases because of atomic emission. The photon number operator for mode λ is

$$\hat{n}_\lambda(t) = \hat{a}_\lambda^\dagger(t) \hat{a}_\lambda(t), \quad (8.9)$$

and $\hat{a}_\lambda(t)$ is composed of “vacuum” and “source” parts

$$\hat{a}_\lambda(t) = \hat{a}_\lambda^v(t) + \hat{a}_\lambda^s(t), \quad (8.10)$$

according to equation 7.40. Then the repeated use of equations 8.6 to 8.8 leads, after making the quantum rotating wave approximation at the end,

to the relation

$$\begin{aligned} \frac{d}{dt} \hat{n}_\lambda(t) = & \left(\frac{\omega_0 d}{\hbar c} \right) \sum_l \left[g_\lambda(\mathbf{r}_l) \{ \hat{R}_{l+} - \hat{R}_{l-} \} \hat{a}_\lambda^v + \text{h.c.} \right] \\ & + i \left(\frac{\omega_0 d}{\hbar c} \right)^2 \sum_l \sum_m g_\lambda(\mathbf{r}_l) g_\lambda^*(\mathbf{r}_m) \left[\hat{R}_{l+} \hat{R}_{m-} \{ \zeta(\omega_\lambda - \omega_0) - \zeta^*(\omega_\lambda - \omega_0) \} \right. \\ & \left. + \hat{R}_{l-} \hat{R}_{m+} \{ \zeta(\omega_\lambda + \omega_0) - \zeta^*(\omega_\lambda + \omega_0) \} \right], \end{aligned} \quad (8.11)$$

where h.c. denotes the Hermitean conjugate of the immediately preceding term. The two main contributions to $\dot{\hat{n}}_\lambda$ have distinct physical origins. The first part contains only a single summation over the atoms and represents energy gain or loss due to the simple dipole interaction of the existing external field with the N atoms. The second part is more interesting because of the products of operators belonging to different atoms in the double summation. Such operator products imply interference by the atoms in each others' emission process.

The rate of change in photon number that might be compared with experiment is of course the expectation value of equation 8.11. The simplest situations are always of two kinds: either the external fields are so strong that the first part of $\dot{\hat{n}}_\lambda$ completely dominates the expectation or the external fields are so weak that a vacuum expectation is called for. In order to discuss the purely spontaneous decay rate, we must assume the latter. Again normal ordering leads to the vanishing vacuum expectation of all terms in $\dot{\hat{n}}_\lambda$ containing \hat{a}_λ^v and $\hat{a}_\lambda^{v\dagger}$. Thus, as should be expected in spontaneous emission, only the source fields lead to changes in photon number:

$$\langle \dot{\hat{n}}_\lambda \rangle = 2\pi \left(\frac{\omega_0 d}{\hbar c} \right)^2 \sum_l \sum_m g_\lambda(\mathbf{r}_l) g_\lambda^*(\mathbf{r}_m) \delta(\omega_\lambda - \omega_0) \langle \hat{R}_{l+} \hat{R}_{m-} \rangle, \quad (8.12)$$

where again $\langle \dots \rangle$ denotes expectation value in the product state

$$|\psi\rangle = |\text{vacuum}\rangle |\Phi_N\rangle, \quad (8.13)$$

representing the field vacuum and an arbitrary N -atom state.

The change in the photon number of a given mode is not quite so directly important as, for example, the power flow into a given solid angle. The conversion is easily arranged. The number of modes per unit solid angle with frequency ω_λ in the range $d\omega_\lambda$ is given by

$$\rho(\omega_\lambda)d\omega_\lambda = \frac{cV}{(2\pi c)^3} \omega_\lambda^2 d\omega_\lambda,$$

so that we may write for the differential power flow in the direction \mathbf{u}_k :

$$d\mathcal{P}(\mathbf{k}_\lambda, t) = \hbar\omega_\lambda \langle \dot{\hat{n}}_\lambda \rangle \frac{cV}{(2\pi c)^3} \omega_\lambda^2 d\omega_\lambda d\Omega(\mathbf{k}_\lambda). \quad (8.14)$$

It is conventional to call $d\mathcal{P}(\mathbf{k}, t)/d\Omega(\mathbf{k})$ the intensity radiated into the direction \mathbf{k} , within solid angle $d\Omega(\mathbf{k})$, when summed over all polarizations and frequencies ω_λ . Thus we write for the intensity

$$I_N(\mathbf{k}, t) = \frac{cV}{(2\pi c)^3} \sum_{\text{pol}} \int \hbar\omega_\lambda \langle \dot{\hat{n}}_\lambda \rangle \omega_\lambda^2 d\omega_\lambda. \quad (8.15)$$

Relation 8.12 may be used to show that this expression for intensity is the same as

$$I_N(\mathbf{k}, t) = I_1(\mathbf{k}, 0) \sum_l \sum_m e^{i\mathbf{k} \cdot (\mathbf{r}_l - \mathbf{r}_m)} \langle \hat{R}_{l+} \hat{R}_{m-} \rangle, \quad (8.16)$$

where I_N is the N -atom spontaneously radiated intensity and

$$I_1(\mathbf{k}, 0) \equiv \frac{\omega_0^4 d^2}{2\pi c^3} \sum_{\text{pol}} |\epsilon(\mathbf{k}) \cdot \mathbf{u}_d|^2 \quad (8.17)$$

is its one-atom counterpart.

A useful check on these relations is provided by equation 7.47. If it is evaluated at $t=0$ with the single atom in its completely excited state so that $\langle \hat{R}_3 \rangle = \frac{1}{2}$, it gives the atom's initial energy-loss rate:

$$\frac{d}{dt} [\hbar\omega_0 \langle \hat{R}_3 \rangle]_{t=0} = -\frac{\hbar\omega_0}{\tau_1}, \quad (8.18)$$

where $1/\tau_1$ is the Einstein A coefficient, given by relation 7.54. But this

rate of change of energy by one atom should be exactly the negative of the power flow from one atom into the radiation field, summed over all frequencies, polarizations, and solid angles. This is the same as saying that

$$\int I_1(\mathbf{k}, 0) d\Omega(\mathbf{k}) = \frac{\hbar\omega_0}{\tau_1}, \quad (8.19)$$

which is easily verified from definition 8.17 by direct integration.

In the Heisenberg picture the dynamical variables are time-dependent and the state vector is constant. The state of the atoms implied by the vacuum expectation can be specified at only one time, by convention at the initial time $t=0$. Before pursuing the expression 8.16 for the N -atom intensity the mode of preparation of the atoms must be specified. For simplicity we adopt the premise that all of the atoms were excited identically by a quasi-monochromatic pumping pulse of radiation with "area" π . The first consequence of such an assumption is that the origin of time for the various dipoles differs according to their location with respect to the wavefront of the pumping pulse. We adjust for this difference by multiplying the dipole operators \hat{R}_{l+} and \hat{R}_{m-} by $\exp[-i\mathbf{k}_0 \cdot \mathbf{r}_l]$ and $\exp[+i\mathbf{k}_0 \cdot \mathbf{r}_m]$ respectively, where \mathbf{k}_0 is the wave vector of the π pulse, so that \hat{R}_{l+} and \hat{R}_{m-} may be taken to have a common time origin [1].

A second important feature of our initial state assumption is that, since all atoms are treated the same, apart from position, the expectation $\langle \hat{R}_{l+} \hat{R}_{m-} \rangle$ is actually independent of the indices l and m . The result is that when the expression 8.16 is broken into the two parts for which $m \neq l$ and $m = l$, the intensity may be written as

$$I_N(\mathbf{k}, t) = I_1(\mathbf{k}, 0) \left[N \langle \hat{R}_{a+} \hat{R}_{a-} \rangle + N^2 \left\{ \Gamma(\mathbf{k} - \mathbf{k}_0) - \frac{1}{N} \right\} \langle \hat{R}_{a+} \hat{R}_{b-} \rangle \right], \quad (8.20)$$

where

$$\Gamma(\mathbf{k} - \mathbf{k}_0) = \left| \frac{1}{N} \sum_{l=1}^N e^{i(\mathbf{k} - \mathbf{k}_0) \cdot \mathbf{r}_l} \right|^2, \quad (8.21)$$

and where atoms a and b have been chosen arbitrarily to serve as the l th

and m th atoms in the expectations. Relations equivalent to formulas 8.20 and 8.21 were first given by Dicke [1] in a study of N -atom spontaneous emission.

The factor $\Gamma(\mathbf{k} - \mathbf{k}_0)$ may be interpreted as the square of the average of $\exp[i(\mathbf{k} - \mathbf{k}_0) \cdot \mathbf{r}]$ taken over all possible positions \mathbf{r} for the atoms:

$$\sum_{l=1}^N e^{i(\mathbf{k} - \mathbf{k}_0) \cdot \mathbf{r}_l} = \int_{\mathcal{V}} d^3 r \mathfrak{N}(\mathbf{r}) e^{i(\mathbf{k} - \mathbf{k}_0) \cdot \mathbf{r}}, \quad (8.22)$$

where $\mathfrak{N}(\mathbf{r})$ is the density of the atoms and \mathcal{V} the volume containing them. Thus $\Gamma(\mathbf{k} - \mathbf{k}_0)$ expresses the interference of incident \mathbf{k}_0 and emitted \mathbf{k} waves. If the collection of atoms is spread over a large enough macroscopic volume, it is clear that there is constructive interference only in the forward direction. If the container volume is small enough, smaller than the wavelength of the emitted light, then $\Gamma \approx 1$ in all directions.

Furthermore, it is known [2] that if the emission line is inhomogeneously broadened, each atom characterized by its own detuning Δ_l from line center, then $\Gamma(\mathbf{k} - \mathbf{k}_0)$ should be multiplied by a factor $H(t)$, which expresses a second kind of interference in the emitted light:

$$H(t) = \left| \frac{1}{N} \sum_{l=1}^N e^{i\Delta_l t} \right|^2. \quad (8.23)$$

The interference implied by $H(t)$ is just that which is due to the dephasing of the individual atomic oscillators associated with the normalized inhomogeneous detuning function $g(\Delta)$:

$$H(t) = \left| \int_{-\infty}^{\infty} g(\Delta) e^{i\Delta t} d\Delta \right|^2. \quad (8.24)$$

A convenient definite expression for $H(t)$,

$$H(t) = e^{-2|t|/T_2^*} \quad (8.25)$$

follows if $g(\Delta)$ is assumed to be Lorentzian with halfwidth $1/T_2^*$ at half maximum amplitude.

Taking account of all N atoms, of the finite volume they occupy, and of their inhomogeneous lineshape, as well as of the relation $\hat{R}_{a+}\hat{R}_{a-} = \frac{1}{2} + \hat{R}_{a3}$,

it follows that

$$I_N(\mathbf{k}, t) = I_1(\mathbf{k}, 0) \left[N \left\{ \frac{1}{2} + \langle \hat{R}_{a3} \rangle \right\} + N^2 \left\{ \Gamma(\mathbf{k} - \mathbf{k}_0) H(t) - \frac{1}{N} \right\} \langle \hat{R}_{a+} \hat{R}_{b-} \rangle \right]. \quad (8.26)$$

Obviously this can be qualitatively very different from single-atom emission. In fact the first main term, proportional to N , is exactly the single-atom intensity taken N times. The second main term vanishes when $N=1$, because then $\Gamma(\mathbf{k} - \mathbf{k}_0) = 1$ and $H(t) = 1$ but it is the major contributor to I_N if N is very large.

The appearance of a term in the emitted intensity proportional to N^2 , rather than N , is a sign of coherence among the emitting oscillators. Such coherence is unexpected in spontaneous emission, and was pointed out explicitly first by Dicke [1] in 1954. The subject of superradiance is concerned with the study of this kind of coherence in multi-atom systems.

8.4. SUPERRADIANCE [3]

To discuss thoroughly multiatom spontaneous emission, it is necessary to invoke the full complexity of equations 8.4 to 8.7. However, an adequate semiquantitative understanding of coherent spontaneous emission, or superradiance, is more easily arrived at. First, however, it is necessary to explain with some care what the term superradiance refers to because it has been used in connection with several effects in the literature.

The N^2 term in equation 8.26 indicates a degree of coherence unexpected at first sight in quantum mechanical spontaneous emission. Actually, the N^2 merely signals the appearance of a well-known classical N -emitter effect: N emitters, phased properly, interfere constructively with each other, resulting in an emission rate proportional to N^2 . Many phenomena, including free induction decay, optical nutation, and photon echoes, share this N^2 feature.

However, the coherence of the wave trains radiated by N emitters in free induction decay, in optical nutation, and in photon echoes, is passive,

induced coherence. It is passive and induced in the sense that it originates in the external agency that acts to prepare the N emitters to radiate synchronously; it does not originate spontaneously in the collective emission process.

The only mechanism available to N emitters that could lead to collective and active coherence is radiation reaction. That is, the essence of superradiance can be taken to be the existence of a significant reaction by each dipole to the fields radiated by all of the other dipoles. One consequence is that superradiant emission is accompanied by a significant energy loss *per dipole*. This is in sharp contrast to the free-precession dephasing that terminates all free-induction decay phenomena. These considerations are closely consistent with the emphasis of Dicke's original paper [1]. For example, only if each dipole experiences significant energy loss is it possible to speak, as Dicke does, of the natural linewidth being broadened in superradiant decay.

In effect, we are describing here a definition of superradiance. As with all definitions, it is neither right nor wrong. However, to have a definition stated may prevent further semantic confusion in the literature. Note that because free induction decay and photon echoes, as they are usually observed, do not entail significant radiative energy loss *per atom*, we will not call them superradiance effects, even though their radiated intensity is proportional to N^2 . Echoes and free induction are discussed at length in the following chapter.

To return to a quantitative discussion of superradiant decay, first note that the choice of the atomic part of the product state 8.13 implied by the vacuum expectation values in expression 8.26 for I_N is to some extent arbitrary. Because it permits a certain amount of semiclassical intuition to be exploited, we make the choice

$$|\Phi_N\rangle = \prod_{l=1}^N |\theta, \phi\rangle_l, \quad (8.27)$$

a product of one-atom states defined by two parameters, θ and ϕ . It is possible to choose to define $|\theta, \phi\rangle_l$ in such a way that θ can be identified with the pseudodipole tipping angle θ that entered the discussions of the Rabi solution in Section 3.2 and of short intense pulses in Section 4.4:

$$|\theta, \phi\rangle_l = \sin \frac{\theta}{2} e^{-i\phi/2} |+\rangle_l + \cos \frac{\theta}{2} e^{i\phi/2} |-\rangle_l, \quad (8.28)$$

where $|+\rangle_l$ and $|-\rangle_l$ are the upper and lower states of the l th atom.

Next we assert, without explicit justification, that the N -atom state 8.27 can be used to compute expectation values at any time. This must be an approximation, because in the Heisenberg picture the state may be chosen only once, traditionally at $t=0$. The implications of this approximation have been commented on by Rehler and Eberly [4]. In the meantime $|+\rangle$ and $|-\rangle$ will be taken to be the eigenstates of $\hat{R}_3(t)$ for any time t , not just $t=0$.

Within the approximation described above it is easy to compute the expectation values needed to evaluate $I_N(\hat{k}, t)$. For example,

$$\langle \hat{R}_{l3}(t) \rangle = -\frac{1}{2} \cos \theta(t), \quad (8.29)$$

$$\langle \hat{R}_{l+}(t) \rangle = \frac{1}{2} \sin \theta(t) e^{i\phi(t)}, \quad (8.30)$$

$$\langle \hat{R}_{l-}(t) \rangle = \frac{1}{2} \sin \theta(t) e^{-i\phi(t)}. \quad (8.31)$$

Equally important, these angles are easily interpreted semiclassically. The vector \mathbf{s}_l shown in Fig. 8.1 and defined by

$$\frac{1}{2}\mathbf{s}_l = (\langle \hat{R}_{l1} \rangle, \langle \hat{R}_{l2} \rangle, \langle \hat{R}_{l3} \rangle) \quad (8.32)$$

is the obvious analogue of the unit vector \mathbf{s} shown in Fig. 2.4.

The explicit evaluation of $I_N(k, t)$ then leads to

$$I_N(\mathbf{k}, t) = I_1(\mathbf{k}, 0) \left[\frac{N}{2} \{1 - \cos \theta(t)\} + \left(\frac{N}{2}\right)^2 \sin^2 \theta(t) \left\{ \Gamma(\mathbf{k} - \mathbf{k}_0) H(t) - \frac{1}{N} \right\} \right], \quad (8.33)$$

a fairly complicated relation with some simple features. For example, the definition 8.21 for Γ and the relation 8.22 make it clear that $\Gamma(\mathbf{k} - \mathbf{k}_0)$ is a very sharply peaked function if \mathcal{V} , the volume of the system, is very large. Thus, for finite values of the dipole tipping angle θ not too close to either 0 or π , the factor $N^2 \Gamma(\mathbf{k} - \mathbf{k}_0)$ will make the largest contribution to the strength and direction of emission. Also, as should be expected, the dipole phase angle $\phi(t)$ is unimportant to the emission, at least in the RWA.

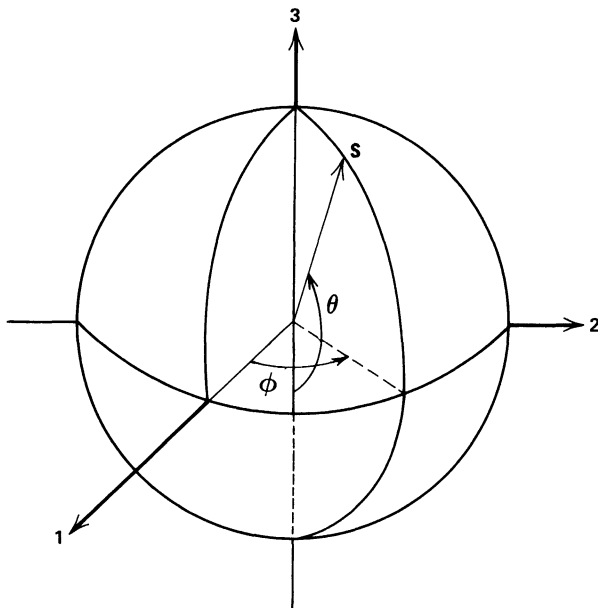


Fig. 8.1 The pseudospin vector for the *l*th atom.

Radiation reaction, or equation 8.5, can be exploited to find an explicit time dependence for the tipping angle. The dimensionless total energy of the *N*-atom system is given by the expectation of \hat{R}_{l3} , summed over all atoms:

$$W_N \equiv \sum_{l=1}^N \langle \hat{R}_{l3} \rangle = -\frac{1}{2} N \cos \theta(t). \quad (8.34)$$

When multiplied by $\hbar\omega_0$, the time derivative of W_N must be equal to $-I_N(\mathbf{k}, t)$ integrated over all solid angles. This equality leads to a differential equation for θ , or to a simpler one for W_N [5]:

$$-\frac{d}{dt} W_N(t) = \left(\frac{\mu}{\tau_1} \right) \left(\frac{N}{2} + W_N \right) \left(\frac{N}{2} - W_N + \frac{1}{\mu} \right). \quad (8.35)$$

The parameter μ embodies the interference effects arising from the finite size and shape of the collection of emitters:

$$\mu \equiv \frac{\int I_1(\mathbf{k}, 0) \left\{ \Gamma(\mathbf{k} - \mathbf{k}_0) H(t) - \frac{1}{N} \right\} d\Omega(\mathbf{k})}{\int I_1(\mathbf{k}, 0) d\Omega(\mathbf{k})}. \quad (8.36)$$

In the limit of negligible inhomogeneous broadening, when $T_2^* \rightarrow \infty$ and $H(t) \rightarrow 1$, equation 8.35 has the solution:

$$W_N(t) = -\frac{N}{2} \left[\left(1 + \frac{1}{N\mu} \right) \tanh \left(\frac{t-t_0}{2\tau_N} \right) - \frac{1}{N\mu} \right]. \quad (8.37)$$

Here τ_N and t_0 are defined in terms of τ and $N\mu$:

$$\frac{1}{\tau_N} \equiv (N\mu + 1) \frac{1}{\tau_1}, \quad (8.38)$$

$$t_0 \equiv \tau_N \ln(N\mu).$$

The shape factor μ has been approximately evaluated by Rehler for several shapes of macroscopic collections of atoms. For circular cylinders, such as that sketched in Fig. 8.2, the expressions

$$\mu = \begin{cases} \frac{3}{8\pi} \left(\frac{\lambda^2}{A} \right), & A \gg \left(\frac{\lambda}{2\pi} \right)^2, \quad L < \frac{A}{\lambda}, \\ \frac{3}{8} \left(\frac{\lambda}{L} \right), & L \gg \frac{\lambda}{2\pi}, \quad A \gg \lambda L, \end{cases} \quad (8.39)$$

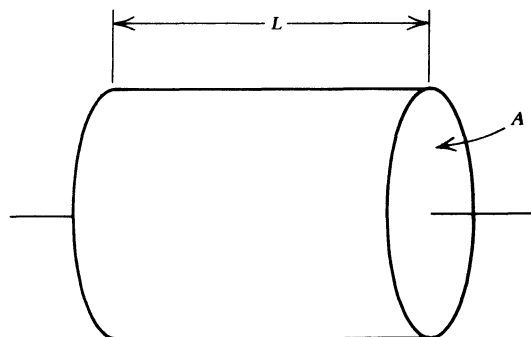


Fig. 8.2 Circular cylinder model of a superradiant emitter. The active atoms are imagined uniformly distributed throughout the cylinder volume.

are good approximations. Additional expressions for μ in the cases of spheres [4b] and rectangular shapes [6] have also been given. In practical laserlike geometries $\Gamma(\mathbf{k} - \mathbf{k}_0)$ is sharply peaked along the system axis, and μ is small as shown in Fig. 8.3. The relation 8.39 shows that the emission solid angle is also small, suggesting that the emission may be considered to be essentially single-mode radiation. Such a restriction, imposed at the outset, is useful in a theory of superradiance due to Bonifacio, Schwendemann, and Haake [7], which avoids the atomic decorrelation implicit in our assumption that initial-time expectation values retain their form for all times.

The integrated intensity function has a very simple time behavior. It may be found by differentiating the solution 8.37 for $W_N(t)$ and multiply-

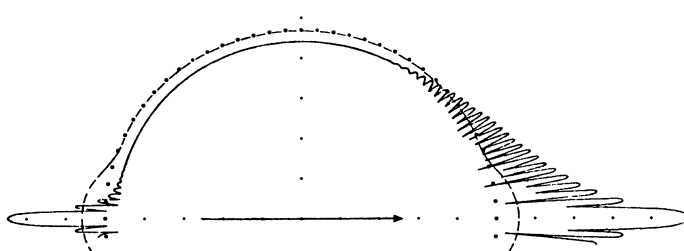


Fig. 8.3 The radiation patterns associated with superradiant emission from two different circular cylinders, each with a “Fresnel number” $A/L\lambda$ equal to 500 and a density of active atoms equal to 61.2 per cubic wavelength. The solid line shows the normalized intensity $i(\psi, t) = (8\pi/3)I_N(\mathbf{k}, t)/NI_1(\mathbf{k}, 0)$ at the time of maximum radiation rate, according to equation 8.33, for a cylinder with volume $V = 10^5\lambda^3/8\pi^2$. The broken line shows $i(\psi, t)$ for a smaller cylinder with volume $V = 10\lambda^3/8\pi^2$. The dotted line is the completely incoherent radiation pattern from either cylinder at the initial time, when all of the atoms are excited. The arrow indicates the direction of an assumed excitation pulse which traveled parallel to the cylinder axis, and ψ is the polar angle of the graphs, indicating the angle between the cylinder axis and the direction \mathbf{k} of emission. The scale is radially logarithmic, each dot along the coordinate axes indicating an order of magnitude. Thus the radiation from the larger cylinder, represented by the solid line, is more than 10^4 times as intense as the radiation from the smaller cylinder, in the forward direction. [From N. E. Rehler and J. H. Eberly, *Phys. Rev. A* **3**, 1735 (1971).]

ing by $\hbar\omega_0$:

$$I_N(t) = \frac{\hbar\omega_0}{4\mu\tau_N} (N\mu + 1)^2 \operatorname{sech}^2\left(\frac{t - t_0}{2\tau_N}\right). \quad (8.40)$$

This function is shown in Fig. 8.4 for several large values of $N\mu$. It exhibits both features commonly associated with superradiance: a strong maximum intensity that can be much larger than the N -atom incoherent intensity $N\hbar\omega_0/\tau_1$, and a shortening of the radiative lifetime.

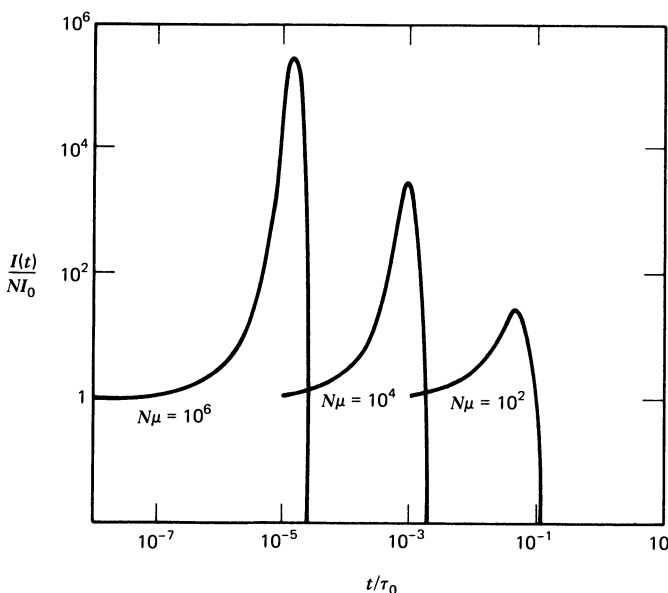


Fig. 8.4 Superradiant intensity as a function of time, as given by equation 8.40, for several large values of the effective number $N\mu$ of cooperating atoms.

The existence of coherence, in the form of a spontaneous emission rate proportional to N^2 rather than N , has often been discussed as if it were completely unexpected. An “explanation” of the existence of superradiance can be offered at several levels of subtlety. In a purely classical theory ([4a], Sec. II) there is little or no subtlety. Classical dipoles radiate at a rate proportional to the square of their dipole moment. Thus N classical dipoles radiate at a rate proportional to the square of their total

moment. If the dipoles are phase-coherent, as in any antenna array, then their radiated power is proportional to N^2 .

The same can be said for most semiclassical quantum treatments of superradiance, such as that of Stroud et al. [3]. In these treatments there is typically no spontaneous emission, although there may be radiation reaction. That is, a semiclassical theory will predict no emission at all if the atoms are exactly in their upper states where the expectation of the dipole moment vanishes. But if a nonzero moment is provided initially, then the radiation by that moment can act back on the system, enhancing the radiation rate and leading to N^2 dependence in the radiated power.

It is only within quantum electrodynamics that superradiance takes on any subtlety. And if superradiance has to do with spontaneous emission in the strict sense, as well as with radiation reaction, only a quantum electrodynamic treatment is possible.

The result 8.33 suggests an interpretation of superradiance that partly answers a basic question. The question is: can an initially incoherent assembly of atoms, all of them in their upper states with zero dipole moments, acquire the coherence that is associated with classical N^2 power dependence, and if so how does it do so? Expression 8.33 shows that during the initial moments of the emission process the emission must be incoherent: when $\theta \approx \pi$, then $I_N \approx NI_1$. This incoherent energy loss requires the atomic Bloch vectors such as that shown in Fig. 8.1 to begin to tip over. As soon as that happens, as soon as θ departs infinitesimally from π , then the $\frac{1}{4}N^2 \sin^2 \theta$ term dominates the emission. Finally, it may be seen from equations 8.30 and 8.31 that

$$\left[\sum_{l=1}^N \langle R_{l1} \rangle \right]^2 + \left[\sum_{l=1}^N \langle R_{l2} \rangle \right]^2 = \frac{1}{4}N^2 \sin^2 \theta. \quad (8.41)$$

In other words to say that $\frac{1}{4}N^2 \sin^2 \theta$ is the dominant term in equation 8.33 is merely to point out that the emission has become entirely classical in its characteristics, the radiated power has become proportional to the square of the N -atom system's total oscillating dipole moment expectation value.

Thus one might say that the only interesting feature of superradiance is the way in which the transition is made from initial incoherence to N^2 coherence during the emission process. The nature of this transition, which has spatial, temporal, and statistical manifestations, is not completely

understood. Its features are connected with a still deeper subtlety that has not yet been mentioned, but is concealed in the simplistic choice of states in equations 8.27 and 8.28. More general states must actually enter the problem.

One set of more general states were introduced in 1954 by Dicke [1] and have the property that the expectations of all the dipole moments vanish at all times, even at the peak of the emission process. But these states still lead to $I_N \sim N^2 I_1$. Thus a classical "explanation" of the N^2 rate based on the existence of radiating dipole moments fails altogether if, as in the case of these more general states, the system dipole moment is zero initially and remains zero during the emission. One could save the classical "explanation" by saying that what is really important is not the oscillating dipole moment, but its square. However, to assert further that even a classical source can have zero dipole moment, but nonzero squared moment, is to introduce in an ad hoc way stochastic elements into the classical theory, stochastic elements whose features are partly quantum mechanical. In the final analysis, quantum theory is essential for a full description of superradiant phenomena. An explanation for the N^2 coherence must then be sought in atom-atom correlations that are necessarily absent from the simple product state 8.27. Further examination of this point may be found in Dicke's papers [1, 8], as well as in the application of the generalized atomic coherent states of Radcliffe [9] and Arecchi, Courtens, Gilmore, and Thomas [9] to the superradiance problem by Narducci, Coulter, and Bowden [10].

8.5. SOME RESTRICTIVE CONSIDERATIONS

In the preceding sections it has been convenient to assume that the collection of atoms undergoing superradiance has been excited by a plane-wave optical pulse, presumably with an area close to π so that all of the atoms would be excited very near their upper states. If the sample containing the atoms is many wavelengths long in every dimension, it may be important to take into account the effects of propagation on the exciting pulse and on the emitted superradiance pulse [11].

The simplest relation connecting superradiance with propagation effects has been derived very directly by Friedberg and Hartmann [12]. They have shown that a very close connection exists between the superradiant lifetime τ_N , the inhomogeneous lifetime T_2^* , and the length L of the sample

measured in Beer's absorption lengths. The Friedberg-Hartmann relation is arrived at by recognizing the similarity between α , Beer's absorption coefficient, and $1/\tau_N$, when τ_N is expressed in terms of the density \mathcal{N} of two-level atoms instead of the total number N . For definiteness, we consider a sample such as that shown in Fig. 8.2, assuming that the exciting pulse travels along the sample axis and that $A \gtrsim \lambda L$. In other words, one end face of the sample presents a large Fresnel number aperture when viewed from the other end face.

First recall the expression for Beer's absorption coefficient, given in equation 4.26,

$$\alpha = \frac{4\pi^2 \mathcal{N} \omega d^2}{\hbar c} g(0), \quad (8.42)$$

and the expression for $1/\tau_1$, the single-atom spontaneous decay rate derived in equation (7.54),

$$\frac{1}{\tau_1} = \frac{4}{3} \frac{\omega^3 d^2}{\hbar c^3}. \quad (8.43)$$

It is clear that the absorption coefficient can be rewritten as

$$\alpha = \frac{3}{4} \frac{\mathcal{N} \lambda^2}{\tau_1} g(0), \quad (8.44)$$

and in this form α is particularly close to $1/\tau_N$ as given in definition 8.37:

$$\frac{1}{\tau_N} = \frac{3}{8\pi} \frac{\mathcal{N} \lambda^2}{\tau_1} L. \quad (8.45)$$

In writing relation 8.45 we have assumed that $N\mu \gg 1$, and have used the first of the alternatives given for μ in expression 8.39, as required by the assumption $A \gtrsim \lambda L$.

Finally, the identification of $\pi g(0)$ with T_2^* leads to the Friedberg-Hartmann relation:

$$\alpha L = 2 \frac{T_2^*}{\tau_N}. \quad (8.46)$$

One way to express this result is to say that superradiance will not occur, because superradiant decay will be slower than free induction dephasing (i.e., $T_2^* < \tau_N$), unless the sample of atoms is at least two Beer's lengths thick (i.e., unless $\alpha L > 2$). Friedberg and Hartmann prefer to say that

"superradiant damping is negligible ($\tau_N \gg T_2^*$) whenever absorption is negligible ($\alpha L \ll 1$)."

It is clear that relation 8.46 must be understood in an order-of-magnitude sense, rather than as a strict equality. We have ignored potentially important factors, such as the index of refraction of the host medium, in deriving it; and the identification of $\pi g(0)$ with T_2^* is unambiguous only if the atomic absorption line is predominantly inhomogeneously broadened and the lineshape is Lorentzian. It is also true that a large value of αL does not necessarily imply large absorption of the exciting pulse. The area theorem guarantees that a pulse with area sufficiently near π will experience very little area change during the first few Beer's lengths of its propagation.

Another consequence of propagation effects on superradiant emission was first pointed out by Arecchi and Courtens [11]. Cooperation among the N superradiating atoms cannot occur if the atoms are too far from each other. The finiteness of the speed of light clearly puts an upper limit on the distance light emitted from any one atom can travel in time τ_N . The dimensions of a cooperating sample are thus restricted. A self-consistency argument based on expression 8.45 for the superradiance lifetime τ_N can be used to determine this upper limit on sample thickness L . If we denote by L_{cr} the critical limit on L imposed by the requirement that the light emitted at one end of the sample be able to reach the other end before the superradiant process ends:

$$L_{\text{cr}} = c\tau_N, \quad (8.47)$$

then the definition of L_{cr} is actually an equation for L_{cr} , since τ_N is a function of L . A corresponding critical limit on the superradiant decay rate $1/\tau_N$ is thereby also implied. These critical values are easily found to be

$$L_{\text{cr}}^2 = \frac{8\pi}{3} \frac{c\tau_1}{\mathcal{N}\lambda^2}, \quad (8.48)$$

$$\left(\frac{1}{\tau_N}\right)_{\text{cr}} = c \sqrt{\frac{3}{8\pi}} \sqrt{\frac{\mathcal{N}\lambda^2}{c\tau_1}}. \quad (8.49)$$

Thus the maximum possible superradiant decay rate does not depend at all on the total number of atoms emitting, but only on their density, in fact on the square root of their density.

At the same time it must be remembered that L is also restricted by the asymptotic form chosen for μ . We have been working under the large-Fresnel-number assumption: $L \lesssim A/\lambda$. It is interesting to see which of these restrictions on L is the more severe. The speed-of-light restriction given by equation 8.48 is stronger than the large-Fresnel-number restriction whenever we have

$$\frac{8\pi}{3} \frac{c\tau_1}{\mathcal{N}\lambda^2} < \left(\frac{A}{\lambda}\right)^2. \quad (8.50)$$

There is one more restriction implicit in everything said so far about cooperative emission. The number N has been assumed to be the total number of two-level atoms present in the sample. Under common experimental situations this may not be true, especially if the sample is to be excited by a coherent optical pulse. In that case only those atoms whose resonant absorption frequency lies within the pulse spectral width will be excited. If the excitation pulse is to affect all of the atoms its spectral width must be at least as wide as the entire atomic line, as wide at $1/T_2^*$ in the case of inhomogeneously broadened absorbers. In other words, the coherent exciting pulse must be on the order of or shorter than T_2^* in duration.

Alternatively, if the exciting pulse spectral width τ_{ex}^{-1} is less than $(T_2^*)^{-1}$, some modification is required in the foregoing formulas. The effective density of atoms is reduced by T_2^*/τ_{ex} and, for example, expression 8.45 becomes

$$\frac{1}{\tau_N} = \frac{3}{8\pi} \frac{\mathcal{N}\lambda^2}{\tau_1} \left(\frac{T_2^*}{\tau_{\text{ex}}} \right) L. \quad (8.51)$$

However, expression 8.44 for αL is modified by approximately the same factor, and so expression 8.46 remains the same. Expressions 8.48 and 8.49 should be modified accordingly, while expression 8.50 becomes

$$\frac{8\pi}{3} \frac{c\tau_1}{\mathcal{N}\lambda^2} \left(\frac{\tau_{\text{ex}}}{T_2^*} \right)^2 < \left(\frac{A}{\lambda} \right)^2. \quad (8.52)$$

One way to summarize these practical restrictions on superradiant emission is to propose specific sample parameters for a “classic” superradiant decay experiment, classic in the sense that propagation effects

are relatively unimportant compared with the dynamics of the decay. This is not difficult to do, at least in an order-of-magnitude way. First of all, we assume that coherent exciting π pulses are available that are as short or shorter than T_2^* .

Next, it is useful if $c\tau_1$ is fairly long; so we imagine working with ruby as the resonant absorber and emitter, for which $\tau_1 \sim 10^{-3}$ sec. The ruby resonance wavelength is roughly 7000 Å. To escape the speed-of-light restriction on sample length we consider a very small sample of ruby, approximately cylindrical in shape, for which $L \sim 10^3\lambda \sim 0.7$ mm and $A \sim 10^5\lambda^2 \sim (0.2 \text{ mm})^2$.

It is necessary to choose N appropriately. In ruby $T_2^* \sim 10^{-10}$ sec; hence we must require that $\tau_N < 10^{-10}$ sec if superradiant damping is to prevail over free induction dephasing. Given the parameters above, this condition is met if we take $N \sim 10^{13}$, in which case $\tau_N \sim 0.8 \times 10^{-10}$ sec. The required doping density of Cr³⁺ ions in the ruby needed to reach this value of N is only $3 \times 10^{17} \text{ cm}^{-3}$, an experimentally feasible value.

It is easy to establish that with these parameter values the sample length is smaller than the critical length L_{cr} as well as substantially smaller than A/λ :

$$L^2 \sim 0.5 \times 10^{-2} \text{ cm}^2, \quad (8.53a)$$

$$L_{cr}^2 \sim 16 \times 10^{-2} \text{ cm}^2, \quad (8.53b)$$

$$\left(\frac{A}{\lambda}\right)^2 \sim 5000 \times 10^{-2} \text{ cm}^2. \quad (8.53c)$$

The Friedberg-Hartmann restriction is not particularly onerous in these circumstances either, since αL is roughly equal to 2.

Of course, substantial experimental difficulties have been ignored in our proposed experiment. It is not easy to design reliable 100 psec π pulses, or to couple them into a sample with cross-sectional area of only 5×10^{-4} cm². We have disregarded all questions of detection. For example, the problem of discriminating the output pulse from the trailing edge of the exciting pulse may be a very difficult one. For these and other reasons an experiment of the pure decay type has yet to be performed.

Nevertheless many experiments claiming some relation to superradiance have been reported [13]. Coherence of the phases of atomic dipoles undergoing emission will automatically lead to an N^2 dependence in the emitted intensity. This is true without even raising the question of the

quantum electrodynamic origin of the phase coherence. Thus photon echoes (see Chapter 9) provided the first observation at optical frequencies of N^2 emission. Any kind of free induction decay [14] shares this characteristic.

References

1. R. H. Dicke, *Phys. Rev.* **93**, 99 (1954).
2. J. H. Eberly, *Acta Phys. Pol.* **A39**, 633 (1971). A much more detailed investigation of the effects of inhomogeneous broadening on multi-atom coherent emission has been made recently: R. Jodoin and L. Mandel, *Phys. Rev. A* **9**, 873 (1974).
3. Many theoretical studies of coherent or cooperative N -atom spontaneous emission have been carried out since 1967, using a variety of semiclassical and quantum electrodynamic treatments. References to this work may be found in two reviews: J. H. Eberly, *Am. J. Phys.* **40**, 1374 (1972); S. Stenholm, *Phys. Reports* **6**, 1 (1973), Sec. 4. In Section 8.4 we follow the approach of Rehler and Eberly, Ref. 4.
4. (a) N. E. Rehler and J. H. Eberly, *Phys. Rev. A* **3**, 1735 (1973); (b) N. E. Rehler, Ph.D. dissertation, University of Rochester, 1972.
5. The validity of equation 8.35 is questionable insofar as it relies on equations 8.27 and 8.28. The point has been investigated by G. S. Agarwal, *Phys. Rev. A* **4**, 1791 (1971), with the conclusion that corrections to equation 8.35 can be expected to be of the order of $1/N$, that is, negligible in the present context.
6. I. D. Abella, N. A. Kurnit, and S. R. Hartmann, *Phys. Rev.* **141**, 391 (1966), App. C.
7. R. Bonifacio, P. Schwendimann, and F. Haake, *Phys. Rev. A* **4**, 302 (1971); *ibid.* **4**, 854 (1971). Other extensive master-equation treatments of superradiance are due to Lehmberg, Ref. 3 and to Agarwal, Refs. 3 and 5.
8. R. H. Dicke, in *Quantum Electronics III*, P. Grivet and N. Bloembergen, eds., Columbia University Press, New York, 1964, p. 35.
9. J. M. Radcliffe, *J. Phys. A* **4**, 313 (1971); F. T. Arecchi, E. Courtens, R. Gilmore, and H. Thomas, *Phys. Rev. A* **6**, 2211 (1973).
10. L. M. Narducci, C. A. Coulter, and C. M. Bowden, *Phys. Rev. A* **9**, 829 (1974).
11. F. T. Arecchi and E. Courtens, *Phys. Rev. A* **2**, 1730 (1970).
12. R. Friedberg and S. R. Hartmann, *Phys. Lett.* **37A**, 285 (1971).
13. A. Compaan and I. D. Abella, *Phys. Rev. Lett.* **27**, 23 (1971); R. L. Shoemaker and R. G. Brewer, *Phys. Rev. Lett.* **28**, 1430 (1972); N. Skribanowitz, I. P. Herman, J. C. MacGillivray, and M. S. Feld, *Phys. Rev. Lett.* **30**, 309 (1973).
14. P. F. Liao and S. R. Hartmann. *Phys. Lett.* **44A**, 361 (1973).

Photon Echoes

9.1 Introduction	195
9.2 Qualitative Considerations	195
9.3 Free Decay	199
9.4 Echo Time Behavior	202
9.5 Directional Character of Echoes	206
9.6 Photon Echoes in Gases	209
9.7 Experimental Observation of Photon Echoes	211
9.8 Propagation and Damping of Photon Echoes	214
References	220

9.1 INTRODUCTION

Irreversibility and decay are powerful partners that dominate much of many-body physics. In the eight preceding chapters we have recognized repeatedly the existence of a wide variety of decay-inducing phenomena: spontaneous emission, soft collisions, hard collisions, phonon scattering in solids, dipole dephasing, and others. The three basic phenomenological decay times T_1 , T'_2 , and T_2^* , have been used again and again in the Bloch and Maxwell equations to express the existence of these decay mechanisms.

In this chapter we examine the rather marvelous notion that not all decay processes need be irreversible. The discovery in 1950 of spin echoes by E. L. Hahn [1,2] showed that free induction decay, in particular, is easily reversed. It is not only easily reversed, but easily reversed long after the free induction signal has disappeared completely. Thus the echo signal, which is the resurrected free induction signal, has the magical quality of something coming from nothing. There is nothing magical about the principles on which echoes are based, of course. As we will show, the possibility of echoes hinges on the simple possibility that an atom retain its own resonance frequency, out of all possible resonance frequencies within the inhomogeneous line of width $1/T_2^*$, for times long compared to T_2^* .

9.2 QUALITATIVE CONSIDERATIONS

In several earlier chapters we encountered the fact that inhomogeneous broadening tends to damp out whatever polarization density P exists in a

macroscopic sample at the rate $1/T_2^*$. We showed in Section 1.4 that such damping is *unrelated* to energy-loss processes which tend to degrade or interrupt the oscillation of individual atoms. In deriving the classical and quantum area theorems in Sections 1.6 and 4.4 we observed that inhomogeneous broadening allowed the atomic absorber to affect the propagating pulse in times much shorter than any homogeneous relaxation time. It was also pointed out in Sections 1.5 and 3.7 that rapid damping of the macroscopic moment can be observed as free-induction decay.

The damping of P due to T_2^* processes is caused by dephasing of individual dipole moments throughout the sample. The corresponding dephasing of the transverse components of the rotating-frame Bloch vectors is shown in Fig. 9.1 [1]. It is natural to ask whether the energy stored in the dephased moments can be recovered in any coherent fashion. If so, the recovery would have to be carried out in the interval between T_2^* and T_2' , after which each individual dipole will have relaxed to its ground state.

At first glance it appears obvious that there can be no way to arrange coherent emission from the dephased dipoles. The individual dipole moments get out of phase with each other because they have slightly different oscillation frequencies. As time goes on they can only get further out of phase. Of course, any two dipoles, with frequencies differing by $\delta\omega$, say, will return to their original phased condition after every interval δt , where $\delta t = 2\pi/\delta\omega$. But in any real collection of atoms the distribution of oscillation frequencies, or the distribution $g(\Delta)$ of detunings from a fixed frequency, is smooth and continuous. Thus there must be many frequencies in the neighborhood of every other frequency with separations $\delta\omega$ which approach zero. Therefore only after an interval $\delta t \rightarrow \infty$ could we expect a return to the original phased condition by any finite fraction of the dipoles.

However, there is another way in which a return to the phased condition could occur. Instead of waiting passively for an extremely unlikely recurrence of the initial condition, it might be possible to interfere with the oscillations after a time t so as to reverse their dephasing, and thus engineer an *inevitable* rephasing at the time $2t$. An analogous diffusion with reversal followed by realignment in a different field is shown in Fig. 9.2.

The difficulty in treating atomic dipoles as the runners are treated in Fig. 9.2 lies in finding a Maxwell demon to serve as the starter. This problem was overcome in 1950 by E. L. Hahn [2], who discovered the

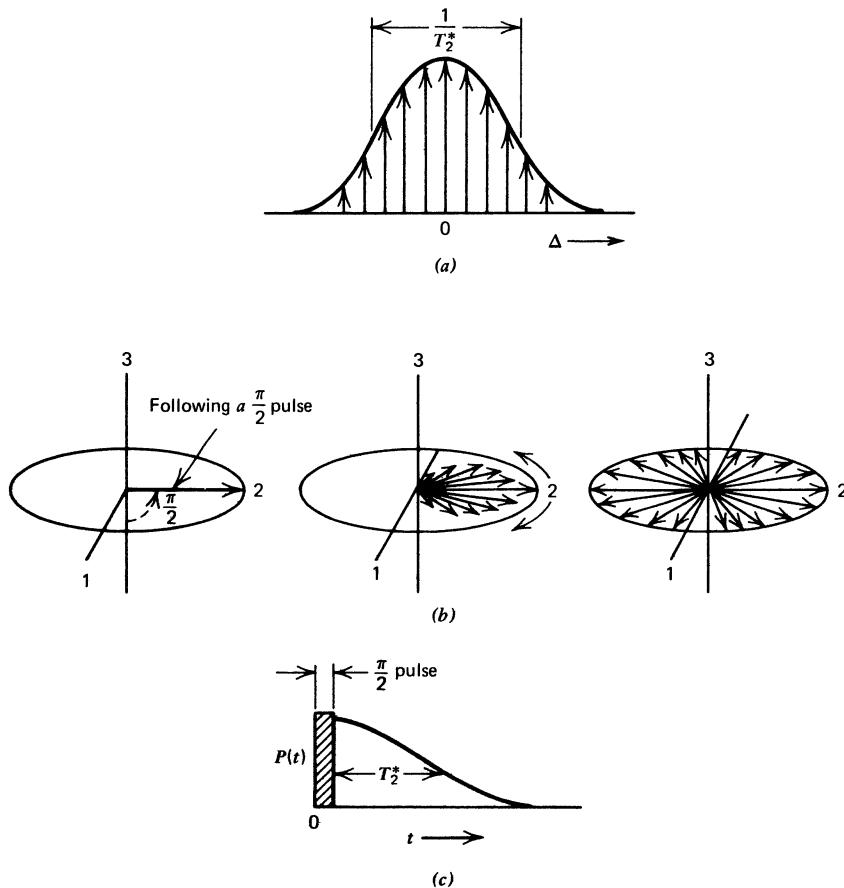


Fig. 9.1 (a) Pictorial representation of an inhomogeneously broadened spectrum of Bloch vectors, with spectral width given by $1/T_2^*$. (b) Following excitation by a 90° pulse, the various pseudospins begin to precess about the 3 axis in the rotating frame, with precession frequencies given by their various detunings, according to equations 2.36 with $\varepsilon = 0$. In the final stage, for time longer than T_2^* , the Bloch vectors are uniformly distributed in the 1–2 plane. (c) The rapid decrease in strength of the polarization density P , and thus of the signal radiated by the atomic dipoles, accompanying the dephasing of their Bloch vectors. The lifetime of the signal is roughly T_2^* . [From E. L. Hahn, *Proc. Roy. Inst. G.B.* **44**, 26 (1970).]

nuclear spin echo, the first of the resonance echo effects in physics. The photon echo is the electric dipole analogue of the spin echo effect. Photon echoes were first observed in 1964 by Kurnit, Abella, and Hartmann [3].

It is not possible to realign the dephased moment vectors shown in Fig. 9.1 in the same way as the runners, because the direction of turning of

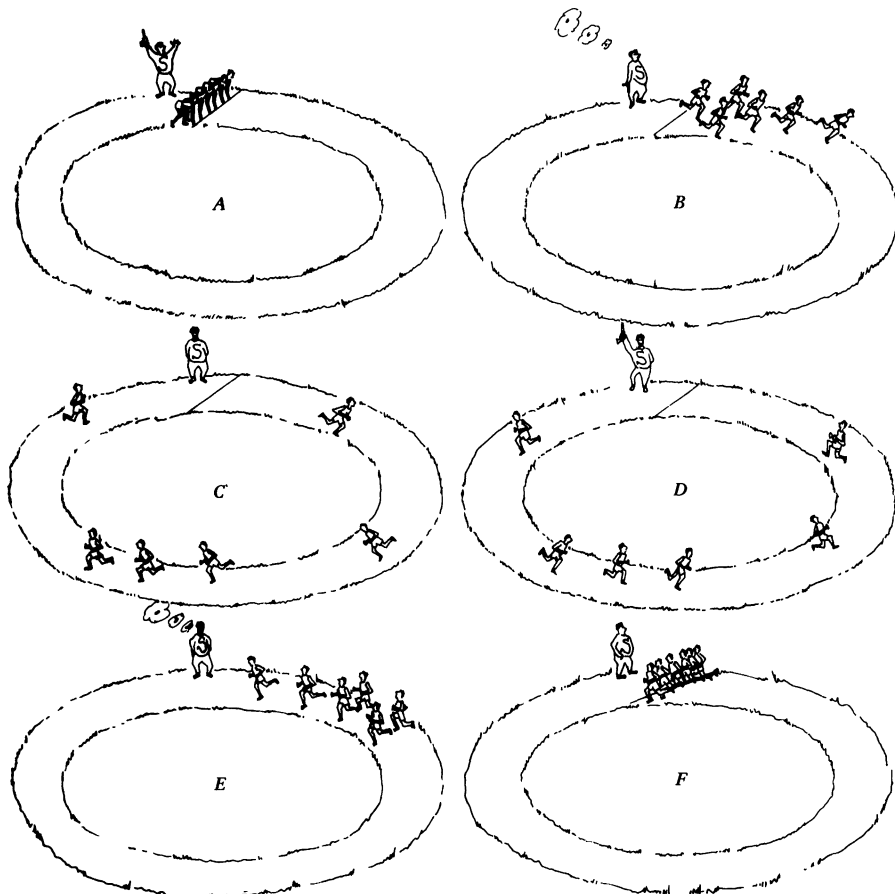


Fig. 9.2 Dephasing and reversal on a race track, leading to coherent rephasing and an “echo” of the starting configuration. [From *Phys. Today*, front cover, November 1953. Reproduced by permission.]

each vector is fixed by its detuning. However, the vectors have a freedom that the runners do not: they are not confined to the horizontal plane. It is easy to see, especially in the case of the partially dephased vectors at stage 2 of Fig. 9.1, that a rotation of all the vectors about the 1-axis through 180° produces a collection of rephasing moments. The reformation of a macroscopic moment with the same magnitude, although opposite sign, as the original macroscopic moment is inevitable. The radiation from this reformed moment is naturally fully coherent because all of the dipoles are in phase.

The rotation of the atomic dipole moments through 180° about the 1-axis is easily accomplished in principle. The formalism of Chapter 3 shows that an externally applied π pulse will do the job. Of course the original alignment along the 2-axis, shown in stage 1 of Fig. 9.1, must also be prepared by a rotation of the Bloch vectors by 90° to lift them from their vertically down equilibrium orientation. Thus an echo experiment can be based on the application of $\frac{1}{2}\pi$ and π pulses in succession. In the next section we examine dipole emission echo phenomena somewhat more quantitatively, basing our calculations on the simple ideas of this section.

9.3 FREE DECAY

Figure 9.1c shows that the polarization density decays in a time approximately equal to T_2^* because of the Bloch vector dephasing in the transverse plane. The detailed nature of this decay has some bearing on subsequent echoes. Let the absorber be subjected to a pulse with area θ_1 , lasting from $t=0$ to $t=t_1$ as shown in Fig. 9.3. We calculate the polarization density

$$P(t_2) = \mathcal{N} d \int d\Delta' g(\Delta') \operatorname{Re} \{(u + iv)e^{i\omega t_2}\} \quad (9.1)$$

for an arbitrary time $t_2 > t_1$.

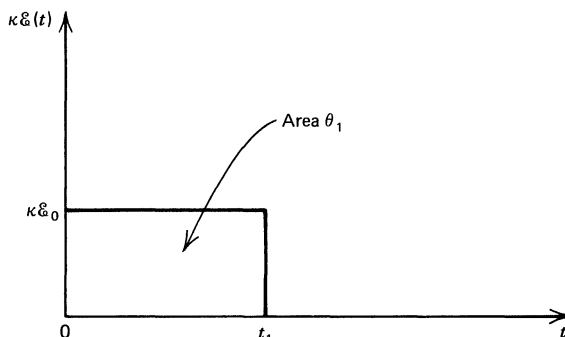


Fig. 9.3 A pulse with area θ_1 .

The transverse components u and v of the Bloch vectors subjected to first the θ_1 pulse from 0 to t_1 , and then the free precession from t_1 to t_2 , may be evaluated at time t_2 easily. Two applications of formula 3.15

suffice. In the first we assume that the atoms begin in their ground states: $u_0 = v_0 = 0$, $w_0 = -1$. It is convenient to assume that the field envelope satisfies $\kappa \tilde{\mathcal{E}}_0 > 1/T_2^*$ so that it is a fair approximation to take $\kappa \tilde{\mathcal{E}}_0 > \Delta$, and ignore all contributions to Bloch vector rotation of order $(\Delta/\kappa \tilde{\mathcal{E}}_0)^2$ and higher. The second application of equation 3.15 corresponds to free precession, that is, rotation of the Bloch vector by a pulse of zero amplitude. Taken together, these two steps lead to:

$$\begin{bmatrix} u(t_2) \\ v(t_2) \\ w(t_2) \end{bmatrix} = \begin{bmatrix} \cos \Delta(t_2 - t_1) & -\sin \Delta(t_2 - t_1) & 0 \\ \sin \Delta(t_2 - t_1) & \cos \Delta(t_2 - t_1) & 0 \\ 0 & 0 & 1 \end{bmatrix} \times \begin{bmatrix} 1 & -\frac{\Delta}{\kappa \tilde{\mathcal{E}}_0} \sin \theta_1 & -\frac{\Delta}{\kappa \tilde{\mathcal{E}}_0} (1 - \cos \theta_1) \\ \frac{\Delta}{\kappa \tilde{\mathcal{E}}_0} \sin \theta_1 & \cos \theta_1 & \sin \theta_1 \\ -\frac{\Delta}{\kappa \tilde{\mathcal{E}}_0} (1 - \cos \theta_1) & -\sin \theta_1 & \cos \theta_1 \end{bmatrix} \begin{bmatrix} 0 \\ 0 \\ -1 \end{bmatrix} \quad (9.2)$$

Therefore, we find the result:

$$\begin{bmatrix} u(t_2) \\ v(t_2) \\ w(t_2) \end{bmatrix} = \begin{bmatrix} \frac{\Delta}{\kappa \tilde{\mathcal{E}}_0} (1 - \cos \theta_1) \cos \Delta t_{21} + \sin \theta_1 \sin \Delta t_{21} \\ \frac{\Delta}{\kappa \tilde{\mathcal{E}}_0} (1 - \cos \theta_1) \sin \Delta t_{21} - \sin \theta_1 \cos \Delta t_{21} \\ -\cos \theta_1 \end{bmatrix}, \quad (9.3)$$

which leads directly to

$$u(t_2) + iv(t_2) = -i \sin \theta_1 e^{i \Delta s} e^{i \Delta t_{21}}, \quad (9.4)$$

where $t_{21} = t_2 - t_1$ and the parameter s is defined by

$$e^{i \Delta s} \equiv 1 + i \left(\frac{\Delta}{\kappa \tilde{\mathcal{E}}_0} \right) \tan \frac{\theta_1}{2}. \quad (9.5)$$

Because we are neglecting terms of order $(\Delta/\kappa\mathcal{E}_0)^2$ and higher, definition 9.5 is the same as

$$s = (\kappa\mathcal{E}_0)^{-1} \tan \frac{\theta_1}{2}. \quad (9.6)$$

The behavior of $P(t)$ may be evaluated at t_2 by inserting the result 9.4 into the definition 9.1 and carrying out the integration. In gases and in many solids at low temperatures $g(\Delta')$ is a Gaussian. If the absorption line center is located at the detuning value Δ , then

$$g(\Delta') = \frac{T_2^*}{\pi} e^{-(\Delta - \Delta')^2 (T_2^*)^2 / \pi}. \quad (9.7)$$

Note that the definition adopted in Chapter 1, $T_2^* \equiv \pi g_{\max}$, has been used in formula 9.7, so that $(T_2^*)^{-1}$ is related indirectly through factors of order unity to the exact halfwidth of g . The value of $P(t_2)$ is given by

$$P(t_2) = \mathcal{N} d \sin(\omega + \Delta)t_2 \exp \left[-\frac{\pi}{4} \left(\frac{t_{21} + s}{T_2^*} \right)^2 \right]. \quad (9.8)$$

That is, at the time $t_{21} + s = 0$, or $t_2 = t_1 - s$, and within limits of about $\pm T_2^*$ before and after that time, the amplitude of P is substantial, approximately equal to the completely phased value $\mathcal{N}d$.

However, because $t_2 > t_1$ and $\theta_1 \approx \pi/2$, the value $t_2 = t_1 - s$ cannot actually be reached. Nevertheless, expression 9.8 can be interpreted by saying that the polarization density during free decay behaves as if its maximum had occurred at a time s earlier than the end of the θ_1 pulse. For this reason an extra delay by the amount s , an extra delay that is not predicted by the simple pictures of Section 9.1, will occur in any subsequent echo pulse. The size of this extra delay is directly related to the duration t_1 of the θ_1 pulse. Since $\theta_1 \approx \kappa\mathcal{E}_0 t_1 \approx \frac{1}{2}\pi$, relation 9.6 shows that

$$s \approx \frac{2}{\pi} t_1. \quad (9.9)$$

Bloom [4] pointed out in 1955 that if $\theta_1 \ll 1$, then $\tan \frac{1}{2}\theta \approx \frac{1}{2}\theta$, and $s \approx \frac{1}{2}t_1$. The existence of an extra delay was confirmed in the earliest photon echo experiments [3].

9.4 ECHO TIME BEHAVIOR

Let two fairly intense pulses, with envelope areas $\frac{1}{2}\pi$ and π , be applied to an absorber in the time sequence shown in Fig. 9.4a. The resonant atoms, according to the rough analysis of Section 9.1, should find their Bloch vectors realigned in the equatorial plane of the Bloch sphere at some time t_4 after the application of the π pulse. The rephased dipole moments will emit an “echo” pulse at that time, as shown in Fig. 9.4b. The figure also shows the free induction decay emission that accompanies the initial dephasing after the $\frac{1}{2}\pi$ pulse.

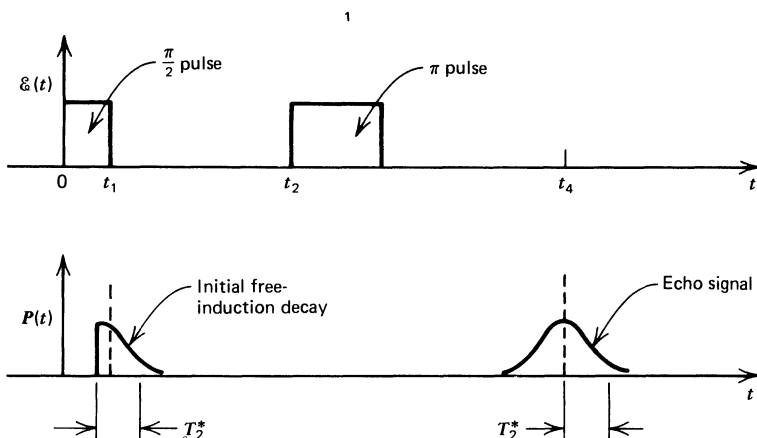


Fig. 9.4 Photon echo time sequence. (a) The two externally applied input pulses, with areas $\frac{1}{2}\pi$ and π . (b) On the same time scale the macroscopic polarization density $P(t)$ which gives rise to the two free induction output pulses, each with a lifetime of roughly T_2^* . The second output pulse is the echo.

The location of the echo in time, and its shape, are easily determined. It is sufficient to calculate the macroscopic polarization density:

$$P(t_4) = \mathfrak{N} d \int d\Delta' g(\Delta') \operatorname{Re} \left\{ [u(t_4; \Delta) + iv(t_4; \Delta)] e^{i\omega t_4} \right\}. \quad (9.10)$$

As in the free decay, the values of the components of the Bloch vector, following excitation for a time t by a field with envelope \mathcal{E}_0 , are given by successive applications of equation 3.15. In the present case we continue to assume that $\kappa \mathcal{E}_0 > 1/T_2^*$, so that it is a fair approximation to take $\kappa \mathcal{E}_0 > \Delta$, and to ignore all contributions of order $(\Delta/\kappa \mathcal{E}_0)^2$ and higher.

At any time $t_4 > t_3$, according to Fig. 9.4a, the Bloch vectors of the absorber atoms have been subjected to a $\frac{1}{2}\pi$ pulse, a period of free precession of duration t_1 , a π pulse, and a second period of free precession of duration $t_4 - t_3$. Since the same formula 3.15 serves for all four time intervals, we find the expression:

$$\begin{aligned}
 \begin{bmatrix} u(t_4) \\ v(t_4) \\ w(t_4) \end{bmatrix} &= \begin{bmatrix} \cos\Delta(t_4 - t_3) & -\sin\Delta(t_4 - t_3) & 0 \\ \sin\Delta(t_4 - t_3) & \cos\Delta(t_4 - t_3) & 0 \\ 0 & 0 & 1 \end{bmatrix} \\
 &\times \begin{bmatrix} 1 & 0 & -2\left(\frac{\Delta}{\kappa\tilde{\mathcal{E}}_0}\right) \\ 0 & -1 & 0 \\ -2\left(\frac{\Delta}{\kappa\tilde{\mathcal{E}}_0}\right) & 0 & -1 \end{bmatrix} \\
 &\times \begin{bmatrix} \cos\Delta(t_2 - t_1) & -\sin\Delta(t_2 - t_1) & 0 \\ \sin\Delta(t_2 - t_1) & \cos\Delta(t_2 - t_1) & 0 \\ 0 & 0 & 1 \end{bmatrix} \\
 &\times \begin{bmatrix} 1 & -\frac{\Delta}{\kappa\tilde{\mathcal{E}}_0} & -\frac{\Delta}{\kappa\tilde{\mathcal{E}}_0} \\ \frac{\Delta}{\kappa\tilde{\mathcal{E}}_0} & 0 & 1 \\ -\frac{\Delta}{\kappa\tilde{\mathcal{E}}_0} & -1 & 0 \end{bmatrix} \begin{bmatrix} 0 \\ 0 \\ -1 \end{bmatrix}. \tag{9.11}
 \end{aligned}$$

By continuing to ignore contributions of order $(\Delta/\kappa\tilde{\mathcal{E}}_0)^2$ and higher, this

sequence of Bloch vector rotations may be reduced directly to:

$$\begin{bmatrix} u(t_4) \\ v(t_4) \\ w(t_4) \end{bmatrix} = \begin{bmatrix} -\sin \Delta[t_{43} - t_{21}] + \frac{\Delta}{\kappa \tilde{\epsilon}_0} \cos \Delta[t_{43} - t_{21}] \\ \cos \Delta[t_{43} - t_{21}] + \frac{\Delta}{\kappa \tilde{\epsilon}_0} \sin \Delta[t_{43} - t_{21}] \\ -2 \frac{\Delta}{\kappa \tilde{\epsilon}_0} \sin \Delta t_{21} \end{bmatrix}, \quad (9.12)$$

where $t_{43} = t_4 - t_3$ and $t_{21} = t_2 - t_1$. Finally, the expression for $u + iv$ is easily found to be:

$$u(t_4; \Delta) + iv(t_4; \Delta) = ie^{i\Delta s} e^{i\Delta[t_{43} - t_{21}]}. \quad (9.13)$$

The phase angle Δs is defined by

$$e^{i\Delta s} = 1 - i \frac{\Delta}{\kappa \tilde{\epsilon}_0},$$

which is the same as

$$s = -\frac{1}{\kappa \tilde{\epsilon}_0} \quad (9.14)$$

up to order $(\Delta/\kappa \tilde{\epsilon}_0)^2$.

The behavior of $P(t)$ at times $t_4 > t_3$ is easily found from equations 9.10 and 9.13, using expressions 9.7 and 9.14 for $g(\Delta')$ and s :

$$P(t_4) = -\mathcal{N}d \sin(\omega + \Delta)t_4 \exp \left[-\frac{\pi}{4} \left(\frac{t_{43} - t_{21} - 1/\kappa \tilde{\epsilon}_0}{T_2^*} \right)^2 \right]. \quad (9.15)$$

Within an interval of size $2T_2^*$ around the time $t_{43} = t_{21} + (\kappa \tilde{\epsilon}_0)^{-1}$, the polarization amplitude is macroscopic, approximately equal to $\mathcal{N}d$. For earlier and later times t_4 we see that $P(t_4) \approx 0$. Thus, as Fig. 9.3b shows, the atomic polarization density grows from zero to a macroscopic value and then decays again to zero, at a time long after the initial free induction decay was completed.

The precise location of the maximum value of P depends on the degree of inhomogeneous broadening, which may invalidate our assumption that $(\Delta/\kappa \tilde{\epsilon}_0)^2 \ll 1$, and on the size of the two externally applied pulses. If the

first external pulse has area $\frac{1}{2}\pi$, then $\kappa\mathcal{E}_0 t_1 = \frac{1}{2}\pi$ and the maximum is reached at

$$t_4 - t_3 = t_2 - t_1 + \frac{2}{\pi}t_1. \quad (9.16)$$

In other words, the interval of free precession after the π pulse must equal the interval of free precession before the π pulse, plus a fraction of the width of the initial $\frac{1}{2}\pi$ pulse. This fraction is exactly the extra delay associated with the apparent beginning of the original free decay following the $\frac{1}{2}\pi$ pulse, as discussed in the preceding section.

It is interesting that the extra delay in the appearance of the echo is so clearly attributable to the $\frac{1}{2}\pi$ pulse, because it confirms an important aspect of the qualitative echo theory of Section 9.1. That is, the echo is a reflection of the initial aligned configuration due to the first pulse, and not a re-creation of any aspect of the intervening π pulse. The absence of additional small delays or other influences on the echo by the π pulse is easily explained. During the first half of the π pulse the Bloch vectors continue to get further out of phase at the rate $1/T_2^*$. But during the second half they begin to rephase at the same rate, so that after the full 180° rotation the Bloch vectors are only as far out of phase as they were before the rotation began.

Obviously this kind of independence of the pulse would fail to hold true if the π pulse were not symmetric in time about its half-area point. A triangularly shaped pulse such as the one shown in Fig. 9.5, for example, takes roughly 70% of its length $t_3 - t_2$ to reach $\frac{1}{2}\pi$ in area. The second $\frac{1}{2}\pi$ is accomplished in less than half the time taken for the first $\frac{1}{2}\pi$. Bloch vectors being flipped by such a pulse would dephase during the first 90° substantially more than they would rephase during the second 90° . As a consequence a new extra delay of about 40% of $t_3 - t_2$ should be introduced into the echo's expected arrival time. This effect does not seem to have been investigated experimentally.

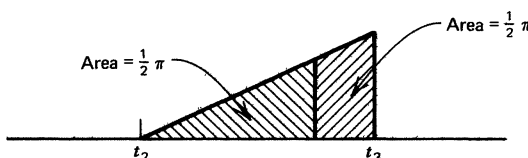


Fig. 9.5 A hypothetical asymmetric π pulse that would have the effect of introducing into the echo time sequence an additional delay not present if the π pulse is symmetric as shown in Fig. 9.4.

9.5 DIRECTIONAL CHARACTER OF ECHOES

In Chapter 8 the directional properties of spontaneous emission were discussed. Any macroscopic emitter, one with dimensions substantially larger than a wavelength, showed pronounced maxima and minima in its radiation pattern [see Fig. 8.3] because of the sharply peaked character of the diffraction function $\Gamma(\mathbf{k} - \mathbf{k}_0)$ appearing in equations 8.20 and 8.33. The same general features should be expected of photon echoes, because in each case the radiation is due to a distribution of dipoles whose relative phases are coherent.

As in the case of superradiance, the relative phasing is governed by the finite speed of light. A plane light wave can be in phase with all of the dipoles lying on any wavefront, obviously, but not with those dipoles more than a fraction of a wavelength ahead or behind the wavefront. Such considerations are unimportant for spin echoes because magnetic resonance wavelengths are comparable to, or even much larger than, the size of the radiating sample. All of the spins automatically lie within a wavelength of each other.

In order to account for the effects of the finite velocity of light on echoes, in expression 9.13 it is only necessary to replace the times t_1, \dots, t_4 by their retarded equivalents. If we remember that these times are defined by reference to the arrival and departure of the two external pulses and the echo pulse, then it is clear that each time, and each time interval, depends on the atom being considered. For the l th atom, located at \mathbf{r}_l , we have:

$$\begin{aligned} t_4 \rightarrow t_{4l} &= t_{40} + \mathbf{n} \cdot \frac{\mathbf{r}_l}{c}, \\ t_3 \rightarrow t_{3l} &= t_{30} + \mathbf{n}_2 \cdot \frac{\mathbf{r}_l}{c}, \\ t_2 \rightarrow t_{2l} &= t_{20} + \mathbf{n}_2 \cdot \frac{\mathbf{r}_l}{c}, \\ t_1 \rightarrow t_{1l} &= t_{10} + \mathbf{n}_1 \cdot \frac{\mathbf{r}_l}{c}. \end{aligned} \tag{9.17}$$

Here t_{40} is the time required for the echo pulse to reach a fictional reference atom located at the origin of the coordinate system. Similarly, t_{30} ,

t_{20} , and t_{10} are the corresponding times for the first and second pulses. The unit vectors \mathbf{n}_1 , \mathbf{n}_2 , and \mathbf{n} give the directions of the first, second, and echo pulses.

As a result of the dependence of the pulse times on the atomic positions, it is necessary to generalize expressions 1.24 or 4.3a for the polarization density. This is because an atom's detuning is now not enough to identify it adequately. We return to the basic definition 4.2, and interpret the average to apply to positions as well as detunings. Then, in place of expression 4.3a, we have

$$\begin{aligned} P(t) = \mathcal{N} d \int d\Delta' g(\Delta') \\ \times \frac{1}{N} \sum_{l=1}^N \operatorname{Re} [\{u_l(t; \Delta') + iv_l(t; \Delta')\} e^{i\omega t}]. \end{aligned} \quad (9.18)$$

With the aid of equations 9.13 and 9.17, the polarization density may be reduced to

$$\begin{aligned} P(t_4) = \mathcal{N} d \int d\Delta' g(\Delta') \operatorname{Re} \left\{ e^{i\Delta'(t_{43} - t_{21})} \right. \\ \left. \times \frac{1}{N} \sum_{l=1}^N e^{i(\omega/c)[(\mathbf{n} - \mathbf{n}_2) - (\mathbf{n}_2 - \mathbf{n}_1)] \cdot \mathbf{r}_l} \right\}. \end{aligned} \quad (9.19)$$

Here ω_l has been replaced by ω in the second exponent, eliminating an extra, but very small, detuning dependence for convenience, and $t_{43} = t_{40} - t_{30}, \dots$, and where the small delay $(\kappa \mathcal{E}_0)^{-1}$ has been ignored.

The fact that $P(t_4)$ splits into two parts, one having to do with atom detunings and the other with atom positions, is not accidental but a consequence of the approximations made. It would be possible for an atom's position to determine its detuning. At the most microscopic level this is true for resonant atoms imbedded in solids, their detuning being largely fixed by local electric fields associated with the site they occupy in the host medium. The assumption made here, which allows this strong correlation between position and detuning to be ignored, is based on the interacting radiation fields' inability to discriminate among the various atoms lying in its wavefront. That is, we have implicitly assumed: that there is always such a large number of atoms at every "effective" position, two positions \mathbf{r}_l and \mathbf{r}_m being effectively the same for the $\frac{1}{2}\pi$ pulse, for example, if $\mathbf{n}_1 \cdot (\mathbf{r}_l - \mathbf{r}_m) = 0$; and that the detunings of these atoms can be

accounted for in an average sense by the smooth function $g(\Delta)$ and need not be treated individually.

Finally, the polarization at time t_4 may be written:

$$P(t_4) = -\mathcal{V}d \sin(\omega + \Delta)t_4 e^{-(\pi/4)[(t_{43} - t_{21})/T_2]^2} \gamma(\mathbf{n} - 2\mathbf{n}_2 + \mathbf{n}_1), \quad (9.20)$$

where the function γ is just the square root of the function Γ introduced in equation 8.21, if the origin of coordinates is located symmetrically so that the sum over atoms in equation 9.19 is real. In any event, $\gamma(\mathbf{m})$ is very sharply peaked near $\mathbf{m} = 0$. This shows that the echo pulse, which is located in time at the point $t_{43} = t_{21}$ as before, is highly directional and has its maximum only if the unit vectors \mathbf{n}_1 , \mathbf{n}_2 , and \mathbf{n} are collinear.

Experimentally it is highly undesirable that the echo pulse be emitted in the same direction as the strong applied $\frac{1}{2}\pi$ and π pulses. For this reason Hartmann and his collaborators [3] adopted a scheme of slightly non-parallel excitation, as shown in Fig. 9.6. If \mathbf{n}_1 is inclined by a small angle ϕ (3° in the original work [3]) to one side of \mathbf{n}_2 , then \mathbf{n} satisfies the condition $\mathbf{n} - 2\mathbf{n}_2 + \mathbf{n}_1 = 0$ to order ϕ^2 if it is in the $\mathbf{n}_1 - \mathbf{n}_2$ plane and inclined by the same angle ϕ to the opposite side of \mathbf{n}_2 .

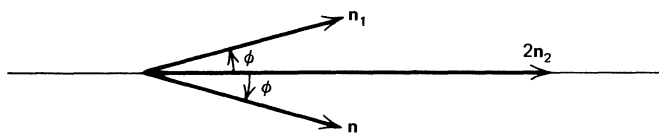


Fig. 9.6 The orientation of the echo pulse \mathbf{n} with respect to the $\frac{1}{2}\pi$ pulse direction \mathbf{n}_1 and the π pulse direction \mathbf{n}_2 .

Obviously it is more convenient for the experimenter if the angle ϕ need not be too small. The limit on ϕ is easily estimated. In order for $\gamma(\mathbf{n} - 2\mathbf{n}_2 + \mathbf{n}_1)$ to be of the order of unity, all of the terms in the sum 9.19 must contribute equally. That is, for all values of \mathbf{r}_i from one end of the sample to the other, the exponent must change by much less than $2\pi i$. If the sample length is L , and its major axis lies along \mathbf{n}_2 , this limit is summarized by the inequality:

$$\frac{\omega}{c} (2\mathbf{n}_2 - \mathbf{n}_1 - \mathbf{n}) \cdot \mathbf{n}_2 L \ll 2\pi. \quad (9.21)$$

This reduces to an expression first derived by Hartmann et al. [3]:

$$\phi^2 \ll \frac{\lambda}{L} \quad (9.22)$$

when use is made of the relations $\mathbf{n}_1 \cdot \mathbf{n}_2 = \mathbf{n} \cdot \mathbf{n}_2 = \cos \phi$ and $2\pi c/\omega = \lambda$, as well as the approximation $4 \sin^2 \frac{1}{2}\phi \approx \phi^2$, valid for small ϕ .

9.6 PHOTON ECHOES IN GASES

Atomic motion in gases adds an extra element of complication to echo phenomena. In equation 9.19 it is apparent that, if the atomic positions \mathbf{r}_i were to drift randomly by even as much as one-quarter wavelength during the time t_{41} between the first applied pulse and the echo, then there would be no direction \mathbf{n} in which the combined atomic phases could produce a macroscopic echo pulse. Of course, at room temperatures, a gas atom drifts as much as 10 or more wavelengths in a typical photon echo delay time of roughly 100 nsec. Thus it might be expected that optical echoes could not be produced in gases at all. This was actually a common view for a time after the original work in solids.

Closer analysis shows that the dephasing due to atomic motion is exactly compensated in the course of the echo development. This was pointed out in 1968 by Scully, Stephen, and Burnham [5] independently of the first photon echo experiments carried out in a gaseous absorber in 1968 by Patel and Slusher [6].

Instead of returning to the quantitative method of the two preceding sections, we simply describe here the compensating effects at work in the echo process in gases. To do that we consider a fictitious model gas in which the atoms move at only two speeds, V^L to the left or V^R to the right, along the direction of the applied $\frac{1}{2}\pi$ and π pulses. Furthermore, we treat only one group of atoms, all located in the plane of the $\frac{1}{2}\pi$ pulse wavefront at time $t_1 = 0$, the instant the $\frac{1}{2}\pi$ pulse reaches the midpoint of the sample.

As Fig. 9.7 shows, the subsequent π pulse reaches the left-moving atoms and begins the rephasing of their moments some time before it catches up with and rephases the right-moving atoms. These two times are denoted by t_2^L and t_2^R , respectively. If the π pulse has negligible time duration, then at times $t_4^L = 2t_2^L$ and $t_4^R = 2t_2^R$ the left- and right-moving atoms' moments have rephased.

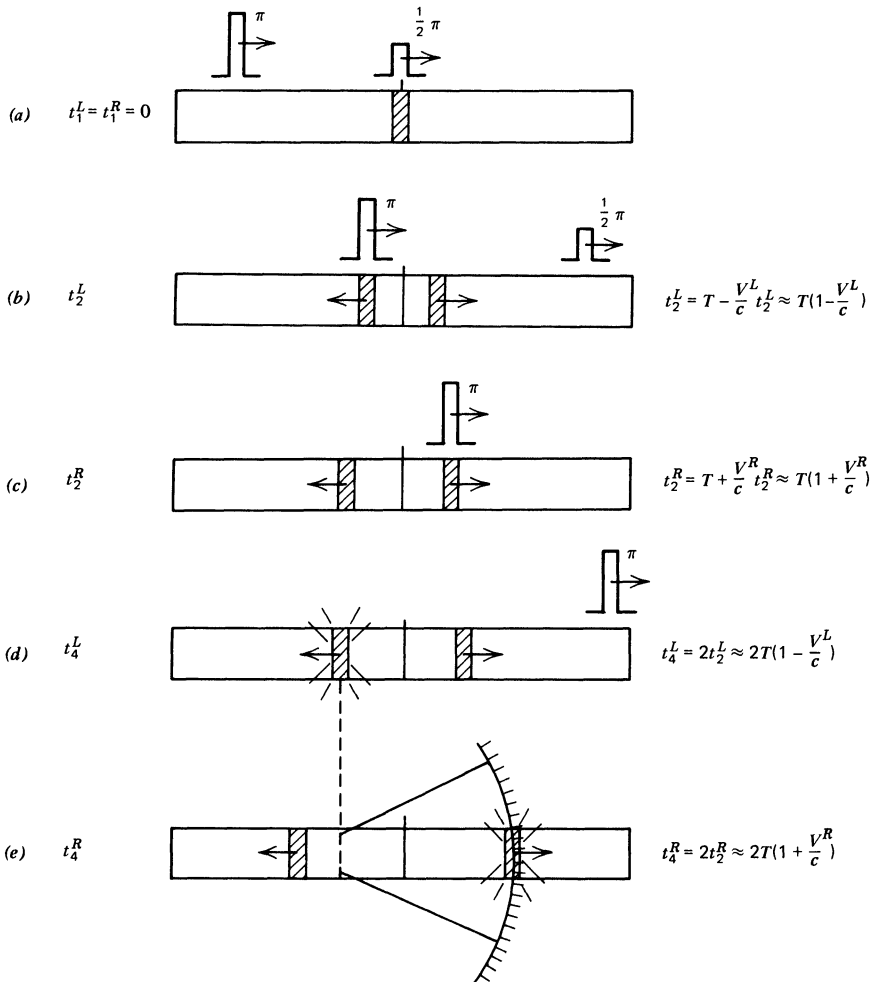


Fig. 9.7 A schematic explanation of the photon echo effect in gaseous absorbers, taking account of atomic motion. (a) At the center of the absorber a group of atoms in the cross-hatched region is irradiated by the $\frac{1}{2}\pi$ pulse. The subsequent time frames (b) to (e) consider only those atoms in the initial group which have speeds lying close to either V^L (left-moving) or V^R (right-moving). Obviously time t_1 , the time of the $\frac{1}{2}\pi$ pulse (see Fig. 9.4), occurs simultaneously for the two groups of atoms. (b) At time t_2^L , the arrival time of the π pulse at the left-moving atoms, both sets of atoms have drifted away from their initial positions. (c) At time t_2^R , the time that the π pulse catches the right-moving atoms, the groups are even farther apart. (d) At some still later time t_4^L the left-moving atom's Bloch vectors will have rephased because of prior action of the π pulse, and they will radiate an echo pulse. (e) Finally, at time t_4^R the right-moving atom's Bloch vectors rephase, and the right-moving atom's echo pulse is emitted. On the assumption that the $\frac{1}{2}\pi$ and π pulses may be taken to be of infinitesimal duration so that $t_2 = t_3$ (in the notation of Fig. 9.4) the various times occurring in the sequence (a) to (e) are all expressed, to first order in V/c , in terms of T , the interval between the two applied pulses.

The left-moving atoms re-phase after they have traveled a distance $-V^L t_4$, which the figure shows to be equal to $D^L = -2V^L T(1 - V^L/c)$ if T is the interval between the $\frac{1}{2}\pi$ and π pulses in the frame of the gas container. The right-moving atoms rephase after having traveled $D^R = 2V^R T(1 + V^R/c)$. The distance between the points where the two groups rephase is given by

$$D = 2(V^R + V^L)T, \quad (9.23)$$

if V^2 contributions are ignored. The importance of this result is that this distance is exactly the distance light travels in the corresponding time interval. That is, it is also true that

$$D = c(t_4^R - t_4^L). \quad (9.24)$$

In other words, the echo emission from the left-moving atoms occurs earlier in time by the right amount so that their echo pulse just catches up with the right-moving atoms at exactly the moment *their* Bloch vectors rephase and emit their echo pulse. Obviously from that time on the echo pulses travel together.

The simple argument given above is rather general. Because the conclusion is independent of the actual values of V^L and V^R , it applies to atoms of every possible velocity. Furthermore, it applies to all the atoms in the sample, since any atom velocity may be decomposed into two components, one along \mathbf{n}_2 and the other orthogonal to it. The orthogonal component, ignored in the discussion above, neither contributes to any additional time of flight nor creates a relative dephasing. Of course, the echo pulses from the various velocity groups overlap and travel together only along the sample axis; that is, along the direction of the $\frac{1}{2}\pi$ and π pulses. The considerations of Section 9.5 show the extent to which the $\frac{1}{2}\pi$ and π pulse directions may deviate from each other. A brief discussion of the contributions to echoes in gases of V^2/c^2 terms and of collisions has been given by Scully, Stephen, and Burham [5].

9.7 EXPERIMENTAL OBSERVATION OF PHOTON ECHO

Kurnit, Abella, and Hartmann [3] observed photon echoes in liquid helium cooled ruby in 1964. At that time the shortest practical pulse that could be produced was of approximately 10 nsec duration. This prescribed a lower limit of about 50 nsec for the time scale of the experiment. In ruby the R_1

fluorescent line width increases from 0.1 cm^{-1} at 77° K to 12 cm^{-1} at room temperature because of phonon-induced transitions in the 2E (\bar{E}) levels. At the temperature of liquid helium the effective relaxation time is of the order of microseconds. The wavelengths of the R_1 and R_2 lines of ruby shift with temperature; hence a laser operating temperature had to be chosen that would permit an overlap of the emission line with the absorption lines of the sample. Happily, since running a ruby laser at liquid helium temperatures would be inconvenient, the wavelength shift of the R_1 line is very small below 77°K . Thus a laser operating at liquid nitrogen temperature allowed appreciable overlap of the R_1 transitions of the sample and the laser just as McCall and Hahn found in the first experiment on self-induced transparency, discussed in Chapter 5.

In the initial experiments the sample had a concentration of 0.005% Cr^{3+} by weight, and the ruby laser was designed to be Q -switched with a Kerr cell. Giant pulses are difficult to obtain at low temperature because of the tendency for weak laser action to occur by reason of Fresnel reflection off any surface inside the cavity. However, the crossed polarizing prisms associated with the Kerr cell prevented the light from leaving the laser.

The two pulses required for exciting the sample were obtained by dividing the beam with a beam-splitter and optically delaying one component of the beam before redirecting it at the sample. In the original experiments, the angle between the two beams was chosen to be about 3° . In consequence a judiciously placed aperture stop allowed a photomultiplier to "see" the echo emitted at an angle of 6° from the first pulse as in Fig. 9.6, without suffering saturation from having observed the first two pulses.

Photon echoes were observed in a manner largely consistent with the theory discussed in the preceding sections. However, an unusual feature of the early work was that in order to observe echoes, a magnetic field had to be applied to the sample along the optic axis. This is a peculiarity of ruby and arises from the time-dependent magnetic field at the Cr^{3+} ion sites because of the precession of the neighboring aluminum nuclei. Similar observations have been made of spin echoes in ruby [7] where rotating the magnetic field away from the optic axis even by as little as 3° causes the spin echo to disappear. This effect is not fundamental to the photon echo process and need not be discussed further here.

It was found that the echo maximum occurred at $t = 2T + s$ after the first pulse where T is the delay between the two excitation pulses and the 5 nsec

extra delay s agreed rather well with the expected extra delay discussed in Section 9.3. The echo spread over a fairly wide angle, but its maximum occurred at the predicted angle of $2\phi \approx 6^\circ$. When the liquid helium was allowed to boil off, echoes could be made to occur for several minutes until incoherent relaxation processes in the warming sample made them undetectable. Since no echoes could be obtained at liquid hydrogen temperatures down to 14°K , it appears that the critical relaxation time is associated with a temperature somewhere in the range from 4.2 to 14°K .

The polarization dependence of the echo was also investigated. The laser output was usually plane-polarized. Using wave plates and linear polarizers in each beam, the relative polarization of each of the pulses could be varied and the echo polarization determined. When the two excitation pulses were plane-polarized in the same direction the echo was found to be polarized similarly. But when the second pulse was plane-polarized at an angle χ_0 to the first, the intensity of the echo was a function of analyzer angle χ and followed the formula

$$I = I_0 \cos^2(\chi - 2\chi_0) \quad (9.14)$$

very closely. It is possible to analyze this result in detail because the transition in ruby is $J = \frac{1}{2} \rightarrow \frac{1}{2}$. Thus the left-hand and right-hand circularly polarized transitions may be looked on as two independent transitions, and each may be investigated separately and the resultant polarization components then recombined to find the final output polarization. Section 5.3 shows that when $\Delta J = 0$ there are no $\Delta M = 0$ transitions.

Patel and Slusher [6] observed photon echoes in the gas SF_6 using 10.6μ pulses produced from two different CO_2 lasers. Unlike ruby, the CO_2 laser allowed single-frequency operation, which together with a high repetition rate allowed the echo phenomena to be studied with rather more ease and accuracy than the earlier work. The pulse width used was 200 nsec and limited the minimum pulse separation to 0.5 μ sec although the pulse separation could be continuously adjusted from 0 to 10 μ sec. As before, the echo occurred at $t = 2T + s$, in agreement with theory. As the incident pulse intensities were decreased or increased so the echo amplitude changed, disappearing when the incident pulse area was estimated to be about $\pi/10$.

In their work on SF_6 Patel and Slusher found the polarization of the echo to be parallel to the polarization of the second exciting pulse when the fields \mathbf{E}_1 and \mathbf{E}_2 of the exciting pulses were polarized at relative angle

χ , and the echo intensity was found to vary as $\cos^2 \chi$. This was in contrast to the original work on ruby, where the variation of polarization with angle went as 2χ and the intensity was independent of χ . Patel and Slusher proposed that the difference was due to the spatial and overlap degeneracy already discussed in Chapter 5 with respect to self-induced transparency, because the circularly polarized components of linearly polarized pulses do not act independently in the case of SF₆.

Alekseev and Evseev independently showed [8] that for $J=0 \rightarrow 1$ or $J=1 \rightarrow 1$ the echo has the polarization of the second pulse, and the echo amplitude is proportional to $\cos \chi$. Furthermore, they showed in agreement with the ruby work that the $J=\frac{1}{2} \rightarrow \frac{1}{2}$ transition has an intensity independent of χ and a polarization vector at 2χ to the first pulse. Subsequently Gordon et al. carried out an extensive theoretical and experimental analysis [9], once again using SF₆, particularly investigating the effects of level degeneracy and echo polarization.

By exploiting the same Stark pulse technique used to observe optical nutation and free induction decay, discussed in Section 3.6, Brewer and Shoemaker [10] were able to obtain photon echoes in C¹³H₃F and NH₂D. Once again they used a cw laser and the $\pi/2$ and π excitation pulses were achieved by briefly Stark shifting the molecules into resonance. The echo observed was different in form from that observed in the other work described here because its frequency was shifted from the laser frequency. The identity of the velocity groups excited during the two pulses was preserved and so the transition frequencies were different for the zero and nonzero Stark fields. Consequently the laser and echo fields produce a beat signal, whose frequency is the Stark shift, at the detector. Because the laser signal was stronger than that of the beat, a pulsed heterodyne signal resulted and the detection sensitivity was greatly enhanced. It was found that increasing the Stark pulse amplitude increased the beat frequency as anticipated and that the plot of the echo amplitude, extrapolated to $T=0$, as a function of molecular density N was linear, showing that the echo intensity varied as N^2 .

9.8 PROPAGATION AND DAMPING OF PHOTON ECHOES

The dephasing of the dipole moments of the resonant atoms in an excited absorber is a deterministic, rather than a stochastic, process. That is, given any two atoms with resonance frequencies differing by $\delta\omega$, it is certain that

after any time δt their dipole moments will have accumulated a phase difference $\delta\phi = \delta\omega\delta t$, simply because of the frequency difference. In the final analysis, it is the deterministic nature of this dephasing that allows rephasing to be accomplished and echoes to be produced.

In discussing echoes we have thus far neglected the effect of stochastic or incoherent damping of the dipole moments. In the semiclassical theory, following Bloch, such incoherent damping of each atom's dipole moment occurs at the rate $(T'_2)^{-1}$. If this rate is substantially smaller than the dephasing rate $(T_2^*)^{-1}$, incoherent processes need have no effect on echo formation.

However, the delay between the two applied pulses that precede the echo can easily be made much larger than T'_2 . If this is done, the echo amplitude is seen to be greatly diminished. Of course, the explanation is simple. Because of T'_2 damping, each dipole moment monotonically decreases in amplitude all the while it is dephasing and rephasing along with the other dipoles to produce the echo. Consequently, when they have rephased, the total dipole moment is no longer $\mathcal{N}d$. The magnitude of the total moment, taking into account T'_2 effects is easily seen to be smaller by the factor $\exp\{-2T/T'_2\}$ if $2T$ is the time between the initial $\frac{1}{2}\pi$ pulse and the echo. This follows from a trivial integration of equations 4.5a and b during the long dephasing and rephasing intervals when there is no applied field present. The equations then reduce to

$$\frac{d}{dt}(u+iv) = -\left(\frac{1}{T'_2} - i\Delta\right)(u+iv), \quad (9.26)$$

with the obvious solution

$$(u+iv)_{2T} = (u+iv)_0 e^{2i\Delta T} e^{-2T/T'_2}. \quad (9.27)$$

Thus the absorber polarization density given in equation 9.15 should be reduced accordingly.

It was pointed out by Hahn [2] in his first discussion of spin echoes that this exponential diminution of echo amplitude provides a natural way to measure T'_2 in many materials. The principal advantage over competing methods lies in the delay T between the last applied pulse and the measured echo. Because of this delay, detector saturation by the exciting pulse can be greatly reduced or eliminated. In Fig. 9.8 the results of photon echo measurements of T'_2 by Patel and Slusher [6] are shown. In their observations the echo intensity decayed exponentially with increasing T in a manner that gave a measure of T'_2 for the vibrational-rotational SF₆

levels excited by the CO₂ laser. T'_2 was changed by mixing the SF₆ with different pressures of He, Ne, or H₂ as a buffer gas. Good fits to straight lines resulted when log (echo amplitude) was plotted against $2T$ as shown in Fig. 9.8.

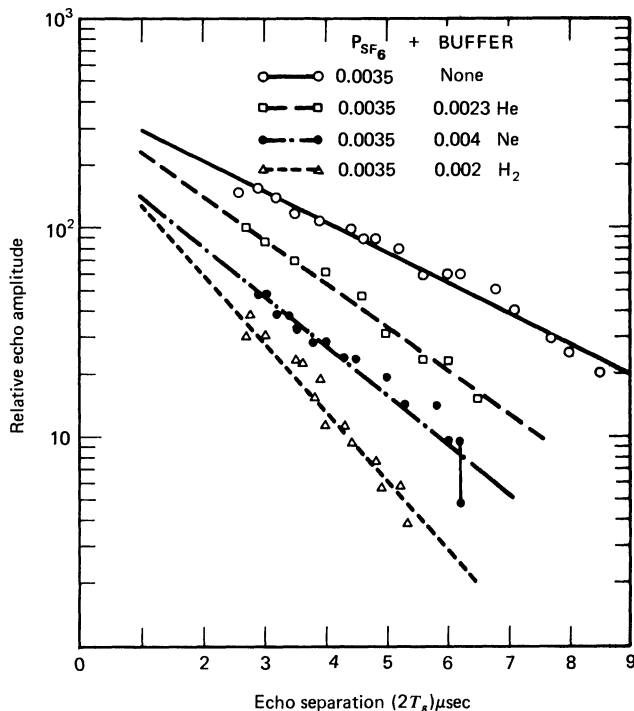


Fig. 9.8 Dependence of echo amplitude on the separation $2T$ between the $\frac{1}{2}\pi$ pulse and the echo pulse in SF₆ vapor, showing an exponential decay. The four curves correspond to SF₆ alone and with He, Ne, and H₂ added as buffer gases. [From C. K. N. Patel and R. E. Slusher, *Phys. Rev. Lett.* **20**, 1087 (1968).]

A detailed treatment [11], using the Bloch equations, of dipole behavior during and after applied pulses shows that the simple picture of damping sketched in the preceding paragraphs is not complete. For example, Hahn pointed out in his original discussion [2] of spin echoes that some circumstances allow T_1 as well as T'_2 to be measured. Although echo experiments to measure T_1 for optical transitions have been discussed, none has yet been reported.

In light of the discussion of superradiance in Sections 8.4 and 8.5, it is natural to consider the possible effect on echo phenomena of cooperative spontaneous emission. A simple argument may be made that superradiant decay, which occurs more rapidly with an increase in the density of resonant atoms, could lead to a decrease in echo amplitude, as follows [12]: At low absorber densities the duration of the echo signal is determined by T_2^* , as explained in Sections 9.2 and 9.3. However, if the density \mathcal{N} were increased sufficiently so that superradiant energy loss occurred more rapidly than free induction dephasing, then each atom's Bloch vector would have to dip significantly below the position in the equatorial plane of the Bloch sphere where the $\frac{1}{2}\pi$ pulse put it initially. But in dropping through an angle consistent with its superradiant energy loss, each Bloch vector's u and v amplitudes automatically decrease. As equation 9.10 shows, it is $u + iv$ that determines the macroscopic polarization density, and through it the echo amplitude. Thus if superradiance led to significant energy loss per excited absorber atom during the dephasing following the initial $\frac{1}{2}\pi$ pulse, the subsequent echo amplitude would have to be diminished.

However, this rough argument ignores too much to be accepted without second thoughts. Photon echoes are almost always observed in samples long enough for light propagation effects to be important. Such effects are deliberately minimized in the discussion of superradiance in Chapter 8. Although Compaan and Abella reported [12] an experimental corroboration of the ideas sketched in the preceding paragraph, it seems clear that other explanations can also account for their results. For example, Hahn, Shiren, and McCall [13a] and Friedberg and Hartmann [13b] show that successive applications of the area theorem to the three pulses involved in an echo experiment can also lead one to expect an eventual decrease in echo amplitude as the absorber density is increased.

It is instructive to explore very briefly the view of echoes implied by the analyses mentioned above [13a, b]. This view emphasizes the propagation of echoes through a long absorber, and is not especially concerned with the timing or shape of the echo. As might be expected, the area theorem is an extremely useful tool when pulse times and shapes are not important. If θ_1 , θ_2 , and θ_e are the areas of the first, second, and echo pulses, then Hahn, Shiren, and McCall give these equations for the three areas:

$$\frac{d\theta_1}{dz} = -\frac{1}{2}\alpha \sin \theta_1(z), \quad (9.28a)$$

$$\frac{d\theta_2}{dz} = -\frac{1}{2}\alpha \cos\theta_1(z) \sin\theta_2(z), \quad (9.28b)$$

$$\begin{aligned} \frac{d\theta_e}{dz} = \frac{\alpha}{2} & [\sin\theta_1(1 - \cos\theta_e \cos\theta_2) \\ & + \cos\theta_1 \sin\theta_2(1 - \cos\theta_e) - \sin\theta_e \cos(\theta_1 + \theta_2)]. \end{aligned} \quad (9.28c)$$

The very complicated last equation follows easily from the fact that the total area $\theta_1 + \theta_2 + \theta_e$ must satisfy the same equation as θ_1 . The second equation has an almost obvious explanation too. The effective attenuation coefficient α seen by the second pulse is reduced in proportion to the inversion produced by the first pulse, as indicated by equation 6.18b, for example.

An estimate of the dependence of echo intensity on \mathcal{N} may be made by integrating equations 9.28 under the assumption that $\theta_1(0)$ and $\theta_2(0)$ are small, and $\theta_e(0)=0$. Then equations 9.28 reduce simply to

$$\frac{d\theta_1}{dz} \approx -\frac{\alpha}{2} \theta_1(z), \quad (9.29a)$$

$$\frac{d\theta_2}{dz} \approx -\frac{\alpha}{2} \theta_2(z), \quad (9.29b)$$

$$\frac{d\theta_e}{dz} \approx \frac{\alpha}{4} \theta_1(z) [\theta_2(z)]^2 - \frac{\alpha}{2} \theta_e(z). \quad (9.29c)$$

The first two of these equations merely express Beer's law, and are easily integrated and substituted into the echo equation, which becomes

$$\frac{d\theta_e}{dz} = -\frac{\alpha}{2} \theta_e(z) + \frac{\alpha}{4} \theta_1(0) \theta_2^2(0) e^{-\frac{3}{2}\alpha z}. \quad (9.30)$$

This equation may also be integrated exactly because it is only first-order and linear in θ_e . The result [13] is:

$$\theta_e(z) = \frac{1}{2} \theta_1(0) \theta_2^2(0) e^{-\alpha z} \sinh\left(\frac{\alpha z}{2}\right). \quad (9.31)$$

From the solution two conclusions may be tentatively drawn if we identify $\theta_e^2(z)$ with the echo intensity detected in the Compaan-Abella experiments [12]. First, for $\alpha z \ll 1$, it is clear that the detected intensity is

proportional to α^2 and thus proportional to \mathcal{N}^2 , as observed. Second, because $\theta_e(z)$ is predicted by solution 9.31 to peak at $\alpha z = \ln 3$, and to decrease for larger values of α (i.e., for higher densities of absorber), it is unnecessary to invoke superradiance in addition to the area theorem in order to show that echo intensities can be expected to fall below an \mathcal{N}^2 dependence on density as \mathcal{N} is made larger and larger.

The second conclusion drawn above is qualitatively obvious, even without the help of the simplified area equations 9.29. It follows that θ_e^2 must eventually decrease as a function of αz simply because of the assumption that $\theta_1(0)$ and $\theta_2(0)$ were very small. The total area was thus initially smaller than π , and its eventual decay to zero a common fate of all pulses lying on the first branch of the area curves in Fig. 4.3.

It is interesting to lift the restriction to very small initial areas. Lamb [14] has emphasized what can be done in the way of approximate analytic solution of area equations like equation 9.28, and Hahn, Shiren, and McCall [13] have integrated those equations numerically for $\theta_1(0) = \frac{1}{2}\pi$ and $\theta_2(0) = 0.99\pi$. In Fig. 9.9 we show their results. The two input pulses are eventually depleted. The final area of the echo pulse is 2π in agreement with the area theorem's prediction that a pulse with area in the range π to 2π will evolve into a 2π pulse, rather than a 0π pulse.

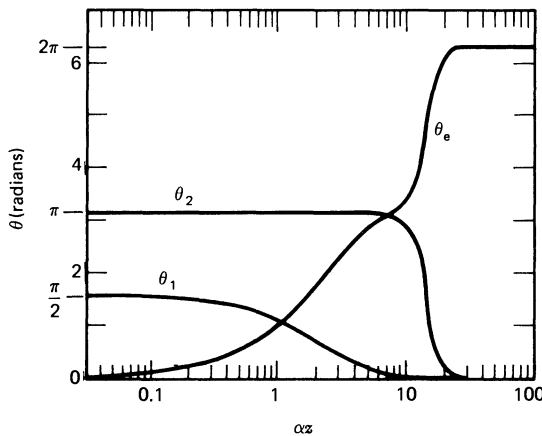


Fig. 9.9 Change with distance of the areas of the $\frac{1}{2}\pi$, π , and echo pulses in a typical echo experiment. In accord with the area theorem, both the $\frac{1}{2}\pi$ and the (slightly less than) π pulses decay to zero. However, the total area, which is greater than π , appears in the echo pulse which eventually grows to 2π . [From E. L. Hahn, N. S. Shiren, and S. L. McCall, *Phys. Lett.* **37A**, 265 (1971).]

References

1. E. L. Hahn, Friday-the-13th Evening Discourse of the Royal Institution, February 1970, in *Proc. Roy. Inst. G. B.* **44**, No. 203, 26–52 (1970).
2. E. L. Hahn, *Phys. Rev.* **80**, 580 (1950).
3. N. A. Kurnit, I. D. Abella, and S. R. Hartmann, *Phys. Rev. Lett.* **13**, 567 (1964). See also I. D. Abella, N. A. Kurnit, and S. R. Hartman, *Phys. Rev.* **141**, 391 (1966), and the review by I. D. Abella, in *Progress in Optics*, E. Wolf, ed., North-Holland, Amsterdam, 1969, Vol. 7.
4. A. L. Bloom, *Phys. Rev.* **98**, 1105 (1955).
5. M. O. Scully, M. J. Stephen, and D. C. Burnham, *Phys. Rev.* **171**, 213 (1968).
6. C. K. N. Patel and R. E. Slusher, *Phys. Rev. Lett.* **20**, 1087 (1968). See also B. Bölgger and J. C. Diels, *Phys. Lett.* **28A**, 401 (1968).
7. D. Grischkowsky and S. R. Hartmann, *Phys. Rev. Lett.* **20**, 41 (1968).
8. A. I. Alekseev and I. V. Evseev, *Sov. Phys. J.E.T.P.* **29**, 1139 (1969).
9. J. P. Gordon, C. H. Wang, C. K. N. Patel, R. E. Slusher, and W. J. Tomlinson, *Phys. Rev.* **179**, 294 (1969).
10. R. G. Brewer and R. L. Shoemaker, *Phys. Rev. Lett.* **27**, 631 (1971).
11. E. T. Jaynes, *Phys. Rev.* **98**, 1099 (1955). See also A. L. Bloom, Ref. 4.
12. A. Compaan and I. D. Abella, *Phys. Rev. Lett.* **27**, 23 (1971).
13. (a) E. L. Hahn, N. S. Shiren and S. L. McCall, *Phys. Lett.* **37A**, 265 (1971)
(b) R. Friedberg and S. R. Hartmann, *Phys. Lett.* **37A**, 285 (1971).
14. G. L. Lamb, Jr., *Phys. Lett.* **28A**, 548, (1969); *Rev. Mod. Phys.* **43**, 99 (1971).

Index

- Abella, 194, 197, 211, 217, 220
Ablowitz, 101, 109
Abragam, 77
Absorber, 23, 69, 78, 87, 88, 89, 96, 99, 106, 110, 111, 112, 113, 115, 116, 117, 119, 121, 124, 125, 127, 138, 140, 143, 144, 145, 151, 203, 214, 219
Absorption, v, 7, 20, 24, 25, 78, 85, 130, 131, 140, 191
Absorption band, 68
Absorption cell, 112, 115
Absorption coefficient, 86, 95, 112, 115, 125, 138, 145, 146, 190
Absorption cross-section, 123, 139
Absorption formula, 1
Absorption length, 24, 25, 95
Absorption line, 26, 30, 70, 112, 117, 121, 141, 201, 212
Absorption linewidth, 26, 145
Absorption profile, 111
Absorption spectrum, 30
Absorptive equation, 137
Absorptive part of the dipole moment, 45, 139, 142
Acke, 169, 172, 173
Adiabatic changes, 103
Adiabatic following, 72-77
Adiabatic following approximation, 75
Adiabatic following assumption, 75
Adiabatic following limit, 74
Adiabatic inversion, 74, 103
Agarwal, 173, 194
Alekseev, 214, 220
Alignment, 54
Alkali metal vapors, 20
Allen, 121, 122, 123, 124, 128, 129, 151
Aluminum nuclei, 212
Ambartsumyan, 151
Amplification, 130, 143-147
Amplification rate, 146
Amplified spontaneous emission, 131
Amplifier, 127, 131, 147, 148, 149
Amplify, 126
Amplifying medium, 67
Amplifying resonant media, 145
Amplitude modulation, 68
Angular momentum, 117, 155
Angular momentum algebra, 44
Angular velocity, 44
Anomalous classical absorption, 21-26
Antenna array, 188
Antialignment, 54
Antinormal ordering, 157, 166, 167
Applied field, 10, 43, 45, 73, 102, 175, 176
Applied pulse, 209
- Area, 15, 23, 54, 85, 86, 88, 90, 91, 94, 115, 119, 179, 199, 219
Area-stable pulse, 91. *See also Pulse*
Area theorem, vi, 2, 20, 78, 85, 86, 91, 96, 104, 105, 110, 113, 119, 138, 191, 217, 219
Arechi, 96, 109, 126, 129, 147, 151, 189, 191, 194
Armstrong, 77, 129
Asher, 115, 116, 128
Ashkin, 151
Atom-atom correlation, 189
Atom fluctuations, 170
Atom's energy, 159
Atomic absorbers, 120, 196
Atomic absorption line, 68, 162
Atomic beam, 116
Atomic Bloch equations, 139; *see Bloch equations*
Atomic coherence, 126
Atomic dipole, 4, 7, 9, 114, 193, 197; *see Dipoles, etc.*
Atomic dipole matrix element, 46
Atomic dipole moment, 90, 142, 199
Atomic dipole moment operator, 167
Atomic frequency, 74
Atomic hydrogen, 35, 42, 141
Atomic inversion, vii, 52, 80, 92, 103, 132, 160
Atomic inversion density, 132
Atomic inversion oscillation, 157-162
Atomic levels, 42
Atomic lifetime, 167
Atomic lowering operators, 158
Atomic motion, 209, 210
Atomic operators, 35, 155, 156, 157
Atomic oscillators, 180
Atomic physics, vii
Atomic polarization density, 204
Atomic population, 55
Atomic raising operators, 158
Atomic reaction, 170
Atomic relaxation times, 130
Atomic resonance, 15
Atomic source field, 170
Atomic structure, 29
Atomic transition, 164
Atomic velocities, 31
Attenuation, 88, 124, 144, 145
Attenuation coefficient, 2, 218
Attenuation rate, 146
Axial modes, 126
- Bandwidth, v, 70
Barnard, 109

- Basov, 151
 Beam-splitter, 212
 Beats, 69, 71, 214
 Beat signal, 214
 Beer's absorption coefficient, 25, 190
 Beer's absorption length, 90, 113, 122, 123, 190, 191
 Beer's law, 14, 20, 23, 24, 25, 26, 78, 85, 88, 120, 125, 145, 218
 Beer's length, 190, 191
 Benney-Newell equation, 101
 Bethe, 173
 Binding field, 42
 Binding forces, 171
 Bjorken, 173
 Bjorkholm, 151
 Bleaching, 110, 111, 127
 Bloch, 28, 47, 51, 52, 60, 61, 77, 142, 151
 Bloch equations, vi, 52, 63, 71, 72, 74, 77, 81, 82, 84, 93, 101, 102, 130, 132, 134-137, 139, 143, 146, 195, 216; *see also* Optical Bloch equations
 Bloch-Sieger (frequency) shift, 29, 47-50, 171
 Bloch sphere, 202, 217
 Bloch variables, 83
 Bloch vector, 53, 54, 55, 56, 57, 67, 72, 73, 74, 75, 81-85, 188, 197, 199, 200, 202, 203, 205, 210, 211, 217
 Bloch vector equations, 53
 Bloch vector tipping angle, 82; *see* Tipping angle
 Bloembergen, 194
 Bloom, 201, 220
 Böller, 220
 Boltzmann's constant, 31
 Bonifacio, 126, 129, 184, 194
 Born, 3, 4, 26
 Bosons, 153
 Bound system, 171
 Boundary conditions, 154
 Bowden, 189, 194
 Break-up, 78, 99, 100, 107
 Brewer, 11, 27, 68, 70, 77, 194, 214, 220
 Brewer-Shoemaker technique, 68
 Brewer-Shoemaker experiments, 70
 Brewer-Shoemaker method, 74
 Broadening, *see* Homogeneous broadening; Inhomogeneous broadening
 Broad-line limit, 115
 Buffer gas, 216
 Bullough, 101, 109
 Burnham, 209, 220

 $\text{C}^1\text{H}_3\text{F}$, 68, 214
 Carrier frequency, 148
 Carrier wave velocity, 149
 Caudrey, 101, 109
 Cavity, 126, 128, 154
 Centre frequency, 31
 Charges, 1
 Cheo, 129
 Chirped, 104, 112

 Churchill, 129
 Circularly polarized light, 107-109, 214
 Circularly polarized light wave, 107
 Circuit analysis, vi
 Classical absorption coefficient, 14, 138
 Classical absorption formula, 145
 Classical area theorem, 15-21, 88
 Classical dialectrics, 21
 Classical dipole, 46, 47, 187
 Classical dipole equations, 6
 Classical dipole interactions, 46-47
 Classical dispersion theory, vi
 Classical electric field, 38
 Classical harmonic oscillator, 29
 Classical linear dispersion theory, 1, 77
 Classical Lorentz oscillator, 157; *see also* Lorentz etc.
 Classical polarization density, 119
 Classical Rabi problem, 5-7
 Classical Rabi solutions, 7
 Classical theories, 80
 Closed shells, 30
 CO_2 laser, 68, 111, 120, 213, 216
 CO_2 laser radiation, 68
 Cohen-Tannoudji, 51
 Coherence, 181, 182, 187, 188, 193
 Coherence time, 124
 Coherent absorption, 78
 Coherent bleaching, 124, 125
 Coherent effects, 130
 Coherent emission, 196
 Coherent external field, 136, 144
 Coherent fields, 66, 72, 136, 141
 Coherent interactions, 29, 32, 77, 114
 Coherent light, v, 54
 Coherent light pulse, 68
 Coherent optical pulses, 112, 192; *see also* Pulses
 Coherent optical transient effects, 71
 Coherent pulses, 96, 115; *see also* Pulses
 Coherent pulse length, 124
 Coherent pulse propagation, vi
 Coherent radiation, 198
 Coherent rephasing, 198
 Coherent resonant effects, 47
 Coherent saturation, 80
 Coherent spontaneous emission, 174, 181
 Coherent stimulating field, 126
 Coherent superposition state, 68
 Coherent transients, v, vii
 Coherent transient effects, 67
 Coherent transient phenomenon, 68
 Collective emission, 182
 Collision damping, 31, 114
 Collision frequency, 31
 Collision linewidth, 32
 Collision process, 97
 Collisions, 6, 30, 31, 52, 60, 61, 64, 99, 133, 139, 195, 211
 Combaud, 124, 129, 137
 Commutation relation, 153
 Compaan, 194, 217, 220
 Compaan-Abella experiment, 218

- Complex dielectric constant, 15
 Complex wave vector, 15
 Compression, 113
 Compton formula, 1
 Conservation laws, 37, 39, 40, 132
 Conservation of probability, 46
 Constant amplitude field, 103
 Convex lens, 150
 Cooperative atoms, 187
 Cooperative effects, vi
 Cooperative emission, 192
 Cooperative phenomenon, 131
 Cooperative spontaneous emission, 217
 Correspondence principle, 1
 Coulter, 189, 194
 Counter-rotating frame, 48
 Counter-rotating torque, 50
 Counter-rotating wave, 171
 Coupled Maxwell-Bloch equations, vi, 90, 91, 92, 95
 Courtness, 77, 125, 129, 189, 191, 194
 Cr^{3+} , 212
 Cr^{3+} ions, 193
 Cr^{3+} ion sites, 212
 Crisp, 21, 23, 24, 25, 26, 27, 74, 75, 76, 77, 96, 109
 Cummings, vi, 152, 159, 161, 162, 172
 Current, 156
 Curry, 151
 C. W. laser, 68, 69, 126, 214
 C. W. laser field, 69
 C. W. signal, 147
 D-lines, 30, 32, 33, 42
 Da Costa, 149, 151
 Damped Bloch equations, 67, 72
 Damping, vi, 6, 11, 17, 61, 68, 72, 81, 195, 196
 Damping rate, 80
 Decay, 5, 11, 21, 61, 132
 Decay law, 167
 Decay rate, 11, 135, 163, 169
 Decay time, 61
 Decorrelation, 165, 186
 Defocussing, 151
 Degeneracy, 32, 112, 118, 119
 Degenerate, 32
 Degenerate absorbers, 110, 117, 120
 DeGiorgio, 109
 Delay, 121; *see also* Pulse delay
 Delay time, 126
 Delta function, 138
 $\Delta m = 0$ transition, 40
 $\Delta m = \pm$ transition, 41, 107, 108, 118
 DeMaria, 77
 Density of states, 133
 Dephasing, 11, 70, 180, 182
 Detuning, 10, 22, 52, 56, 57, 59, 60, 73, 74, 82, 83, 84, 105, 115, 116, 135, 136, 138, 140, 141, 143, 145, 149, 180, 196, 197, 198, 201, 207
 Detuning function, 11
 Dicke, 155, 172, 174, 180, 181, 182, 189, 194
 Dielectric, v, vii, 1, 2, 7, 9, 12, 14, 20, 26, 85
 Dielectric absorber, 80; *see also* Absorber
 Dielectric absorption line, 25
 Dielectric constant, 14, 23
 Diels, 115, 128, 220
 Diffraction function, 206
 Dimensionless intensity, 134, 138, 141, 144
 Dipoles, 1, 4, 5, 6, 7, 8, 10, 17, 20, 47, 71, 78, 79, 82, 103, 155, 157, 175, 179, 182, 187, 196, 198, 206
 Dipole amplitude, 20, 21, 75
 Dipole approximation, 155
 Dipole correlation function, 168
 Dipole damping, 85
 Dipole decay time, 60
 Dipole dephasing, 195
 Dipole emission, 199
 Dipole envelope function, 7, 91
 Dipole equations, 13
 Dipole interaction, 177
 Dipole magnitude, 132
 Dipole matrix element, 36, 156
 Dipole moment, vii, 8, 28, 29, 42, 45, 61, 80, 107, 108, 109, 112, 115, 117, 118, 142, 175, 187, 188, 189, 202, 214, 215
 Dipole moment decay time, 61
 Dipole moment dephasing, 196
 Dipole moment operator, 34, 35, 36, 40, 108, 165, 167, 168
 Dipole oscillations, 4, 60, 61
 Dipole oscillator, 2, 3, 96
 Dipole phase, 132
 Dipole phase angle, 183
 Dipole phase interruption, 64, 135
 Dipole relaxation, 20
 Dipole relaxation time, 128
 Dipole spectral response function, 82, 83
 Dipole tipping angle, 183; *see also* Tipping angle
 Dipole transients, 14, 17
 Dipole transient response, 17
 Dipole transitions, 42; *see also* Electric dipole transitions
 Dipole turning angle, 90, 104
 Dipole variables, 81
 Dirac, 172, 174
 Directional character of echoes, 206-209
 Dispersion, 29, 45
 Dispersion characteristics, 126
 Dispersion formula, 1
 Dispersion relations, 14, 15, 96, 148
 Dispersion in saturated media, 147-151
 Dispersion theory, vi
 Dispersive effects, 130
 Dispersive part of dipole moment, 139
 Dissipative processes, 32
 Dissipative system, 20
 Doppler broadened, 70
 Doppler effect, 8, 31, 32, 61
 Doppler width, 32, 112, 116; *see also* T_2^* , Inhomogeneous width

- Doublet structure, 30
 Drell, 173
 Driving field, 60, 103
 Driving frequency, 5
 Duguay, 129
 DuPont-Roc, 51
 Dye lasers, v, 120
 Eberly, 92, 94, 96, 109, 151, 172, 183, 186, 194
 Echo, v, vii, 182, 198, 199, 205, 209, 212, 213, 215; *see also* Photon echo
 Echo amplitude, 213, 216, 217
 Echo delay, 205
 Echo emission, 211
 Echo in gases, 211
 Echo intensity, 214, 215, 218, 219
 Echo phenomena, 199, 213, 217
 Echo polarization, 213, 214
 Echo pulse, 201, 202, 206, 207, 208, 209, 210, 211, 216, 219
 Echo signal, 195, 217
 Echo time behavior, 202-205
 Effective field, 103
 Effects of degeneracy, 117-120
 Eigenstates, 35
 Eilbeck, 101, 109
 Einstein, 131
 Einstein's A coefficient, 167, 174, 178
 Einstein's B coefficient, 174
 Electric dipole, 40, 78; *see also* Dipole
 Electric dipole matrix elements, 117
 Electric dipole pseudospin vector, 40, 43
 Electric dipole radiation, 4, 78
 Electric dipole transitions, 30, 34, 42, 78, 117, 119
 Electric discharge, 61
 Electric field, vii, 1, 2, 11, 34, 39, 84, 85, 119, 145, 153
 Electric field amplitude, 52, 84, 153
 Electric field area, 21
 Electric field envelope, 15, 85
 Electric field envelope area, 85
 Electric field operator, 34, 37
 Electric field strength, 132
 Electric spin vector, 28
 Electromagnetic energy, 3, 4
 Electromagnetic field, 152
 Electromagnetic field-dipole coupling, 159
 Electromagnetic radiation field, 153
 Electromagnetic wave propagation, 12-15
 Electron, 30, 42, 124, 153
 Electron spin resonance, v
 Elliptic functions, 82, 97
 Emission, 7, 183, 188
 Emission line, 7, 30, 180, 212
 Emission process, 174, 177
 Energy, 20, 24, 45, 47, 61, 80, 107, 146, 184
 Energy absorption, 53, 142
 Energy conservation, 3, 4, 12, 92
 Energy decay, 5, 64, 120
 Energy decay rate, 167
 Energy density, 3, 80
 Energy of the dipole, 4
 Energy flux, 120
 Energy flux conservation, 80
 Energy levels, v, 29, 33, 34, 110, 140
 Energy level diagram, 32
 Energy loss, 4
 Energy loss mechanisms, 88
 Energy-loss processes, 196
 Energy loss rate, 88, 178
 Energy shift, 171
 Energy stored, 140
 Ensemble of atoms, 176
 Envelope amplitude, 98, 99, 106; *see also* Field envelope
 Envelope area, 55, 86, 87, 103, 115, 117, 124, 128, 202; *see also* Pulse area
 Envelope function, 6, 13, 21, 80, 94, 109, 134
 Envelope propagation velocity, 125
 Envelope shape, 96
 Evseev, 214, 220
 Exact resonance, 64
 Exact resonance atoms, 160
 Excitation number operator, 159
 Excitation pulse, 32, 186, 192, 212
 Excited atom, 176
 Excited state lifetime, 30
 Exciting pulse, 191
 Experimental observation of photon echo, 211-214
 Exponential decay, 20, 21
 External field, 42, 65, 140, 175, 177, 207
 F, 32
 Fabre, 51
 Fain, 170, 173
 Feld, 194
 Feynman, 37, 51
 Field, vi, vii, 7, 20, 32, 42, 54, 61, 75, 128, 139, 140, 143, 148, 153, 154, 158, 159
 Field amplification, 130
 Field amplitude, 103
 Field energy, vii, 21
 Field energy density, 134
 Field energy flux, 92
 Field envelope, 23, 53, 72, 93, 94, 108, 200, 202; *see also* Envelope
 Field envelope function, 91
 Field equations, 73, 97
 Field frequency, 6, 101
 Field intensity, 132, 137
 Field modes, 158, 162, 175
 Field mode creation operators, 157
 Field mode destruction operators, 157
 Field mode operators, 156
 Field operators, 157
 Field operator solution, 174
 Field phase, 105
 Field phase reversals, 120
 Field-polarization vector, 133
 Field strength, 42, 135, 136, 148
 Flash lamp, 61

- Fluorescence, 59, 174
Fluorescence intensity, 59
Fluorescent linewidth, 212
Fluorescent output, 174
Focus, 150
Fourier, 23
Fourier transform, 23
Fox, 126, 127, 129
Free decay, 199-201, 202, 205
Free electron, 171
Free field, 163
Free field operator, 166
Free induction decay, v, 2, 11, 21, 52, 69-72, 181, 182, 194, 195, 196, 204, 214
Free induction dephasing, 190, 193, 217
Free induction pulses, 202
Free induction signal, 195
Free precession, 182, 199, 200, 203, 205
Frequency, 34, 179
Frequency distribution function, 11
Frequency modulated field, 102
Frequency modulation, 103-107
Frequency profile, 115
Frequency range, 9
Frequency shift, 169, 170, 172
Frequency spectrum, v
Frequency sweep, 102, 103
Frequency width, 116
Fresnel number, 186, 190, 192
Fried, 172
Friedberg, 189, 190, 194, 217, 220
Friedberg-Hartmann relation, 190
Friedberg-Hartmann restriction, 193
Friedman, 109

Gain, 126, 146
Gain curve, 128
Garrett, 129
Gaseous absorbers, 31, 111, 151, 210
Gases, 81, 201, 209, 211
Gas laser, 126
Gauge transformation, 155
Gaussian, 19, 24, 25, 26, 31, 201
Gibson, 101, 109
Gibbs, 88, 89, 99, 107, 109, 112, 113, 114, 115, 116, 128, 129
Gilmore, 189, 194
Ginsburg, 173
Gires, 124, 129, 137
Goldhar, 129
Gordon, 129, 214, 220
Green's function, 163
Grieneisen, 129
Grishkowsky, 77, 220
Grivet, 194
Ground state, 30, 32, 46, 54, 60, 67, 73, 88, 104, 136, 176
Ground state population, 74
Gruhl, 129

 H_2 , 216
Haake, 186, 194
Hahn, 11, 27, 77, 78, 83, 84, 85, 86, 88, 90, 91, 108, 109, 110, 115, 126, 127, 128, 129, 195, 196, 197, 212, 215, 216, 217, 219, 220
Halfwidth, 22
Hannaford, 51
Hansch, 51, 141, 151
Hard collisions, 195
Harmonic oscillator, 47
Hartmann, 189, 190, 194, 197, 208, 209, 211, 217, 220
He, 216
Heisenberg, vii, 1, 37
Heisenberg equations, 36, 37, 132, 153, 154, 156, 160, 163, 170
Heisenburg operator, 162, 169
Heisenburg picture, vii, 153, 159, 179, 183
Heitler, 51, 164, 172, 173
Hellworth, 37, 51
He-Ne 6328 Å, 128
He-Ne laser cavity, 127
Hepp, 172
Hercher, 51
Herman, 194
Hermitian operator, 36
Heterodyne signal, 214
 $^{202}\text{Hg II}$ laser, 112
High-power lasers, 111
Hioe, 172
Hocker, 68, 77
Hole, 19, 124, 141, 143
Hole-burning, 111, 130, 143, 144
Hole width, 141
Hollow cathode discharge tube, 112
Holmes, 94, 109
Homogeneous absorber, 124
Homogeneous broadening, 8, 14, 15, 120, 137
Homogeneous damping, 31, 61
Homogeneous effects, 61
Homogeneous field, 164
Homogeneous lifetime, 11
Homogeneous line, 148
Homogeneous linewidth, 30, 141
Homogeneous relaxation time, 139, 196
Homogeneous width, 8
Homogeneously broadened absorbers, 145, 150; *see also* Absorber
Homogeneously broadened linewidth, 133
Homogeneously broadened resonance line, 120
Hopf, 27, 126, 129, 151
Hydrogen, 35, 42, 141
Hyperbolic secant pulse, 83, 116
Hyperbolic secant steady-state pulse, 116
Hyperfine level, 32
Hyperfine structure, 32, 33, 34

I, 32
Isevgi, 146, 147, 151
Impurities, 8
Incident pulse, 117
Incident pulse area, 213
Incoherence, 188

- Incoherent bleaching, 11, 123, 124, 125
 Incoherent damping, 215
 Incoherent decay rate, 124
 Incoherent dipole interruptions, 139
 Incoherent energy, 136
 Incoherent energy input, 61, 62, 140, 145
 Incoherent energy loss, 188
 Incoherent interactions, 6, 61
 Incoherent line-broadening processes, 52
 Incoherent optical effects, 130
 Incoherent optical saturation, 124
 Incoherent processes, 127
 Incoherent pulse, 121
 Incoherent relaxation processes, 110, 213
 Incoherent relaxation rates, 135
 Incoherent resonance phenomena, 130
 Incoherent saturable absorber theory, 124
 Incoherent saturation, 80, 110, 111, 114,
 120, 121-126
 Incoherent threshold, 124
 Incoherently saturating field, 140
 Index of refraction, 2, 148, 149, 150, 191
 Induced emission, 131
 Induced transition rate, 133-134
 Inducing field, 131
 Infinite pulse-train solutions, 96
 Inhomogeneous broadening, 8, 9, 10, 11,
 14, 17, 31, 59, 68, 79, 103, 109, 119,
 138, 142, 143, 175, 185, 191, 195-197,
 204
 Inhomogeneous dephasing, 85
 Inhomogeneous effects, 61
 Inhomogeneous halfwidth, 11
 Inhomogeneous lifetime, 10, 11, 17
 Inhomogeneous line, 11, 116, 141, 180,
 195
 Inhomogeneous lineshape, 10, 12, 180
 Inhomogeneous lineshape function, 8, 143
 Inhomogeneous linewidth, 72
 Inhomogeneous spectral broadening, 32
 Inhomogeneous width, 32, 115, 117
 Inhomogeneously broadened absorber, 96,
 119, 125, 192
 Inhomogeneously broadened absorption
 line, 140, 144
 Inner shell electrons, 42
 In-phase dipole amplitude, 5, 6, 92
 In-phase Maxwell equation, 79, 96, 105,
 147
 Input area, 91, 117
 Input energy, 114, 115
 Input pulse, 116
 In-quadrature dipole amplitude, 5, 6, 142
 In-quadrature Maxwell equation, 79, 86, 92,
 105, 108, 119
 Instantaneous frequency shift, 103
 Intensity, 145, 146, 178
 Intensity dependent pulse delay, 120
 Intensity modulation, 67
 Intensity rate equation, 139, 144
 Interference, 11, 177, 180, 184
 Intermode competition, 126
 Internal energy, 40
 Inverse scattering, 101
 Inversion, vii, 28, 45, 46, 58, 59, 60, 61, 69,
 76, 127, 132, 134, 135, 136, 139, 140,
 141, 143, 144, 146, 160, 161
 Inversion oscillation, 53
 Inversion process, 103
 Inverted media, 126
 Ionization energy, 42
 J, 29, 30, 32
 Jacobs, 51, 109
 Javan, 111, 128, 129, 149, 151
 Jaynes, 64, 77, 152, 159, 161, 162, 172,
 220
 Jaynes-Cummings approach, 161
 Jaynes-Cummings atom, 162
 Jaynes-Cummings problem, vi
 Jodoin, 194
 Jones, vii, 129
 Kaup, 101, 109
 Kelley, 149, 151
 Kerr cell, 212
 Khanin, 170, 173
 Kinetic energy, 97
 Knight, vii, 172
 Korteweg-de Vries equations, 101
 Kramers, 1
 Kramers-Heisenberg dispersion formula, 46
 Kryukov, 151
 Kuhn, 51
 Kurnit, 129, 194, 197, 211, 220
 L, 30
 L-S coupling, 29
 Lamb, G. L. (Jr), 27, 97, 99, 106, 109, 129,
 147, 151, 219, 220
 Lamb, W. E. (Jr), 128, 129, 131, 146, 147,
 151
 Lamb shift, 141, 152, 153, 169, 170
 Lamb theory of the laser, 128
 Laplace transforms, 62, 63
 Laser, v, 42, 68, 71, 81, 111, 112, 120, 121,
 126, 127, 128, 131, 151, 212, 213
 Laser amplitude, 71
 Laser cavity, 127
 Laser field, 53, 69, 71, 214
 Laser frequency, 70, 214
 Laser light, 112
 Laser source, 141
 Laser threshold, 126
 Laser tube, 127
 Lead vapor, 121, 122, 123, 124
 Lead vapor cell, 121
 Lead vapor laser, 121
 Lee, 151
 Lehmburg, 194
 Letokhov, 151
 Levels, 29
 Level degeneracy, 110, 214
 Level population, 131; *see also* Inversion
 Liao, 194
 Lieb, 172

- Lifetime, 5, 6, 11, 163, 164, 167, 168, 169, 170
 Light emission, 174
 Light pulse, 67, 81; *see also* Pulse
 Linear absorption, 115, 145
 Linear dipole oscillator, 2-5
 Linear dispersion theory, 125
 Linear oscillator, 80
 Linear polarization, 107
 Linear polarized light, 214
 Linear polarizer, 213
 Linearly polarized wave, 107
 Lineshape, 7-10, 163, 164, 168, 169, 191
 Lineshape function, 119
 Line shift, 163, 164, 169
 Linewidth, 7-10, 67
 Liquid helium, 211, 212, 213
 Liquid hydrogen, 213
 Liquid nitrogen, 212
 Local strain field, 61
 Locked three-mode pulses, 128
 Locking, 126, 127
 Locking regime, 128
 Logarithmic divergence, 169, 172
 Longitudinal decay rates, 65
 Longitudinal homogeneous lifetime, 61;
see also T₁
 Longitudinal modes, 126
 Longtime steady-state solution, 62
 Lorentz, 1, 26
 Lorentz force equation, 5
 Lorentz force law, 3
 Lorentzian, 8, 10, 12, 22, 30, 31, 83, 135,
 138, 168, 180, 191
 Lorentzian absorption formula, 1
 Lorentzian detuning function, 24
 Lorentzian dielectric, v, vii
 Lorentzian dispersion formula, 1, 46
 Lorentzian emission, 9
 Lorentzian line, 31, 133
 Lorentzian oscillator, 46
 Lorentzian theory, 1
 Loss-free optical Bloch equations, 72; *see also* Bloch equations
 Loss mechanisms, 11
 Loss medium, 127
 Louisell, 44, 51, 151, 172, 173
 Lowering operator, 164
 Lower state, 68
 Low temperature, 201
 MacGillivray, 194
 Macroscopic moment, 196, 198
 Macroscopic polarization, 17, 61, 204
 Macroscopic polarization density, 11, 20,
 202, 217
 Magnetic degeneracy, 32; *see also* Degeneracy
 Magnetic dipole radiation, 78
 Magnetic field, 1, 32, 54, 61, 112, 115, 117,
 212
 Magnetic force, 3
 Magnetic quantum number, 117
 Magnetic resonance, 28, 40, 41, 43, 61, 71,
 72, 74, 78, 103, 143, 206
 Magnetic resonance absorption, 142
 Magnetic resonance phenomena, 7, 52, 78
 Magnetic resonance theory, 52
 Magnetic spin, 61
 Magnetic states, 119
 Magnetic transient phenomena, 71
 Magnetic transitions, 78
 Magnetic tuning, 112
 Mandel, vii, 194
 Mandelbaum, 51, 109
 Many-atom cooperative phenomena, 131;
see also Superradiance
 Many-atom effects, 176
 Many-atom operator equations, 174-176
 Many mode problem, 162
 Many- π pulse, 68
 Markovian Heisenberg equation, 172
 Markovian source field, 164
 Marth, 94, 109
 Maser, v
 Masserini, 151
 Mass renormalization, 171
 Mass-renormalized frequency shift, 169
 Matrix commutators, 37
 Matrix element, 36
 Matulic, 92, 106, 109
 Maxwell-Bloch equations, vi; *see also*
 Coupled Maxwell-Bloch equations
 Maxwell-Boltzmann distribution, 31
 Maxwell demon, 196
 Maxwell's equations, vi, 12, 13, 21, 22, 38,
 78-80, 81, 84, 85, 102, 107, 108, 130,
 137, 143, 156, 195
 Maxwell field equations, 139
 McCall, 78, 83, 84, 85, 86, 88, 90, 91, 108,
 109, 110, 115, 126, 127, 128, 129, 212,
 217, 219, 220
 McCall-Hahn, 109
 McCall-Hahn area theorem, 85-89; *see also*
 Area theorem
 McCall-Hahn experiment, 111
 McCall-Hahn quantum optical area theorem,
 87; *see also* McCall-Hahn area theorem
 Mensuration, v
 Microwelding, v
 Milonni, iii, 169, 173
 Modes, 127, 128, 162, 164, 176, 178
 Mode frequency, 126
 Mode function, 154
 Mode locked lasers, 81, 126-128
 Mode locked laser pulse, 126
 Mode locking, 128
 Mode operators, 166
 Mode phase, 126
 Mode resonances, 128
 Mode sum, 167, 168
 Molecular dipoles, 70
 Molecular transitions, 68
 Mollow, 172
 Moment vectors, 197
 Monochromatic classical radiation field, 158

- Monochromatic field, v, vi, 133-134
 Monochromatic radiation field, 28, 157
 Multiatom spontaneous emission, 181; *see also* N-atom spontaneous emission
 N-atom incoherent intensity, 187
 N-atom intensity, 178, 179
 N-atom spontaneous emission, 176-181
 N-atom spontaneously radiated intensity, 178
 N-atom state, 177, 183
 N-atom system, 184, 188
 N^2 coherence, 189
 N^2 dependence, 181, 182, 187, 188, 193
 N^2 dependence of echo intensity, 214, 219
 N^2 emission, 194
 Na, 30, 32, 33, 42
 Narducci, 172, 189, 194
 Natural frequency, 5, 6, 20
 Natural lifetime, 5, 11, 112; *see also* Lifetime
 Natural line broadening, 162; *see also* Homogeneous broadening
 Natural linewidth, 182
 Natural precession, 47, 49
 Natural precession frequency, 48
 Natural radiative lifetime, 30
 Natural transition frequency, 169
 Nayfeh, 151
 Near resonance, v, 2, 5, 10, 13, 14, 156
 Near resonant, v, vi, 160
 Near resonant transitions, 34
 Ne (neon), 216
 Neon absorber cell, 127
 Newell, 101, 109
 NH_2D , 68, 70, 71, 214
 NH_3 , 74
 No-damping limit, 72
 Nonadiabatic inversion, 104
 Nondegenerate absorbers, 110
 Nondegenerate magnetic sublevels, 112
 Nondegenerate systems, 112
 Nonlinear circuit analysis, vii
 Nonlinear pulse propagation, viii
 Nonlinear spectroscopy, 139-141
 Nonlinear threshold, 116
 Nonlinear transmission, 111, 112, 114
 Nonlinearities, 86, 140
 Nonrelativistic bound-state calculations, 171
 Nonresonant, 145
 Normal ordering, 157, 165, 166, 168, 170
 Nuclear magnetic resonance, 11, 117; *see also* Magnetic resonance
 Nuclear spin, 32, 60
 Nuclear spin resonance, v
 Nucleus, 42, 153
 Number of modes, 178
 Nutation, v, 67, 69, 70, 71
 Off-resonance, 56, 68, 72, 82, 143
 Off-resonance single-atom absorption coefficient, 139
 One-atom states, 182
 On-resonance, 84, 135, 139
 On-resonance absorption, 20
 On-resonance atom, 53, 55, 56, 59, 67, 68, 69, 81, 102, 135
 On-resonance dipole amplitude, 86
 On-resonance equation, 139
 Operator, 39
 Operator fields, 38
 Operator Maxwell equation, 38
 Operator products, 165
 Optic axis, 212
 Optical adiabatic inversion, 21, 74
 Optical Bloch-equations, vi, viii, 28, 72, 79, 81, 107; *see also* Bloch equations
 Optical delay, 111, 212
 Optical dye laser, v
 Optical echoes, 209; *see also* Echo and Photon echo
 Optical energy, 114
 Optical free induction decay, 71; *see also* Free induction decay
 Optical frequency, 29, 45, 50, 194
 Optical interaction, 152
 Optical maser, v; *see also* Laser
 Optical nutation, v, 21, 53, 67-69, 70, 71, 130, 181, 214
 Optical path length, 111
 Optical pulse, 32, 90, 127; *see also* Pulse
 Optical pulse compression, 89
 Optical pulse equations, 100
 Optical radiation field, 28
 Optical resonance, v, vi, vii, 28, 29, 43, 71, 87
 Optical spectrum, v
 Optical transition, 42, 216
 Optical wavelength, 12, 174
 Orbit, 42
 Ordering, 169; *see also* Normal ordering, etc.
 Ordering of operators, 153, 157, 169
 Orszag, 172
 Oscillation frequency, 196
 Oscillator, 4
 Oscillator energy, 5
 Overlap degeneracy, 214; *see also* Degeneracy
 Pake, 151
 Parity, 35
 Passive cavity resonance, 126
 Patel, 111, 128, 129, 209, 213, 214, 215, 216, 220
 Pauli, 36
 Pauli matrix, 36, 37, 155
 Pauli matrix operators, 37
 Pauli principle, 30
 Pb vapor, 121, 122, 123, 124
 Peak amplification, 89, 125
 Pegg, 51
 Pendulum, 82, 83
 Pendulum solutions, 82
 Perturbation theory, 46, 146, 153, 170
 Perturbation theory, third order, 146
 Phase, 20

- Phase changes, 21
 Phase coherence, 194
 Phase-coherent, 188
 Phase function, 101, 103
 Phase modulation, 101-107
 Phase relaxation time, 115
 Phase velocity, 131, 148, 150
 Phenomenological damping terms, 74
 Phenomenological decay constants, 52, 59-61
 Phenomenological decay time, 195
 Phenomenological relaxation constants, 52
 Phonon-induced transitions, 212
 Phonon scattering, 60, 195
 Photomultiplier, 212
 Photon, 162
 Photon creation operator, 153
 Photon destruction operator, 153
 Photon echo, v, vi, 21, 181, 182, 193, 195, 197, 201, 202, 206, 209, 210, 211, 212, 214, 217
 Photon echo delay, 201
 Photon echo delay time, 209
 Photon echo in gases, 209-211
 Photon field, 160
 Photon flux, 122
 Photon matrix element, 166
 Photon number, 159, 176, 177, 178
 Photon number operator, 176
 Photon number states, 154
 Photon statistics, v
 π components, 118
 π -pulse, *see also* Pulse
 π transitions, 118
 Picosecond pulses, 72
 Planck, 131
 Planck's constant, vii
 Planck distribution function, 131
 Plane-polarized light, 213
 Plane-wave, 111
 Plane-wave propagation, 12
 Plasma, 124
 Plasma frequency, 14
 Pockels cell, 112
 Polarization, 118, 119, 154, 178, 179, 208
 Polarization decay, 22, 85
 Polarization density, 7, 10, 11, 12, 79, 108, 195, 197, 199, 201, 207
 Polarization sum, 171
 Polarization vector, 3, 154, 214
 Population, 126, 127, 131
 Population density, 132
 Population difference, 45
 Population rate equations, 135
 Potential energy, 97
 Power, E. A., 155, 172, 173
 Power, v
 Power absorbed, 142
 Power broadening, 52, 140, 143
 Power densities, 42, 124, 125
 Power flow, 142, 178, 179
 Power level, 68
 Precession, 41, 43, 44, 47, 55, 56, 71, 73
 Precession equation, 72
 Precession frequencies, 72, 197
 Probability amplitudes, vii
 Probability conservation, 80, 83, 102, 132
 Probe beam, 140
 Prokhorov, v
 Propagation, v, vi, 13, 20, 88, 89, 90, 91, 119, 130, 146, 147, 191, 214
 Propagation and damping of photon echoes, 214
 Propagation effects, 72, 189, 191, 192, 217
 Propagation experiments, 117
 Propagation of radiation, 78
 Propagation vector, 125
 Propagating lossless pulses, 97
 Propagating pulse, 196
 Propagating wave attenuation and amplification, 143-147
 Pseudodipole tipping angle, 182
 Pseudo-spin, 29, 40, 45, 57, 197
 Pseudo-spin equations, 41, 44, 80
 Pseudo-spin precession, 42
 Pseudo-spin vector, 28, 41, 43, 46, 57, 67, 184
 Pulling, 115
 Pumping pulse, 179
 Pulse, v, 12, 13, 16, 17, 20, 22, 24, 25, 26, 32, 54, 68, 73, 78, 85, 87, 88, 89, 90, 91, 93, 110, 111, 112, 113, 116, 120, 144, 145, 147, 149, 199, 204
 Pulse, 0π , 99, 100, 110, 120, 219
 Pulse, $\frac{1}{2}\pi$, 197, 199, 202, 205, 207, 208, 209, 210, 211, 214, 216, 217, 219
 Pulse, π , 50, 53-56, 124, 126-128, 179, 189, 191, 193, 199, 202, 205, 208, 210, 211, 214, 219
 Pulse, 2π , 90, 91, 96, 98, 99, 104, 105, 106, 107, 112, 113, 114, 115, 125, 219
 Pulse, 3π , 113, 115, 125
 Pulse, 4π , 96, 98, 99, 106, 107, 113, 114
 Pulse, 5π , 113
 Pulse, 6π , 99, 113, 114
 Pulse, $n\pi$, 110, 112
 Pulse, $2n\pi$, 110
 Pulse, $2\pi^\infty$, 96
 Pulse, many π , 68
 Pulse, near π , 115
 Pulse, π propagation, 128
 Pulse, ultrashort, 2
 Pulse absorption, 16, 23
 Pulse amplitude, 16, 97, 103
 Pulse area, 13, 17, 20, 59, 82, 89, 90, 91, 93, 94, 104, 113, 117, 119, 120, 126, 199, 205, 213
 Pulse attenuation, 144
 Pulse break up, 78, 99, 113, 125, 128
 Pulse collision, 107
 Pulse compression, 78, 115
 Pulse delay, 95, 111, 113, 115, 120, 121-126, 127
 Pulse distortion, 124
 Pulse duration, 32, 68, 127, 128
 Pulse energy, 21, 25, 26, 88, 112, 113, 120

- Pulse envelope, 96, 112, 125, 128, 144
 Pulse envelope area, 15, 55, 128; *see also*
 Pulse area
 Pulse field, 16
 Pulse frequency shift, 105
 Pulse intensity, 93
 Pulse length, 26, 81, 83, 84, 90, 93, 95, 97,
 112, 120
 Pulse narrowing, 124
 Pulse propagation, v, vi, vii, 26, 91, 97, 116,
 121, 122, 123, 125
 Pulse reshaping, 120
 Pulse scattering, 97
 Pulse shapes, 115
 Pulse shaping, 117
 Pulse shortening, 90
 Pulse spectral width, 26, 192
 Pulse spectrum, 25
 Pulse steepening, 120
 Pulse tails, 113
 Pulse transmission, 121
 Pulse velocity, 91, 95, 97, 127
 Pulse width, 124, 127, 213
- Q-switch, 81, 111, 212
 Quantization, 174
 Quantized field theory, 152, 161
 Quantized radiation theory, 152
 Quantized field, 152, 161
 Quantized radiation field, 170
 Quantum, 46
 Quantum area theorem, 85, 88, 90; *see also*
 Area theorem
 Quantum correlations, 37
 Quantum dipole, 46, 47, 148, 156
 Quantum dipole envelope functions, 79
 Quantum dipole equations, 84
 Quantum electrodynamics, v, 34, 152, 153,
 158, 159, 160, 161, 162, 174, 188, 194
 Quantum electrodynamic field attenuation,
 162
 Quantum electrodynamic Rabi problem,
 157-162
 Quantum electrodynamic perturbation
 theory, 170-173
 Quantum mechanical absorption coefficient,
 138; *see also* Absorption coefficient
 Quantum numbers, 30
 Quantum optical free induction decay, 11;
 see also Free induction decay
 Quantum optical nonlinear theory, 77
 Quantum optics, vi, 20, 21, 34
 Quantum rotation theory, 44
 Quantum rotating wave approximation, 176;
 see also Rotating wave approximation
 Quantum theory, 47
 Quasi-monochromatic field, 34
 Quasi-monochromatic pulse, 179
 Quasi-steady state, 134
 Quasi-steady state Bloch equations, 135
 Rabi, 7, 27, 52, 53, 56, 77
 Rabi frequency, 54, 57, 58, 59, 67, 68,
 160, 161
 Rabi oscillation, 60
 Rabi problem, 2, 71, 102, 157-162
 Rabi solution, 53, 56-59, 67, 82, 182
 Radcliffe, 189, 194
 Radiated field, 11
 Radiated power, 188
 Radiation, vi, 78
 Radiation field, 80, 130, 152, 156, 162,
 174, 179
 Radiation gauge, 153
 Radiation mode, 161
 Radiation pattern, 186
 Radiation rate, 186, 188
 Radiation reaction, 5, 38, 169, 175, 182,
 184, 188
 Radiative damping, 31, 114
 Radiative decay, 6, 61
 Radiative effects, 30
 Radiative frequency shift, 152, 153
 Radiative level shifts, 170
 Radiative lifetime, 6, 187
 Radiative lineshape, 163
 Radiative rate, 6
 Radiative reaction, 170
 Rate equation, v, vi, 76, 121, 123, 124, 126,
 130, 131, 132, 133, 135, 137, 139
 Rate equation approximation, 131
 Rate equation limit, 134-137, 141
 Rate equation limit of the Maxwell equations
 137
 Rayleigh scattering formula, 1
 Rb, 112, 114, 115, 116
 Reciprocal Beer's absorption length, 87
 Refraction, index of, 2, 148, 149, 150, 191
 Rehler, 183, 184, 186, 194
 Relativistic limit, 3
 Relaxation, 111, 136
 Relaxation processes, 67, 68
 Relaxation times, 14, 141, 212, 213
 Resonance, v, vi, 5, 14, 32, 34, 42, 43, 45,
 53, 54, 59, 60, 67, 68, 70, 75, 111, 112,
 115, 116, 125, 140, 143, 145, 146, 149,
 214
 Resonance centre frequency, 8, 10
 Resonance condition, 48, 49, 50
 Resonance echo effects, 197
 Resonance frequency, 47, 195, 214; *see also*
 Resonant frequency
 Resonance frequency shift, 172
 Resonance line, 68
 Resonance optics, 84
 Resonance wavelength, 193
 Resonant absorber, 91, 96, 110, 124, 193
 Resonant absorption frequency, 192
 Resonant atoms, 8, 61, 73, 90, 143, 145,
 214, 217
 Resonant dipoles, 82
 Resonant field amplitude, 61
 Resonant frequency, 7, 8, 29, 61, 151, 162
 Resonant interactions, v, 132
 Resonant levels, 110
 Resonant medium, 146

- Resonant phenomena, vi
 Resonant pulse interactions, 60
 Resonant pulse propagation experiments, 117
 Resonant transitions, 42, 150
 Retarded solution, 164
 R. f. field, 53
 Rhodes, 27, 111, 128, 129
 Rotating coordinate system, 52
 Rotating frame, 44, 45, 46, 53, 55, 56, 60, 67, 73, 101, 102, 103, 108, 197
 Rotating frame Bloch vectors, 196
 Rotating frame equations, 47
 Rotating wave approximation, 28, 29, 44, 45, 47, 107, 158, 159, 162, 176, 183
 Rotation, 48
 Rotation matrix, 44
 Rubenstein, 100, 109
 Rubidium, 112, 114, 115, 116
 Ruby, 110, 111, 115, 116, 193, 211, 212, 213, 214
 Ruby laser, 111, 212
 Russell-Saunders coupling, 30
 RWA, *see* Rotating wave approximation
- S, 30
 Salamo, 129
 Salpeter, 173
 Saturable dyes, 127
 Saturated, 69, 111, 140
 Saturated absorption, 111, 142-143
 Saturated inhomogeneous lineshape function, 143
 Saturated media, 147
 Saturation, vi, vii, 130, 139-141, 146, 150, 151
 Saturation effects, 131, 140
 Saturation and nonlinear spectroscopy, 139-141
 Saturation phenomena, 68, 130
 Saturating field, 141, 142, 143
 Saturating field frequency, 40
 Sayers, 129
 Scattering formula, 1
 Schawlow, v, 51, 141, 151
 Schiff, 151
 Schrödinger, vii, 37
 Schrödinger equation, 28, 36
 Schrödinger picture, vii, 170
 Schuda, 51
 Schwarz, 129
 Schwendimann, 151, 186, 194
 Scully, 27, 115, 116, 126, 128, 129, 151, 220
 Sech envelope, 102
 Sech pulse, 84, 104, 113
 Sech pulse, 2 π , 94, 96
 Sech shape, 91
 Secular determinant, 62
 Secular effects, 29, 30
 Secular equation, 64
 Segur, 101, 109
 Selden, 124, 129
- Selden's theory, 122
 Selection rules, 29
 Self-focusing, 131, 147, 149, 150, 151
 Self-induced transparency, vi, 21, 32, 89-101, 110, 111, 114, 115, 116, 117, 120, 121, 124, 125, 130, 212, 214
 Self-locked, 126
 Semiclassical dipole interactions, 46
 Semiclassical equations, 46
 Semiclassical laser theory, 135
 Semiclassical optical Bloch equations, vii
 Semiclassical Rabi problem, 152
 Semiclassical radiation theory, 34-41, 38, 39, 79, 80
 Semiclassical rate equations, vi
 Senitzky, 169, 172
 Series, 51
 SF₆, 68, 111, 120, 213, 214, 215, 216
 SF₆ vapor, 216
 Shahin, 51, 141, 151
 Shape-preserving pulse, 105
 Shape-stable pulse, 91
 Sharp-line limit, 116
 Shift, 29, 115
 Shireen, 217, 219, 220
 Shirley, 48, 51, 141, 151
 Shoemaker, 11, 27, 68, 70, 77, 194, 214, 220
 Short intense pulses, 182
 Siegert, 47, 51
 Signal decay, 71
 Simple harmonic oscillator, 2
 Sine-Gordon equation, 100, 101
 Single-atom absorption cross-section, 143
 Single-atom decay, 167
 Single-atom dipole oscillator, 2
 Single-atom emission, 181
 Single-atom intensity, 181
 Single-atom small-signal absorption coefficient, 145
 Single-atom spontaneous emission, 143, 162-170
 Single-frequency operation in CO₂, 213
 Single-mode field, 157
 Single-mode quantized field, 162
 Single-mode quantized radiation field, 152
 Single-mode radiation, 186
 Skribanowitz, 194
 Slowly varying envelope, 13
 Slowly varying Maxwell equations, 108
 Slusher, 88, 89, 99, 107, 109, 111, 112, 113, 114, 115, 116, 128, 129, 209, 213, 214, 215, 216, 220
 Small-signal absorption coefficient, 145, 150
 Small-signal absorption constant, 125
 Small-signal limit, 145, 148
 Smith, K. W., 121, 122, 123, 124, 129
 Smith, P. W., 126, 127, 129
 Smith, W. A., 169, 173
 Sodium, 30, 32, 33, 42
 Sodium vapor, 151

- Soft collisions, 195
 Solids, 201, 207
 Solid state lasers, 127
 Someda, 109
 Source field, 164, 165, 167, 169, 175, 176, 177
 Spatial degeneracy, 117, 214
 Spectral distribution, 31
 Spectral line, 8, 30
 Spectral lineshape, 8
 Spectral width, 8, 23, 32, 112, 192, 197
 Spectroscopy, 130
 Spectrum, v, 25, 26, 78, 133
 Speed of light, 149, 191, 192, 193, 206
 Spins, 28, 44, 67, 103
 Spin echoes, 195, 197, 206, 215, 216
 Spin echoes in ruby, 212
 Spin exchange, 61
 Spin nutation, 67
 Spin resonance, v
 Spin vector, 28
 Spontaneous absorption, 170
 Spontaneous cooperative effects, vi
 Spontaneous decay, 34, 52, 169, 176
 Spontaneous decay rate, 177, 190
 Spontaneous emission, 38, 152, 158, 161, 162, 164, 169, 174, 177, 181, 188, 195, 206
 Spontaneous emission rate, 187
 Spontaneous radiative decay, 163
 Stark field, 69, 214
 Stark-field switching, 70
 Stark pulse, 214
 Stark shift, 69, 70, 214
 Stark splitting, 68
 State functions, vii, 35
 State vectors, 35, 179
 Statz, 67, 77
 Steady-state inversion, 140, 141
 Steady-state pulse, 91, 92, 106, 116
 Steady-state pulse envelope, 94
 Stenholm, 51
 Stephen, 209, 220
 Stevenson, 51
 Stimulated absorption rate, 124
 Stimulated emission, 131
 Stimulating field, 127
 Stochastic, 174, 189
 Stochastic damping, 215
 Stored energy, 20
 Strain fields, 8
 Strong collisions, 64
 Strong collision limit, 67
 Stroud, vii, 51, 188
 Sub-picosecond pulses, 32
 Superradiance, 174, 181-189, 190, 193, 206, 217, 219
 Superradiance effects, 182
 Superradiant damping, 191, 193
 Superradiant decay, 182, 190, 192, 217
 Superradiant decay rate, 191
 Superradiant emission, 182, 184, 191, 192
 Superradiant energy loss, 217
 Superradiant lifetime, 189, 191
 Superradiant intensity, 187
 Superradiant phenomena, 189
 Superradiant process, 191
 Superradiant transmitter, 184
 Szöke, 111, 125, 128, 129
 T_1 , 6, 7, 8, 11, 12, 14, 15, 16, 17, 18, 19, 20, 22, 24
 T_1^* , 11, 12, 14, 17, 18, 19, 20, 22, 24
 T_2 , 61, 62, 69, 71, 73, 76, 79, 80, 81, 88, 91, 93, 116, 124, 125, 126, 130, 131, 132, 134, 135, 136, 138, 139, 140, 141, 142, 143, 144, 147, 195, 216
 T_2' , 61, 116
 T_2'' , 30, 61, 62, 69, 71, 73, 75, 76, 79, 80, 81, 88, 90, 91, 93, 110, 115, 116, 120, 125, 126, 130, 133, 134, 135, 136, 138, 139, 140, 141, 142, 143, 144, 145, 146, 147, 149, 150, 195, 196, 215, 216
 $T_{2\perp}$, 60, 72, 73, 90, 103, 116, 120, 144, 180, 184, 189, 191, 192, 193, 195, 196, 197, 199, 200, 201, 202, 204, 208, 215
 Tang, 67, 68, 77
 Tanh frequency sweep, 102
 Tavis, 172
 Taylor expansion, 75
 Terms, spectroscopic, 29
 Thermal reservoir, 61
 Thermal tuning, 111
 Third subharmonic, 50
 Thomas, 189, 194
 Thomson scattering formula, 1
 Time-dependent Bloch equations, 95; *see also* Bloch equation
 Tipping angle, 53, 54, 173
 Tomlinson, 129, 220
 Torque, 41, 42, 43, 44, 47, 48, 50, 55, 56, 67, 72, 73, 74
 Torque vector, 41, 42, 43, 44, 45, 48, 56, 72, 73, 103
 Torrey, 52, 62, 64, 67, 71, 72, 77
 Torrey rate constants, 64
 Torrey's solutions, 62-67
 Total decay rate, 6
 Total linewidth, 12, 22
 Total relaxation rate, 12
 Total transverse decay time, 61
 Townes, v
 Transient optical resonance effects, 68
 Transient phenomena, vi
 Transition, v, 32, 34, 35, 40, 43, 67, 111, 112, 118, 121, 140, 155, 161
 Transition dipole moment, 42
 Transition frequency, 28, 31, 34, 37, 42, 47, 133, 155, 214
 Transition line, 169
 Transition moment, 45
 Transition rate, 54
 Transition wavelength, 150
 Transitions, σ , $\Delta M=\pm 1$, 107, 108, 118
 Transitions, π , $\Delta M=0$, 118

- Transmittance, 124
Transparency, 91, 114, 120, 121, 126;
 see also Self-induced transparency
Transparency threshold area, 115
Transport equation, 12
Transverse decay rate, 65
Transverse homogeneous lifetime, 61; *see also* T_2'
Transverse moment lifetime, 61
Traveling wave, 147
Treacy, 47, 51, 74, 77, 103, 109
Tuft, 172
Tunable laser, 151
Two-level absorber, 121; *see also* Absorber
Two-level approximation, vi
Two-level atom, v, vi, 28, 29, 32, 34-41,
 52, 53, 71, 80, 110, 118, 119, 131, 140,
 152, 155, 158, 160, 166, 169, 170, 192
Two-level atom operators, 40
Two-level model, 131, 132
Two photon absorption, v

Ultrashort pulses, 2
Ultraviolet divergence, 168
Undamped solutions, 62
Unit sphere, 84
Upper state, 68

Vacuum, 149
Vacuum expectation, 177
Vacuum field, 161, 164, 165, 167, 168,
 169, 175, 176
Vacuum field operator, 166
Vacuum fluctuations, 169, 170
Vacuum state, 171
Vacuum wave vector, 13, 21, 101
Valence electrons, 30, 42

Vapor density, 112
Vector electric field operator, 38
Vector model, 72
Vector operator, 35
Vector potential, 153, 154, 175
Vector space, 35
Velocity, 61
Velocity distribution, 31
Velocity of light, 206
Vernon, 37, 51

Wang, C. H., 129, 220
Wang, Y. K., 172
Wave attenuation, 143-147
Wave equation, 78
Wave plates, 213
Wave propagation, 71
Wave vector, 13, 21, 31, 96, 101, 148,
 154, 167
Wavefront, 111, 112
Wavelength, 32, 78, 206
Weisskopf, 162, 163, 172
Weisskopf-Wigner approach, 163, 169
Wigner, 162, 163, 172
Wolf, vii, 3, 4, 26, 128, 129, 220
Woodgate, 51

X-ray, 1

Zeeman, 112
Zeeman field, 61
Zembrod, 129
Zero-area pulses, 99; *see also* Pulses, Or
Zero-point energy, 153
Zeta function, 164
Zienau, 155, 172
Zuev, 151